

Austrian Journal of Technical and Natural Sciences

**Nº 1–2 2017
January–February**



«East West» Association for Advanced Studies and Higher Education GmbH

**Vienna
2017**

Austrian Journal of Technical and Natural Sciences

Scientific journal

№ 1–2 2017 (January–February)

ISSN 2310-5607

Editor-in-chief
International editorial board

Hong Han, China, Doctor of Engineering Sciences
Andronov Vladimir Anatolyevitch, Ukraine, Doctor of Engineering Sciences
Bestugin Alexander Roaldovich, Russia, Doctor of Engineering Sciences
S.R. Boselin Prabhu, India, Doctor of Engineering Sciences
Frolova Tatiana Vladimirovna, Ukraine, Doctor of Medicine
Inoyatova Flora Ilyasovna, Uzbekistan, Doctor of Medicine
Kambur Maria Dmitrievna, Ukraine, Doctor of Veterinary Medicine
Kurdzeka Aliaksandr, Russia, Doctor of Veterinary Medicine
Khentov Viktor Yakovlevich, Russia, Doctor of Chemistry
Kushaliyev Kaiser Zhalitovich, Kazakhstan, Doctor of Veterinary Medicine
Mambetullaeva Svetlana Mirzamuratovna, Uzbekistan, Doctor of Biological Sciences
Manasaryan Grigoriy Genrihovich, Armenia, Doctor of Engineering Sciences
Martirosyan Vilena Akopovna, Armenia, Doctor of Engineering Sciences
Miryuk Olga Alexandrovna, Kazakhstan, Doctor of Engineering Sciences
Nagiyev Polad Yusif, Azerbaijan, Ph.D. of Agricultural Sciences
Nemikin Alexey Andreevich, Russia, Ph.D. of Agricultural Sciences
Nenko Nataliya Ivanovna, Russia, Doctor of Agricultural Sciences
Ogirko Igor Vasilievich, Ukraine, Doctor of Engineering Sciences
Platov Sergey Iosifovich, Russia, Doctor of Engineering Sciences
Rayiha Amenzade, Azerbaijan, Doctor of architecture
Shakhova Irina Aleksandrovna, Uzbekistan, Doctor of Medicine
Skopin Pavel Igorevich, Russia, Doctor of Medicine
Suleymanov Suleyman Fayzullaevich, Uzbekistan, Ph.D. of Medicine
Tegza Alexandra Alexeevna, Kazakhstan, Doctor of Veterinary Medicine
Zamazay Andrey Anatolievich, Ukraine, Doctor of Veterinary Medicine
Zhanadilov Shaizinda, Uzbekistan, Doctor of Medicine

Proofreading

Cover design

Additional design

Editorial office

Kristin Theissen

Andreas Vogel

Stephan Friedman

European Science Review

“East West” Association for Advanced Studies
and Higher Education GmbH, Am Gestade 1
1010 Vienna, Austria

Email:

info@ew-a.org

Homepage:

www.ew-a.org

Austrian Journal of Technical and Natural Sciences is an international, German/English/Russian language, peer-reviewed journal. It is published bimonthly with circulation of 1000 copies.

The decisive criterion for accepting a manuscript for publication is scientific quality. All research articles published in this journal have undergone a rigorous peer review. Based on initial screening by the editors, each paper is anonymized and reviewed by at least two anonymous referees. Recommending the articles for publishing, the reviewers confirm that in their opinion the submitted article contains important or new scientific results.

East West Association GmbH is not responsible for the stylistic content of the article. The responsibility for the stylistic content lies on an author of an article.

Instructions for authors

Full instructions for manuscript preparation and submission can be found through the “East West” Association GmbH home page at: <http://www.ew-a.org>.

Material disclaimer

The opinions expressed in the conference proceedings do not necessarily reflect those of the «East West» Association for Advanced Studies and Higher Education GmbH, the editor, the editorial board, or the organization to which the authors are affiliated.

East West Association GmbH is not responsible for the stylistic content of the article. The responsibility for the stylistic content lies on an author of an article.

Included to the open access repositories:



© «East West» Association for Advanced Studies and Higher Education GmbH

All rights reserved; no part of this publication may be reproduced, stored in a retrieval system, or transmitted in any form or by any means, electronic, mechanical, photocopying, recording, or otherwise, without prior written permission of the Publisher.

Typeset in Berling by Ziegler Buchdruckerei, Linz, Austria.

Printed by «East West» Association for Advanced Studies and Higher Education GmbH, Vienna, Austria on acid-free paper.

Section 1. Biology

DOI: <http://dx.doi.org/10.20534/AJT-17-1.2-3-11>

*Nenko Natalya Ivanovna,
Federal State Budgetary Scientific Institution
“North-Caucasian Zonal Research Institute
of Horticulture and Viticulture” (FSBSI NCZRIHV),
Professor, Doctor of Agricultural Sciences,
Head of Laboratory of Plant Physiology and Biochemistry
E-mail: nenko.nataliya@yandex.ru*

*Ilyina Irina Anatolyevna,
FSBSI NCZRIHV, Professor,
Doctor of Engineering Sciences, Deputy Director
E-mail: kubansad@kubannet.ru*

*Kiselyova Galina Konstantinovna,
FSBSI NCZRIHV, Associate Professor,
Candidate of Biological Sciences, Senior Research Associate
of Laboratory of Plant Physiology and Biochemistry
E-mail: galina-kiseleva-1960@mail.ru*

*Sundyeva Mariya Andreyevna,
FSBSI NCZRIHV, Candidate of Agricultural Sciences,
Research Associate of Laboratory of Plant
Physiology and Biochemistry
E-mail: kubansad@kubannet.ru*

Physiological and biochemical characteristics of resistance of grape varieties of different ecological and geographical origin to the stress factors of summer season

Abstract: This article is devoted to determination of physiological and biochemical regularities of adaptation of grape plants of different ecological and geographical origin to drought and high temperature stress. The identified regularities let us assume that there are mechanisms of biochemical processes in plant leaves, which are focused on provision of resistance of grape varieties to drought and high temperature. Knowledge of biochemical fundamentals of plant resistance allows us to develop evaluation methods and techniques, which increase resistance of plants to drought and high temperature stress.

Keywords: grape, high temperature stress, drought, heat resistance, regularities, adaptive resistance.

Introduction

The study of physiological and biochemical fundamentals of plant resistance allows to develop methods for evaluation of this characteristic, as well as techniques focused on its increase [1; 2]. Detection of physiological and biochemical mechanisms for provision of resistance

of grape plants to abiotic factors is a basis of management of adaptive and production processes for stabilization of perennial agrocenosis.

It is known that a long stay of grape bushes during summer months and early autumn on unprovided boghara under high pressure of atmospheric factors and strong

air and soil drought has a negative impact on physical and biochemical processes, growth and productivity of plants [3; 4]. The study on physiological and ecological condition of grape plants, their responses to abiotic stresses becomes relevant due to frequent stresses associated with drought against the background of high temperature during summer season. In conditions of constantly varying environmental factors, activation of protective-compensatory and other adaptive responses of grape plants, including regulation and preservation of a relative constancy of internal water medium of plants, plays an important role as one of the main means of adaptation to variable environmental conditions and the influence of disturbing factors [5–8].

Adaptation of plant organism to the environment on a molecular level is based on a flexible provision of its vital functions, controlled by a complex system of regulatory mechanisms [6].

The objective of the study was to reveal physiological and biochemical regularities of adaptation of grape plants of different ecological and geographical origin to high temperature and water stresses.

Materials and methods

Field investigations and sampling (grape leaves) for laboratory studies were performed on the ampelographic collection of Federal State Budgetary Scientific Institution of Anapa Zonal Experimental Station of Viticulture and Winemaking in North Caucasian Zonal Research Institute of Horticulture and Viticulture, located in Anapa City. Objects of the study were grape varieties of industrial purpose: European-Amur-American interspecies hybrid of early ripening — *Kristall*, grape of middle ripening — interspecies hybrids of European-American group — *Dostoiny* and *Krasnostop AZOS*. Plants of the same planting year; rootstock Kober SBB. Shaping — two-sided high-stem spiral cordon AZOS. Cultivation of grape plants — in bare fallow with landing procedure 3×2.5 m.

Adaptive resistance of grape plants to high temperature and water stresses of summer period in Anapa-Taman zone was studied in Laboratory of Plant Physiology and Biochemistry and in Common Use Center of Federal State Budgetary Scientific Institution in North Caucasian Zonal Research Institute of Horticulture and Viticulture. Influence of low moisture availability and high temperature in summer season on grape plants was studied both in vivo and in a model experiment by the following indicators: membrane damage coefficient (by cation yield according to conductometric method), content of free and bound water in plant tissues (grape leaves) — by weight method, content of proteins, carbohydrates — by spectral method [9], content of organic

acids (malic, succinic, citric) [10] and phenolcarbonic acids [11; 12] — by capillary electrophoresis with the use of the instrument “Capel 105 P”. Intensity of photosynthesis was measured by pigment content in leaves, and resistance of chlorophyll-protein complex was measured by dynamics of protein and chlorophyll content (a and b) and anatomical structure of lamina. Anatomical-morphological and histochemical investigations were conducted with the use of microscopes MBI-3, MBI-10, Olympus [13]. Experimental data were processed with standard methods of variation statistics.

Results and discussion

Grape is considered to be drought-resistant culture, because thanks to a deeply penetrating root system it can survive and produce crop in dry weather conditions. However, experience of grape cultivation evidences that grape-vine produces high and conditioned crops only in conditions of optimal water supply. Therefore, estimation of hydrothermal resources of vine cultivation areas is especially important. In this context, we studied the influence of hydrothermal conditions of summer season 2014–2016 in Anapa-Taman zone on grape plants of different ecological and geographical origin.

During the analyzed period in summer season on the territory of Anapa-Taman zone we noted a gradual reduction of precipitation depth in June by 72.3 %, in July by 83.3 %; in August 2014–2015 drought was observed; besides, the maximum air temperature increased in June by 7 °C, in July — by 7 °C and in August — by 4 °C, respectively. August in 2014 and 2015 was characterized by a low moisture availability (precipitation — 0–11 mm.), and precipitation in 2016 amounted to 47 mm. (fig. 1).

In these conditions during the summer season 2016 we noted the decrease of water content in grape leaves of the variety *Kristall* by 19.2 %, in the variety *Krasnostop AZOS* — by 13.2 % and in the variety *Dostoiny* — by 11.8 % (fig. 2).

During the analyzed period in 2016 in comparison with 2014, water content of leaves of the examined varieties decreased in June by 0.6–2 %, in July — by 0.68–1.85 % and in August — by 4.39–11.37 %.

During summer in 2014–2016 water content of leaves of the examined grape varieties correlated in a greater degree with minimal air temperature (correlation ratio = 0.6–0.9) (fig. 3).

Drought-resistant varieties in the case of increasing dehydration preserve synthetic processes for a longer time and have biochemical mechanisms of protection, which contribute to maintenance of homeostasis in conditions of drought.

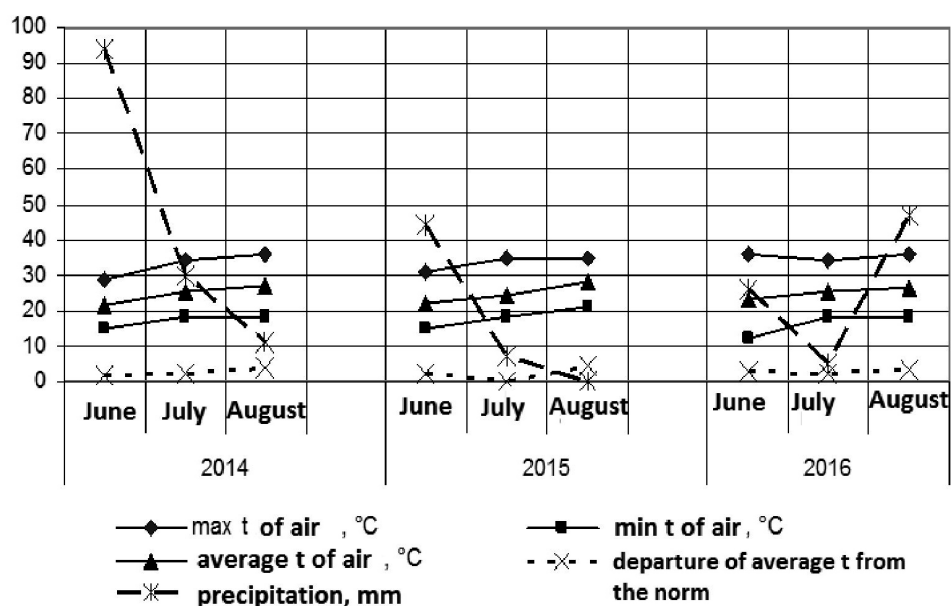


Fig. 1. Hydrothermal conditions of summer season 2014–2016 in Anapa-Taman zone

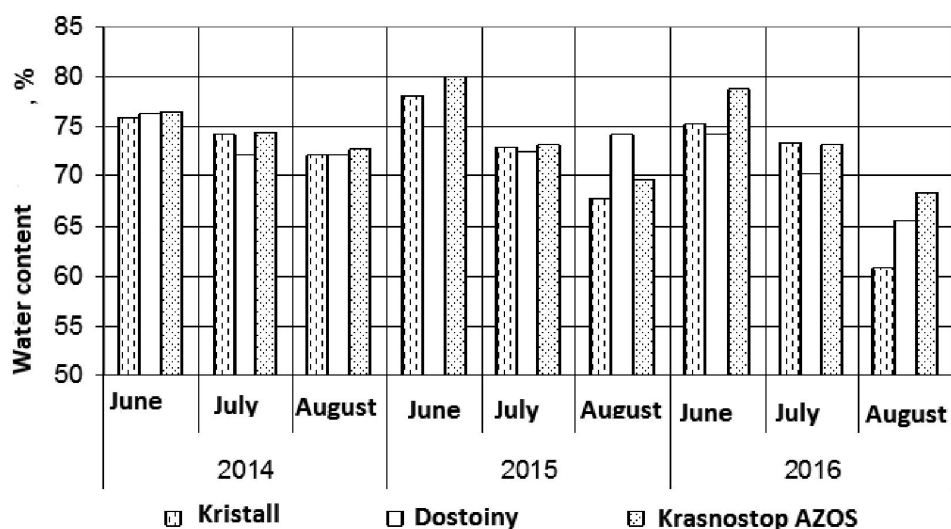


Fig. 2. Water content of grape leaves in vegetation period 2014–2016

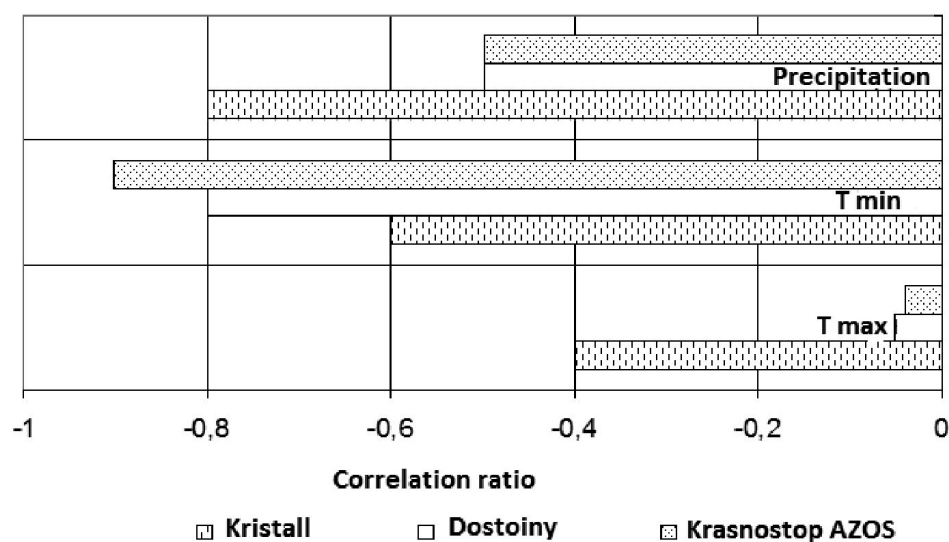


Fig. 3. Dependence of water content of grape leaves from hydrothermal conditions of vegetation period 2014–2016

These mechanisms prevent dehydration of a cell due to accumulation of low-molecular hydrophilic proteins, which bind a considerable amount of water, proline, the concentration of which significantly increases; due to the growth of monosucrose content, which provide the detoxication of decay products and contribute to the recovery of damaged structures of cytoplasm under the condition of prevention of cells from damage of genetic apparatus. In July 2016 compared to June, the ratio between content of bound and free water in the studied grape varieties decreased by 8.5–11.7%, in August compared to July increased by 21–29% and in greater degree — in the varieties *Kristall* and *Dostoiny*; the variety *Krasnostop AZOS* was in intermediate position, at the same time the change of this indicator in the variety *Dostoiny* correlated with the precipitation depth (correlation ratio = 1) (fig. 4).

The content of bound water in conditions of drought decreases along with the increase of proline

content (by 3.7–5.7 times), what characterizes its stress-protective properties. During the analyzed period, water-retaining capacity of all studied grape varieties in conditions of drought is conditioned by high content of proline that constitutes a part of osmoprotective proteins (correlation ratio = 0.82–0.99), in 2015 — in the variety *Krasnostop AZOS*, and in 2016 in the variety *Kristall* — also with sucrose content (correlation ratio = 0.85–1.0) (fig. 5, 6).

The proteins of protoplasm are characterized by hydrophilism and easily come into contact with water, forming a colloidal system; therefore, the increase of their content contributes to the formation of protective mechanisms in grape plants against abiotic stresses.

Under the influence of drought in August 2016 the protein content in leaves decreased as a result of its hydrolysis (fig. 7).

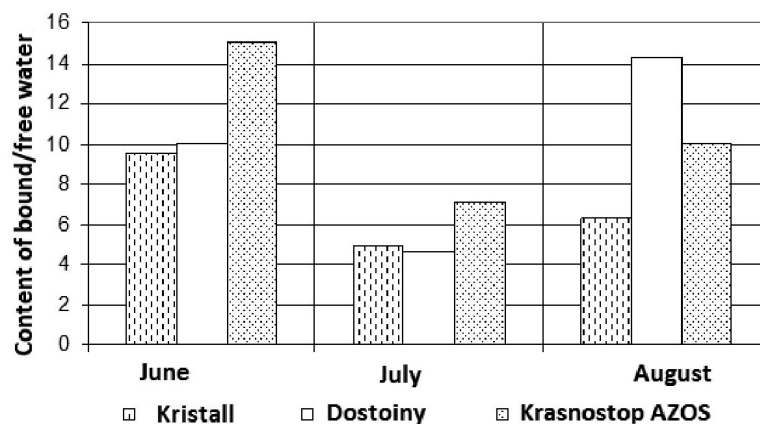


Fig. 4. Dynamics of ratio between content of bound and free water in grape leaves in summer season 2016

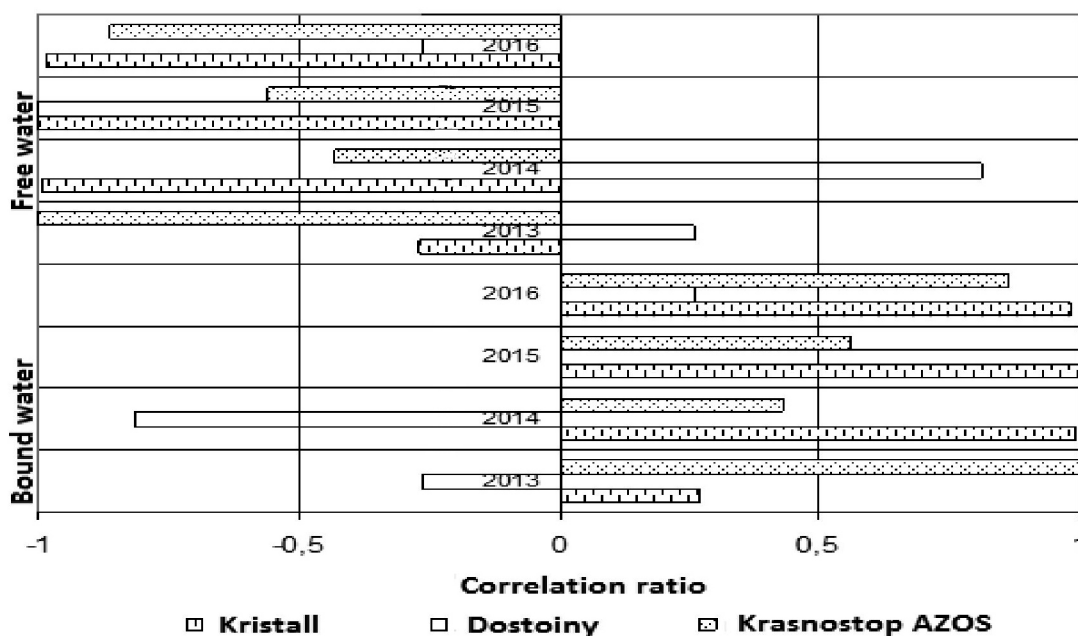


Fig. 5. Dependence of the content of bound and free water from the content of proline in grape leaves during the vegetation period 2013–2016

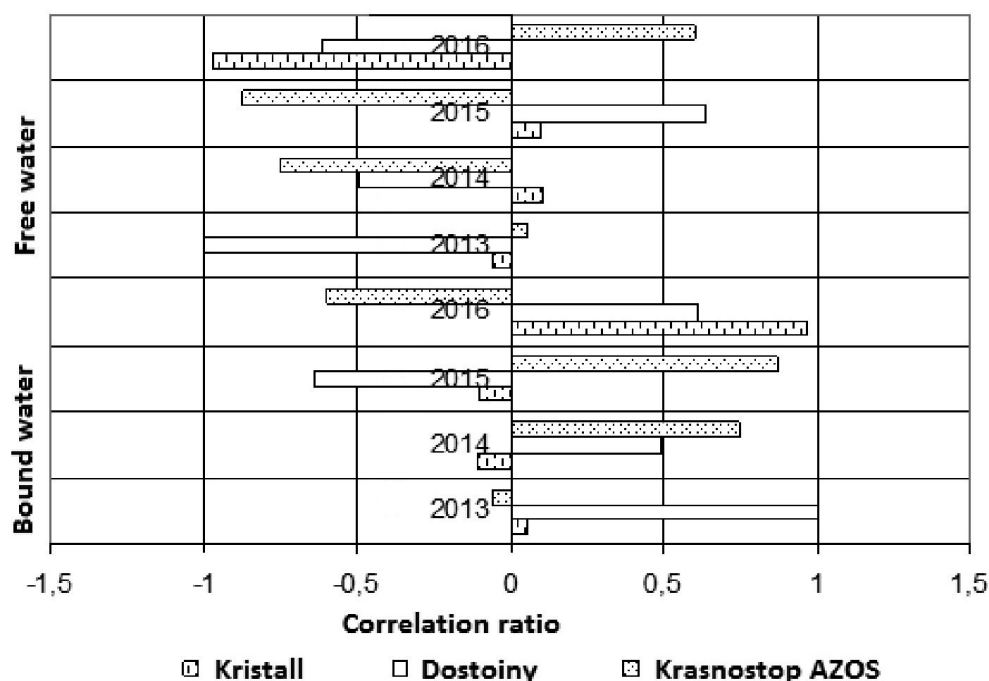


Fig. 6. Dependence of the content of bound and free water from the content of sucrose in grape leaves during the vegetation period 2013–2016

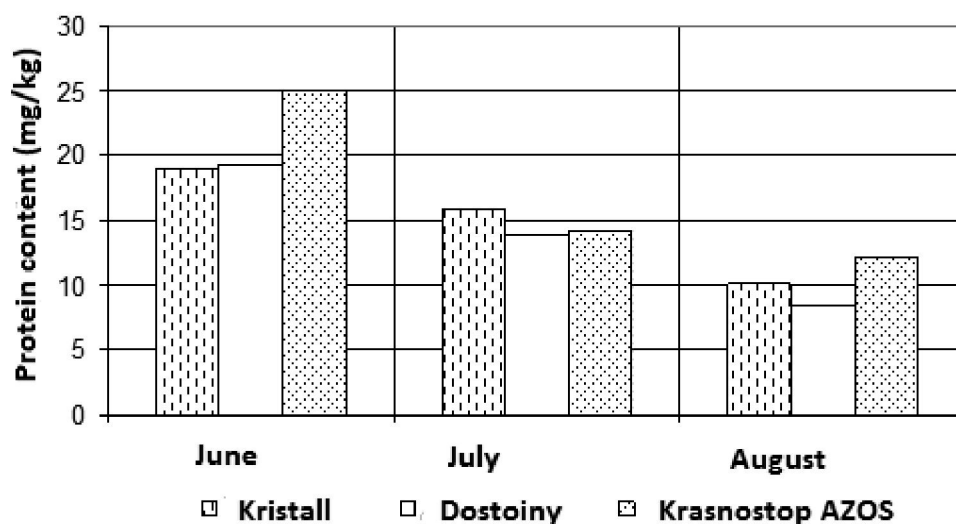


Fig. 7. Dynamics of protein content in grape leaves during the vegetation period 2016

The decrease of protein content in leaves of the studied grape varieties in August is conditioned by its more active decay as a result of activation of metabolic processes.

It is known that stresses provoke the emergence of free radicals and singlet oxygen, what leads to development of destructive effects. The more intensive oxidation-reduction processes in plant cells, the more resistant is the variety to the influence of stress factors. This is also evidenced by the increase of organic acids of Krebs cycle. Increase in the content of free organic acids in grape leaves under the conditions of drought in 2015 and 2016 denotes the activation of breathing and, thus, metabolic processes, what may be connected with

response of the studied varieties to high temperature stress and low moisture availability (fig. 8).

Drought has a negative impact on photosynthesis. One of the indicators of photosynthetic activity is pigment content in leaves.

In August 2015 and in July 2016, as compared to 2014, we noted the increase of chlorophyll content (a + b) in leaves of the studied varieties, what is consistent with high content of carotinoids that protect chlorophyll from destruction, especially in the variety *Dostoiny*, what allows to assume that there are different manifestation effects of their protective properties with regard to chlorophyll in varieties of different origin (fig. 9, 10).

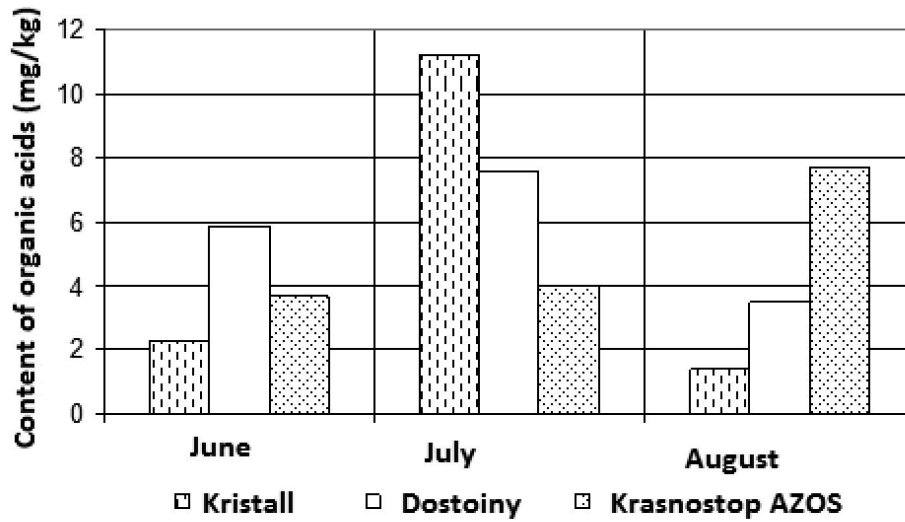


Fig. 8. Dynamics of organic acid content in grape leaves during the vegetation period 2016

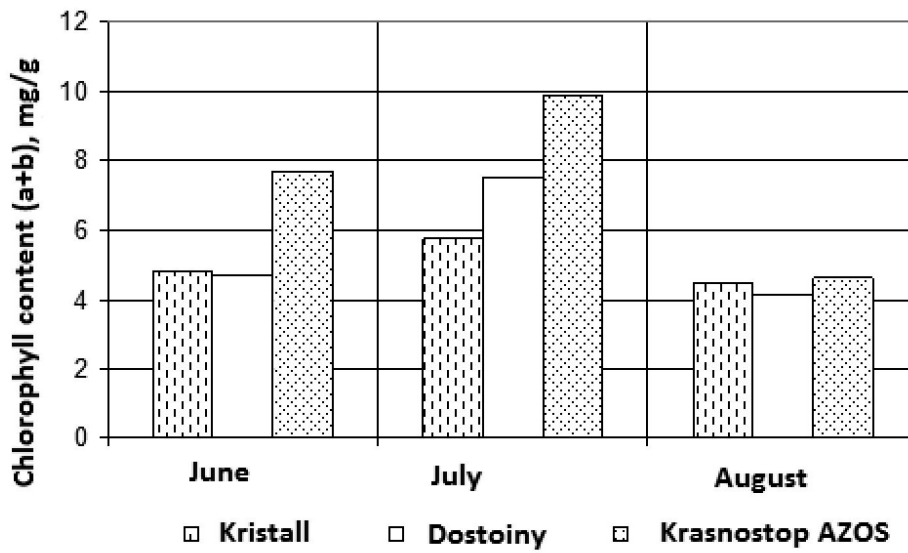


Fig. 9. Dynamics of chlorophyll content (a+b) in grape leaves during vegetation period

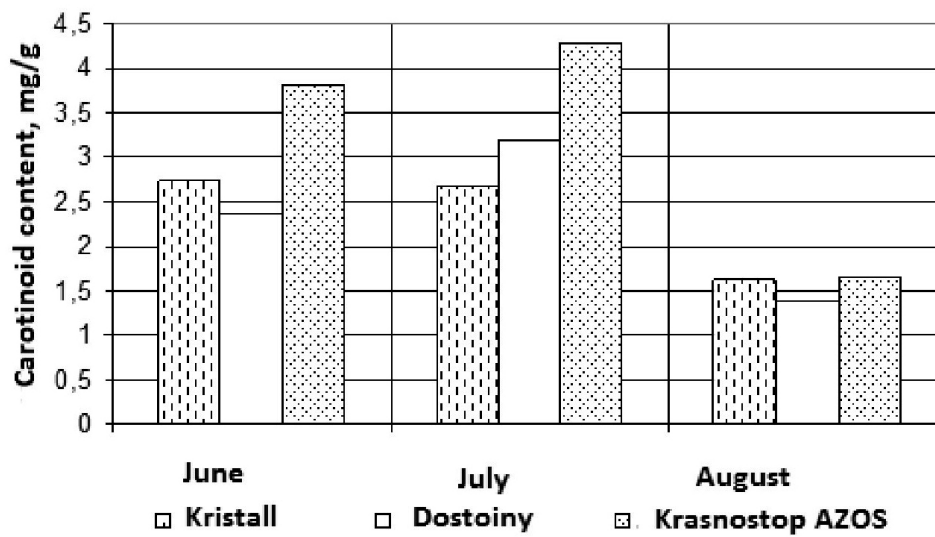


Fig. 10. Dynamics of carotene content in grape leaves during the vegetation period 2016

Heat resistance of grapes was estimated by such indicator as membrane damage coefficient.

In July 2016 as compared to June, the studied varieties demonstrated the increase of membrane damage coefficient in the case of high temperature stress in model experiment, what indicates the decrease of heat resistance (fig. 11).

Heat resistance of the studied grape varieties was higher in June and August 2016 than in July. In July and August, heat resistance of the variety *Dostoiny* was higher than heat resistance of the varieties *Kristall* and *Krasnostop AZOS*. In August the varieties *Dostoiny* and

Kristall demonstrated the increase of resistance of cell membranes to destruction, caused by the influence of drought and heat.

Resistance of cell membranes to destruction is influenced considerably by phenolcarmonic and ascorbic acids that protect membrane lipids from destruction. It was established that ascorbic acid content in the leaves of the grape varieties of European-American origin has a greater influence on the resistance of cell membranes to destruction under the influence of high temperature, as compared to *Kristall* variety of European-Amur-American origin (fig. 12).

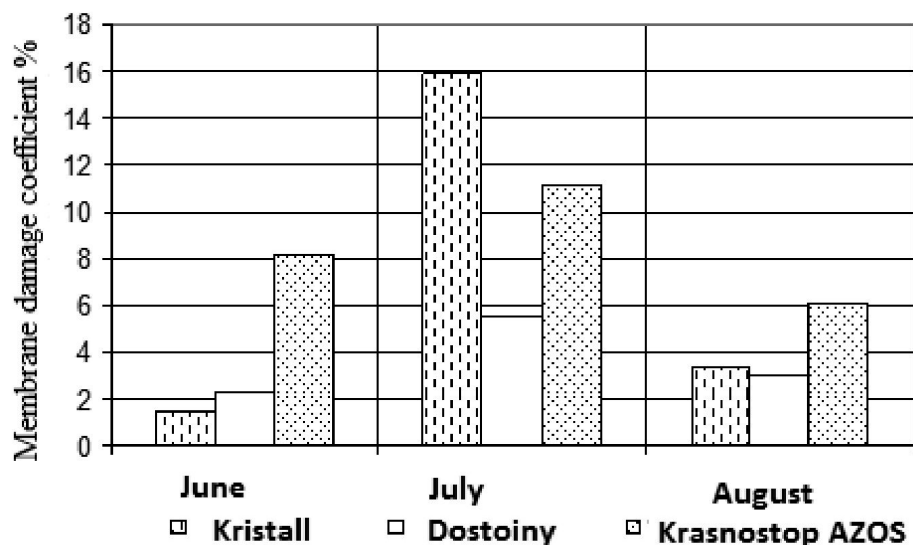


Fig. 11. Heat resistance of grape varieties in summer season 2016

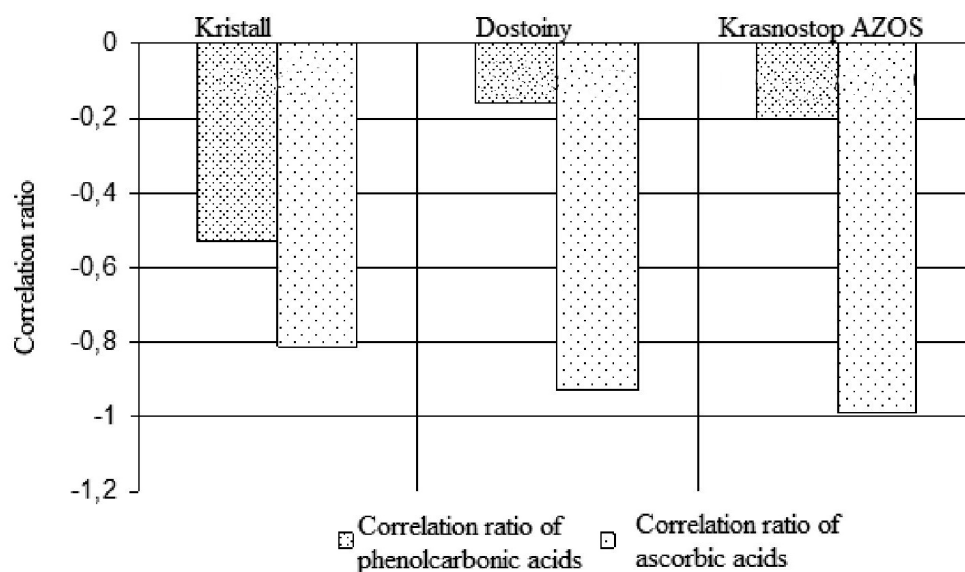


Fig. 12. Dependence of membrane damage coefficient from the content of phenolcarmonic and ascorbic acids in grape leaves during the summer season 2016

Phenolcarmonic acid content (chlorogenic and caffeic acids) has a greater influence on heat resistance of *Kristall* variety than on heat resistance of varieties *Dostoiny* and *Krasnostop AZOS*.

Therefore, the studied varieties adapt to drought in different ways.

This allowed us to conclude that mechanisms of resistance to low moisture availability in the studied

varieties during adaptation change specifically and are conditioned by their genetic potential.

This fact evidences a high degree of adaptation of the studied interspecies hybrids to hydrothermal conditions of the growth area.

In terms of anatomic and morphological indicators, in June 2016 the most evident signs of xeromorphic structure of lamina were observed in the varieties *Dostoiny* and *Kristall*, and in July — in the variety *Dostoiny* (table 1, 2).

Table 1. – Biometric parameters of lamina of grape varieties of different ecological and geographical origin (2.06.16)

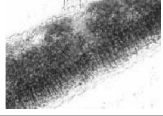

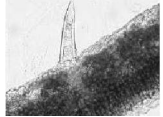
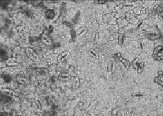
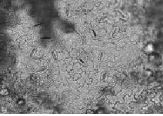
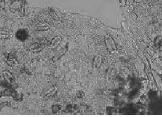
Variety	Thickness of lamina	Thickness of palisade layer	Thickness of spongy layer	Thickness of upper epidermis	Palisadness index	Micro-photo of lamina cross-section
Dostoiny	125.3	61.8	53.1	10.4	1.16	
Krasnostop AZOS	141.4	64.7	65.7	11.0	0.98	
Kristall	135.4	66.2	58.4	10.8	1.13	

Table 2. — Biometric parameters of stomatal apparatus of grape varieties of different ecological and geographical origin (2.06.16)

Variety	Parameters of stomatal apparatus, standard units			Micro-photo of stomatal apparatus
	Length	Depth	quantity, piece/mm ²	
	of stomatal guard cells			
Dostoiny	25.8	17.2	196	
Krasnostop AZOS	29.7	14.9	205	
Kristall	30.3	15.5	202	

In these varieties we noted the greatest development of palisade parenchymal layer, as compared to spongy layer, more intense development of upper epidermal cells with cuticle, more stomas per unit of lamina surface, smaller linear sizes of stomatal guard cells, what represents the signs of xeromorphic structure and causes resistance of plants to drought.

Conclusions

As result of the studies we determined physiological and biochemical criteria that characterize resistance of the studied grape varieties to high temperature and low moisture availability in summer seasons 2014–2016 in Anapa-Taman zone. We revealed biochemical and anatomical-

morphological specific features of adaptation of grape plants of different ecological and geographical origin to high temperature stresses. We determined correlation dependence of plant moisture status from hydrothermal conditions of summer season. We determined the influence of content of osmoprotectors (sucrose, proline), plastic substances (protein), organic and phenolcarboxylic acids, pigment complex (chlorophyll (a + b), carotene) on the resistance of grape plants to water and high temperature stresses. This allowed us to assume that there is a difference between mechanisms of biochemical protection of grape varieties of different ecological and geographical origin against abiotic stresses during summer season.

References:

1. Алехина Н. Д. Физиология растений: учебник для студ. вузов/Н. Д., Алехина, Ю.В. Балконин, В. Ф. Гавриленко [и др.]; под ред. И. П. Ермакова. – М., 2005. – 640 с.
2. Петров В. С. Селекционно-технологические методы повышения стрессоустойчивости винограда/ В. С. Петров, И. А., Ильина Т. А. Нудьга, М. А. Сундырева//Методы и способы повышения стрессоустойчивости плодовых культур и винограда: сб. науч. тр. – Краснодар, 2009. – С. 144–156.
3. Yordanov I. Plant responses to drought and stress tolerance/I. Yordanov, V. Velikova, T. Tsonev: Environmental Stress and Sustainable Agriculture «ESSA»: proceedings of the European Workshop (Varna. 7–12 Sept., 2002)//Bulg. J. Plant Physiol, Spec. Issue. – 2003. – V. XXIX, No 3–4. – P. 187–206.
4. Ильина И. А. Физиологические и биохимические изменения технических сортов винограда в весенне-летний период/И. А. Ильина, В. С. Петров, Н. И. Ненько, В. В. Кудряшова, Н. М. Запорожец, Т. А. Схалыхо//Виноделие и виноградарство. – 2009. – № 5. – С. 20–22.
5. Sauerborn J. Site productivity, the key to crop productivity/J. Sauerborn//J. Agron. and Crop Sci. – 2002. – 188, № 6. – С. 363–367.
6. Kishor Kavi P. B. Regulation of proline biosynthesis, degradation, uptake and transport in higher plants: its implications in plant growth and abiotic stress tolerance/P. B. Kavi Kishor, S. Sangam, R. N. Amrutha, P. SriLaxmi [et. al.]//Curr. Sci. – 2005 – Vol. 88, № 3. – P. 424–438.
7. Kaldenhoff R. Aquaporins and plant water balance/R. Kaldenhoff, M. Ribas-Carbo, Sans J. Flexas, C. Lovisolo [et. al.]//Plant, Cell & Environment. – 2008. – Vol. 31. – P. 658–666.
8. Ненько Н. И. Сопряженная устойчивость сортов винограда к абиотическим стрессорам летнего периода/Н. И. Ненько, И. А. Ильина, В. С. Петров, Г. К. Киселева, М. А. Сундырева, Т. В. Схалыхо//Европейска наука XXI век – 2014: матеріалы X Міжнародowej naukowo-praktycznej konferencji (07–15 maja 2014 roku). Vol. 28. – Rolnictwo Weterynaria: Przemysł. Nauka i studia. – S. 20–40.
9. Воробьев Н. В. Определение содержания сахарозы, фруктозы и глюкозы в растительных тканях с помощью антронового реактива/Н. В. Воробьев//Бюллетень НТИ ВНИИ риса. – Краснодар, 1985. – Вып. 33. – С. 11–13.
10. Захарова М. В. Методика определения массовой концентрации винной, яблочной, янтарной, лимонной кислот с применением капиллярного электрофореза/М. В. Захарова, И. А. Ильина, Г. К. Киселева, Г. В. Лифарь, Ю. Ф. Якуба//Методическое и аналитическое обеспечение исследований по садоводству: сб. науч. тр. – Краснодар: ГНУ СКЗНИИСиВ, 2010. – С. 283–288.
11. Захарова М. В. Методика определения массовой концентрации аскорбиновой, хлорогеновой и кофейной кислот с применением капиллярного электрофореза/М. В. Захарова, И. А. Ильина, Г. К. Киселева, Г. В. Лифарь, Ю. Ф. Якуба//Методическое и аналитическое обеспечение исследований по садоводству: сб. науч. тр. – Краснодар: ГНУ СКЗНИИСиВ, 2010. – С. 279–283.
12. Якуба Ю. Ф. Способ определения индолилуксусной кислоты методом капиллярного электрофореза/Ю. Ф. Якуба, Н. И. Ненько, Е. К. Яблонская, В. В. Шестакова, М. А. Сундырева//Пат. 2517219 Российская Федерация, МПК G01N 33/15 (2006.01), G01N 27/26 (2006.01). заявитель и патентообладатель ГНУ СКЗНИИСиВ. – № 2012145879/15; заявл. 26.10.12; опубл. 27.05.14, Бюл. № 15. – 7 с.
13. Киселева Г. К. Анатомо-морфологическая оценка адаптивного потенциала сортов плодовых культур и винограда/Г. К. Киселева//Современные методологические аспекты организации селекционного процесса в садоводстве и виноградарстве. – Краснодар: СКЗНИИСиВ, 2012. – С. 199–205.

Sukhov Evgeny Evgenyevich,
 Doctor of Geology and Mineralogy,
 Kazan Federal University, Kazan City
 E-mail: evgeny.sukhov@yandex.ru

Kungurian foraminifera of Starostinskaya suite of Spitsbergen Island

Abstract: The article presents new data on Kungurian foraminifera of Spitsbergen island. As a result of the researches, two foraminiferal complexes were detected in Starostinskaya suite of Kungurian stage, which concur with layers *Nodosaria longa* and *Gerkeina komiensis*, previously identified by G. P. Sosipatrova [1]. The first complex relates to Lower Kungurian deposits and the second complex — to Upper Kungurian deposits. In both complexes we discovered foraminifera, found in the stratotypical sections, what increases reliability of the results. The detected complexes are widely spread and observed on the whole territory of Bjarmaland.

Keywords: Bjarmaland, Spitsbergen, Permian system, Starostinskaya suite, Kungurian stage, Foraminifera, province.

Introduction

Palaeo-biogeographical Bjarmaland includes extensive sea basins, which during Permian period covered the territories of Greenland, Spitsbergen, Canadian Arctic archipelago and the adjoining water areas and also the northern part of Alaska, the north-east of Asia, Trans-Baikal, Mongolia. Exactly the water area of Spitsbergen is most interesting, which is located in the propagation center of Permian deposits and is meant to be a unique connecting link between the water basins of the North America, Eastern-European and Taymyr-Kolyma sub-regions.

Due to its geographical position, Spitsbergen province is the least explored region of Bjarmaland. Small foraminifera on the Spitsbergen Island have not been practically studied, and until now the studies of G. P. Sosipatrova are considered to be the most significant [1]. The current materials supplement the stratigraphic and paleontological picture of Permian sections of the Spitsbergen Island.

Rock materials were collected in the stratotypical region (Western Spitsbergen) at the bottom and in the middle part of Starostinskaya Suite.

Permian deposits, which are widespread almost on the whole island, represent a considerable interest because of continuity of the sections, which were formed due to the calcareous sedimentation.

Results. Foraminiferal complexes of Kungurian stage

The Carboniferous and Permian sedimentary deposits of Spitsbergen Island according to these foraminifera are divided into I–XII complexes, which are named on the basis of the most characteristic forms. The intervals from VIII to XII complexes fall on the formation of Permian system.

The sections of Spitsbergen Island belong to the lower boreal basins of Eastern-European platform and Ural, and as opposed to the neighboring provinces of Bjarmaland there were other conditions of sedimentation on Spitsbergen island, and its sections are composed of black thick-layer argillaceous-siliceous and calcareous-siliceous rocks, while in Pechora and Novozemelskaya provinces — they are composed mainly of argillites and aleurolites.

1. Foraminifera were detected in complexes X (layers with *Nodosaria longa*) and XI (layers with *Gerkeina komiensis*).

The layers with *Nodosaria longa*, which were detected in spiriferous limestone, fall to the bottom of Starostinskaya suite. This oryctocoenosis is represented mainly by agglutinated shells *Saccammina arctica* Gerke (family Psammosphaeridae); *Hyperammina borealis* Gerke, *Kechenotiske aff. hadzeli* (Crespin) (family Hyperamminidae); *Ammodiscus semiconstrictus* Cush. et Wat., *Turritella* sp. nov. (family Ammodiscidae); *G. shikhanensis* Moroz., *Globivalvulina ex gr. shikhanensis* Moroz., *G. orbiculata* Zol. (family Biseriamminidae); *Orthovertella eximia* Suchov (family Pseudocornuspiridae). Calcareous forms are of secondary importance, in particular the forms from the family *Nodosariidae*, which includes the genera *Protonodosaria* and *Nodosaria*, and the following species: *Protonodosaria proceriformis* (Gerke), *Nodosaria krotowi* Tscherd., *N. longa* Moroz., *N. pseudoincelebrata* Sossip.

Dc.le zfgbcfnm Saccammina arctica Gerke, *Hyperammina borealis* Gerke are determinants among the agglutinated species. The species *Dc.le zfgbcfnm Saccammina arctica* Gerke is extremely widespread in Bjarmaland and found almost everywhere in all Permian deposits

(see table 1). Especially significant large agglomerates are observed in postartinsky formations of the northern Siberia [2]: in Nordviksky region, in the upper part of Tustakhskaya suite; in Ilyino-Kozhevnikovo area “in the horizon of sandy foraminifera” and “in the horizon of large *sakkammins*”; large quantity of this species was detected in the lower reaches of the Lena river on the West wing of Bulkurskaya anticline, “in the horizon of sandy foraminifera”. The complex is also extremely widespread in Eastern-European sub-region, for example in the north of Pechora basin — in Rudnitskaya sub-suite (package “Na”); on the Kozhim river in Kozhimrudnitskaya suite (foraminiferal zone *Nodosaria monile*) [3]; in Abzalskaya suite of Kungurian stage of Aktyubinsky Cisurals.

The species *Hyperammina borealis* Gerke is very popular in the Permian deposits of Bjarmaland [4; 5]. Massive concentrations are observed in Central Siberia: in the sections of Lower Kozhevnikovskaya Suite of Nordvik, Ilyino-Kozhevnikovo area, in some parts — in Tyagino-Anabarskaya anticline. In Taymyr it was found in Kungurian stage of Sokolinskaya Suite. The species *Hyperammina borealis* Gerke was detected on the whole territory of Eastern-European sub-region. For example, in Pechora province in the north of Chernyshev ridge, in the sections of Adzva river and Nelyn-Shor brook; in Padimey Taryuskaya anticline in the well BK-21, depth 1 440–1 260 m. (Kungurian stage, Talatinskaya suite); in Aktyubinsky Cisurals, in rivers Syntas, Borlya, Sogchursay, Kungurian stage, Abzalskaya suite.

The species *Hyperammina borealis* Gerke and *Dc.le zfgbcfnm Saccammina arctica* Gerke are found both separately and together. If *Hyperammina borealis* Gerke forms massive agglomerates, except for *Dc.le zfgbcfnm Saccammina arctica* Gerke, then the deposits are of Artinskian age. If there is only *Saccammina arctica* Gerke, which is found in large quantity, then it points most probably at the Ufimian age. If the complex is mixed, as in this case, then it attests its Kungurian age, and namely Filippovsky horizon.

In the layers with *Nodosaria longa* we detected a considerable complex of *Globivalvulin*, among which there are species *Globivalvulina shikhanensis* Moroz., *G. ex gr. shikhanensis* Moroz, typical for lower Kungurian deposits, *G. orbiculata* Zol., obtained in Filippovsky horizon of the stratotypical region and found in the north of Pechora province in the same deposits.

In the complex there are also club-shaped forms, including the species *Orthovertella eximia* Suchov, which is principal for Filippovsky horizon of Kungurian stage. The species was found in Pechora province on Chernyshev ridge at the foot of Kozhimskaya suite (Filippovsky








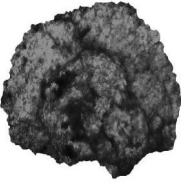



horizon), as well as in Kosyu-Rogovskaya and Korotai-khinskaya depressions in the lower part of Talatinskaya suite (Filippovsky horizon).

The species *Ammodiscus semiconstrictus* Cush. et Wat. is transit, it comes from the middle Carbonic period of Texas, in the lower Permian system of Bjarmaland it is uncommon, in the middle Permian — it is rare. The layers with *Nodosaria longa* acquire archaic shade due to the genus *Protonodosaria* (which was found on the whole territory of Bjarmaland), in particular, the species *Protonodosaria proceriformis* (Gerke), which is more typical for Artinskian deposits, where it can form large clusters, in Kungurian deposits — it is less common. The genus *Nodosaria* is represented by rejuvenescent species. The species *Nodosaria krotowi* Tscherd was found for the first time in Kazanian deposits. The species was observed in all Bjarmaland: in Talatinskaya suite of Pechora province, in Kungurian deposits in Novaya Zemlya, in the Eastern Taymyr in the upper part of Baykursky horizon, in the horizon of various foraminifera in Pur-Oleneksky area of Oleneksky region. The species *Nodosaria pseudoincelebrata* Sossip was obtained in Kungurian stage of the Permian Cisurals, it was found almost in all Kungurian deposits of the Eastern-European sub-region, especially large concentrations were observed in stratotypical area of Filippovsky horizon and in Talatinskaya suite of Pechora province. The species *Nodosaria longa* Moroz is also a principal species for Kungurian deposits and it is widespread in the north of the Eastern-European platform.

Due to the predominant number of lower Kungurian species, including species from the stratotypical area of Filippovsky horizon, the complex X (layers with *Nodosaria longa*) should be attributed to Filippovsky horizon.

2. Oryctocoenosis of the complex XI (the layers with *Gerkeine komiensis*) is of the greatest interest, due to the representative material and absolute preservation. Paleobiocoenosis, isolated from light gray siliceous limestone, is represented by calcareous and agglutinated shells and has about three dozen species. It consists of the orders *Astrorhizida* (family *Psammospaeridae*), *Hyperamminida* (families *Hyperamminidae*, *Hippocrepinidae*), *Earlandita* (family *Earlandiidae*), *Ammodiscida* (families *Ammodiscidae*, *Tolypamminidae*, *Pseudolituotubidae*), *Endothyrida* (family *Endothyridae*), *Ataxophragmiida* (family *Globivalvulina*), *Cornuspirida* (family *Pseudocornuspiridae*) *Nodosariida* (family *Nodosariidae*), as well as the genera: *Saccammina*, *Hyperammina*, *Hyperamminoides*, *Erlandia*, *Glomospira*, *Ammovertella*, *Tolypammina*, *Palaeonubecularia*, *Endothyra*, *Endothyranella*, *Orthovertella*, *Nodosaria*, *Rectoglandulina*, *Geinetzina*.

Table 1

№	Explanation of the table	Fig. (Extension × 80)	№	Explanation of the table	Fig. (Extension × 80)
1	Nodosaria psedoincelebratd Sossip., Kungurian stage, Filippovsky horizon; thin section.		7	Hemigordius glomospiridalis Sossip., Kungurian stage, Irensky horizon; thin section.	
			8	Geinitzina foliata Zolot., Kungurian stage, Irensky horizon; thin section.	
2	Hyperamminoides proteus (Cushm. et Waters), Kungurian stage, Filippovsky horizon; thin section.		9	Orthovertella flexuosa Suchov, Kungurian stage, Irensky horizon; thin section.	
3	Nodosaria longa Moroz., Kungurian stage, Filippovsky horizon; thin section.		10	Glomospira compressiformis Igonin, Kungurian stage, Irensky horizon; thin section.	
4	Pseudonodosaria starostinaensis Sossip., Kungurian stage, Irensky horizon; thin section.				
5	Ichtyolaria partilulata Zolot., Kungurian stage, Irensky horizon; thin section.		11	Saccamina arctica Gerke, Kungurian stage, Filippovsky horizon; thin section.	
6	Geinitzina chussovensis Raus., Kungurian stage, Irensky horizon; thin section.				

From the unilocular species in paleobiocoenosis we discovered a rare archaic form *Erlandia minuta* (Cushman et Waters), attributed to the Cisurals, and also *Delella zfgbcfnm Saccammina arctica* Gerke and *Hyperamminoides ex gr. elegans* (Cushman et Waters), which were found in all Bjarmaland. For example, in Taymyr-Kolyma sub-region the species is observed in Nordviksky area “in the horizon of sandy foraminifera” in Oleneksky area “in the horizon of various foraminifera”; in the lower reaches of the Lena river (the western wing of Bulkurskaya anticline) it was observed much below the horizon of sandy foraminifera. In the Eastern-European sub-region, in particular in Pechora province, this species was found on Chernyshev ridge in the confining layer of Artinskian deposits; in Korotaihinskaya depression in Talatinskaya suite in Kungurian deposits. The species *Hyperamminoides ex gr. elegans* (Cushman et Waters) is transit; and in Bjarmaland it is found from the Artinskian to Ufimian deposits. However, it was found seldom in Artinskian deposits, while during Kungurian age it formed numerous complexes. The genus *Hyperamminoides proteus* (Cushman et Waters) is also widespread in Bjarmaland and confined to the Lower Permian period.

Foraminiferal complex of the layers with *Gerkeina komiensis* includes a significant amount of club-shaped forms, among which there is *Glomospira compressiformis Igon.*, which is observed mainly in Pechora province and the northern Bashkiria in the deposits of Kungurian stage of Irensky horizon. The species *Orthovertella verchojanica* Sossipat is quite widespread in Bjarmaland; it is transit and common from Artinskian till Ufimian ages. But the species experienced the greatest prosperity at the boundary of Kungurian and Ufimian stages. *Palaeonubecularia uniserialis Reitlinger* is found in the Eastern-European platform, Southern Pritimanye, Western Cisurals, it has a wide distribution — from the middle Carbonic to Permian period. The species is also found in areas of the northern Cisurals, — the Shchugor River, Kungurian stage of Irensky horizon, Kyrtadinskaya suite.

The complex of Nodosariids is fairly representative, among which there are the species *Nodosaria*, *Rectoglandulina*, *Geinetzina*. The species *Nodosaria ustritskyi* Sossip is typical in a greater degree for Taymyr-Kolyma sub-region, where it is a rejuvenescent element. For example, it was discovered in Dzhigdalinsky horizon; in the eastern Taymyr in Baykurskaya suite of Tsvetochinsky horizon; in the Eastern-European sub-region the species was found in Denisovsko-Moreyuskaya zone (Malozemelskaya monocline) in the Upper Telvisskaya sub-suite, (Upper Kazanian sub-stage);

in Novozemelskaya province (Southern Novozemelsky anticlinorium) it was found in the upper part of the Sokolovskaya suite (Ufimian stage). The species *Nodosaria cassiaformis Igonin* was detected in Abzalskaya suite of Aktyubinsky Cisurals. However, it is also widespread in other regions of Eastern-European sub-region; for example, it is common in numerous sections of the upper part of Kozhimskaya suite of Pechora province, attributable to the Upper Kungurian deposits. The genus *Ichtyolaria* has a decisive importance in determination of age. The species *Ichtyolaria semiovalis* Zol. and *Ichtyolaria partita* Zol. were detected in the stratotypical area; they are principal species of Irensky horizon. The species *Gerkeina komiensis Grozd. et Lebed.* was detected for the first time in Lower Kachgortskaya sub-suite of stratigraphic well “Naryan-Mar” and was attributed to Upper Kungurian stage.

In the complex XI we found about 10 species of foraminifera, identified in the deposits of Irensky horizon of the Permian Cisurals, and its analogs; moreover, there are several species, which undoubtedly have upper Kungurian age; therefore, we can conclude that the middle part of Starostinskaya suite should be attributed to the upper Kungurian deposits.

Discussion

The age of Starostinskaya suite (Kapp Starostin formation) is also controversial up to the present time. Chernyshev F. N. [6] attributed the deposits of Starostinskaya suite to Artinskian stage, D. L. Stepanov [7] — to the united Kungurian-Ufimian stage, V. I. Ustritsky — to Ufimian stage [8], and Japanese experts, who worked on Spitsbergen island [9; 10], attributed the lower part of Starostinskaya Suite to Kazanian stage. Grunt T. A. attributes the lower part of Starostinskaya Suite to Kazanian stage too [11].

Conclusions

1. According to the research results we detected 2 foraminiferal complexes, belonging to the layers with *Nodosaria longa* and the layers with *Gerkeina komiensis*. Foraminifera, detected in complexes X (layers with *Nodosaria longa*) and XI (layers with *Gerkeina komiensis*), have stratigraphic significance and belong to Philippovsky and Irensky horizons of Kungurian stage, respectively.

2. The layers with *Nodosaria longa* and the layers with *Gerkeina komiensis* of Taymyr province are fully independent; they have fauna, which is significantly different from the adjacent paleogeographic areas. However, according to taxonomic composition the Taymyr complex is similar to paleocomplex of foraminifera of

Novozemelskaya and Pechora provinces. We should conclude that during all Kungurian age the water areas of Taymyr province had a stable relationship with the Pre-Ural foredeep, which were occupied by sea basins, in which there was an intense *faunal* exchange.

3. We detected a wide stratigraphic distribution of some principal species, which were found almost in all Bjarmaland. For example, among the agglutinated foraminifera we know *Hyperammina borealis* Gerke, *Dicellograptus* *Saccammina arctica* Gerke, *Orthovertella ver-*

chojanica Sossipat., and among the calcareous foraminifera — *Nodosaria cassiaformis* Igonin, *Ichtyolaria semi-ovalis* Zol. and *Ichtyolaria partita* Zol.

4. Complexes of foraminiferal layers with *Nodosaria longa* and layers with *Gerkeina komiensis*, which were detected in Starostinskaya suite, correspond to the final development stage of foraminifera of Permian system of Spitsbergen province, as evidenced by the highly organized Nodosariids, such as *Nodosaria*, *Rectoglandulina*, *Ichtyolaria*.

References:

1. Сосипатрова Г.П. Верхнепалеозойские фораминиферы Шпицбергена//Материалы по стратиграфии Шпицбергена. – Л.: Из-во НИИГА, 1967. – С. 94–120.
2. Герке А.А. Фрондикулярии из пермских, триасовых и лейасовых отложений Севера Центральной Сибири//Сб. статей по палеонтологии и биостратиграфии. – Л.: Тр. НИИГА, 1961. – Т. 127. – С. 97–174.
3. Сухов Е.Е. Пермские мелкие фораминиферы Биармийской палеобиогеографической области. – Казань: Изд-во Казан. ун-та, 2003. – 320 с.
4. Сухов Е.Е. Пермские фораминиферы Биармийской области. – Deutschland, Saarbrücken: Verlag LAR LAMBERT Academic Publishing, 2013. – 454 s.
5. Сухов Е.Е. Биполярность пермских фораминифер. – Deutschland, Saarbrücken: Verlag LAR LAMBERT Academic Publishing, 2014. – 161 s.
6. Чернышев Ф.Н. Верхнекаменноугольные брахиоподы Урала и Тимана. – С.-Пб: Тр. Геол. ком. 1902. – Т. 16, № 2, вып. 1/2. – 749 с.
7. Степанов Д.Л. О новом ярусе пермской системы в Арктике//Вест. ЛГУ. Сер. Геол. и географ. – Л.: Из-во ЛГУ, 1957. – Вып. 4, № 24. – С. 20–24.
8. Устрицкий В.И. Биостратиграфия верхнего палеозоя Арктики. – Л.: Изд-во НИИГА, 1971. – 280 с.
9. Nakamura K., Kimura G., Winsnes Th. Brachiopod zonation and age of the Permian Kapp Starostin Formation (Central Spitsbergen)//Polar Research. – 1989. – V. 5, № 9. – P. 207–219.
10. Nakamura K., Kimura G., Winsnes Th. Permian brachiopods of the Kapp Starostin//Investigations of the Upper Carboniferous – Upper Permian Succession of Western Spitsbergen 1989–1991. Hokkaido University. – Sapporo, 1992. – P. 77–95.
11. Грунт Т.А. Биостратиграфия и биогеография Западной Арктики в середине пермского периода//XVI Геологический съезд Коми. Стратиграфия и палеонтология. – Сыктывкар: Из-во ИГ Коми НЦ УрО РАН, 2014. – С. 149–151.

Sukhov Evgeny Evgenyevich,
 Doctor of Geology and Mineralogy, Kazan Federal University
 E-mail: evgeny.sukhov@yandex.ru

Permian foraminifera of parastratotype of the river Usolka

Abstract: The article presents information on detection of significant complexes of small foraminifera in the interval between Asselian and Artinskian stages. According to the results of the study, three layers with foraminifera were detected. The first layer with *Nodosaria shikhanica* falls on the lower part of Shikhansky horizon of Asselian stage, in which there is a considerable complex of agglutinated and calcareous foraminifera. The second layer with *Hyperammina borealis*, which is represented by several tens of specimens, corresponds to the lower part of Tastubsky horizon of Sakmarian stage; and the third foraminiferal layer with *Kechenotiske hadzeli* was detected in the lower part of Artinskian stage of Irginsky horizon. All three foraminiferal layers had principal species, what confirms the specified age and supplements the faunistic palette of the Permian parastratotype. Moreover, the detected layers are observed in Bjarmaland, as well as in all Notalnaya area.

Keywords: Bjarmaland, Permian period, parastratotype, the river Usolka, stage, Asselian, Sakmarian, Artinskian, foraminifera, species, complex.

Introduction

The geological section of the river Usolka is located on the territory of Gafuriysky area and confined to the southern part of Pre-Ural foredeep, which is bordered from the east by the Russian platform. The section is a parastratotype of the boundary between Carboniferous and Permian systems, and also it serves as an additional benchmark of lower boundary of Sakmarian stage of Pre-Ural series of Lower Permian age, included in the International stratigraphic scale. The section is represented mostly by Asselian, Sakmarian and Artinskian deposits. In the interval between Asselian and Artinskian stages, an impressive complex of small foraminifera was discovered for the first time, which numbered hundreds of specimens and tens of species with agglutinated and calcareous composition.

Results. Layers with foraminifera

The section of the river Usolka uncovers a carbonate-argillaceous layer of Asselian, Sakmarian and Artinskian deposits. Continuity of the section is evidenced by present fusulinids, ammonoidea and also by the analysis of conodont complexes [1].

Paleobiocoenosis of foraminifera includes 5 orders: *Astrorhizida* (family *Psammospaeridae*), *Hyperamminida* (families *Hyperamminidae*, *Hippocrepinidae*), *Ammodiscida* (families *Ammodiscidae*, *Tolypamminidae*, *Calcivertellidae*), *Endothyrida* (family *Endothyridae*), *Nodosariida* (family *Nodosariidae*), and also ten genera: *Saccammina*, *Hyperammina*, *Kechenotiske*, *Hyperamminoides*, *Turritellella*, *Tolypammina*, *Trepeilopsis*, *Endothyra*, *Protonodosaria*, *Nodosaria*, among which there are already known species that were found in different regions of Bjarmaland

(Taymyr-Kolyma and Eastern-European sub-regions), such as *Hyperammina borealis* Gerke, *Hyperamminoides proteus* Gerke, as well as new species, for example, from the genus *Turritellella*. In the studied section we clearly identified three layers with foraminifera, which can be traced on the whole territory of Bjarmaland (see table 1).

1. The first foraminiferal complex: layers with *Nodosaria shikhanica* fall on the lower part of Shikhansky horizon of Asselian stage, which is represented by the interchange of carbonate and argillaceous rocks. The complex consists mainly of calcareous and agglutinated shells, among which there are such genera as *Hyperammina*, *Tolypammina* and also the genus *Nodosaria*, which is predominant in paleobiocoenosis (4 new species).

The complex detected in the section is comparable with paleobiocoenoses of foraminifera contained at the bottom of Sezymyskaya suite of Pechora basin [2] in Shikhansky horizon of Denisovsko-Moreyuskaya zone, in Parensky horizon of the North-East of Russia. Stratigraphic units combine several general types, including two principal species *Nodosaria shikhanica* Lip. and *Nodosaria galinae* ex. gr. Gerke et Kar. (known from Parensky horizon of the North-East of Russia, analogue of Asselian stage), what allows to make a conclusion about Asselian age of the correlative levels. The species *Tolypammina kusjapkulensis* Lipina is widespread in Asselian stage, and was detected by O.A. Lipina from the so-called "Lower Permian buried masses of Bashkiria" [3]. It may be found in the East of the Russian platform and in the Western Cisurals (at the bottom of the Lower Permian system), and also in Pechora province on Chernyshev ridge (Talatinskaya suite, Kungurian stage).

Table 1. – Characteristic species of parastratotype of the river Usolka

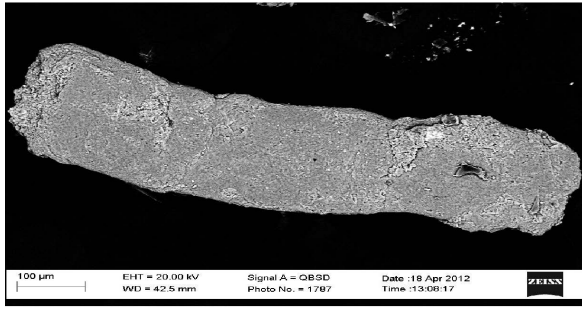


Fig. 1. *Nodosaria* sp. 1: specimen, general view; the lower part of Artinskian stage, Irginsky horizon, layers with *Kechenotiske hadzeli*

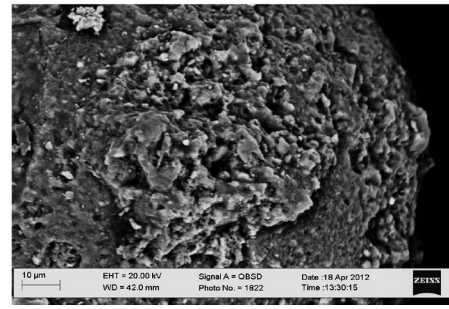


Fig. 5. *Nodosaria* sp. 2: the same specimen, lateral face of the shell, on which calcareous nodes can be observed

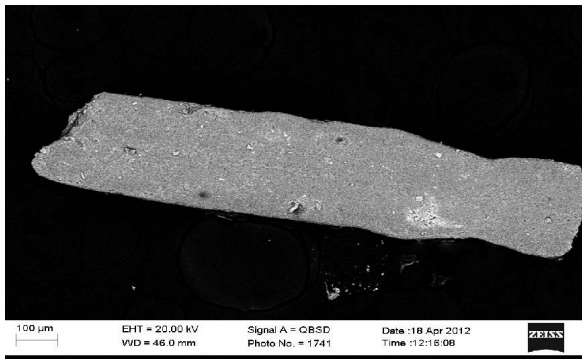


Fig. 2. *Nodosaria* sp. 1: the same specimen; middle part of the shell; the greatest number of pores is concentrated in lower areas; the system of pores presents a somewhat annual orientation

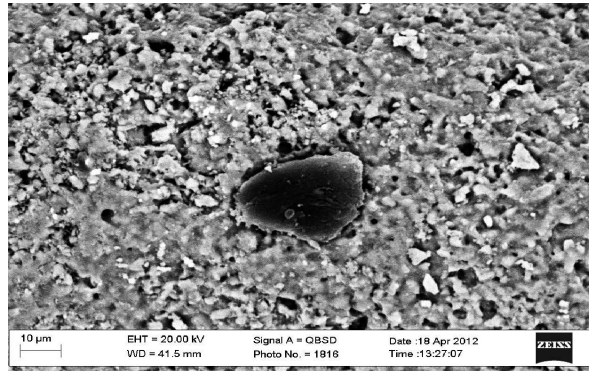


Fig. 6. *Nodosaria* sp. 2: the same specimen; initial locus with numerous calcareous formations, where a porous system of pores is distinctly seen

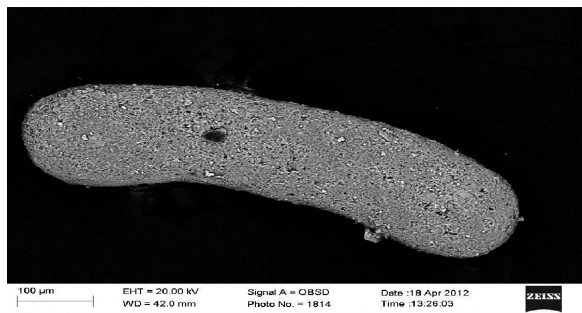


Fig. 3. *Nodosaria* sp. 2: specimen, the lower part of Artinskian stage, Irginsky horizon, layers with *Kechenotiske hadzeli*, general view

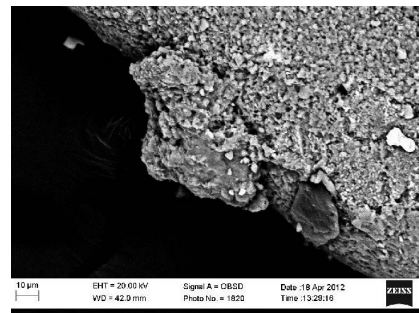


Fig. 7. *Hyperammia borealis subtilensis* Voron; general view; the lower part of Tastubsky horizon of Sakmarian stage, layers with *Hyperammia borealis* Gerke

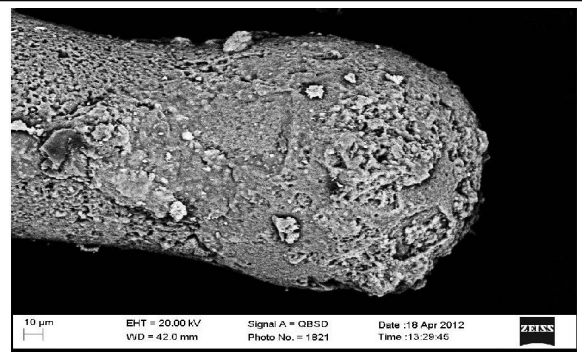


Fig. 4. *Nodosaria* sp. 2: the same specimen; terminal locus with a large amount of pores, which are concentrated in the most elevated areas

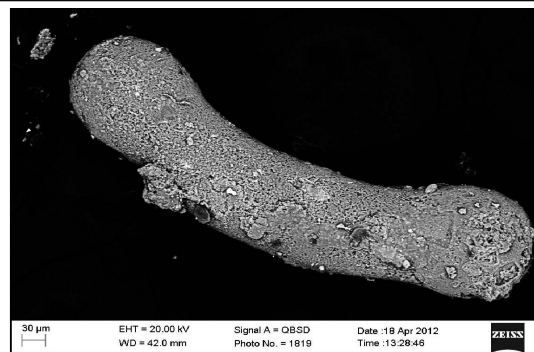


Fig. 8. *Hyperammia borealis* Gerke; general view; the lower part of Tastubsky horizon of Sakmarian stage, layers with *Hyperammia borealis*

Due to the predominant amount of Asselian species, including principal species, the layers with *Nodosaria shikhanica* fully correspond to Asselian stage.

2. The second foraminiferal complex: the layers with *Hyperammina borealis* are represented by several tens of specimens of foraminifera, they fall on the lower part of Tastubsky horizon of Sakmarian stage, and are composed mainly of thin-layer marls. The complex numbered two species of the genus *Saccammina*, several species of the genus *Hyperammina* (including three new species), two new species of the genus *Nodosaria*, and one new species of the genera *Endothyra* and *Protodonodosaria*.

According to the composition of agglutinated forms, the obtained complex resembles "the horizon of sandy foraminifera" [4]. Characteristic species for this complex are *Saccammina ampulla* (Crespin), *Hyperammina borealis* Gerke, which are widespread in Bjarmaland; however, a significant number of *Nodosaria* allows us to make a suggestion about a younger age of the oryctocoenosis.

As for the species composition, the obtained complex is comparable with a similar complex of Nelynyashorskaya suite of Pechora province, where also there are *Saccammina ampulla* (Crespin), *Hyperammina borealis* Gerke; with the middle part of Sezysmskaya Suite (with the presence of the genus *Hyperammina borealis* Gerke), which belongs to Sakmarian age according to these fusulinids. The complex also correlates with similar types in the whole Taymyr-Kolyma sub-region, for example, in Tustakhskaya suite we found a considerable complex of agglutinated species, including general species *Hyperammina borealis* Gerke, *H. borealis subtilensis* Voron., *H. borealis delicatula* Voron.

A significant amount of species was found outside the territory of Bjarmaland. They resemble especially the foraminifera from Notalnaya area. For example, the species *Saccammina ampulla* (Crespin), which has a significant population in the layer [4], was found everywhere in Sakmarian deposits of Australia and Tasmania.

According to a significant number of agglutinated species, found exclusively in Sakmarian stage, the layers with *Hyperammina borealis* point at the Sakmarian interval.

3. The third foraminiferal complex: the layers with *Kechenotiske hadzeli* were detected in the bottom of Artinskian stage of Irginsky horizon and represented mainly by argillites. Paleobiocoenosis consists of agglutinated genera *Saccammina*, *Kechenotiske* and *Turritellella*, which numbers about two dozen shells, among which there are new species: one species of the genera *Saccammina*, *Kechenotiske* [5] and two species of the genus *Turritellella*. The obtained complex, due to the principal species *Saccammina arctica* Gerke, which appeared for the

first time in Artinskian stage, can be easily traced in the even-aged sections of the Eastern-European sub-region. This species was also found in Chernyshevskaya suite of Chernyshev ridge [6], in Kosinskaya suite of the sections of Kosyu-Rogovskaya depression, which are attributable to Artinskian stage. The genus *Kechenotiske hadzeli* (Crespin) is also widespread in Bjarmaland. It may be found in the Northern territories of Pechora province: in Belkovskaya suite of Kosyu-Rogovskaya depression and in Kosinskaya suite of Chernyshev ridge, which are attributable to Artinskian stage. This species is widely spread in Notalnaya area [7; 8]: in Australia (Queensland) and in Western Australia in Artinskian stage [9; 10].

Conclusion

1. On the basis of the collected material and further research work in parastratotype of the river Usolka in Cisurals of Permian system (Asselian, Sakmarian and Artinskian stages) we obtained three considerable complexes that are significantly different from each other in species composition. Oryctocoenosis in Asselian stage (foraminiferal layers with *Nodosaria shikhanica*) is represented mainly by agglutinated unilocular and club-shaped species, which supplement the ancient *Nodosariida*. Sakmarian oryctocoenosis (foraminiferal layers with *Hyperammina borealis*) is quite numerous, consists predominantly of agglutinated primitive species. However, there is a small quantity of calcareous species of the genera *Nodosaria*, *Endothyra*, and *Protodonodosaria*. The most impressive paleobiocoenosis is in Artinskian stage (foraminiferal layers with *Kechenotiske hadzeli*), which includes the species of wide planetary distribution.

2. Parastratotype of Permian system of the river Usolka, which contains Asselian, Sakmarian and Artinskian deposits, is quite promising for research of small foraminifera and for a detailed biostratigraphy. Oryctocoenoses include quite rich agglutinated and calcareous paleocomplexes. Foraminifera were found almost along the whole section, what allows us to make a suggestion about formation of more fractional stratigraphic units in para-geological units.

3. Detected foraminiferal layers in parastratotype can be traced in the whole Bjarmaland. Moreover, there is a number of species, such as *Saccammina ampulla* (Crespin), *Kechenotiske hadzeli* (Crespin), *Hyperammina subtilensis* Voron., *H. borealis delicatula* Voron, which are widespread in tropical basins of the North American platform and the north of Southern America, as well as in the water areas of Notalnaya climatic zone, what gives to the detected complexes a great importance and significant reasons for the planetary correlation.

References:

1. Черных В. В., Чувашов Б. И. Лимитотипы нижней границы сакмарского и артинских ярусов на Урале. Литосфера. № 1. – С. 35–52.
2. Сухов Е. Е. Пермские мелкие фораминиферы Биармийской палеобиогеографической области. – Казань: Изд-во Казан. гос. ун-та, 2003. – 320 с.
3. Липина О. А. Мелкие фораминиферы погребенных массивов Башкирии//Тр. ГИН АН СССР. – 1949. – Геол. серия. – Вып. 105. – С. 198–233.
4. Герке А. А. Фораминиферы пермских, триасовых и лейасовых отложений нефеносных районов севера Центральной Сибири. – Л.: Изд-во Гостоптехиздат, 1961. – 656 с.
5. Crespin J. Permian Foraminifera of Australia//Australia Bureau of Mineral Resources Bulletin. – 1958. – № 48. – P. 3–98.
6. Сухов Е. Е. Пермские фораминиферы Биармийской области. – Deutschland, Saarbrucken: Verlag LAP LAMBERT Academic Publishing, 2013. – 454 s.
7. Сухов Е. Е. Биполярность пермских фораминифер. – Deutschland, Saarbrucken: Verlag LAP LAMBERT Academic Publishing, 2014. – 161 s.
8. Sukhov E. E. Correlation of Foraminiferal Zones of Biarmia and Notal Regions//2 International Congress on Stratigraphy. STRATI 2015. 19–23. July 2015. – Graz, Austria, 2015. – P. 363.
9. Palmieri V. First record of shared species of Late Permian small foraminiferids in Australia and Russia: time correlations and plate reconstructions//Journal of Australian Geology & Geophysics. – 1994. – № 15(3). – P. 359–365.
10. Palmieri V. Foraminifera zonation in the Permian stratigraphy of the Denison Trough (Bowen Basin), Central Queensland//Strzelecki International Symposium on Permian of Eastern Tethys: Biostratigraphy, Palaeogeography and Resources. – 1998. – V. 110. № 1/2. – P. 173–195.

DOI: <http://dx.doi.org/10.20534/AJT-17-1.2-20-22>

Khuzhanazarov Uktam Eshtemirovich,

Islamov Imongali,

Sadinov Jasur Samandarovich,

Tashkent State Pedagogical University named after Nizami

Ishmuminov Bobur,

Karshi State University

E-mail: Khuzhanazarov74@mail.ru

A description of some pasture plant communities in adyr (steppe) territory of Chirakchi district in Kashkadarya basin

Abstract: In the article pasture plant cover decreasing conditions are described and seed productivity of plants is given in the researched territory of Kashkadarya region in Chirakchi district.

Keywords: pasture, cenopopulation, desertification, productivity, adyr (steppe), mesophytes, xerophytes, ephemers, ephemerooids.

Introduction

We must know, that many people have not realized the desertification and anthropogenic influence to the nature and pollution facts that there are so many endangered plants and that species of plants need to survive. Our researches belong to upper part of Kashkadarya region including of Chirakchi district, so south-west Zarafshan mountain ranges have rich biodiversity. But

last years we defined the shortening of rare, relict and medicine plants in researched territory. So we describe the adyr (steppe) plants it belongs to Otchopar and Hayitkul adyrs (mezophytes and xerophytes).

Results and discussion

The description is formed in September 25, 2016 in adyr Otchopar in Chirakchi district in Kashkadarya region. Covering of soil is about 70%. The background plant is

Carex pachystylis, amongst which Salsola collina is absently grown and we defined some other single growing plants. The whole on area 7 species were noted and from 5 species belong to group of autumn-summer plants and ephemeroids involve the 2 species. The weeds were absent. The cover is more monotonous, than ephemeral-girgensohnia pasture. Hay harvests showed, the fluctuation of gross productivity of the dry mass has from 127 till 200.5 gr./m, or at the average of 143 gr./m, that at translation on hectare it gives 14.3 centner/hectare of fodder productivity.

An analyze of hayrick	
Carex pachystylis	19.0 gram
Poa bulbosa	0.4 gram
Diartronvesiculosun	0.3 gram
Cousiniarresinosa	0.2 gram
Salsolacollina	142.9 gram
Dry herbs	13.0 gram

Comparatively high productivity given type of pasture is conditioned, as this shows the specific analysis, in big quantity of saltwort in herbage; the specific mass of last reaches 78 %; on share of well eaten plants forms only 15 %. So, at determination of the eaten part, we must take into consideration and protection measures are demanded [1].

Ephemeral-acanthophyll pasture. It occupies the most lowering west part of the adyr Otchopar. The area was described in September 25, 2016. The vegetation was dried, Cousinia is torn off wind and piles up with the heap in western area and besides of natural barriers. Acanthophyllum is spilled on segments. Exception of transferred species, background plants are Carex pachystylis and Poa bulbosa.

Covering of soil is 55 %. The whole on area 11 species were noted, referring to the following biological groups: autumn-summer plants — 4, spring-summer plants — 2, ephemeroids — 3, ephemers — 2, moreover, the last two species are weed plants. Hay harvests showed, the fluctuation of the dry mass of the herbs is from 46 till 111 gr./m, and at the average it is 49 gr./m, that it gives at translation on hectare — 4.9 centner/hectare gross productivity or 2.7 centner/hectare fodder plants.

An analyze of hayrick	
Acanthophyllum brevibracteatum	22.0 gram
Salsola collina	10.0 gram
Stipa Hohenackeriana	17.3 gram
Carex pachystylis	4.1 gram
Poa bulbosa	3.6 gram
Taeniatherum crinitum	1.3 gram
Psoralea drupacea	10.9 gram

On square meter 7 species of plants were noted. From data of weight analysis it is clear that large role in herbage

belongs to three first species, on share which it shows 50 gr./from 58.9 gr. on total weight of herbage/that it involves bad eaten plants. Ephemeral, the most valuable part of herbage, here it was showed till minimum — 7.6 gr. All this enables to refer the described difference to winter pasture with low productivity.

Ephemeral-girgensohnia-acanthophyllum pasture. It occupies the flat tops of the hills in adyr Otchopar. The area was described in September 28, 2016. This is the most usual variant of vegetation. On background ephemeroids of Carex and Poa are absently, there are perennial xerophytes of Cousinia resinosa and Acanthophyllum brevibracteatum and dry saltwort Girgensohnia oppositiflora.

The total 8 species are registered, from them: autumn-summer plants — 4, spring-summer plants — 2, ephemera — 0, ephemeroids — 2. There are no weeds. Hay harvests showed that spares of the dry mass of the herbs on square meter are differentiates from 22 till 71 gr., or at the average — 41.8 gr./m., that at translation on hectare it gives 41.8 centner of gross productivity, or about 3 centner/hectare fodder herbs.

An analyze of hayrick	
Carex pachystylis	8.2 gram
Acanthophyllum brevibracteatum	18.6 gram
Poa bulbosa	2.0 gram
Girgensohnia oppositiflora	11.2 gram
Haplophyllum hirsutum	1.8 gram

On square metre 5 species of plants were noted. Thereby, on share of well eaten plants/Poa and Carex/it forms only 10.2 gr., rests of plants — 31.6 gr. fall to bad eaten plants, moreover half of this weight belongs to Acanthophyllum, which it easy breaks apart to segments. At the bottom of the table is described in which ephemeral-saltwort pasture is given on all area.

We additional position defined the following data: ephemeral-saltwort pasture exceedingly is poor with species, which the amount varies from 7 till 9 and in ephemeral-acanthophyll pasture this cipher increase still 11. The amount of species on square meter for three differences pasture is on 5 and only on ephemeral-acanthophyll fodders it reaches to 7. Such this distribution of species has biological group: so, summer-autumn plants has 4 for three differences pasture and ephemeral-saltwort pasture has 5 species that it forms from 36.3 till 71.4 % (Table 1).

We could give our view, that the pasture plants area are decreasing as a result of desertification and we can increase the plant diversity according to the cenopopulation protection by law measures with the help of the committee of nature protection in the district and by increasing of ecological culture among the people [2].

Table 1. – The data of pasture plants of Chirakchi district in September, 2016

№	Name of pasture	A quantity of species	A quantity of species on 1 square meter	summer-autumn		spring-autumn		ephemerals		ephemerals		weeds		productivity	
				number	%	number	%	number	%	Number	%	number	%	gross	fodder
1.	ephemer-girgensohnia	9	5	4	44.4	2	22.2	1	11.1	2	22.3	–	–	3.5	2.5
2.	ephemer-saltwort-girgensohnia	7	5	5	71.4	–	–	–	–	2	28.6	–	–	16.4	11.9
3.	ephemer-saltwort-acanthophyll	11	7	4	36.3	2	18.2	2	18.2	3	27.3	2	18.2	5.3	3.7
4.	ephemer-girgensohnia-acanthophyll	8	5	4	50.0	2	25.0	–	–	2	25.0	–	–	4.3	3.0

References:

1. Khuzhanazarov U., Khasanov O. Natural fodder resources of Uzbekistan, prospects their use//Ecology information journal. – Tashkent, 2006. – № 7 – P. 37.
2. Khuzhanazarov U. Modern condition of upper Kashkadarya region pasture//Uzbekistan agricultural information journal. – 2012. – № 1–2 (47–48). – P. 111.

Section 2. Mathematics

DOI: <http://dx.doi.org/10.20534/AJT-17-1.2-23-25>

*Druzhinin Victor Vladimirovich,
Holuskin Vladimir Semenovich,
National research nuclear University «MEPhI»,
Sarov Institute of physics and technology,
Department of mathematics, Sarov
E-mail: vvdv@newmail.ru*

Necessary conditions of the existence the sums of fermat

Abstract: The General necessary conditions for the solution of Diophantine equations, which includes the latest task of Fermat, formulated. The generalization of small Fermat's theorem is used. There are large number of examples.

Keywords: small and the last Fermat's theorem, comparison, deductions.

Under the sums of Fermat we understand Diophantine equation of the form:

$$F(n; t) = \sum_{k=1}^n \beta_k a_k^t = 0, \quad (1)$$

where $\beta_k = \pm 1$, a_k and t natural number, $t \geq 2$. The Fermat's last theorem $a^t + b^t - c^t \neq 0$ for $t \geq 3$ refers to the form (1). It is fully proven in 1995 by the British mathematician Edward Wiles [1], for which he in 2016 has the Abel prize. We consider the solution of equation (1) for an arbitrary number of summands and analyzed the necessary conditions of their existence. Trivial cases of subtraction of identical numbers or compensation for the expense of the pieces we reject. If these conditions are not met, then (1) in integers is not solved. If these conditions are met, then the evidence (1) requires additional analysis. Many such conditions are known, but we have found some new requirements. List them.

1. Signs β_k can't all be the same and odd numbers a_k must be an even number.

2. If only one $\beta_k = -1$, then $\sum_{k=1}^n \beta_k a_k > 0$.

3. If $t = p$ is a Prime number, due to the small Fermat's theorem $a_k^t \equiv a_k \pmod{t}$ and $\sum_{k=1}^n \beta_k a_k = Cp$, where C is an integer.

4. If we write $a_k^t = 10a_{kt1} + a_{kt0}$ in the decimal system, where $a_{kt0} \geq 0$ the last digit of the number, $\sum_{k=1}^{p-1} \beta_k a_{kt0} = 10C$. If $\sum_{k=1}^{p-1} \beta_k a_{kt0} \neq 10C$ (1) in integers is

not solved. Moreover, if we increase t to $t + 4k$, this amount will not change, i. e., with such increased amount of Fermat does not exist.

5. Choose randomly a Prime number p_2 greater then t and all $\{a_k\} \perp p_2$ (p_2 mutually simple with a_k). Generalization a small of Fermat's theorem in [2] for any $t < p_2$ gives such a comparison:

$$a_k^t \equiv \mu(a_k; t; p_2) \pmod{p_2}, \quad (2)$$

where $\mu(a_k; t; p)$ deduction from the full set of minimum to module deduction, i. e. :

$$-(p_2 - 1)/2 \leq \mu(a_k; t; p_2) \leq (p_2 - 1)/2.$$

The calculation of these deductions is relatively simple, and they have the following properties:

$$\mu(a_k; p_2 - 1; p_2) = 1;$$

$$\mu(a_k; (p_2 - 1)/2; p_2) = \pm 1;$$

$$\mu(1; t; p_2) = 1;$$

$$\mu(p_2 - 1; t; p_2) = (-1)^t; \quad (3)$$

$$\mu(a_k; 2t_1; p_2) = \mu(p - a_k; 2t_1; p_2);$$

$$\mu(a_k; 2t_1 + 1; p_2) = -\mu(p_2 - a_k; 2t_1 + 1; p_2);$$

$$\sum_{k=1}^{p-1} |\mu(a_k; t; p_2)| \leq (p_2^2 - 1)/4.$$

$$\mu(a_k; t; p_2) = \mu(a_k; t + p - 1; p_2);$$

$$\sum_{k=1}^{p-1} \mu(a_k; (p_2 - 1)/2; p_2) = 0.$$

As an example we give the matrix of the Fermat (tab. 1) the generalized small Fermat's theorem for $p_2 = 7$.

Table 1. – The matrix of Fermat.
Deductions μ for $p_2 = 7$

$t \backslash a$	1	2	3	4	5	6
6	1	1	1	1	1	1
5	1	-3	-2	2	3	-1
4	1	2	-3	-3	2	1
3	1	1	-1	1	-1	-1
2	1	-3	2	2	-3	1
1	1	2	3	-3	-2	-1

Write the Fermat's amount $F(n;t)$ by applying the generalized small Fermat's theorem in the form:

$$F(n;t) = \sum_{k=1}^n \beta_k a_k^t = F_1(n;t) + F_2(n;t), \quad (4)$$

where:

$$\begin{aligned} a_k^t &= C_k p_2 + \mu_k; \\ F_1(n;t) &= p_2 \sum_{k=1}^n \beta_k C_k; \\ F_2(n;t) &= \sum_{k=1}^n \beta_k \mu(a_k; t; p_2). \end{aligned} \quad (5)$$

From (4, 5) follows the fifth necessary condition in the form of a theorem: if $F(n;t) = 0 \Rightarrow p_2 \setminus F_2(n;t)$. If the Fermat's amount exists, $F_2(n;t)$ divided by p_2 , including F_2 may be zero. A special role plays the Central line $t = (p_2 - 1)/2$. We will continue to operate with two simple numbers: the control p_2 and the real $t = p_1$. At the same $p_2 > p_1$. They are connected: $p_2 = p_1 + 1$; $p_2 = 2p_1 + 1$; $p_2 = 4p_1 + 1$; $p_2 = 8p_1 + 1$ and so on.

If there is a control Prime number $p_2 = 2p_1 + 1$, all of $\{a_k\} \perp p_2$, n is odd, then for $3 \leq n \leq p_2 - 2$ $F_2(n; p_1) \neq 0$, i. e. in whole numbers the Fermat's amount does not exist. Give proof. Since $F_2(n; p_1)$ is the sum of an odd number of numbers $\ll \pm 1 \gg$, then $F_2(n; p_1) \neq 0$ $|F_2(n; p_1)| \leq (p_2 - 2)$ and the condition $p_2 \setminus F_2(n; p_1)$ fails. Hence the quotient proof of the last Fermat's theorem. If $\{a; b; c\} \perp 7$, then $a^3 + b^3 - c^3 \neq 0$ as the amount $\{\pm 1; \pm 1; \pm 1\}$ gives the number of $\{-3; -1; 1; 3\}$ is not a multiple of $\ll 7 \gg$. Further, since $11 = 2 \cdot 5 + 1$ and all $\{a_k\} \perp 11$, the sum of three, five, seven, and nine numbers to the fifth power will never be equal to zero. In particular the calculation of $F_2(n; p_1)$ number of terms can be more $(p_2 - 2)$. For example, consider the sum $F(5; 3) = (4^3 + 5^3 + 10^3 + 11^3 - 16^3)$. Then the residues modulo $\ll 7 \gg$ are respectively equal to $\{1; -1; 1; -1; 1\}$, $F_2(5; 3) = -1$, and the sum $F(5; 3) = -1576 = -7 \cdot 225 - 1$, as it should be not equal to zero.

Let specific degrees. At $t = 2$ the control $p_2 = 3$. Hence, it follows that Pythagorean triple (type

$3^2 + 4^2 - 5^2 = 0$) must contain one number is a multiple of $\ll 3 \gg$. If not, deductions of squares modulo $\ll 3 \gg$ equal to 1, and $F_2(2; 1) = \sum_k^3 \beta_k = \pm 1$ is not divisible by $\ll 3 \gg$. This requirement also follows from the quadratic identities:

$$4a^2b^2 + (a^2 - b^2)^2 = (a^2 + b^2)^2. \quad (6)$$

As shown by the author [3] for $F(n; 2) = 0$ we can obtain any length. For example:

$$3^2 + 4^2 + 12^2 + 84^2 + 3612^2 - 3613^2 = 0. \quad (7)$$

Here are only two numbers not divisible by $\ll 3 \gg$: $\{4; 3613\}$ and $F_2(6; 2) = 0$.

Consider the degree $t = 3$. It is known that the triple of numbers $(a^3 + b^3 - c^3) \neq 0$, and this equality was proved by Euler. However, the evidence is apparently so cumbersome that not a single textbook we never found him. Our method shortens the proof. Let $a + b = c + 3T$, $T > 0$, we must take $a = 3a_1 + 1, b = 3b_1 + 1, c = 3c_1 - 1$. If we build this equation in the cube, we get $1 = 3K$, which is impossible. Now let $a = 3a_1$. In this case, we come to quadratic equation :

$$Tc^2 + c(3T^2 - a_1b) + 3T(T - a_1b) = 0.$$

The discriminant $D = (3T^2 + a_1b)^2 - 12T^4$. According to the quadratic identity (5) to $\sqrt{D} \in \mathbb{N}$ requires that $T^2 = a_1b$. But this gives $c = \{0; -2T\}$, which is unacceptable. So always $(a^3 + b^3 - c^3) \neq 0$. If the number of summands is more, there are chains of any length. We received the the Fermat's amount f forty-one components by the method of [4]:

$$\begin{aligned} &2 \cdot 2^3 + 3^3 + 5^3 + 2 \cdot 4^3 + 2 \cdot 6^3 + 7^3 + 10^3 + 12^3 + \\ &+ 13^3 + 3 \cdot 14^3 + 2 \cdot 15^3 + 4 \cdot 16^3 + 17^3 + 19^3 + 24^3 + \\ &+ 26^3 + 27^3 + 2 \cdot 28^3 + 3 \cdot 29^3 + 30^3 + 2 \cdot 31^3 + 32^3 + \\ &+ 35^3 + 36^3 + 38^3 + 39^3 + 62^3 - 92^3 = 0 \end{aligned} \quad (8)$$

Go to a degree $t = 4$. $F(3; 4) \neq 0$. This inequality has proved by Fermat himself. We it looks so. Let $\{a; b; c\} \perp 5$, then $a^4 + b^4 - c^4 = 5T + 1$ at the second small Fermat's theorem. To the right of zero is impossible. Need to take, for example, $a = 5a_1$. But there is superimposed a stronger necessary condition. We write $a^4 + b^4 - c^4 = (a^2)^2 + (b^2)^2 - (c^2)^2 = 0$. From to (6) $b^2 = (\alpha^2 - \beta^2)$, $c^2 = (\alpha^2 + \beta^2)$. In integers the equation impossible. So, all $a^4 + b^4 - c^4 \neq 0$. Hence this inequality is in many other even t .

Euler put forward the hypothesis that the Quartet Quartets $F(4; 4) \neq 0$ for any integers. However, in recent years it was experimentally refuted. Computer calculations have a few two quartet quartets [5; 6]. For example:

$$95800^4 + 217519^4 + 414560^4 - 422481^4 = 0, \quad (9)$$

$$2682440^4 + 15365639^4 + \\ + 18796760^4 - 20615673^4 = 0. \quad (10)$$

Consider the necessary conditions for the existence of such quartets. If all four numbers $a_k \perp 5$, then $F_2(4;4) = 3 - 1 = 2$, and therefore $F(4;4) \neq 0$. If only one number is a multiple of «5», $\sum_k \beta_k = \{1;3\}$ and we get the same result. Only when two numbers are multiples of «5» $\sum_k \beta_k = 0$ and the equalities (9, 10) is possible. Offer the Fermat's amount of six terms: $2^4 + 2^4 + 3^4 + 4^4 + 4^4 - 5^4 = 0$.

6. There is also a sixth necessary condition for the existence of the Fermat's amounts. Before that we used or the top row of the Fermat's matrices with $t = p - 1$ or

the Central line at $t = p_1 = (p_2 - 1) / 2$. Sure you can use other strings. Let $t = p_1 = (p_2 - 1) / 4$. In this line deductions there are only four different numbers $(\pm 1; \pm B)$. For example, when: $p_2 = 13, B = 5$; $p_2 = 29, B = 12$; $p_2 = 53, B = 30$. The result is easily calculated F_2 . For example, it is necessary to check $F(5;13)$. Can we of the five numbers $\{\pm 1; \pm 30\}$ to get the number «53»? It's impossible. Therefore, $F_2(5;13) \neq 53C$ and all amounts with $a_k \perp 53$ give $F(5;13) \neq 0$.

If we take $t = p_1 = (p_2 - 1) / 8$ then a row will have eight different deductions.

For example, if $p_2 = 41, t = 5$ — a line contains deductions $\{\pm 1; \pm 3 \pm 9; \pm 14\}$. From the sum of the five numbers will receive a «41» is impossible. Therefore, if $\{a; b; c; d; f\} \perp 41$ then $a^5 + b^5 + c^5 + d^5 - f^5 \neq 0$.

References:

1. Wils A.//Annals of Mathematics. – 1995. – 141. – P. 443–551.
2. Druzhinin V. V.//NTVP – 2015. – № 5. – P. 22–24.
3. Druzhinin V. V.//NTVP – 2014. – № 1. – P. 19–21.
4. Druzhinin V. V., Holuskin V. S.//AJTNS – 2016. – № 4–5. – P. 3–4.
5. Graham Z., Knuth D., Patashnik O. Concrete mathematics. – Moscow: “Mir”, 1998. – P. 313.
6. Science. № 18. Fermat. – Moskow: De Agostini, 2015. – P. 82.

Section 3. Materials Science

DOI: <http://dx.doi.org/10.20534/AJT-17-1.2-26-30>

*Bukleshev Dmitry Olegovich,
Federal State Budgetary Educational Institution of High Education
«Samara State Technical University»,
graduate student, SamSTU
E-mail: bukleshev-dima@mail.ru*

*Sharaukhova Anastasia Grigoryevna,
graduate student, SamSTU*

*Buzuev Igor Ivanovich,
Candidate of technical science, SamSTU*

Industrial danger reduction of the pipelines operation by assessment of the weld-affected zones in a stress-strain state

Abstract: Reliability of the pipelines operation directly depends on the performed works quality on technical diagnosing, which assumes analytical procedures of technical condition assessment and forecasting. The result of the technical diagnosing to a great extent depends on completeness and quality of the analysis results received at the inspection. That, in turn, depends on the relevant normative documents existence, assessment techniques and other materials which allow estimating negative influence of all revealed defects at the maximum degree. A lot of the corresponding standard documentation is developed, but the cases of pipelines accidents and breakages, under the condition of essential amounts of the performed work on technical diagnosing, nevertheless can confirm problems regarding negative influence assessment of some defects types.

One of the reasons of accidents on pipelines is the stress-corrosive destruction (SCD). The problem of the main pipelines SCD came to the world's forefront as one of the main reasons for pipe body destructions. However because of the significant complexity of SCD emergence process the mentioned phenomenon is insufficiently studied today and therefore not all factors, which influence it, are enough considered when determining potentially dangerous segments. Along with the general regularities SCD process has considerable number of specific features inherent in the particular studied pipeline (a particular steel brand resistance to the stress corrosion process, chemical characteristics of the pipe surrounding environment, regulations of the pipeline operation and its construction features, stress in the pipelines joints and weld-affected zone).

In literature and according to the research works results one of the main reasons for a stress — corrosive cracks incubation is a stress which arises in a pipe body near to the concentrators (welded seams are referred to them as well) and exceeds the material fluidity limit. According to the authors' opinion, besides other factors (the corrosion environment, a relief, mounting conditions, set-on weight presence etc.), inherent in any pipe irrespective of the way and place of its production, emergence of rather essential local additional stress is caused by two-joint pipes geometrical form defects which are generally formed at a stage of their production [6, 10].

Keywords: pipeline, stress-corrosive destruction, weld-affected zone, stress, crack.

It is known that the centers of metal construction destruction, including the main pipelines, are most often located near the welded connections. The reason of it besides the defects arising in metal during welding because of various deviations from the established norms and technical requirements, and considerable internal stress which are formed in metal during welding near the welded joints, is also the fact that the structure of material and its physical and mechanical properties respectively change in metal during welding [3, 3].

Stress conditions and corrosion are the main reasons for accidents on the main and distributing steel pipelines. In such segments during the time at the metal stress condition development, a change of residual magnetization usually occurs [2, 4].

Practice of gas pipelines operation shows that the main sources of damages at the gas-main pipelines operation are stress local zones — local corrosion, cracks on the corrosion cracking under the stress basis (CCS), and deformations from joints mounting which are formed under the working loadings influence [4].

Corrosion cracking under the stress (CCS) currently is the most frequent reason for failures on a line part of the gas-main pipeline. Corrosion and active environment influence, temperature fluctuation, working loadings and stress during the time change structure and properties of the operated pipe metal in comparison with the initial characteristics. Repeatedly static loadings along with the geometrical (a welded joint, mechanical damages of a pipe surface, corrosion damages) and structural heterogeneity (grains boundary, nonmetallic inclusions) cause the inevitable metal damages owing to irreversible microplastic deformations accumulation.

Dislocation density increase and damages accumulation is the first stage of destruction process the subsequent stages of which are microcracks incubation, their stable growth and spontaneous destruction. Destruction processes are intensified in zones of double plastic deformation caused by a technique of pipe manufacturing (edges turn-up for welding and subsequent calibration), by sections of cold bending, by pipeline laying with a compulsory bend at the mounting, and by pipeline deformations caused by geophysical processes [1, 8].

At load influence on the pipe metal there is a proneness to the stress concentration zones (SCZ) accumulation and formation. Stress concentration is understood as a local stress increase in a deformable body's zones with abrupt change in section [9]. Defects of orifice welding production, pores, inclusions, notching and others can be such concentrators in the weld-affected zones. Stress

concentration in the welded connections is defined by the connected elements general structure, by geometrical form of the pipeline joint welded with the base metal and by transition way and energy power of welding process as well. Circular butt joints are such concentrators for pipelines undoubtedly. And the fact of their existence and counterbalancing in a pipe material without being influenced by the external factors is a residual stress characteristic. SCZ are determined by a total contribution of all inheritance forms accumulated at the stages of rolling sheet manufacturing, pipe production, performance of the pipeline construction assembly, welding and installation work and also metal structure and properties changes which are accumulated in it during the time.

With the stress gradient growth as it is near to the crack-like defects, stress distribution is influenced by separate structural elements, such as grain blocks, separate grains which are variously focused in relation to a power flow, grains boundary, etc. All this causes the metal inhomogeneity contribution to the stress growth. Low-volume real constructional materials of a crystal structure, isotropy conditions, homogeneity and material continuity are violated. Because of various orientation of separate structural components stress distribution in low-volume real material can't be smooth. Therefore real material structural microinhomogeneity is revealed in the form of its deformation heterogeneity.

Currently a lot of works are actively carried out on nondestructive methods elaboration of a metal structural condition determination and assessment of a product's intense deformed state (IDS) changes at operational loadings, but the majority of these works don't consider the fact that the pipe can undergo an additional plastic deformation at a stage of production, and when transporting a pipe to the mounting place and directly at the pipe mounting.

In the welded constructions, as a rule, three following zones are distinguished: base metal, welded joint and weld-affected zone (WAZ). Fig. 2 displays the scheme of thermal influence zone structure in the welding of a single-layer butt weld at the constructional steel [8]. At the same time, as well as the mentioned zones differ on structure, physical and mechanical properties, and residual stress level, material of various welded constructions segments in the course of production, transporting, mounting and operation will react differently to loadings activity. Respectively, preliminary plastic deformation will affect differently the behavior of metal magnetic characteristics of various welded connection segments of a pipe at their subsequent elastic deformation [3, 3].

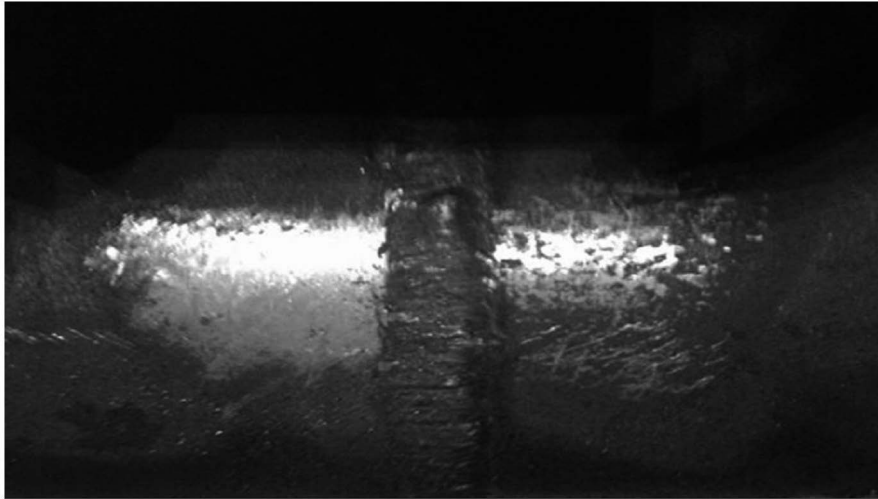


Fig. 1. Sample of a gas-main pipeline fragment (a welded joints fragment of the Central Asia-Center gas-main pipeline, steel 09GSF, diameter of 1420 mm, ball hardness HRB = 110)

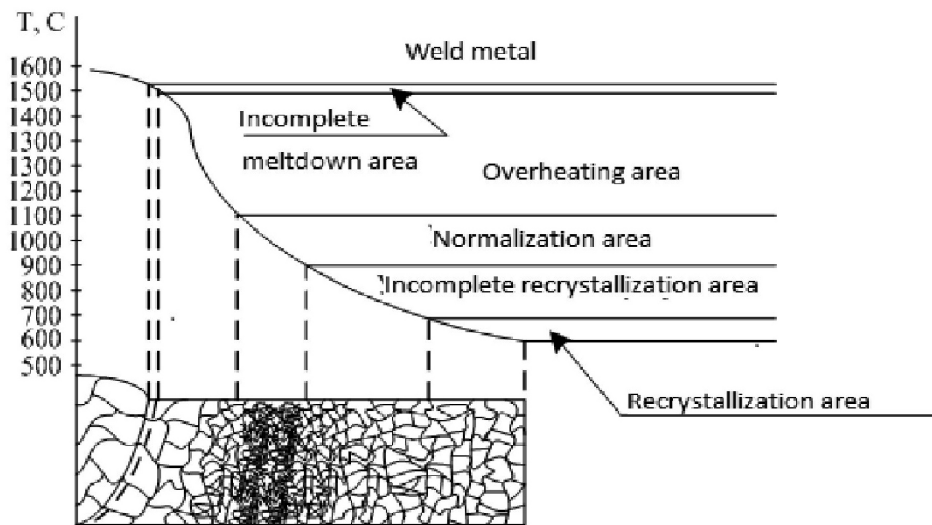


Fig. 2. Structural scheme of the weld-affected zone in welded connection

It is known that welding stress and deformation emergence is caused:

- 1) irregular temperature distribution in welded connection at a stage of its heating and subsequent cooling;
- 2) metal casting shrinkage of a joint — metal volume reduction of a welding puddle when hardening;
- 3) metal volume changes of a joint and weld-affected zone at phase transformations of heating and cooling stages [7].

The following reasons of internal residual stress formation can be distinguished in the weld-affected zones:

1. Local irregular metal heating. It is known that all metals expand when heating, and compress when cooling. In the course of welding, as a result of local metal heating and its subsequent cooling, irregular temperature field is formed in the welded connection. Thus, in the welded detail there is a squeezing and (or) stretching thermal internal stress. Stress magnitude depends mainly on heating temperature, coefficient of linear expansion

and the welded metal thermal conductivity. At the firmly fixed construction welding, thermal stress magnitude can increase because of its transfer limitation in the course of heating and cooling. At the same time in the heating-up construction, because of its expansion, there will be a squeezing internal stress at first, and at the subsequent cooling in the course of its shortening there will be a stretching stress. When the stress internal magnitude reaches fluidity limit level, plastic deformations causing a change of the welded product form size will occur in metal. After the end of welding process, residual stress will occur in the areas which have undergone irregular plastic deformation.

2. Irregular structural transformations in metal. At the gas-main pipelines joints welding, when heating the temperature above critical, there can be stress caused by phase transformations with a change in a crystal lattice type and formation of the phase having a large specific volume and other linear expansion coefficient.

Structure transformations in the pipe steel cause a formation of the so-called quenching structures (martensite) having a large specific volume, higher hardness, fragility and lowered plasticity. Such transformation is followed by increase in volume; metal adjoining to it will undergo the stretching stress, and martensite-structured segments will have a phase fluidity limit. In non-plastic alloys it can cause cracks formation.

3. Casting shrinkage of the weld metal. There is a metal shrinkage at the process of its cooling and hardening in the welded joint and weld-affected zone of a joint. This results from the fact that the metal density increases when hardening therefore its volume decreases. According to the welded metal indissoluble connection with the

base metal, remaining in its invariable volume and counteracting shrinkage, longitudinal and cross internal stress, causing the corresponding welded connection deformations, occur in the welded connection.

In fig. 3 gives “geometrical” multitudes of elastic stress concentration at the pure gas pipeline bending. In the segments with the largest mechanical heterogeneity of joint properties SCZ is shown, which results in the form of deformations stress in thermal influence zone in testing. It is possible to notice that extreme damages begin to be shown from the inside of a pipe body at dynamic loadings, forming defective areas. This effect can be explained with pipeline metal compression and stretching process in testing [5, 25].

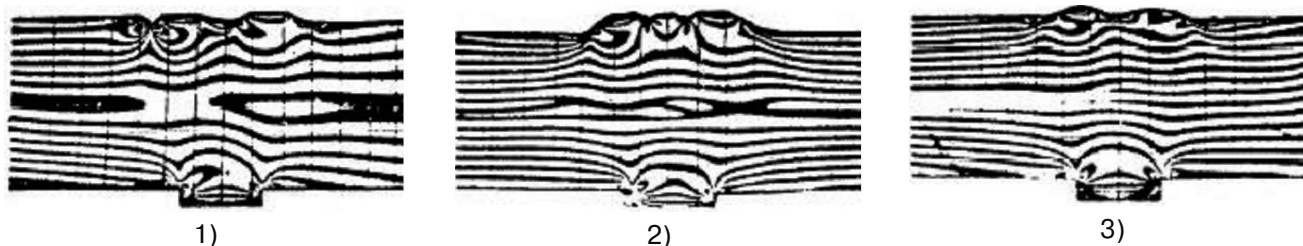


Fig. 3. Stress concentration of a sample at dynamic loading: 1) — load of 80 kN; 2) — load of 120 kN; 3) — without loading

When calculating the of welded construction durability it is important to consider a stress and deformations existence at a thermal and deformation welding cycle. On the basis of the approximate calculations, used in the theory of welding deformations and stress, welded elements deformations for the establishment of admissions and allowances for elements of the bearing and protecting construction are usually defined. At the same time with a certain probability, calculation of the residual welding stress and deformations generally is a quite complex challenge as it has to consider all reasons causing their emergence, and material heat and physical properties as well.

Conclusion

The main sources of damages at the gas-main pipelines operation are local stress zones — local corrosion, cracks on the corrosion cracking under the stress, and also deformations from joint assembly mounting which are formed under the influence of working loadings. Reliable pipeline operation can be provided only in the absence of defects of various nature: chemical and structural homogeneity of a pipeline body. In turn, lack of defects will guarantee the main pipeline reliability and

service life, maintaining operating abilities, pipe material qualitative characteristics which will be as close as possible to their theoretical (calculated) values.

Stress in the weld-affected zone is an indicator of the stress and strain state. Metal stress in the weld-affected zone is a source of defects emergence. This stress adds up to the working stress, accelerating a process of crack formation in the weld-affected zones of pipe connections, and causes continuous corrosion process, and also contributes to a crack propagation until the pipeline destruction. Stress in the weld-affected zone is a result of internal stress existence which can be caused by various reasons. Among the main reasons for their emergence can be referred: irregular heating and a welded joint shrinkage, structural changes in metal and the weld-affected zone. Also among the reasons for their emergence is an inappropriate application of welding equipment and technology (electrode diameter is incorrectly chosen, the welding modes aren't observed etc.), low welder qualification, violation of the welded joints sizes, etc. One of the reasons for a stress in the weld-affected zone is a pressure created by a transportation product.

References:

1. Varlamov D. P. Risks forecasting of safe operation of the gas-main pipeline linear segment subject to corrosion cracking under the stress: thesis, doctor of engineering sciences/D. P. Varlamov. – Mosow, 2014. – 349 p.
2. Venkova Y. A. Technical condition of oil and gas pipelines monitoring on the induced and residual magnetization: thesis, doctor of engineering sciences./Y. A. Venkova. – Saint Petersburg, 2016. – 149 p.

3. Gorkunov E. S. Behavior features of metal magnetic characteristics of separate pipe zones of big diameter with various initial stress-strain state at elastic deformation/E. S. Gorkunov, A. M. Polovotskaya, S. M. Zadvor-kin, E. A. Putilova//NDT days 2016. – 2016. – No. 1 (187). – P. 3–7.
4. Kasyanov A. N. Working capacity assessment of the weld-affected zones in the main pipeline circular welded connections: thesis, doctor of engineering sciences/A. N. Kasyanov. – Moscow, 2012. – 151 p.
5. Makovetskaya-Abramova O. V., Hlopova A. V., Makovetsky V. A. A research of stress concentration at pipelines welding/O. V. Makovetskaya-Abramov, A. V. Hlopova, V. A. Makovetsky//Service technical and technological problems. – 2014. – No. 2 (28). – P. 25–27.
6. Okhrimchuk S. A., Babelsky R. M., Rudenko S. N. The review of the possible reasons for crack formation on the two-joint Urengoy – Pomary – Uzhhorod gas-main pipeline/S. A. Okhrimchuk, R. M. Babelsky, S. N. Ruden-ko//Gas industry. – 2011. – No. 814 (Application). – P. 7–10.
7. Welding of building metal constructions/V. M. Rybakov, Y. V. Shirshov, D. M. Chernavsky [etc.]. – Moscow: Stroyizdat, 1993. – 267 p.
8. Dictionary on welding, soldering, sawing and adjacent types of metal processing//[Electronic resource]. – Avail-able from: <http://svarka-info.com/node/170>
9. Burkov P. V., Burkova S. P., Timofeev V. Y. Analysis of stress concentrators arising during MKY.2SH-26/53 sup-port unit testing/Burkov P. V., Burkova S. P., Timofeev V. Y.//Applied Mechanics and Materials. – 2014. – Vol. 682. – P. 216–223.

DOI: <http://dx.doi.org/10.20534/AJT-17-1.2-30-34>

*Maksudova Nasima Atkhamovna,
Senior Lecturer, department: Strength of Materials,
faculty: Mechanical Engineering
Tashkent State Technical University
Iskandarov Asilbek Akrom ugli,
bachelor, department: Thermal Engineering, faculty: Energetics,
Tashkent State Technical University
named after Abu Raykhon Beruni,
Tashkent, Republic of Uzbekistan
E-mail: asilbek.iskandarov17@gmail.com*

Research project of metal oxide nanofluids reaching an increase of heat transfer rate capacity in solar absorption refrigerator

Abstract: Solid metallic materials, such as silver, copper and iron, and non-metallic materials, such as Alumina, CuO, SiC and carbon nanotubes, have much higher thermal conductivities than heat transfer fluids (HTFs). It is thus an innovative idea trying to enhance the thermal conductivity by adding solid particles into HTFs and can be used as heat transfer media in the solar absorption refrigeration system. AgO nanofluid with weights percent of 0.1, 0.2, 0.3 and 0.4 %, which compared in the ability of transfer and storage the heat with distilled water, it is found that the suitable weight percent was 0.1 wt %. The flow rate required supplying heat input to generator and the volume of hot fluid storage required to operate the refrigerator for 24 hours has been calculated. Experimental and theoretical results obtained from the present work show a good improvement by comparing with literatures.

Keywords: nanofluid, absorption refrigeration system, energy storage, heat transfer, heat capacity.

Generally, nanofluids are formed by dispersing nanometer-sized particles (1–100 nm) or droplets into HTFs. Nanoparticles have unique properties, such as large surface area to volume ratio, dimension-dependent physical properties, and lower kinetic energy, which can be exploited by the nanofluids. At the same time, the large

surface area make nanoparticles better and more stably dispersed in base fluids. Compared with micro-fluids or milli-fluids, nanofluids stay more stable, so nanofluids are promising for practical applications without causing problems mentioned above. Nanofluids well keep the fluidic properties of the base fluids, behave like pure liquids and incur little penalty in pressure drop due to the fact that the dispersed phase (nanoparticles) are extremely tiny, which can be very stably suspended in fluids with or even without the help of surfactants [4].

Solar energy conversion to electricity is achieved primarily by using (a) photovoltaic technology, or (b) by harnessing solar thermal-energy. At larger scales of production, solar thermal techniques are more reliable and cost effective (as opposed to photovoltaic technologies), since these platforms can provide uninterrupted power supply in the off peak time (at night and during cloud cover). Solar thermal power plants rely on high temperature thermal storage units for continuous operation. Typical solar thermal-energy storage facilities require the storage medium to have high heat capacity and thermal conductivity. Contemporary commercial solar thermal units use energy storage facilities that operate at 400 °C and typically use mineral oil based storage medium as well as heat transfer fluids. It is estimated that pushing the storage facility to operate at 500–600 °C or higher can make the cost of solar power competitive with coal fired power plants in near future. However, few materials are compatible with the cost and performance requirements for such high-temperature thermal-energy storage. Typical materials used as HTF and for high-temperature thermal-energy storage include Na–K eutectics and alkali metal salt eutectics (e. g., NaNO_3 , KNO_3 , KCl , etc.). However, these materials have low thermo-physical properties. Hence, there is a need to find better performing thermal-energy storage technologies and materials that are cost effective. It should be noted that novel materials (such as nano material additives) can become cost effective if they can increase the operating range of the storage facilities to higher range of temperatures. For high temperature thermal-energy storage, compatible materials include molten salts and their eutectics, such as alkali-nitrate, alkali- carbonate, or alkali-chlorides. However, those molten salts have relatively low heat capacity — usually less than $0 \text{ J}/(\text{g } ^\circ\text{K})$ (in contrast to specific heat capacity of water which is $4.1 \text{ J}/(\text{g } ^\circ\text{K})$ at room temperature) [1].

Due to energy shortage in some regions, especially after the energy crisis of the 1970's, solar energy as

a renewable energy source has once again become a popular energy source. Research and development in the solar energy field has grown rapidly, along with research in solar cooling. With the invention of the DC-motor, photovoltaic (pv) technology was first used for pumping water. Later the pump motor was modified to drive the vapour compression system. PV-driven water pumps and refrigerators have since become a relatively large business. Subsequently, researchers have integrated so-called Peltier coolers with PV-panels to simple, yet inefficient solar coolers. These systems are used in the cold chain projects of the World Health Organization [2]. Contradictory reports in the literature demonstrate the degradation in specific heat of the fluids on doping with nanoparticles. Zhou and Ni [5] reported the reduction in specific heat of water by as much as 50%, when doped with aluminum oxide nanoparticles, with progressive increase in volume fraction from 0% to 21.7%. The aim of this research is to enhance the heat transfer rate in the solar absorption refrigeration system by replacing liquid paraffin wax by AgO nanofluid.

Solar Driven Cooling System

Any solar cooling system design essentially consists of two parts: the cooling unit that uses thermal cycle is not different from those used in conventional refrigerators, and heat source with the solar flat plat collector or focus operation [5].

1. The cooling unit

The absorption diffusion refrigerator machine is designed according to the operating principles of the refrigeration machine mono pressure invented by Platen and Muntter (Unique Gas Products Ltd). This machine used three operating fluids, water as the absorbent, the ammonia as refrigerant, and hydrogen as inert gas used in order to maintain the total pressure constant, which is composed of the principal following elements:

1.1. The boiler

A precise heat (electric heater element or gas flame) is applied to the boiler to begin operation. Heat is transferred from the outer shell of the boiler through the weak ammonia solution to the perk tube. The perk tube is provided with a rich ammonia solution (a high percentage of ammonia to water) from the absorber tank. When heated, the ammonia in the rich ammonia solution begins to vaporize (sooner than the water would) creating bubbles and a percolating effect. The ammonia vapor pushes the now weakening solution up and out of the perk tube. The ammonia vapor (gas) leaving the perk tube goes upward towards the top of the cooling unit, passing through the rectifier. The rectifier is just

a slightly cooler section of pipe that causes water that might have vaporized to condense and drop back down. The water separator at the top of the cooling unit (only on some models) prevents any water that might have escaped the rectifier to condense and fall back. After this point, pure ammonia vapor is delivered to the condenser. Meanwhile, back at the perk tube, the weaker solution expelled from the perk tube by the ammonia vapor drops into the weak ammonia solution surrounding the perk tube. Here, a little more ammonia vapor is generated and rises. The weak ammonia solution flows downward and through the outer shell of the liquid heat exchanger, where heat is transferred to the rich ammonia solution on its way to the perk tube. The weak ammonia solution then flows to the top of the absorber coils and enters at a cooler temperature.

1.2. The condenser

Ammonia vapor enters the condenser where it is cooled by air passing through the metal fins of the condenser. The cooling effect of the condenser coupled with a series of step-downs in pipe size forces the ammonia vapor into a liquid state, where it enters the evaporator section.

1.3. The evaporator

Liquid ammonia enters the low temperature evaporator (refrigerator/freezer) and trickles down the pipe, wetting the walls. Hydrogen, supplied through the inner pipe of the evaporator, passes over the wet walls, causing the liquid ammonia to evaporate into the hydrogen atmosphere at an initial temperature of around -28.88°C . The evaporation of the ammonia extracts heat from the refrigerator/freezer. At the beginning stages, the pressure of the hydrogen is around 24.5 kg/cm^2 , while the pressure of the liquid ammonia is near 0.98 kg/cm^2 . As the ammonia evaporates and excess liquids continues to trickle down the tube, its pressure and evaporation temperature rise. The liquid ammonia entering the high temperature evaporator (refrigerator portion) is around 3.08 kg/cm^2 , while the pressure of the hydrogen has dropped to 22.75 . Under these conditions, the evaporation temperature of the liquid ammonia is -9.44°C . Heat is removed from the refrigerator box through the fins attached to the high temperature evaporator. The ammonia vapor created by the evaporation of the liquid ammonia mixes with the already present hydrogen vapor, making it heavier. Since the ammonia and hydrogen vapor mixture is heavier than the purer hydrogen, it drops down through the evaporators, through the return tube to the absorber tank.

1.4. The absorber

When the ammonia and hydrogen vapor mixture enters the absorber tank through the return tube, much of the ammonia vapor is absorbed into the surface of the rich ammonia solution, which occupies the lower half of the tank. Now lighter, the ammonia and hydrogen mixture (now with less ammonia) begins to rise up the absorber coils. The weak ammonia solution trickling down the absorber coils from the top (generated by the boiler) is "hungry" for the ammonia vapor rising up the absorber coils with the hydrogen. This weak ammonia solution eventually absorbs all the ammonia from the ammonia and hydrogen mixture as it rises, allowing pure hydrogen to rise up the inner pipe of the evaporator section and once again do its job of passing over the wetted walls of the evaporator. The absorption process in the absorber section generates heat, which is dissipated.

1.5. The Fuse

The fuse on many cooling units and in this graphic is a steel tube, the end of which is filled with solder. The plug is hollow and filled with solder. In either case, the fuse is the weak link of the system. If pressure inside the cooling unit were to rise beyond a reasonable level for some reason, the fuse is designed to blow and release the pressure. This would make the cooling unit inoperable, but is necessary for safety.

2. The solar Collectors

The major energy gains in the receiver in a solar collector are from the direct absorption of visible light from the sun and, additionally, the absorption of infrared radiation from the warm glass as shown in fig. 1. Important energy losses are infrared radiation emission, convective heat due to natural convection between the receiver and glass, as well as conduction of heat through the rear and sides of the collector. Therefore, the efficiency of the solar collector depends on all of these factors. The efficiency of the solar collector sub-system can be defined as the ratio of useful heat output to the total incident solar radiation (insolation) [2].

Results and Discussion

Results were obtained for using AgO nanofluid with different weights percent which are 0.1, 0.2, 0.3, and 0.4. Fig. 2 shows variation of temperature of fluid with time, from which we can see that the favorite weight percent that above the line of pure water and the suitable is 0.1 wt.%, which behave as high heat absorption to transfer it to the refrigeration system in the solar absorption refrigeration system.

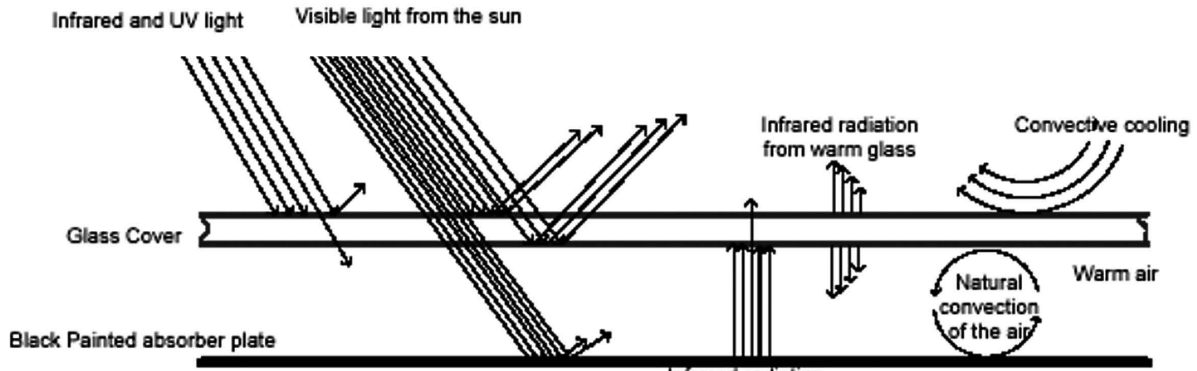


Fig. 1. Energy Flows in a Single-Glazed Collector [8]

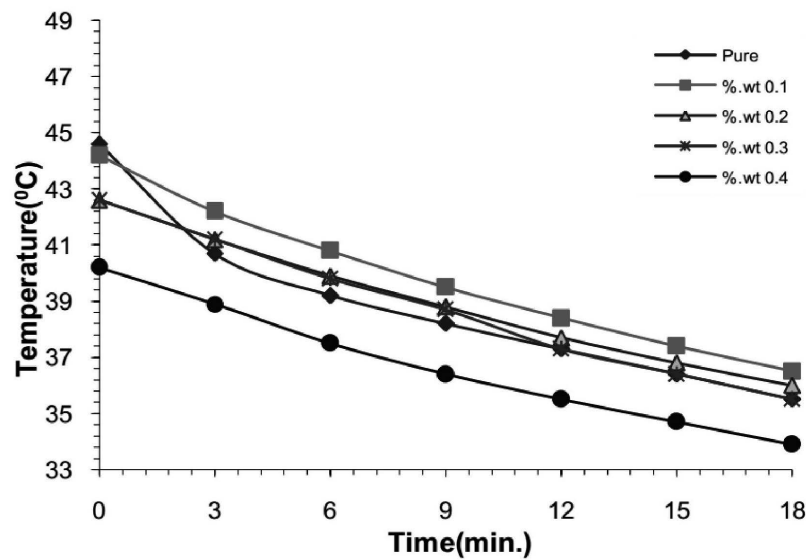


Fig. 2. Variation of Fluid Temperature with Time Heat Loss

From the T\Log diagram (Carl) the boiling point of rich ammonia-water mixture (33%) is 130 °C and the weak mixture (12%) temperature at 23 bar is about 190 °C. To operate the cooling unit with above condition, inlet generator temperature about 200 °C, and outlet temperature about 140 °C must be supplied from solar concentrator, then the flow rate of the working fluid required to achieve this operation is calculate as follow:

In this study 2.52 hr. was measured to generate 1 kg. of ammonia with 649 kcal, and then the energy demand of the generator is:

$$Q_g = \frac{649}{2.52} = 257.5 \text{ kcal/hr} = 257.5 \cdot 1.166667 = 300 \text{ W.} \quad (1)$$

$$Q_g = m \cdot c_p \cdot \Delta T. \quad (2)$$

$$\Delta T = (T_{go} - T_{gi}). \quad (3)$$

The specific heat (c_p) of AgO is 66 J/(mole °K), then the mass flow rate of heat exchange fluid required (AgO + water) can be calculated based on the proposed entrance and exit temperatures of the oil in the generator [3]:

C_p of water = 4.2 J/(g °K). We select 0.1 wt. % of AgO nanofluid.

Molecular weight of AgO = 232 g/gmole;

$$C_{p \text{ mix}} = 0.284 \cdot 0.1/100 + 4.2 = 4.2 \text{ J/(g °K)};$$

$$C_p \text{ of AgO} = 66/232 = 0.284 \text{ J/(g °K)} \quad m = \frac{300}{4.2 \cdot (200 - 140)} = 1.19 \text{ g/s}.$$

The density of AgO is 7.5 g/cm^3 then:

The density of water = 1 g/cm^3 ;

$$\rho_{\text{mix}} = 7.5 \cdot 0.1/100 + 1 \cdot 0.9 = 0.907 \text{ g/cm}^3.$$

The volumetric flow rate is:

$$\frac{1.19}{0.907} = 1.3 \text{ cm}^3/\text{s} = 4.68 \text{ liter/hr.} \quad (4)$$

The required hot fluid volume for 24 hr. is:

$$4.68 \cdot 24 = 112.3 \text{ liter/day}$$

Table 1. – Comparison Between Results of the Present Work and Obtained from Ref. (1)

Item	Ref. [5]	Present work	Improvement Ratio (%)
Mass Flow Rate (g/s)	2.28	1.19	46.49
Volumetric Flow Rate (liter/hr)	10.27	4.68	54.43
Hot Fluid Volume (liter/day)	246.5	112.3	54.44
Heat Capacity (J/(g°K))	2.19	4.2	91.78

Conclusions

From the present work we can report the following conclusions:

1. Using AgO nanofluid increase the heat transfer rate.
2. Using AgO nanofluid reduce the required hot fluid volume if compared with [5] as shown in table 1.
3. Using AgO nanofluid reduce the volumetric flow rate if compared with [5] as shown in table 1.
4. Using AgO nanofluid increasing the heat capacity if compared with [5] as shown in table 1.

Nomenclature

C_p — Specific heat capacity (J/(g °C));

$C_{p\text{mix}}$ — Specific Heat Capacity of the Mixture (AgO and water) (J/(g °C));

m — Generator mass flow rate (kg/s);

Q_g — Generator heat input (W);

T_{gi} — Generator inlet temperature (°C);

T_{go} — Generator outlet temperature (°C).

Greek Symbols

ρ_{mix} — Density of mixture (AgO and Water);

$\Delta T_g = (T_{go} - T_{gi})$ — Temperature Difference of the generator.

References:

1. Donghyun Shin et al. Enhancement of specific heat capacity of high-temperature silicananofluids synthesized in alkali chloride salt eutectics for solar thermal-energy storage applications//International Journal of Heat and Mass Transfer. – 2011. – № 54. – P. 1064–1070.
2. Pridasawas W. Solar-Driven Refrigeration Systems with Focus on the Ejector Cycle. Doctoral Thesis submitted to Division of Applied Thermodynamic and Refrigeration, Department of Energy Technology, School of industrial Engineering and Management, Royal Institute of Technology, KTH, 2006.
3. Narziev A. N., Iskandarov A. A. Improvement of autonomous system of the electrical supply, maintaining renewable power sources//International Scientific Review. – 2016. – № 3 (13). – P. 14–17.
4. Zenghu Han. Nanofluids with Enhanced Thermal Transport Properties. – Department of Mechanical Engineering University of Maryland at College Park College Park, Maryland, 2008.
5. Zhou, S. Q., and Ni, R., , Measurement of the Specific Heat Capacity of Water-Based Al_2O_3 Nanofluid//Appl. Phys. Lett. – 2008. – № 92. – P. 93–123.

Turaev Erkin,
Ph. D. Independent researcher,
Tashkent chemical-technological institute,
The faculty of chemical technology of fuel
and organic substances, Uzbekistan, Tashkent
E-mail: turaev08@yahoo.com

Mikitaev Abdulah,
Doctor of Chemistry, Professor of Kabardino-Balkarian State
University named by H. M. Berbekov, Russia, Nalchik

Djalilov Abdulakhat,
Doctor of Chemistry, Professor,
Director of Tashkent State Unitary
Enterprise Research Institute, Uzbekistan, Tashkent

The properties of polyethylene nanocomposites based on organo-modified montmorillonite

Abstract: Research the possibility of obtaining nanocomposite materials by the process of melt-mixing using organo-modified montmorillonite. Studied the the effect of the organoclay on the physical and mechanical, thermal properties of high density polyethylene.

Keywords: Polyethylene; Organo-modified montmorillonite; nanocomposite; Mechanical properties; Thermal stability.

Introduction

In recent decades, the task of developing new materials is achieved by the modification of the base grades of industrial polymers. One way of adjusting the properties of polymer materials, is to obtain composite materials filled with nano size particles. It's due to the fact that such composite materials have a number of significant advantages. When incorporating nanoscale fillers in a polymer matrix, there is an increase of modulus, impact strength, thermal stability, chemical stability to solvents, flammability and decrease gas diffusion and permeability in polymers occurs.

In connection of above mentioned, the development and study of the properties of nanocomposites based on high density polyethylene (PE) and nanoscale particles is a very urgent task that allows to expand the scope of PE.

Methods of organic modification of montmorillonite

It is known that the main problem of creating layered silicate nanocomposites is the incompatibility of the organic (polymer) and inorganic (layered silicate) constituent of composites. This problem can be solved by using organo-modified layered silicate as an alternative. This product is the replacement of inorganic cations in the galleries of the layered silicates with organic cations, as shown in fig. 1.

As a nanoscale PE filler, we used montmorillonite (MMT), which is derived from bentonite clay deposits of Gerpegezh (Kabardino-Balkarian Republic).

Organic modifier that has been used for modification of organic MMT is shown in table 1.

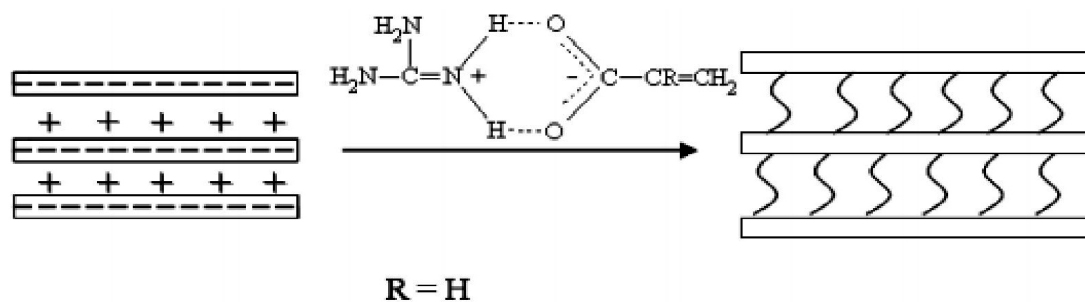


Fig. 1. Scheme of organic modification of montmorillonite

Table 1. – Composition of organo-modified MMT

MMT	Acrylate guanidine	
-----	--------------------	--

To achieve the maximum possible effect of increasing the properties of nanocomposites, the optimal content of organic modifier-Acrylate guanidine in MMT is 3–10 wt. %. It is determined that increase in the concentration of organic modifier in MMT above 10 % leads to the destruction of natural structure of layered silicates (disorients the silicate layers) and premature exfoliation of layered silicates reduces the physical and mechanical properties of nanocomposites [1].

Mechanical properties of PE/organoclay nanocomposites

Introduction of organoclay in the PE changes the whole complex of its physical and mechanical properties. The observed effect is also found conformation in the comparison of developed organoclay with unmodified natural MMT.

Table 3. – The physical and mechanical properties of nanocomposites depending on the content of organoclay

Polymer matrix	Filler, wt. %	MI, gr/10min 2.16 kg	Izod impact, J/m	Modulus, MPa	Tensile yield strength, MPa	Tensile yield at break, MPa	Elongation at break, %
PE	–	0.8	88	950	24	25	500
	3 % organoclay	0.8	58	1180	24	23	480
	5 % organoclay	0.85	51	1300	26	23	350
	7 % organoclay	0.85	48	1330	25	23	330
	5 % compoline	0.79	116	880	21	23	500
	3 % organoclay + 5 % compoline	0.8	82	1200	22	23	500
	5 % organoclay + 5 % compoline	0.76	80	1250	24	23	450
7 % organoclay + 5 % compoline	0.78	62	1260	24	24	450	

As can be seen from table 3, even at a low content of organoclay, there is observed a significant increase in modulus in tension with a tendency to increase with increasing organoclay content. For example, introducing 5 wt. % organoclay increases the modulus of the material to about 1.37 times. Thus an increase in yield strength by 8 %.

PE strength increases when the content of the organoclay is in an amount of up to 5 wt. % in the polymer matrix, which is probably due to the very resistance clay, which is a reinforcing element in the matrix.

Apparently, there is a threshold concentration at which the organo-modified silicate layer capable to be distributed at the nanoscale level, given the nature of the polymer to form a nanocomposite exfoliated structure.

Table 2. – Influence of the nature of organoclay on the properties of PE

Matrix	Modulus, MPa	Tensile yield strength, MPa	Elongation at break, %
PE	950	24	500
PE + 5 % MMT	1020	24	330
PE + 5 % organoclay	1300	26	350

As the result of the experiments shows, introducing 5 wt. % natural MMT and organoclay increases the modulus of the PE to 10 % and 37 %, the yield strength is 0 % and 8 % respectively. Table 2 shows that, the presence of organomodifier in clay, leads to the increase in adhesion strength and modulus of nanocomposites.

To determine the optimal concentration of organoclay, by extrusion process it was obtained composites containing 3, 5, 7 wt. % organoclay and mixture of 5 % compoline (compatibilizer) with organoclay. The results of this study are shown below.

Large concentrations of organoclay lead to the formation of intercalated structure [2].

Additional introduction in 5 % Compoline composition increases of the modulus by 24 %, thus further increasing the concentration of organoclay does not effect on modulus of nanocomposites, which is probably due to the nature of compoline. Introducing 5 % compoline contributes to the preservation of the elongation at break at the level of the base PE. Introducing 5 and 7 wt. % organoclay, nanocomposites elongation decreases slightly to 10 %. This suggests that, Compoline acts as an elastic bridge, thereby maintains high elongation values of nanocomposites.

Reduced elongation of 30 % with the introduction of organoclay in PE, it is assumed that, it's due to the blocking

of the mobility of the polymer segments of the layered silicates at the nanoscale. Meanwhile, the modulus increases monotonously in the entire range of concentrations.

Established fact of reduced izod impact strength of nanocomposites when introduction of organoclay in PE, can be explained by the blocked mobility of the polymer segments of the layered silicates at the nanoscale.

Structure of nanocomposites based on PE/organoclay

One of the methods of studying the degree of dispersion of organically modified layered silicates in a polymer matrix is an X-ray analysis. Diffractogram of nanocomposites obtained by melt mixing with PE/organoclay, is shown in fig. 2.

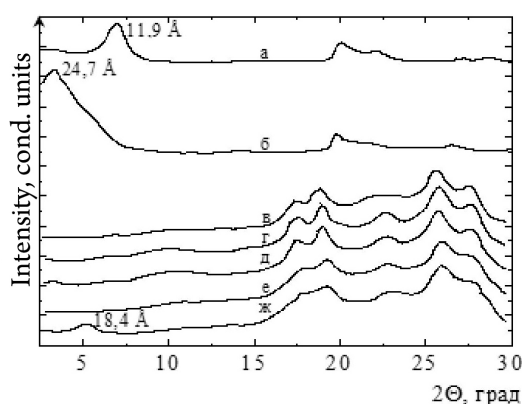


Fig. 2. The X-ray diffraction data: a — MMT; b — organoclay; PE with x% of organoclay content: at c — 0%; d — 1%; e — 3%; f — 5%; g — 7%

From the diffractogram, it can be seen that, for unmodified clay the characteristic peak is observed in $2\Theta = 7.0^\circ$ ($d = 1.19$ nm), which corresponds to the organoclay in $2\Theta = 3.0^\circ$ ($d = 2.47$ nm). When introduced into the polymer matrix PE organoclay in an amount of 5 wt. %, a characteristic peak for organoclay is absent, indicating the division of organoclay plates into separate silicate layers. The results of the analysis of the diffractogram suggest a complete exfoliation of the clay.

By increasing organoclay content to 7 wt. %, in the diffractogram in $2\Theta = 5.0^\circ$ a peak appears, the intensity of which is very small. The maximum intensity of this peak corresponds to $d = 1.84$ nm. This suggests that, in the resulting composite regions in which there was a complete exfoliation of organoclay, coexist with areas, which partially preserved the order in the arrangement of layers of packages.

Based on these results, it can be concluded that the composites obtained by melt mixing using an organoclay, when its content in an amount up to 5 wt. %, inclusive, are exfoliated, and when the content of organoclay in an amount of 7 wt. % composites have a mixed structure comprising intercalated and exfoliated packets.

Thermal properties of nanocomposites based on PE/organoclay

The method of thermogravimetric analysis (TGA) confirmed an increase in the degradation temperature (the temperature of the beginning of the slump) of the nanocomposites with the content of 3, 5, 7 wt. % organoclay on 5, 8, 11°C respectively. This is connected with the effect thermo-protection, influencing on macromolecules of polymers from the side of silicate layers.

In contrast to the base PE, nanocomposites are degraded in air to the form of coke, the quantity of which increases with increasing organoclay content. The presence of carbon residue indicates a more complex characteristic of the process of thermal destruction of nanocomposites.

The complexity of the thermal destruction process can be the result of the organoclay which plays the role of initiator of coking due to the barrier and blocking effects rendered by them to the volatile products. These results of TGA nanocomposites are shown in table 4.

Table 4. – The results of TGA nanocomposites based on PE/organoclay.

Matrix	Degradation temperature, °C	The coke residues at 600 °C, %
PE	394	0
PE + 3 % organoclay	399	5
PE + 5 % organoclay	402	8
PE + 7 % organoclay	405	10

Conclusion

The experimental data allow to draw conclusions about the prospects of given direction of research, as the development of new polymer nanocomposite materials based on MMT and polyethylene, permits to modify the basic properties of polymer significantly. Such materials with a low content of organoclay (about 5.3 wt. %) possess a new set of improved and new properties comparing to the base unfilled polymers, including high rigidity in a wide temperature range and increased thermal properties.

References:

1. Khashirov S. Guanidine containing polymers and nanocomposites based on them. Doctoral dissertation. – Nalchik, 2009.
2. Alexandre M., Dubois Ph. Polymer/layered silicate nanocomposites: preparation, properties and uses of a new class of materials // Mater. Sci. and Eng. – 2000. – V. 28. – P. 1–63.

Section 4. Mechanical engineering

DOI: <http://dx.doi.org/10.20534/AJT-17-1.2-38-50>

Vasenin Valery Ivanovich,
Perm National Research Polytechnic University,
Associate professor of the Department of materials,
technologies and machinery design, Candidate of technical sciences
E-mail: vaseninvaleriy@mail.ru
Bogomyagkov Aleksey Vasilievitch,
Senior teacher

Investigation of the work of the P-shaped gating system

Abstract: The description of laboratory P-shaped gating system is provided. The results of theoretical and experimental determination of speeds and flow of the fluid were stated, depending on the quantity of feeders that work simultaneously. Not only ramification of some part of the stream from collector to collector (or to feeder) takes place in the system, but also the confluence of fluid streams from two collectors, and between the rings with feeders there are working feeders. It was demonstrated that Bernoulli's equation is suitable for calculation of gating systems with variable flow (mass), which varies a lot in collector in the course of stream distribution to feeders. For calculation the gating system is divided into two half-rings. Calculation is performed, using the method of successive approximations until the given value of pressure loss divergence in half-rings reaches the zero point. Pressure losses, speed and fluid flow in the feeder are calculated and compared with each other during flow of the fluid in two parallel hydraulic lines. Four types of pressure losses are taken into account: for friction along the length, in local resistances, for split of the stream into parts, for confluence of streams.

Keywords: pouring basin, down gate, collector, feeder, pressure, resistance coefficient, flow coefficient, speed of the stream, fluid flow.

Introduction

L-shaped, ramified, combined, crosspiece, stepped gating systems (GS), one- and two-ring GS [1; 2], vertical ring GS [3], ring system with feeders of different cross sections [4], GS with 2 down gates [5], GS with collector of variable section were studied previously. The difference between calculated and experimental values of speed and flow amounted to 1–6%, although Bernoulli's equation (BE) was used in the calculation for stream of the fluid with variable flow (mass). And it was derived for a particular case — for the stream with a constant flow (mass), in the absence of distribution of fluid to feeders [5, 205; 6, 10], that is, for the simplest gating system — the system with one feeder. Therefore, BE is applicable for the stream with variable flow, although it is unclear why it works. The possibility of using BE in the calculation of GS with flow in the collector (scum riser) varying from maximum to zero in the split and confluence of

fluid streams is theoretically not proved. Therefore, it seems reasonable to research through experiments and calculations apparently the most complex GS — ring system, which has 2 rings with feeders and between the rings there are also working feeders (fig. 1). This system is widely used in the founding of magnesium alloys.

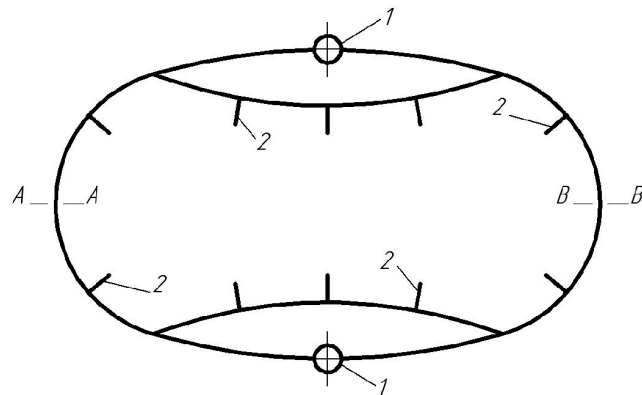


Fig. 1. Ring gating system: 1 — down gate; 2 — feeder

Research methods

In the fig. 1 in GS in sections A–A and B–B, the fluid speed is equal to 0. So, only half of GS can be investigated. The fig. 2 shows half of the ring GS — laboratory P-shaped GS. The system consists of pouring basin, down gate, collector and 5 feeders I–V. Internal diameter of pouring basin is 272 mm, height of water in the pouring basin is 103.5 mm. Longitudinal axes of collectors and feeders are located in the same horizontal plane. The level of liquid H — vertical distance from the section 1–1 in the pouring basin to the longitudinal axes of the collector and feeders — was kept constant by continuous filling-up the water in the pouring basin and discharge of its surplus through a special slit in the pouring basin: $H = 0.3615$ m. The fluid is poured from the top out of the feeders into the moulds. In the sections of the collector 5–5, ..., 16–16 piezometers are installed in order to measure the pressure — glass tubes with a length of 370 mm. and internal diameter of 4.5 mm. 90° curved piezometers were placed in the sections of the down gate 2–2, 3–3 and 4–4 (not shown in the fig. 2). The time of liquid outflow from each feeder was 50–150 s. — depending on the number of simultaneously operating feeders, and the volume of water discharged from each of the feeder was about 8 L. These time and weight restrictions provided the deviation from the average speed — no more than ± 0.0005 m/s. The fluid flow in each feeder was determined at least 6 times.

Major part

First we calculate the characteristics of GS for the cases, when the hydraulic system is open-circuited in the section 16–16 (there is no ring). We work out Bernoulli's equation (BE) for the sections 1–1 and 17–17 of GS (let's assume that only feeder I is in operation):

$$H = \alpha \frac{v_{17}^2}{2g} + h_{1-17}, \quad (1)$$

where: α — the coefficient of speed distribution irregularity in a section of the stream (Coriolis coefficient); assume that $\alpha = 1,1$ [7, 108]; v_{17} — speed of metal in the section 17–17, m/s; g — free fall acceleration; $g = 9.81$ m/s²; h_{1-17} — pressure loss when fluid flows from the section 1–1 to the section 17–17, m. These pressure losses are as follows:

$$h_{1-17} = \left(\zeta_{cm} + \lambda \frac{l_{cm}}{d_{cm}} \right) \alpha \frac{v_{cm}^2}{2g} + \left(\zeta_{\kappa} + \lambda \frac{l_{cm-1}}{d_{\kappa}} + 2\zeta \right) \alpha \frac{v_{\kappa}^2}{2g} + \left(\zeta_n + \lambda \frac{l_n}{d_n} \right) \alpha \frac{v_{17}^2}{2g}. \quad (2)$$

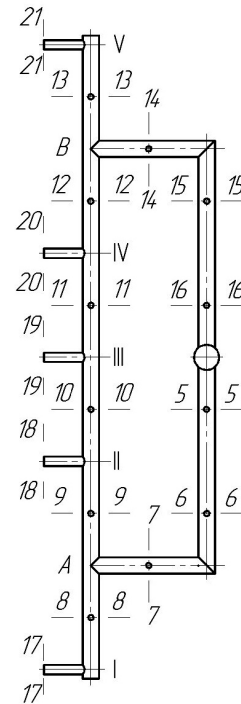
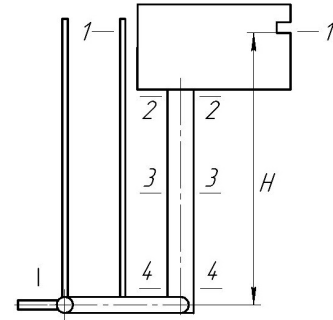


Fig. 2. P-shaped gating system

In equation (2): ζ_{cm} , ζ_{κ} and ζ_n — local resistance coefficients of entering of metal from the pouring basin into the down gate, turn from the down gate to the collector and turn from the collector to the feeder I; ζ — local resistance coefficient of 90° -turn from the section 6–6 to the section 7–7 and from the section 7–7 to the section 8–8 (without change of collector sectional areas); λ — friction loss coefficient; l_{cm} — length (height) of the down gate, m; d_{cm} , d_{κ} and d_n — hydraulic diameters of the down gate, collector and feeder, m; v_{cm} and v_{κ} — fluid speed in the down gate and collector, m/s; l_{cm-1} — distance from the down gate to the feeder I, m; l_n — length of the feeder I, m. The flow in GS during water discharge from the top is determined by the metal speed v_{17} in the exit section 17–17 of the feeder I and by its cross sectional area: $Q = v_{17}S_n$. Other fluid speeds in gates of GS are determined by using the flow continuity equation:

$$Q = v_{cm}S_{cm} = v_{\kappa}S_{\kappa} = v_{17}S_n, \quad (3)$$

where: S_{cm} , S_{κ} — cross sectional areas of the down gate and collector, m². Let's express all speeds in the

formula (2) through the speed v_{17} , using the flow continuity equation (3):

$$h_{1-17(17)} = \alpha \frac{v_{17}^2}{2g} \left[\left(\zeta_{cm} + \lambda \frac{l_{cm}}{d_{cm}} \right) \left(\frac{S_n}{S_{cm}} \right)^2 + \left(\zeta_{\kappa} + \lambda \frac{l_{cm-1}}{d_{\kappa}} + 2\zeta \right) \left(\frac{S_n}{S_{\kappa}} \right)^2 + \zeta_n + \lambda \frac{l_n}{d_n} \right]. \quad (4)$$

We denote the formula in square brackets as $\zeta_{1-17(17)}$ — system resistance coefficient from the section 1–1 to the section 17–17, added to the fluid speed in the section 17–17:

$$\zeta_{1-17(17)} = \left(\zeta_{cm} + \lambda \frac{l_{cm}}{d_{cm}} \right) \left(\frac{S_n}{S_{cm}} \right)^2 + \left(\zeta_{\kappa} + \lambda \frac{l_{cm-1}}{d_{\kappa}} + 2\zeta \right) \left(\frac{S_n}{S_{\kappa}} \right)^2 + \zeta_n + \lambda \frac{l_n}{d_n}. \quad (5)$$

Now the formula (1) may be presented as:

$$H = \alpha v_{17}^2 (1 + \zeta_{1-17(17)}) / 2g. \quad (6)$$

The system flow coefficient from the section 1–1 to the section 17–17, added to the speed v_{17} , is as follows:

$$\mu_{1-17(17)} = (1 + \zeta_{1-17(17)})^{-1/2}. \quad (7)$$

Speed:

$$v_{17} = \mu_{1-17(17)} \sqrt{2gH / \alpha}. \quad (8)$$

The flow Q is calculated using the formula (3). Length of the down gate $l_{cm} = 0.2675$ m, length of the feeder $l_n = 0.0495$ m, distance from the down gate to the feeder I $l_{cm-1} = 0.494$ m. Diameters of feeder, collector and down gate: $d_n = 0.00903$ m, $d_{\kappa} = d_5 = \dots = d_{16} = 0.01603$ m, $d_{cm} = 0.02408$ m. We assume, the same as in the works [8; 9], that the friction loss coefficient $\lambda = 0.03$. The local resistance coefficient of the entering from the pouring basin into the down gate, depending on the radius of rounding of the entering lip, is determined using the reference data [10, 126]: $\zeta_{cm} = 0.12$. The local resistance coefficient of the 90°-turn from the down gate to the collector and change of flow areas $\zeta_{\kappa} = 0.396$ [11]. The local resistance coefficient of the 90°-turn in the collector from the section 6–6 to the section 7–7 (without change of the flow areas before and after the turn) $\zeta = 0.885$ [11]. $\zeta = \zeta_{6-7} = \zeta_{7-8} = \zeta_{7-9} = \zeta_{14-12} = \zeta_{14-13} = \zeta_{15-16}$. The local resistance coefficient of the 90°-turn from the collector to the feeder I (with change of the flow areas) $\zeta_n = 0.334$

[11]. Calculation results according to the formulas (5), (7), (8) and (3): $\zeta_{1-17(17)} = 0.818621$, $\mu_{1-17(17)} = 0.741530$, $v_{17} = 1.882939$ m/s, $Q_{17} = 120.587295 \cdot 10^{-6}$ m³/s.

If the hydraulic system is open circuited in the section 5–5, then for calculation of characteristics of the feeder I in the formula (5) it is necessary to replace l_{cm-1} by $l_{cm-1(16-8)}$ — distance from the down gate to the feeder I on the way through the sections 16–16, 14–14, 12–12, 8–8; $l_{cm-1(16-8)} = 0.992$ m. We have: $\zeta_{1-17(17)} = 0.912471$, $\mu_{1-17(17)} = 0.723107$, $v_{17} = 1.836157$ m/s, $Q_{17} = 117.591311 \cdot 10^{-6}$ m³/s.

The work of feeders II and III is calculated in the same way. The results of calculations and experiments (in the denominator) are given in the table 1.

$$N = 100(Q - Q_{\text{акт}}) / Q_{\text{акт}}, \%$$

Let us calculate a simultaneous work of the feeders I and V. This is a ramified GS. $v_9 = v_{10} = v_{11} = v_{12} = 0$. Work out Bernoulli's equation for the sections 1–1 and 17–17 (for the way through the sections 2–2, 5–5, 7–7, 8–8):

$$H = \left(\zeta_{cm} + \lambda \frac{l_{cm}}{d_{cm}} \right) \alpha \frac{v_{cm}^2}{2g} + \left(\zeta_{4-5(5)}^{\partial} + \lambda \frac{l_{cm-1}}{d_{\kappa}} + 2\zeta \right) \alpha \frac{v_5^2}{2g} + \left(\zeta_n + \lambda \frac{l_n}{d_n} + 1 \right) \alpha \frac{v_{17}^2}{2g}, \quad (9)$$

and for the sections 1–1 and 21–21 (for the way through the sections 2–2, 16–16, 14–14, 13–13):

$$H = \left(\zeta_{cm} + \lambda \frac{l_{cm}}{d_{cm}} \right) \alpha \frac{v_{cm}^2}{2g} + \left(\zeta_{4-16(16)}^{\partial} + \lambda \frac{l_{cm-V}}{d_{\kappa}} + 2\zeta \right) \alpha \frac{v_{16}^2}{2g} + \left(\zeta_n + \lambda \frac{l_n}{d_n} + 1 \right) \alpha \frac{v_{21}^2}{2g}, \quad (10)$$

where v_5 , v_{16} , v_{21} — fluid speeds in the sections 5–5, 16–16 and 21–21, m/s; $v_5 = v_{16}$, $v_{17} = v_{21}$; l_{cm-V} — distance from the down gate to the feeder V; $l_{cm-1} = l_{cm-V} = 0.494$ m; $\zeta_{4-5(5)}^{\partial}$ — the resistance coefficient for split of the stream in the down gate in the section 4–4 between the sections 5–5 and 16–16, added to the speed of metal in the section 5–5; $\zeta_{4-16(16)}^{\partial}$ — the resistance coefficient for split of the stream in the down gate in the section 4–4 between the sections 5–5 and 16–16, added to the fluid speed in the section 16–16. These coefficients are calculated by the following formula [10, 277]:

$$\zeta^\partial = \left[1 + \phi \left(v_\partial / v \right)^2 \right] / \left(v_\partial / v \right)^2, \quad (11)$$

where ϕ — coefficient, which depends on the rounding of the edges of the place of stream split; in the case of big

rounding radius $\phi = 0.3$; in the case of zero rounding radius $\phi = 1.5$; for our GS $\phi = 1.5$; v — fluid speed before split of the stream, m/s; v_∂ — fluid speed in one of the gates after split of the stream, m/s.

Table 1. – Characteristics of gating system in the case of work of the feeder I

Indicators	Operating feeders						
	I*	I**	I	II*	II	III*	III
ζ	0.819	0.912	0.693	0.819	0.639	0.844	0.637
μ	0.742	0.723	0.769	0.742	0.781	0.736	0.782
v	$\frac{1.883}{1.89}$	$\frac{1.836}{1.83}$	$\frac{1.952}{1.98}$	$\frac{1.883}{1.88}$	$\frac{1.983}{1.99}$	$\frac{1.870}{1.86}$	$\frac{1.986}{2.01}$
$Q \cdot 10^{-6}$	$\frac{120.58}{121.04}$	$\frac{117.59}{117.20}$	$\frac{124.99}{126.80}$	$\frac{120.58}{120.40}$	$\frac{127.01}{127.44}$	$\frac{119.74}{119.12}$	$\frac{127.19}{128.72}$
$N, \%$	-0.4	0.3	-1.4	0.2	-0.3	0.5	-1.2

Note: * — the hydraulic system is open circuited in the section 16–16; ** — the hydraulic system is open circuited in the section 5–5.

The fluid flow:

$$Q = v_{cm} S_{cm} = v_5 S_\kappa + v_{16} S_\kappa = 2v_5 S_\kappa = v_{17} S_n + v_{21} S_n = 2v_{17} S_n.$$

$v_5 / v_{cm} = S_{cm} / 2S_\kappa = 1.128277$ — this is a ratio v_∂ / v in the formula (11). We arrive at the following conclusion:
 $\zeta_{4-5(5)}^\partial = \zeta_{4-16(16)}^\partial = 2.285540.$

The formula (9) will be written as follows:

$$H = \alpha \frac{v_{17}^2}{2g} + \left[\left(\zeta_{cm} + \lambda \frac{l_{cm}}{d_{cm}} \right) \left(\frac{2S_n}{S_{cm}} \right)^2 + \left(\zeta_{4-5(5)}^\partial + \lambda \frac{l_{cm-1}}{d_\kappa} + 2\zeta \right) \left(\frac{S_n}{S_\kappa} \right)^2 + \zeta_n + \lambda \frac{l_n}{d_n} + 1 \right].$$

The function in square brackets (except for “1”) is $\zeta_{1-17(17)}$, the system resistance coefficient from the section 1–1 to the section 17–17, adduced to the speed v_{17} and considering the work of both feeders (I and V). We formulate:

$$\zeta_{1-17(17)} = \zeta_{1-21(21)} = 1.035783,$$

$$\mu_{1-17(17)} = \mu_{1-21(21)} = 0.700865,$$

$$v_{17} = v_{21} = 1.779679 \text{ m/s},$$

$$Q_{17} = Q_{21} = 113.974307 \cdot 10^{-6},$$

$$Q = 2Q_{17} = 227.948615 \cdot 10^{-6} \text{ m}^3/\text{s}.$$

If the I and II feeders work and the hydraulic system is open circuited in the section 16–16, then this is a ramified GS. $v_{10} = v_{12} = v_{16} = 0$. Let us work out Bernoulli's equation for the sections 1–1 and 17–17:

$$H = \left(\zeta_{cm} + \lambda \frac{l_{cm}}{d_{cm}} \right) \alpha \frac{v_{cm}^2}{2g} + \left(\zeta_{4-5(5)}^\partial + \lambda \frac{l_{cm-A}}{d_\kappa} + \zeta \right) \alpha \frac{v_5^2}{2g} + \left(\zeta_{7-8(8)}^\partial + \lambda \frac{l_{A-1}}{d_\kappa} \right) \alpha \frac{v_8^2}{2g} + \left(\zeta_n + \lambda \frac{l_n}{d_n} + 1 \right) \alpha \frac{v_{17}^2}{2g}, \quad (12)$$

and for the sections 1–1 and 18–18:

$$H = \left(\zeta_{cm} + \lambda \frac{l_{cm}}{d_{cm}} \right) \alpha \frac{v_{cm}^2}{2g} + \left(\zeta_{4-5(5)}^\partial + \lambda \frac{l_{cm-A}}{d_\kappa} + \zeta \right) \alpha \frac{v_5^2}{2g} + \left(\zeta_{7-9(9)}^\partial + \lambda \frac{l_{A-II}}{d_\kappa} \right) \alpha \frac{v_9^2}{2g} + \left(\zeta_n + \lambda \frac{l_n}{d_n} + 1 \right) \alpha \frac{v_{18}^2}{2g}. \quad (13)$$

Here v_8, v_9 — fluid speeds in the sections 8–8 and 9–9, m/s; $v_8 = v_9$; l_{cm-A} — distance from the down gate to the point A on the way through the sections 5–5, 6–6, 7–7; $l_{cm-A} = 0.378$ m; l_{A-1}, l_{A-II} — distance from the point A to the feeders I and II; $l_{A-1} = l_{A-II} = 0.116$ m; $\zeta_{7-8(8)}^\partial$ — the resistance coefficient for split of the stream in the collector in the section 7–7 between the sections 8–8 and 9–9, adduced to the metal speed in the section 8–8; $\zeta_{7-9(9)}^\partial$ — the resistance coefficient for split of the stream in the collector in the section 7–7 between the sections 8–8 and 9–9, adduced to the fluid speed in the section 9–9. The fluid flow:

$$\begin{aligned}
 Q &= v_{cm} S_{cm} = v_5 S_{\kappa} = v_7 S_{\kappa} = v_8 S_{\kappa} + v_9 S_{\kappa} = \\
 &= 2v_8 S_{\kappa} = v_{17} S_n + v_{18} S_n = 2v_{17} S_n. \\
 v_8 / v_7 &= S_{\kappa} / 2S_{\kappa} = 0.5, \quad \zeta_{7-8(8)}^{\partial} = \zeta_{7-9(9)}^{\partial} = 5.5 \text{ — according} \\
 &\text{to the formula (11).}
 \end{aligned}$$

Now the formula (12) may be written as follows:

$$H = \alpha \frac{v_{17}^2}{2g} \left[\begin{aligned} &\left(\zeta_{cm} + \lambda \frac{l_{cm}}{d_{cm}} \right) \left(\frac{2S_n}{S_{cm}} \right)^2 + \\ &+ \left(\zeta_{4-5(5)} + \lambda \frac{l_{cm-A}}{d_{\kappa}} + \zeta \right) \left(\frac{2S_n}{S_{\kappa}} \right)^2 + \\ &+ \left(\zeta_{7-8(8)}^{\partial} + \lambda \frac{l_{A-1}}{d_{\kappa}} \right) \left(\frac{S_n}{S_{\kappa}} \right)^2 + \zeta_n + \lambda \frac{l_n}{d_n} + 1 \end{aligned} \right].$$

The ratio in square brackets (except for “1”) — $\zeta_{1-17(17)}$, the system resistance coefficient from the section 1–1 to the section 17–17, adduced to the speed v_{17} and considering the work of both feeders (I and II). Formulate:

$$\begin{aligned}
 \zeta_{1-17(17)} &= \zeta_{1-18(18)} = 1.910914, \\
 \mu_{1-17(17)} &= \mu_{1-18(18)} = 0.586118, \quad v_{17} = v_{18} = 1.488307 \text{ m/s,} \\
 Q_{17} &= Q_{18} = 95.314284 \cdot 10^{-6} \text{ m}^3/\text{s,} \\
 Q &= 2Q_{17} = 190.628568 \cdot 10^{-6} \text{ m}^3/\text{s.}
 \end{aligned}$$

The work of the feeders I, II, III and the rupture of the hydraulic system in the section 16–16 lead to the formation of combined GS. $v_5 = v_6 = v_7$, $v_{11} = v_{14} = v_{16} = 0$, $v_8 \neq v_9 \neq v_{10}$. Bernoulli's equation for the sections 1–1 and 17–17 is already formulated — this is a formula (12). The formula (13) is valid for the sections 1–1 and 18–18; however, it is necessary to replace in it the local resistance coefficient of the feeder ζ_n by the resistance coefficient ζ_{18} (for ramification of some part of the stream from the section 9–9 of the collector to the feeder II). Bernoulli's equation for the feeder III for the sections 1–1 and 19–19 is as follows:

$$\begin{aligned}
 H &= \left(\zeta_{cm} + \lambda \frac{l_{cm}}{d_{cm}} \right) \alpha \frac{v_{cm}^2}{2g} + \\
 &+ \left(\zeta_{4-5(5)} + \lambda \frac{l_{cm-A}}{d_{\kappa}} + \zeta \right) \alpha \frac{v_5^2}{2g} + \\
 &+ \left(\zeta_{7-9(9)}^{\partial} + \lambda \frac{l_{A-1}}{d_{\kappa}} \right) \alpha \frac{v_9^2}{2g} + \\
 &+ \left(\zeta_{10} + \lambda \frac{l_{10-III}}{d} \right) \alpha \frac{v_{10}^2}{2g} + \left(\zeta_n + \lambda \frac{l_n}{d_n} + 1 \right) \alpha \frac{v_{19}^2}{2g}.
 \end{aligned} \quad (14)$$

Here ζ_{10} — the resistance coefficient for the passage of the stream in the collector from the section 9–9 to the section 10–10 in the case of ramification of some part of the stream from the section 9–9 to the feeder II.

Resistance coefficients, resulting from ramification of the stream from the collector to the feeder and for the passage of the stream, will be calculated using the formulas for the circulating T-joint [6, 112–115]. Resistance coefficient for the passage in the collector in the case of ramification of some part of the stream to the feeder:

$$\zeta_{np} = 0,4 \left(1 - v_{np} / v_{\kappa} \right)^2 / \left(v_{np} / v_{\kappa} \right)^2, \quad (15)$$

and resistance coefficient for ramification of some part of the stream to the feeder:

$$\zeta_{oms} = \left[1 + \tau \left(v_n / v_{\kappa} \right)^2 \right] / \left(v_n / v_{\kappa} \right)^2, \quad (16)$$

where v_{κ} and v_{np} — metal speeds in the collector before and after ramification of some part of the stream to the feeder, m/s; v_n — fluid speed in the feeder, m/s; τ — coefficient. For our case at $S_n / S_{\kappa} = 0.317$, $\tau = 0.15$ [12]. The coefficient ζ_{np} turns out adduced to the speed of the passing stream v_{np} , and ζ_{oms} — to the speed in the feeder v_n . As we can see, the coefficients ζ_{np} and ζ_{oms} depend on the unknown speed ratios v_{np} / v_{κ} and v_n / v_{κ} , namely, on v_{10} / v_9 and v_{18} / v_9 .

Let us introduce the following notations: $x_1 = v_{18} / v_{19}$, $x_2 = v_{17} / v_{19}$. Fluid flow in the system:

$$\begin{aligned}
 Q &= v_{cm} S_{cm} = v_5 S_{\kappa} = v_{17} S_n + v_{18} S_n + v_{19} S_n = \\
 &= S_n \left(v_{17} + x_1 \cdot v_{17} / x_2 + v_{18} / x_2 \right) = \\
 &= v_{17} S_n \left(x_2 + x_1 + 1 \right) / x_2 = v_{17} S_{np(17)},
 \end{aligned}$$

where $S_{np(17)} = S_n \left(x_2 + x_1 + 1 \right) / x_2$ — the area of feeders, adduced to the speed v_{17} . Similarly we write down: $Q = S_n \left(v_{17} + v_{18} + v_{19} \right) = S_n \left(x_2 \cdot v_{18} / x_1 + v_{18} + v_{18} / x_1 \right) =$

$$= v_{18} S_n \left(x_2 + x_1 + 1 \right) / x_1 = v_{18} S_{np(18)}.$$

Here $S_{np(18)} = S_n \left(x_2 + x_1 + 1 \right) / x_1$ — the area of feeders, adduced to the speed v_{18} . For the feeder III the area of feeders, adduced to the speed v_{19} — $S_{np(19)} = S_n \left(x_2 + x_1 + 1 \right)$.

$$\begin{aligned}
 v_{cm} &= v_{17} S_{np(17)} / S_{cm} = v_{18} S_{np(18)} / S_{cm} = v_{19} S_{np(19)} / S_{cm}, \\
 v_5 &= v_{17} S_{np(17)} / S_{\kappa} = v_{18} S_{np(18)} / S_{\kappa} = v_{19} S_{np(19)} / S_{\kappa}.
 \end{aligned}$$

Ratios x_1 , x_2 , v_8 / v_7 , v_9 / v_7 , v_{18} / v_9 , v_{10} / v_9 are unknown. Let us assume, that $x_1 = x_2 = 1$.

$$\begin{aligned}
 \frac{v_8}{v_7} &= \frac{Q_8}{Q_7} = \frac{Q_{17}}{Q_{17} + Q_{18} + Q_{19}} = \frac{v_{17} S_n}{v_{17} S_n + v_{18} S_n + v_{19} S_n} = \\
 &= \frac{x_2 v_{19}}{x_2 v_{19} + x_1 v_{19} + 1} = \frac{x_2}{x_2 + x_1 + 1}.
 \end{aligned}$$

Similarly we determine: $\frac{v_9}{v_7} = \frac{x_1 + 1}{x_2 + x_1 + 1}$. At

$x_1 = x_2 = 1$, $v_8 / v_7 = 1/3$, $v_9 / v_7 = 2/3$. $\zeta_{7-8(8)}^{\partial} = 10.5$, $\zeta_{7-9(9)}^{\partial} = 3.75$ — according to the formula (11).

$$v_8 = v_{17} S_n / S_{\kappa}.$$

$$v_9 = \frac{(v_{18} + v_{19})S_n}{S_\kappa} = \frac{(v_{18} + v_{18}/x_1)S_n}{S_\kappa} = v_{18} \frac{(1 + 1/x_1)S_n}{S_\kappa}.$$

$$v_9 = \frac{(v_{18} + v_{19})S_n}{S_\kappa} = \frac{(x_1 v_{19} + v_{19})S_n}{S_\kappa} = v_{19} \frac{(1 + x_1)S_n}{S_\kappa}.$$

$$v_{10} = v_{19} S_n / S_\kappa.$$

Now Bernoulli's equation for the feeders I, II and III may be formulated as follows:

$$H = \alpha \frac{v_{17}^2}{2g} \left[\begin{aligned} & \left(\zeta_{cm} + \lambda \frac{l_{cm}}{d_{cm}} \right) \left(\frac{S_{np(17)}}{S_{cm}} \right)^2 + \\ & + \left(\zeta_{4-5(5)} + \lambda \frac{l_{cm-A}}{d_\kappa} + \zeta \right) \left(\frac{S_{np(17)}}{S_\kappa} \right)^2 + \\ & + \left(\zeta_{7-8(8)}^\partial + \frac{l_{A-1}}{d_\kappa} \right) \left(\frac{S_n}{S_\kappa} \right)^2 + \zeta_n + \lambda \frac{l_n}{d_n} + 1 \end{aligned} \right],$$

$$H = \alpha \frac{v_{18}^2}{2g} \left[\begin{aligned} & \left(\zeta_{cm} + \lambda \frac{l_{cm}}{d_{cm}} \right) \left(\frac{S_{np(18)}}{S_{cm}} \right)^2 + \\ & + \left(\zeta_{4-5(5)} + \lambda \frac{l_{cm-A}}{d_\kappa} + \zeta \right) \left(\frac{S_{np(18)}}{S_\kappa} \right)^2 + \\ & + \left(\zeta_{7-9(9)}^\partial + \frac{l_{A-II}}{d_\kappa} \right) \left(\frac{(1+1/x_1)S_n}{S_\kappa} \right)^2 + \\ & + \zeta_{18} + \lambda \frac{l_n}{d_n} + 1 \end{aligned} \right],$$

$$H = \alpha \frac{v_{19}^2}{2g} \left[\begin{aligned} & \left(\zeta_{cm} + \lambda \frac{l_{cm}}{d_{cm}} \right) \left(\frac{S_{np(19)}}{S_{cm}} \right)^2 + \\ & + \left(\zeta_{4-5(5)} + \lambda \frac{l_{cm-A}}{d_\kappa} + \zeta \right) \left(\frac{S_{np(19)}}{S_\kappa} \right)^2 + \\ & + \left(\zeta_{7-9(9)}^\partial + \frac{l_{A-III}}{d_\kappa} \right) \left(\frac{(1+x_1)S_n}{S_\kappa} \right)^2 + \\ & + \left(\zeta_{10} + \lambda \frac{l_{III}}{d_\kappa} \right) \left(\frac{S_n}{S_\kappa} \right)^2 + \zeta_n + \lambda \frac{l_n}{d_n} + 1 \end{aligned} \right].$$

The ratios in square brackets (except for "1") are resistance coefficients $\zeta_{1-17(17)}$, $\zeta_{1-18(18)}$ and $\zeta_{1-19(19)}$. At $x_1 = x_2 = 1$, $Q_{10} = 0,5Q_9$, $v_{10} / v_9 = 0,5$. Using the formula (15) we find out, that $\zeta_{10} = 0,4$. $\frac{Q_{18}}{Q_9} = \frac{v_{18} S_n}{v_9 S_\kappa} = 1 - Q_{10} / Q_9$,

$$\frac{v_{18}}{v_9} = \frac{v_{18} S_n}{v_9 S_\kappa} = (1 - Q_{10} / Q_9) \frac{S_\kappa}{S_n}. \quad v_{18} / v_9 = 1,575657, \text{ and}$$

$\zeta_{18} = 0,552788$ — according to the formula (16). Calculation results:

$$\zeta_{1-17(17)} = 3,460359, \quad \zeta_{1-18(18)} = 4,197866,$$

$$\zeta_{1-19(19)} = 4,04667, \quad \mu_{1-17(17)} = 0,473495,$$

$$\mu_{1-18(18)} = 0,438619, \quad \mu_{1-19(19)} = 0,445273,$$

$$v_{17} = 1,202326 \text{ m/s}, \quad v_{18} = 1,113768 \text{ m/s},$$

$$v_{19} = 1,130665 \text{ m/s}.$$

$$x_1 = v_{18} / v_{19} = 0,985055, \quad x_2 = v_{17} / v_{19} = 1,063380.$$

And we prescribed the values $x_1 = x_2 = 1$. We assume that $x_1 = 0,985055$, $x_2 = 1,063380$, perform calculation once again and receive the results: $x_1 = 0,974609$, $x_2 = 1,102053$. After successive approximations we determine that $x_1 = 0,946411$, $x_2 = 1,150917$. At the same time:

$$\zeta_{1-17(17)} = 2,915719, \quad \zeta_{1-18(18)} = 4,790815,$$

$\zeta_{1-19(19)} = 4,186801$. The results of calculations and experiments are presented in the table 2. Similarly we calculate the work of GS with the feeders I–IV and I–V. Note that for the feeders I–III: $v_{17} / v_{19} = 1,151$, for the feeders I–IV: $v_{17} / v_{20} = 1,342$, for the feeders I–V: $v_{17} / v_{21} = 1,553$.

Bernoulli's equation in the case of work of the feeder I for the sections 1–1 and 17–17 of GS on the way through the sections 2–2, 5–5, 7–7, 8–8:

$$H = \alpha v_{17}^2 / 2g + h_{1-17(5-8)}. \quad (17)$$

Bernoulli's equation for the sections 1–1 and 17–17 of GS on the way through the sections 2–2, 16–16, 14–14, 12–12, 8–8:

$$H = \alpha v_{17}^2 / 2g + h_{1-17(16-8)}. \quad (18)$$

Pressure losses when the fluid flows from the section 1–1 to 17–17 on the way through the sections 2–2, 5–5, 7–7, 8–8:

$$h_{1-17(5-8)} = \left(\zeta_{cm} + \lambda \frac{l_{cm}}{d_{cm}} \right) \alpha \frac{v_{cm}^2}{2g} +$$

$$+ \left(\zeta_{4-5(5)}^\partial + \zeta + \lambda \frac{l_{cm-A}}{d_\kappa} \right) \alpha \frac{v_5^2}{2g} + \quad (19)$$

$$+ \left(\zeta_{7-8(8)}^\partial + \lambda \frac{l_{A-1}}{d_\kappa} \right) \alpha \frac{v_8^2}{2g} + \left(\zeta_n + \lambda \frac{l_n}{d_n} \right) \alpha \frac{v_{17}^2}{2g}.$$

Pressure losses when the fluid flows from 1–1 to 17–17 on the way through the sections 2–2, 16–16, 14–14, 12–12, 8–8:

$$h_{1-17(16-8)} = \left(\zeta_{cm} + \lambda \frac{l_{cm}}{d_{cm}} \right) \alpha \frac{v_{cm}^2}{2g} +$$

$$+ \left(\zeta_{4-16(16)}^\partial + 2\zeta + \lambda \frac{l_{cm-A(16-9)}}{d_\kappa} \right) \alpha \frac{v_{16}^2}{2g} + \quad (20)$$

$$+ \left(\zeta_{9-8(8)}^{np} + \lambda \frac{l_{A-1}}{d_\kappa} \right) \alpha \frac{v_8^2}{2g} + \left(\zeta_n + \lambda \frac{l_n}{d_n} \right) \alpha \frac{v_{17}^2}{2g}.$$

Table 2. – Characteristics of gating system

Indicators	Operating feeders							
	I, II*	I, II	I-III*	I-III	I-IV*	I-IV	I-V*	I-V
$\zeta_{1-17(17)}$	1.911	1.258	2.916	1.960	3.588	2.682	3.956	3.696
$\mu_{1-17(17)}$	0.586	0.665	0.505	0.581	0.467	0.521	0.449	0.461
v_{17}	$\frac{1.488}{1.50}$	$\frac{1.690}{1.74}$	$\frac{1.283}{1.25}$	$\frac{1.476}{1.50}$	$\frac{1.185}{1.12}$	$\frac{1.323}{1.32}$	$\frac{1.141}{1.09}$	$\frac{1.172}{1.17}$
$\zeta_{1-18(18)}$	1.911	1.025	4.791	1.746	11.029	2.638	22.357	4.421
$\mu_{1-18(18)}$	0.586	0.703	0.416	0.603	0.288	0.524	0.207	0.429
v_{18}	$\frac{1.488}{1.48}$	$\frac{1.784}{1.83}$	$\frac{1.055}{1.09}$	$\frac{1.532}{1.56}$	$\frac{0.732}{0.76}$	$\frac{1.331}{1.32}$	$\frac{0.525}{0.55}$	$\frac{1.091}{1.12}$
$\zeta_{1-19(19)}$			4.187	1.713	8.226	2.564	16.147	4.435
$\mu_{1-19(19)}$			0.439	0.607	0.329	0.530	0.241	0.429
v_{19}			$\frac{1.115}{1.14}$	$\frac{1.542}{1.51}$	$\frac{0.836}{0.85}$	$\frac{1.345}{1.33}$	$\frac{0.613}{0.64}$	$\frac{1.089}{1.17}$
$\zeta_{1-20(20)}$					7.264	3.272	12.157	4.421
$\mu_{1-20(20)}$					0.348	0.484	0.276	0.429
v_{20}					$\frac{0.883}{0.92}$	$\frac{1.229}{1.25}$	$\frac{0.700}{0.72}$	$\frac{1.091}{1.14}$
$\zeta_{1-21(21)}$							10.957	3.696
$\mu_{1-21(21)}$							0.289	0.461
v_{21}							$\frac{0.734}{0.74}$	$\frac{1.172}{1.15}$
$Q \cdot 10^{-6}$	$\frac{190.63}{190.85}$	$\frac{222.48}{228.63}$	$\frac{221.16}{222.87}$	$\frac{291.38}{292.67}$	$\frac{232.92}{233.75}$	$\frac{334.82}{334.30}$	$\frac{237.83}{239.52}$	$\frac{359.53}{368.24}$
$N, \%$	-0.1	-2.7	-0.8	-0.4	-0.4	0.2	-0.7	-2.4

Note: * — the hydraulic system is open circuited in the section 16–16.

Here $l_{cm-A(16-9)}$ — distance from the down gate to the point A on the way through the sections 16–16, 14–14, 12–12, 9–9; $l_{cm-A(16-9)} = 0.876$ m.

In the formula (19) $\zeta_{7-8(8)}^6$ — the resistance coefficient in a sideward ramification in the confluence of the stream from the section 7–7 with the stream from the section 9–9 in the section 8–8. And in the equation (20) $\zeta_{9-8(8)}^{np}$ — the resistance coefficient for the passage in the confluence of the stream from the section 9–9 with the stream from the section 7–7 in the section 8–8. The coefficients of resistances, which are conditioned by confluence of the streams in the collector, will be calculated using the formulas for the circulating T-joint [6, 114–115]. Resistance coefficient for the passage in the collector in the case of confluence of the steams:

$$\zeta_{np(cn)} = 1.55v_{\delta} / v_{\kappa} - (v_{\delta} / v_{\kappa})^2, \quad (21)$$

and resistance coefficient in a sideward ramification (at $v_{\delta} > 0.4v_{\kappa}$):

$$\zeta_{om\theta(cn)} = 0.75 \left[1 + (v_{\delta} / v_{\kappa})^2 - 2(1 - v_{\delta} / v_{\kappa})^2 \right], \quad (22)$$

where: v_{κ} — metal speed in the collector after the confluence of streams, m/s; v_{δ} — fluid speed in a sideward ramification, m/s. Coefficients $\zeta_{np(cn)}$ and $\zeta_{om\theta(cn)}$ are added to the stream speed after the confluence of streams.

Let us introduce the following notation:

$z = v_5 / v_{16}$. Fluid flow in the system:

$$\begin{aligned} Q &= v_{cm} S_{cm} = v_{17} S_n = (v_5 + v_{16}) S_{\kappa} = \\ &= (z \cdot v_{16} + v_{16}) S_{\kappa} = v_{16} (z + 1) S_{\kappa}. \end{aligned}$$

Let us assume that $v_5 = 1,1v_{16}$, i. e. $z = 1,1$. Then:

$v_{16} / v_{cm} = S_{cm} / (z + 1) S_{\kappa} = 1.074550$. Using the formula (11) we find out that $\zeta_{4-16(16)}^{\delta} = 2.366058$.

Similarly we determine the following:

$$\begin{aligned} v_{cm} S_{cm} &= (v_5 + v_{16}) S_{\kappa} = (v_5 + v_5 / z) S_{\kappa} \\ &= v_5 (1 + 1/z) S_{\kappa}, \\ v_5 / v_{cm} &= S_{cm} / (1 + 1/z) S_{\kappa} = 1.182005, \\ \zeta_{4-5(5)}^{\delta} &= 2.215750. \quad v_{cm} = v_{17} S_n / S_{cm}, \quad v_8 = v_{17} S_n / S_{\kappa}, \\ v_5 &= v_{cm} S_{cm} / (1 + 1/z) S_{\kappa} = v_{17} S_n / (1 + 1/z) S_{\kappa}. \end{aligned}$$

Now the formula (19) may be written as follows:

$$h_{1-17(5-8)} = \alpha \frac{v_{17}^2}{2g} \left[\begin{aligned} &\left(\zeta_{cm} + \lambda \frac{l_{cm}}{d_{cm}} \right) \left(\frac{S_n}{S_{cm}} \right)^2 + \\ &+ \left(\zeta_{4-5(5)}^{\delta} + \zeta + \lambda \frac{l_{cm-A}}{d_{\kappa}} \right) \times \\ &\quad \times \left(\frac{S_n}{(1 + 1/z) S_{\kappa}} \right)^2 + \\ &+ \left(\zeta_{7-8(8)}^{\delta} + \lambda \frac{l_{A-1}}{d_{\kappa}} \right) \left(\frac{S_n}{S_{\kappa}} \right)^2 + \\ &\quad + \zeta_n + \lambda \frac{l_n}{d_n} \end{aligned} \right]. \quad (23)$$

The function in square brackets will be denoted as $\zeta_{1-17(5-8)}$ — the system resistance coefficient when the fluid flows from the section 1-1 to the section 17-17 through the sections 2-2, 5-5, 7-7, 8-8. The coefficient is added to the fluid speed in the section 17-17.

$$\frac{v_7}{v_8} = \frac{v_5}{v_5 + v_{16}} = \frac{v_5}{v_5 + v_5 / z} = \frac{1}{1 + 1/z}.$$

At $z = 1.1$ using the formulas (21) and (22) we determine the following: $\zeta_{9-8(8)}^{np} = 0.537528$, $\zeta_{7-8(8)}^{\delta} = 0.247392$. Using the formulas (23), (7), (8) and (3) we find out: $\zeta_{1-17(17)} = 0.659403$, $\mu_{1-17(17)} = 0.776290$, $v_{17} = 1.971203$ m/s,

$$Q_{17} = 126.239922 \cdot 10^{-6} \text{ m}^3/\text{s}.$$

The value z was taken randomly. It must be determined through calculations. The ring consists of 2 half-rings: the first half-ring — from the down gate through the sections 5-5, 6-6 and 7-7 to the point A, the second half-ring — from the down gate through the sections 16-16, 14-14, 12-12 and 9-9 to the point A. Pressure losses in these half-rings — parallel pipelines — must be equal. Pressure losses in the first half-ring:

$$h_{cm-A(5-7)} = \left(\zeta_{4-5(5)}^{\delta} + \zeta + \lambda \frac{l_{cm-A}}{d_{\kappa}} + \zeta_{7-8(7)}^{\delta} \right) \alpha \frac{v_5^2}{2g}.$$

Pressure losses in the second half-ring:

$$h_{cm-A(16-9)} = \left(\zeta_{4-16(16)}^{\delta} + 2\zeta + \lambda \frac{l_{cm-A(16-9)}}{d_{\kappa}} + \zeta_{9-8(9)}^{np} \right) \alpha \frac{v_{16}^2}{2g}.$$

Coefficients $\zeta_{7-8(8)}^{\delta}$ and $\zeta_{9-8(8)}^{np}$ must be added to the speeds before confluence of the streams, using the following equations:

$$\begin{aligned} \zeta_{7-8(7)}^{\delta} &= \zeta_{7-8(8)}^{\delta} (v_7 / v_8)^2, \quad \zeta_{9-8(9)}^{np} = \zeta_{9-8(8)}^{np} (v_9 / v_8)^2. \\ \zeta_{7-8(7)}^{\delta} &= 0.901653, \quad \zeta_{9-8(9)}^{np} = 2.3705. \\ v_5 &= 0.327652 \text{ m/s}, \quad v_{16} = 0.297866 \text{ m/s}, \\ v_8 &= 0.625518 \text{ m/s}. \end{aligned}$$

After calculations we obtain the following results:

$$\begin{aligned} h_{cm-A(5-7)} &= 0.028348 \text{ m}, \quad h_{cm-A(16-9)} = 0.040521 \text{ m}, \\ h_{5-16} &= h_{cm-A(5-7)} - h_{cm-A(16-9)} = -0.012173 \text{ m}. \end{aligned}$$

Losses $h_{cm-A(5-7)}$ are less than the losses $h_{cm-A(16-9)}$. In order to make them equal, it is necessary to increase the speed v_5 and decrease the speed v_{16} .

Changing z , we alter the speeds and pressure losses in the half-rings of the hydraulic system. At $z = v_5 / v_{16} = 1.384552615$, $h_{5-16} = 1.99 \cdot 10^{-10}$ m. The difference of pressure in 10^{-10} m. is surely meaningless. It was necessary to verify efficiency of the proposed calculation method.

Bernoulli's equation in the form (17), (18) and pressure losses in the form (19), (20) are questionable. The characteristics of the feeder I may be calculated using the formulas (18) and (20). Let us compare the characteristics of the feeder I, using the formulas (17), (19) and (18), (20):

$\zeta_{1-17(5-8)} = 0.6926712053$, $\zeta_{1-17(16-8)} = 0.6926712043$. The difference is in the ninth sign after the coma. But the calculation of pressure losses for the same feeder is conducted in different hydraulic lines. Apparently, the equations in the form (17)–(20) are valid.

The results of calculations and experiments are presented in the table 1.

During work of the feeders I and II two different streams exist in the ring: one is counterclockwise (16-14-12-10), and the other one is clockwise (5-6-7), moreover, the flow is divided into two parts at the point A. In the feeder II the confluence of the streams from sections 9-9 and 10-10 takes place. The streams meet on entering into the feeder II at the point C, which is called the water-parting point or the zero point [7, 240-241]. In the mind's eye we cut our ring along the designated water-parting line and get the circuit, which is depicted in the figure 3. Then using common formulas, we calculate pressure losses for the line 16-14-12-10 h_{16-10} and for the line 5-7-9 h_{5-9} . Then we compare two obtained values of the

pressure losses. If $h_{16-10} = h_{5-9}$, we conclude that pressure in the points C' and C'' will be identical, as it must be, since the points C' and C'' physically constitute one point C . Therefore, after obtaining the specified equality, we may state that we designated right values of liquid flow Q_5, Q_9 and Q_{16} . If the specified equality fails, then we have to change the liquid flow values. We make the 2nd, 3rd and subsequent attempts to ensure that the above mentioned equality is achieved with a given accuracy.

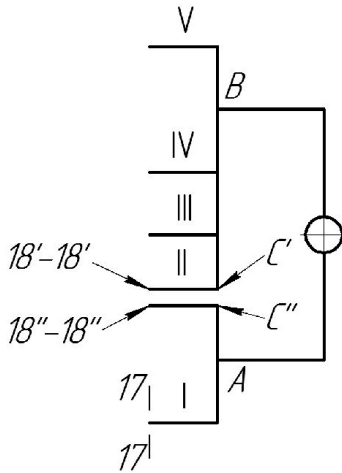


Fig. 3. Calculation scheme for the ring system during the work of the feeders I and II

Bernoulli's equation for the sections $I-I$ and $17-17$ of the feeder I (for the way through the sections 2-2, 5-5, 7-7, 8-8):

$$H = \left(\zeta_{cm} + \lambda \frac{l_{cm}}{d_{cm}} \right) \alpha \frac{v_{cm}^2}{2g} + \left(\zeta_{4-5(5)}^{\partial} + \lambda \frac{l_{cm-A}}{d_{\kappa}} + \zeta \right) \alpha \frac{v_5^2}{2g} + \left(\zeta_{7-8(8)}^{\partial} + \lambda \frac{l_{A-1}}{d_{\kappa}} \right) \alpha \frac{v_8^2}{2g} + \left(\zeta_n + \lambda \frac{l_n}{d_n} + 1 \right) \alpha \frac{v_{17}^2}{2g}. \quad (24)$$

Bernoulli's equation for the feeder II (for the way through the sections 2-2, 16-16, 14-14, 12-12, 10-10):

$$H = \left(\zeta_{cm} + \lambda \frac{l_{cm}}{d_{cm}} \right) \alpha \frac{v_{cm}^2}{2g} + \left(\zeta_{4-16(16)}^{\partial} + \lambda \frac{l_{cm-II(16-10)}}{d_{\kappa}} + 2\zeta \right) \alpha \frac{v_{16}^2}{2g} + \left(\zeta_n + \lambda \frac{l_n}{d_n} + 1 \right) \alpha \frac{v_{18}^2}{2g}. \quad (25)$$

Here $l_{cm-II(16-10)}$ — distance from the down gate to the feeder II on the way through the sections 16-16, 14-14, 12-12, 10-10, m. $l_{cm-II(16-10)} = 0.760$ m.

For the feeder II (on the way through the sections 2-2, 5-5, 7-7, 9-9) Bernoulli's equation may be formulated as follows:

$$H = \left(\zeta_{cm} + \lambda \frac{l_{cm}}{d_{cm}} \right) \alpha \frac{v_{cm}^2}{2g} + \left(\zeta_{4-5(5)}^{\partial} + \lambda \frac{l_{cm-A}}{d_{\kappa}} + \zeta \right) \alpha \frac{v_5^2}{2g} + \left(\zeta_{7-9(9)}^{\partial} + \lambda \frac{l_{A-II}}{d_{\kappa}} \right) \alpha \frac{v_9^2}{2g} + \left(\zeta_n + \lambda \frac{l_n}{d_n} + 1 \right) \alpha \frac{v_{18}^2}{2g}. \quad (26)$$

Let us introduce the following notations: $x = v_{17} / v_{18}$, $z = v_5 / v_{16}$, $w = v_8 / v_9$. Fluid flow in the system:

$$Q = v_{cm} S_{cm} = (v_{17} + v_{18}) S_n = (x \cdot v_{18} + v_{18}) S_n = v_{18} (x + 1) S_n = v_{18} S_{np(18)},$$

where $S_{np(18)} = (x + 1) S_{18}$ — the area of the feeders, adduced to the speed v_{18} . Similarly we write down:

$$Q = (v_{17} + v_{18}) S_n = (v_{17} + v_{17}/x) S_n = v_{17} S_n (1 + 1/x) = v_{17} S_{np(17)}.$$

Here $S_{np(17)} = (1 + 1/x) S_n$ — the area of the feeders, adduced to the speed v_{17} . Also we have:

$$Q = v_{cm} S_{cm} = (v_5 + v_{16}) S_{\kappa} = (v_5 + v_5/z) S_{\kappa} = v_5 (1 + 1/z) S_{\kappa},$$

$$\frac{Q_5}{Q} = \frac{v_5 S_{\kappa}}{v_{cm} S_{cm}} = \frac{v_5 S_{\kappa}}{v_5 (1 + 1/z) S_{\kappa}} = \frac{1}{1 + 1/z},$$

$$v_5 = \frac{v_{cm} S_{cm}}{(1 + 1/z) S_{\kappa}} = \frac{v_{17} S_{np(17)}}{(1 + 1/z) S_{\kappa}} = v_{17} \frac{z S_{np(17)}}{(1 + z) S_{\kappa}}.$$

Now the formula (24) may be written as follows:

$$H = \alpha \frac{v_{17}^2}{2g} \left[\left(\zeta_{cm} + \lambda \frac{l_{cm}}{d_{cm}} \right) \left(\frac{S_{np(17)}}{S_{cm}} \right)^2 + \left(\zeta_{4-5(5)}^{\partial} + \lambda \frac{l_{cm-A}}{d_{\kappa}} + \zeta \right) \left(\frac{z S_{np(17)}}{(1 + z) S_{\kappa}} \right)^2 + \left(\zeta_{7-8(8)}^{\partial} + \lambda \frac{l_{A-1}}{d_{\kappa}} \right) \left(\frac{S_n}{S_{\kappa}} \right)^2 + \zeta_n + \lambda \frac{l_n}{d_n} + 1 \right].$$

The ratio in square brackets (except for "1") — $\zeta_{1-17(17)}$, the system resistance coefficient from the section $I-I$ to the section $17-17$, adduced to the speed v_{17} and considering the work of both feeders (I and II).

$$\frac{v_8}{v_7} = \frac{Q_8}{Q_7} = \frac{v_8 S_{\kappa}}{v_8 S_{\kappa} + v_9 S_{\kappa}} = \frac{v_8}{v_8 + v_8/w} = \frac{1}{1 + 1/w}.$$

We assume (randomly) that: $x = 1$, $z = 1,1$, $w = 1$. In this case $S_{np(17)} = 2S_n$, $S_{np(18)} = 2S_n$. At $w = 1$, $v_8 / v_7 = 0,5$, $\zeta_{7-8(8)}^{\partial} = 5,5$ — according to the formula (11). Coefficients

$\zeta_{4-5(5)}^\partial$ and $\zeta_{4-16(16)}^\partial$ were already determined. Calculation results:

$\zeta_{1-17(17)} = 1.530863$, $\mu_{1-17(17)} = 0.628587$, $v_{17} = 1.596147$ in m/s, $Q_{17} = 102.220587 \cdot 10^{-6}$ m³/s.

For the feeder II on the way through the sections 2–2, 16–16, 14–14, 12–12, 10–10 the following ratios are valid:

$$Q = v_{cm} S_{cm} = (v_5 + v_{16}) S_\kappa = (z v_{16} + v_{16}) S_\kappa = v_{16} (z + 1) S_\kappa,$$

$$v_{16} / v_{cm} = S_{cm} / (1 + z) S_\kappa, v_{16} = v_{10} = \frac{v_{cm} S_{cm}}{(1 + z) S_\kappa} = \frac{v_{18} S_{np(18)}}{(1 + z) S_\kappa},$$

$$\frac{Q_{16}}{Q} = \frac{v_{16} S_\kappa}{v_{cm} S_{cm}} = \frac{v_{16} S_\kappa}{v_{16} (1 + z) S_\kappa} = \frac{1}{1 + z}.$$

The formula (25) will be formulated as follows:

$$H = \alpha \frac{v_{18}^2}{2g} + \left[\left(\zeta_{cm} + \lambda \frac{l_{cm}}{d_{cm}} \right) \left(\frac{S_{np(18)}}{S_{cm}} \right)^2 + \left(\zeta_{4-16(16)}^\partial + \lambda \frac{l_{cm-III(16-10)}}{d_\kappa} + 2\zeta \right) \times \left(\frac{S_{np(18)}}{(1 + z) S_\kappa} \right)^2 + \zeta_n + \lambda \frac{l_n}{d_n} + 1 \right] \times.$$

In square brackets (except for “1”) — the system resistance coefficient $\zeta_{1-18(18)}$ from the section 1–1 to the section 18–18, added to the speed v_{18} and considering a simultaneous work of the feeders I and II. We find: $\zeta_{1-18(18)} = 1.113125$, $\mu_{1-18(18)} = 0.687919$, $v_{18} = 1.746806$ m/s, $Q_{18} = 111.869076 \cdot 10^{-6}$ m³/s.

The flow in the system:

$$Q = Q_{17} + Q_{18} = 214.089664 \cdot 10^{-6} \text{ m}^3/\text{s}.$$

$v_5 = v_6 = v_7 = 0.555664$ m/s, $v_{10} = v_{14} = v_{16} = 0.505149$ in m/s, $x = v_{17} / v_{18} = 0.913752$,

$w = v_8 / v_9 = Q_{17} / (Q_{16} - Q_{18}) = 10.302815$.

In the ring hydraulic system the pressure losses $h_{cm-II(5-9)}$ from the down gate to the feeder II on the way through the sections 5–5, 7–7 and 9–9 should be equal to the pressure losses $h_{cm-II(16-10)}$ from the down gate to the feeder II on the way through the sections 16–16, 14–14 and 10–10. These pressure losses may be calculated using the following formulas:

$$h_{cm-II(5-9)} = \left(\zeta_{4-5(5)}^\partial + \lambda \frac{l_{cm-A}}{d_\kappa} + \zeta \right) \alpha \frac{v_5^2}{2g} + \left(\zeta_{8-9(9)}^\partial + \lambda \frac{l_{A-II}}{d_\kappa} \right) \alpha \frac{v_9^2}{2g}; \quad (27)$$

$$h_{cm-II(16-10)} = \left(\zeta_{4-16(16)}^\partial + \lambda \frac{l_{cm-III(16-10)}}{d_\kappa} + 2\zeta \right) \alpha \frac{v_{16}^2}{2g}. \quad (28)$$

All values in the formulas (27) and (28) are known. We find out that:

$h_{cm-II(5-9)} = 0.090665$ m, $h_{cm-II(16-10)} = 0.079521$ m, the difference between them $h_{II} = 0.011144$ m. The losses $h_{cm-II(5-9)}$ are greater, than $h_{cm-II(16-10)}$, it is necessary to decrease the fluid speed on the way through the sections 5–5, 6–6 and 7–7. At $x = 0.913752$, $w = 10.302815$ and $z = 1.1$ as per calculation $h_{II} = 0.004235$ m, $x = 0.938313$, $w = 12.186871$. Using such approximations with further changes of x , w and z we bring h_{II} to the value, which is less than 10^{-6} m. The table 2 presents calculation results for the feeders I and II at $x = 0.947055$, $z = 1.070017$ and $w = 15.943246$. $v_9 / v_7 = 0.059021$, i.e. only 5.9% of the fluid flow comes to the feeder II in the section 7–7, the rest — to the feeder I.

Characteristics of the feeder II may be also calculated using the formula (26). Let us compare the characteristics of the feeder II using the formulas (26) and (25): $\zeta_{1-18(5-9)} = 1.025445$, $\zeta_{1-18(16-10)} = 1.025438$. The difference is in the sixth sign after the comma. But the calculation of pressure losses for the same feeder was conducted in different hydraulic lines. Apparently, the formulas (24)–(26) can be regarded as proven — considering their experimental verification.

During work of the feeders I, II and III, the zero point is apparently in the feeder II. Bernoulli's equation for the feeders I and II is already formulated — these are the formulas (24) and (26). For the feeder III for the sections 1–1 and 19–19 (on the way through the sections 2–2, 16–16, 14–14, 12–12, 11–11) Bernoulli's equation is as follows:

$$H = \left(\zeta_{cm} + \lambda \frac{l_{cm}}{d_{cm}} \right) \alpha \frac{v_{cm}^2}{2g} + \left(\zeta_{4-16(16)}^\partial + \lambda \frac{l_{cm-III(16-11)}}{d_\kappa} + \zeta \right) \alpha \frac{v_{16}^2}{2g} + \left(\zeta_{19} + \lambda \frac{l_n}{d_n} + 1 \right) \alpha \frac{v_{19}^2}{2g}.$$

Here $l_{cm-III(16-11)}$ — distance from the down gate to the feeder III on the way through the sections 16–16, 14–14, 12–12, 11–11, m. $l_{cm-III(16-11)} = 0.631$ m. ζ_{19} — the resistance coefficient for ramification of some part of the stream from the section 11–11 of the collector to the feeder III.

Let us introduce the following notations: $x_1 = v_{18} / v_{19}$, $x_2 = v_{17} / v_{19}$, $z = v_5 / v_{16}$, $w_1 = v_8 / v_9$, $w_2 = v_{10} / v_{11}$. The added areas of the feeders will be as follows: $S_{np(17)} = S_n (x_2 + x_1 + 1) / x_2$, $S_{np(18)} = S_n (x_2 + x_1 + 1) / x_1$,

$$\begin{aligned}
S_{np(19)} &= S_n (x_2 + x_1 + 1). \text{ Let us write down the evident} \\
\text{equations: } & v_8 = v_7 w_1 / (1 + w_1), \quad v_9 = v_7 / (1 + w_1), \\
v_8 &= v_{17} S_n / S_\kappa, \quad v_{11} = w_2 v_{12}, \quad Q_5 = Qz / (1 + z), \\
Q &= v_{cm} S_{cm} = (v_5 + v_{16}) S_\kappa = \\
&= (v_5 + v_5 / z) S_\kappa = v_5 (1 + 1/z) S_\kappa, \\
Q_{16} &= Q / (1 + z), \quad v_5 = v_7, \quad v_{11} = v_{16}, \\
v_{cm} &= v_{17} S_{np(17)} / S_{cm} = v_{18} S_{np(18)} / S_{cm} = v_{19} S_{np(19)} / S_{cm}, \\
v_5 &= \frac{z v_{cm} S_{cm}}{(1+z) S_\kappa} = v_{17} \frac{z S_{np(17)}}{(1+z) S_\kappa} = \\
&= v_{18} \frac{z S_{np(18)}}{(1+z) S_\kappa} = v_{19} \frac{z S_{np(19)}}{(1+z) S_\kappa}.
\end{aligned}$$

Acting as abovementioned, we define the characteristics of GS in the course of work of the feeders I, II and III. Similarly we calculate GS with the feeders I–IV and I–V. The zero point in these systems is in the feeder III. The results are given the table 2.

Research results and their discussion

The difference between the experimental and calculation results is from — 2.7 % to +0.5 %. The difference is not big, and it is difficult to make any conclusions. In general, we may believe that a good conformity of theoretical and experimental data is obtained. And Bernoulli's equation, adduced for the particular case — for the system with one feeder, also works in the gating system with many feeders and in the most complex one — P-shaped system, in which there is not only a split of the stream in the collector into parts, but also a confluence of streams in the collector, and there are also operating feeders between the rings with the feeders.

Let us note the influence of circularity of a hydraulic circuit on the characteristics of GS. In the case of work of 1, 2, 3, 4 and 5 feeders, the flow in a closed-circuit system, as opposed to an open-circuit system, is higher by 3.7, 16.7, 31.8, 43.7 and 51.2 % respectively — due the work of the second parallel collector (see the table 1 and 2).

Regardless of the number of working feeders, the calculation is based on Bernoulli's equation in the form of the formula (1). Initially we randomly assume speed ratios in feeders and collector after split or confluence of streams, and determine the fluid flow in each feeder and all system. Then we divide the system into two half-rings. The pressure losses in half-rings must be equal to each other. We try to achieve it by increasing or decreasing the fluid speed in separate lines of GS. This difference of pressure losses in half-rings may be adduced to any pre-assigned infinitely small value.

Pressure losses, fluid speed and flow in each feeder can be calculated when fluid flows in two parallel hydraulic lines (but not against flow of the stream). Although the fluid speeds in different parts of the collector can differ from each other by many times. And the difference of the feeder characteristics in the case of its calculation by different hydraulic lines can also be adduced to any pre-assigned infinitely small value. This unexpected result requires surely a further verification and discussion.

So, we use Bernoulli's equation for stream sections with different flow and for different hydraulic lines in the same system, and, surprisingly enough, the experiments confirm this seemingly absurd assumption. And due to this it became possible to calculate the P-shaped ring GS. Without any additional principles. Only evident features:

$$Q = \sum_{i=1}^n Q_i,$$

where Q_i — the fluid flow in i -feeder. In any section of hydraulic system the pressure H consists of velocity and piezometric pressures and pressure losses.

In calculations apart from 2 conventional hydraulic losses — for friction along the length and in local resistances, we consider the losses for the pressure change, which are calculated using the formulas (11), (15) and (16) — in split of the stream, and using the formulas (21) and (22) — in confluence of the streams. The possibility of summing the losses for pressure change and the losses for friction along the length and in local resistances is theoretically not substantiated. However, now we do not have experimental data that contradict this assumption.

Bernoulli's equation for elementary filament of ideal ("dry") liquid in stable motion was derived strictly theoretically, without use of experimental data [2, 95–97]: $h + p / \gamma + v^2 / 2g = const$ (along the filament), where h — excess of the section above the plane of reference. However, for the flow of real (viscous) fluid in a stable motion we have to introduce the pressure losses for friction and in local resistances and the coefficient of speed distribution irregularity along the section of the stream [2, 108–111]. And in order to determine the friction losses, we calculate the loss coefficient λ through experiments, and to determine the losses for local resistances — we calculate the local resistance coefficients ζ . The coefficients λ and ζ depend on the speed of stream flow, roughness of pipeline inner surface and other aspects. So, Bernoulli's equation becomes a calculation-experimental one. And the extension of its work field into streams with variable fluid flow with the use of experimental formulas (11), (15), (16), (21) and (22) should not draw protest.

Let's note that the feeders "know" about each other, so switching on or off at least one of the feeder causes the work restructuring of the entire hydraulic system. Moreover, the process of liquid outflow is established experimentally very quickly, within 5–10 seconds, even in the case of serious malfunction of the system, when, for example, only feeders I and II work.

The question arises about conformity between the results of experiments with water and liquid metals. We may give the following answer to it. In 1946 E. Z. Rabinovich proved [13; 14] that «the movement of liquid metal in the region of turbulent flow does not have any peculiarities in comparison with ordinary motion of "normal liquids"; the hydraulic resistances in the studied motion of liquid metal follow the common laws of hydraulics». In the article [15], published in 1958, E. Z. Rabinovich came to the following conclusion: "Now we may regard it as the established fact, that in turbulent conditions, the local resistance coefficients depend only on the form and structural peculiarities of resistances; the influence of viscosity starts to manifest itself only in the region of laminar flow, where these coefficients are also regarded as a function of the Reynolds number. Thus, for record of local pressure losses in calculation of gating systems we may proceed from resistance coefficients, which are usually recommended for this purpose. The mechanism of molten metal movement changes significantly, if the initial pouring temperature is not sufficient".

The experiments, which were conducted for study of the gating channels, confirm applicability of the laws of hydraulics to liquid aluminum and titanium alloys and cast iron [16–18]. In the review of the works on hydrodynamics of molten metals [19, 340–341], including the works on foundry hydraulics, it was formulated the following: "In the whole region of turbulent flow, the molten metals act like normal, Newtonian liquids. A considerable change of the flow coefficient is observed only when temperatures are close to the solidification temperature, i. e. in the region where the molten mass is presented by Newtonian liquid". According to the

book [20, 57]: "A frequent calibration of orifice meters on water, mercury, tin and other molten metals also confirms the absence of differences in the local resistance coefficients during the flow of water and molten metal".

In the works [21; 22] the hydrodynamics of filling of a foundry mould with aluminum alloy AK12 was investigated theoretically and experimentally. In the articles [23–25] we studied the filling of gating system with alloy AK12 with the same dimensions as in the filling of a system with water. And thus far we have not detected any contradictions, using water instead of liquid metals in experimental studies of gating systems.

Considering the previously investigated GS, which are listed in the introduction, the possibility of using Bernoulli's equation to the stream sections with different flow may be regarded as proven, i. e. for calculations of gating systems with many feeders. However, theoretically it is not substantiated.

Conclusion

Thus, the most complex gating system (P-shaped) was theoretically and experimentally investigated for the first time — with identification of speeds and flow of the fluid in each feeder and all system. In the system there is not only a ramification of some part of the stream from collector to collector, but also confluence of fluid streams from two collectors, and some feeders are located outside the rings with feeders. In the calculation of such hydraulic system with variable fluid flow we used Bernoulli's equation, although it is theoretically derived and practically tested for the fluid flow with a constant flow, that is, for GS with one feeder. For calculation the GS is split into two half-rings. The calculation is performed by successive approximations until the predetermined value of the pressure loss divergence in half-rings reaches the zero point. Pressure losses, speed and flow of fluid in each feeder are calculated during flow of fluid in two parallel hydraulic lines (but not against the flow of the stream). And the difference of the feeder characteristics in calculation by different hydraulic lines may be adduced to any pre-determined infinitely small value. A good conformity of experimental and calculation results is obtained.

References:

1. Vasenin V. I., Bogomyagkov A. V. Investigation of the operation of a ring-shaped gating system // Austrian Journal of Technical and Natural Sciences. – 2016. – № 9–10. – P. 18–28.
2. Vasenin V. I. Investigation of the double-ring-shaped gating system performance // European Journal of Technical and Natural Sciences. – 2016. – № 3. – P. 15–23.
3. Vasenin V. I., Bogomyagkov A. V., Sharov K. V. The study of the work of the vertical ring-shaped gating system // Science, Technology and Higher Education: materials of the XII international research and practice conference. – Westwood (Canada): Accent Graphics communications, 2016. – P. 146–174.

4. Vasenin V. I., Bogomyagkov A. V. The study of the ring-shaped gating system//European Science and Technology: materials of the XV international research and practice conference. – Munich (Germany): Vela Verlag, 2016. – P. 69–87.
5. Vasenin V. I. Investigation of the work of the gating system with two sprues//Austrian Journal of Technical and Natural Sciences. – 2016. – № 5–6. – P. 6–12.
6. Меерович И. Г., Мучник Г. Ф. Гидродинамика коллекторных систем. – М.: Наука, 1986. – 144 с.
7. Чугаев Р. Р. Гидравлика. – М.: изд-во “Бастет”, 2008. – 672 с.
8. Токарев Ж. В. К вопросу о гидравлическом сопротивлении отдельных элементов незамкнутых литниковых систем//Улучшение технологии изготовления отливок. – Свердловск: изд-во УПИ, 1966. – С. 32–40.
9. Jonekura Koji (et al.) Calculation of amount of flow in gating systems for some automotive castings//The Journal of the Japan Foundrymen’s Society. – 1988. – Vol. 60. – № 8. – P. 326–331.
10. Идельчик И. Е. Справочник по гидравлическим сопротивлениям. – М.: Машиностроение, 1992. – 672 с.
11. Васенин В. И., Васенин Д. В., Богомягков А. В., Шаров К. В. Исследование местных сопротивлений литниковой системы//Вестник Пермского национального исследовательского политехнического университета. Машиностроение, материаловедение. – 2012. – Т. 14. – № 2. – С. 46–53.
12. Васенин В. И., Богомягков А. В., Шаров К. В. Исследования L-образных литниковых системы//Вестник Пермского национального исследовательского политехнического университета. Машиностроение, материаловедение. – 2012. – Т. 14. – № 4. – С. 108–122.
13. Рабинович Е. З. О гидравлических сопротивлениях при движении жидких металлов//Известия АН СССР. Отделение технических наук. – 1946. – № 7. – С. 943–948.
14. Рабинович Е. З. Экспериментальное исследование движения расплавленного металла в открытом канале//Доклады АН СССР. – 1946. – Том 4. – № 3. – С. 152–157.
15. Рабинович Е. З. Некоторые вопросы гидравлики расплавленных металлов//Гидродинамика расплавленных металлов. – М.: Издательство АН СССР, 1958. – С. 85–89.
16. Кальман А. Исследование явлений, протекающих в каналах литниковой системы чугунных отливок, с точки зрения равномерного заполнения формы//28-й Международный конгресс литейщиков. – М.: Машгиз, 1964. – С. 319–337.
17. Токарев Ж. В. Расчет литниковых систем с равномерным распределением металла по питателям//Новое в теории и практике литейного производства. – Пермь, 1966. – С. 28–35.
18. Серебряков С. П., Васенин В. И., Ковалев Ю. Г., Гладышев Г. П. Некоторые вопросы литья титана под электромагнитным давлением//Применение магнитной гидродинамики в металлургии. – Свердловск: издательство УНЦ АН СССР, 1977. – С. 87–92.
19. Брановер Г. Г., Цинобер А. В. Магнитная гидродинамика несжимаемых сред. – М.: Наука, 1970. – 384 с.
20. Жидкометаллические теплоносители. – М.: Атомиздат, 1976. – 328 с.
21. Васенин В. И., Ковалев Ю. Г. Экспериментальное исследование кондукционного МГД-насоса постоянного тока//Магнитная гидродинамика. – 1984. – № 3. – С. 142–143.
22. Васенин В. И. Исследование заполнения литейных форм с разными гидравлическими сопротивлениями расплавленным алюминием под давлением кондукционного МГД-насоса//Магнитная гидродинамика. – 1986. – № 2. – С. 142–144.
23. Васенин В. И., Богомягков А. В., Шаров К. В. Определение величины напора в потоке жидкого металла в коллекторе литниковой системы//Литейное производство. – 2015. – № 8. – С. 16–17.
24. Vasenin V. I., Bogomyagkov A. V., Sharov K. V. Research of the mould filling with metal through the ringshaped gating system//8th International Scientific and Practical Conference “Science and Society”. – London: Scieuro, 2016. – P. 20–25.
25. Vasenin V. I., Bogomyagkov A. V., Sharov K. V. Research of the mould filling with metal through the step gating system//Austrian Journal of Technical and Natural Sciences. – 2016. – № 3–4. – P. 32–34.

Maslov Ivan Vasilevich,
 Don State Technical University,
 master's degree student of the Department
 of Welding Engineering, Rostov-on-Don, Russia
 E-mail: deagls666@mail.ru

Numerical simulation of underwater curtain welding with various configurations of water nozzle

Abstract: The article tells about the unsteady numerical simulation of hydrodynamic characteristics of underwater welding with water curtain nozzle. The simulation is based of CAD-models with various configurations of water nozzle exit. The simulations are performed with the help of the software package computational fluid dynamics ANSYS CFX.

Keywords: water curtain welding, local cavity, underwater welding, computational fluid dynamics, finite element method (FEM).

Technology of underwater mechanized solid wire welding with a water curtain nozzle is known from the beginning of the 1970s [1; 2]. This welding method is implemented by means of burner with two concentrically arranged nozzles (fig. 1), a shielding gas is fed into the welding zone from the inner nozzle, and water at the angle to the workpiece surface is fed from the outer nozzle. A high-speed water flow forms the water curtain at the exit from the nozzle, which provides shielding of the welding zone from exposure to the aqueous environment. The initial laboratory tests of the welding process have been carried out in Japan (Government Industrial Research Institute, Shikoku), later in Germany (Laboratorium für Werkstoffkunde und Schweißtechnik, Hamburg), South Korea and other countries [3]. This technology of local protection of the welding zone allows realizing the underwater electric arc and laser beam welding [1; 4].

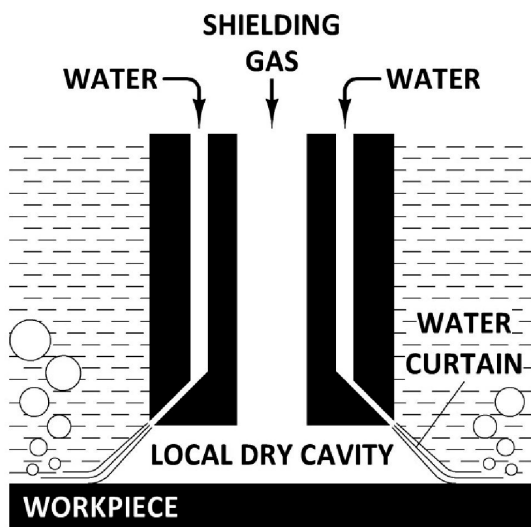


Fig. 1. Diagram of local dry cavity formed by water curtain

The numerical study [5] of the hydrodynamic characteristics of a water curtain at various configurations of the water nozzle exit has been performed. The simulation has been performed without the shielding gas in a stationary setting with a closed local protection zone area. It was found that at configurations A and B (fig. 2) of water nozzle exit, the water curtain has similar hydrodynamic characteristics that justify the practicability of simulation to the shielding gas in the unsteady setting. The purpose of this work is the numerical simulation of underwater welding process with a water curtain nozzle, in order to determine the optimal configuration of the water nozzle exit.

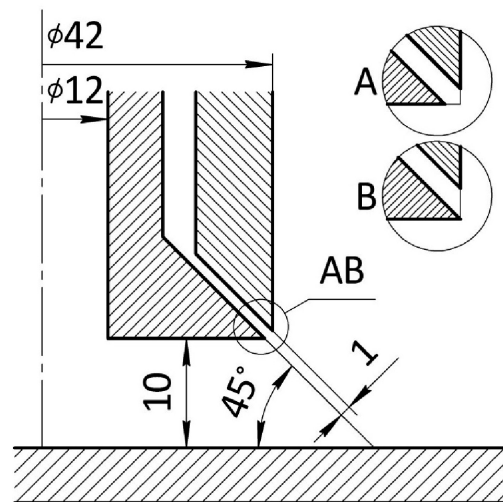


Fig. 2. Structure and size of water curtain nozzle

Obtaining of accurate hydrodynamic characteristics of this process is complicated by the inhomogeneity of the environment, between which the streams of water curtain flow, the pressure difference in the local protection zone and the aquatic environment, as well as the

impact of the shielding gas flow on the curtain. In order to track the impact of the water nozzle exit location on the process the high resolution capability visualization is required, which can be implemented in CFD-packages. The simulations are performed with the help of the software package computational fluid dynamics ANSYS CFX. The geometrical parameters of the burners, used to generate the CAD-models of the computational domain, are shown in fig. 2.

Settlement areas are part of the pie geometry angle 6° . The numerical integration of differential Navier-Stokes equations is carried out by finite volume method.

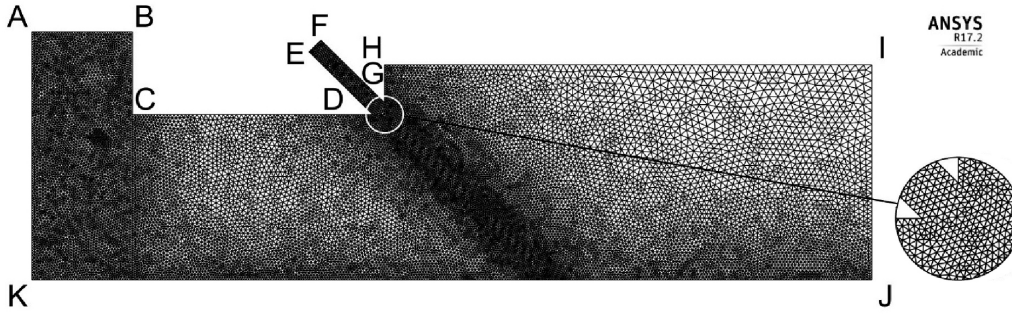


Fig. 3. Computational grid

In this case, the water curtain is a free submerged jet of viscous fluid directed to the planar obstacle at an angle of 45° . By interacting with the obstacle, the free jet forms the wall-adjacent jet which spreads radially from the burner axis. In this regard, in order to get the quality results, both in the flow core and the wall-adjacent, the turbulence model is necessary that describes well both free and near-wall flows. Until recently, the most popular among differential turbulence models were the two-parameter turbulence models, based on the examination of the kinetic energy of turbulent fluctuations k . Either equation of energy dissipation rate ϵ transfer, or specific energy dissipation rate ω [6] are used as the second equation. The drawback of k - ϵ -model is a low accuracy in simulation of flows with separation from smooth surfaces, but Wilcox k - ω models do not have such drawback. Based on the fact that the turbulence model of k - ϵ type with a high degree of reliability describes the shear flow at a distance from the wall, and models of k - ω type have the advantage in the simulation of near-wall flows, Menter in 1993 proposed the SST (Shear Stress Transport) model [7], combining the best features of these models.

After the CAD-models of calculation area have been coated with the grid control volumes the calculation model was established by imposing initial and boundary conditions, parameters of the simulated processes and tasks of the solver settings. First of all, this is the set of equations that needs to be solved:

Calculated fields are split (discretized) into non-crossing volumes so that each junction point is contained in a finite volume. The differential equation is integrated under each finite volume, at that, the piecewise constant functions are used, describing the behavior of the dependent variable between junctions. At the result we have a discrete analogue of the solved equation. The grid models are presented by tetrahedral elements and have thickenings in the area of the boundary layer on the surface of the welded workpiece, as well as in the channels and exits of the nozzles (fig. 3). The total number of nodes in the computational grids $>320\,000$, elements $>1\,770\,000$.

Navier-Stokes equation:

$$\frac{\partial}{\partial t}(\rho \bar{U}_i) + \frac{\partial}{\partial x_j}(\rho \bar{U}_i \bar{U}_j) = -\frac{\partial P^*}{\partial x_i} + f_i + \frac{\partial}{\partial x_j} \left\{ \mu_{eff} \left(\frac{\partial \bar{U}_i}{\partial x_j} + \frac{\partial \bar{U}_j}{\partial x_i} \right) - \frac{2}{3} \mu_{eff} \frac{\partial \bar{U}_i}{\partial x_i} \delta_{ij} \right\}.$$

Continuity equation:

$$\frac{\partial \rho}{\partial t} + \frac{\partial}{\partial x_j}(\rho \bar{U}_j) = 0.$$

Energy equation:

$$\frac{\partial}{\partial t}(\rho h) + \frac{\partial}{\partial x_j}(\rho U_j h) = \frac{\partial P}{\partial t} + U_j \frac{\partial P}{\partial x_j} - \tau_{ij} \frac{\partial U_i}{\partial x_j} - \frac{\partial Q_j}{\partial x_j}.$$

Equation of state:

$$P = \rho RT.$$

The SST-model of turbulence was used as the final equation:

$$\begin{aligned} \frac{\partial \rho k}{\partial t} + \frac{\partial}{\partial x_i}(\rho v_i k) &= \tau_{ij} \frac{\partial v_i}{\partial x_j} - \beta^* \rho \omega k + \\ &+ \frac{\partial}{\partial x_i} \left((\mu_n + \sigma_k \mu_T) \frac{\partial k}{\partial x_i} \right); \\ \frac{\partial \rho \omega}{\partial t} + \frac{\partial}{\partial x_i}(\rho v_i \omega) &= \frac{\gamma}{v_T} \tau_{ij} \frac{\partial v_i}{\partial x_j} - \beta \rho \omega^2 + \\ &+ \frac{\partial}{\partial x_i} \left((\mu_n + \sigma_k \mu_T) \frac{\partial \omega}{\partial x_i} \right) + 2\rho(1 - F_1) \sigma_{\omega 2} \frac{1}{\omega} \frac{\partial k}{\partial x_j} \frac{\partial \omega}{\partial x_j}. \end{aligned}$$

The computation has been carried out for the following parameters: depth — 0.5 m, volumetric feeding of CO₂—60l/min, water — 60l/min. In the initial moment of time all the volume of the computed region was filled with water. Arrangement and main values of the boundary conditions are presented in the Table 1.

This mode of water and shielding gas feeding does not ensure the stable weld zone protection from the

surrounding aqueous environment and the water entering into the local protection area is periodic. The water is displaced from the area inside the water curtain at the initial moment of time, and then the water curtain begins to deviate from the axis of the water nozzle and the water penetrates into local protection area. The results of CO₂ volume fraction simulation are presented in the fig. 4.

Table 1. – Used boundary conditions for the equation system

REGION (Fig. 3)	TYPE	SETTINGS	
AB	INLET (CO ₂)	mass flow rate	0.032946 g/s
EF	INLET (water)	mass flow rate	16.667 g/s
H-J	OPENING	relative pressure	0.0 Pa
B-E, F-H, JK	WALL	wall roughness	smooth wall
remaining surfaces	SYMMETRY		
DEFAULT DOMAIN			
CO ₂ at STP, water		material library	
reference pressure		1.05 atm	
buoyancy reference density		1000 kg/m ³	
gravity Y component		-9.81 m/s ²	
ANALYSIS TYPE/SOLVER CONTROL			
analysis type		transient	
total time		0.6 s	
timesteps		0.001 s	
min./max. coefficient loop iteration		3	



Fig. 4. CO₂ volume fraction. Left configuration A, the right configuration B

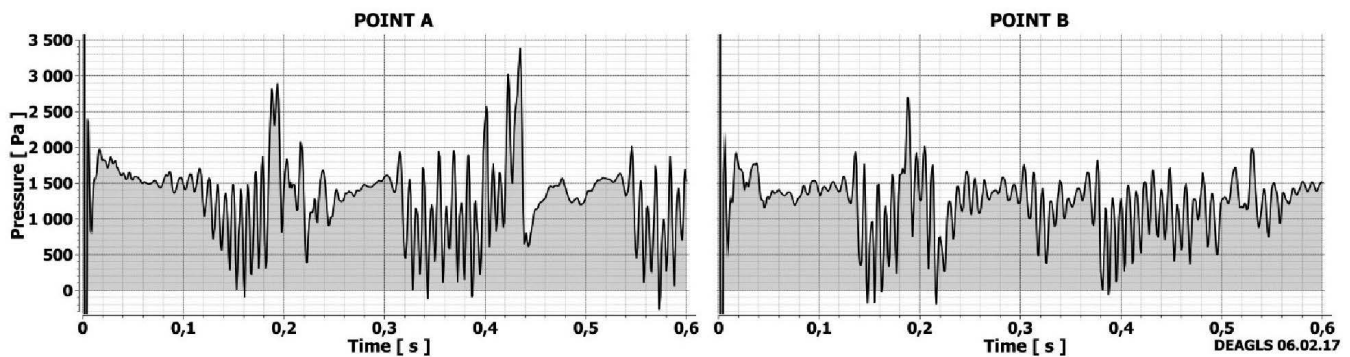


Fig. 5. The pressure at points A and B on time

The water jet focusing is directly dependent on the shape of the water nozzle exit. Improvement of focus increases the rigidity of the jet, which in turn improves the stability of the process. The rigid jet is also capable of holding increased pressure in the local protection area. The pressure charts for the points A and B were constructed for analysis of the pressure change in local protection area on time (see fig. 5).

It may be noted that the chart for the point A has long intervals with the stable pressure and sudden changes have the periodic nature. The average pressure for the point A at a given interval of time has the more value — 1321.056 Pa, against 1234.910 Pa. for the

point B, indicating the greater rigidity of the jet in the first case. This, in turn, is explained by the fact, that at the configuration A at the angle 45° the water nozzle exit in longitudinal section is axisymmetric.

From the overall image of the results, we can conclude that the configuration A of the water nozzle outlet contributes to a more sustainable water jet, which in turn improves the stability of the process. In this case the ability of a water curtain to hold the greater pressure in the local protection area also shows that in this configuration the less water consumption is required to maintain the non-aqueous environment in the welding zone.

References:

1. Hamasaki M. and Sakakibara J. Studies on the Underwater CO₂ Arc Welding Method with a Curtain Nozzle // J. Japan Weld. Society. – 1973. – Vol. 42, No. 9. – P. 897 (in Japanese).
2. Mitsubishi Jukogyo. Welding Torch for Underwater Welding [P]. USA:4029930. 1977–06–14.
3. Maslov I. V., Rogozin D. V. The numerical investigation of shielding gas flow at the underwater welding with water curtain of a nozzle. UNIVERSUM: Technical Sciences. – 2017. – 1 (34) // [Electronic resource]. – Available from: <http://7universum.com/ru/tech/archive/item/4197> (in Russian).
4. Zhang X. D., Ashida E., Shono S., Matsuda F. Effect of shielding conditions of local dry cavity on weld quality in underwater Nd: YAG laser welding // J. Mater. Process. Technol. – 2006. -No. 174. – P. 34–41.
5. Rogozin D. V., Maslov I. V., Koronchik D. A. Numerical calculation of hydrodynamic parameters for underwater welding with water curtain nozzles // Young Researcher of the Don. – 2017. – № 1 (4) // [Electronic resource]. – Available from: http://mid-journal.ru/upload/iblock/5b2/94_100.pdf (in Russian).
6. Hitryh D. P. Turbomachinery Design: review of turbulence models // ANSYS Advantage. Russian edition. – 2005. – № 1 (1). – P. 9–11 (in Russian).
7. Menter F. R. Zonal two equation k- ω turbulence models for aerodynamic flows. In: 24th Fluid Dynamics Conference, Florida, USA, 6–9 July 1993. – Paper No. AIAA 93–2906.

DOI: <http://dx.doi.org/10.20534/AJT-17-1.2-55-58>

*Salahov Timur Zufarovitch,
Ufa state aviation technical university,
postgraduate student,
the Faculty of aviation technologic system
E-mail: Tim-DoctorD@yandex.ru*

*Migranov Mars Sharifullovitch,
Ufa state aviation technical university, professor,
the Faculty of aviation technologic system*

*Nigmatullin Rashit Gajazovich,
Manager of Company "Himmotolog",
Ufa state aviation technical university,
professor, the Faculty of aviation technologic system*

*Hamidullin Ruslan Galeevitch,
director of Company "GasAutoCentre-Ufa"*

Economic calculation of efficiency of introduction of the gauge of deterioration and temperature in the car engine

Abstract: The deterioration and temperature gauge allows:

- to reveal lacks at an early stage;
- to supervise temperature in oil-filled units;
- to supervise deterioration under the maintenance of particles of deterioration in oil-filled units;
- to fix a current condition of knots of a friction;
- to store in memory of the computing block the information in the form of tables and schedules of concentration of particles of deterioration depending on time;
- to predict and give out recommendations about terms of replacement of greasing and to carrying out of repair work;
- to save the finance.

Keywords: economic calculation, deterioration, a friction, the analysis of oil, an expenditure of labour, engine repair.

Introduction

The analysis of a technical condition of the equipment is based on equipment diagnostics under the analysis of lubricant working in it [1]. In article economic calculation of cost of introduction of the gauge of deterioration and temperature in the engine of the car the Gazelle and its comparison with existing service in the conditions of real use is resulted.

Question condition

Data from the device on wireless communication Bluetooth are transferred to phone or a tablet where the owner can see data on a current condition of knots of a friction, schedules of concentration of particles of deterioration depending on time, the forecast and recommendations about terms of replacement of greasing and to carrying out of repair work.

The gauge of products of deterioration has already proved the efficiency: during tests the raised maintenance of particles of iron in a distributing box that has proved to be true results of the analysis трансмиссионного oils on spectrometer OSA Metallab has been revealed. The device is patented, has successfully passed bench tests, and also operational tests for car «Gazelle».

Research technique

For economic benefit calculation used the formula:

$$EE_y = E_y - E_{nc} \cdot C, \quad (1)$$

where: E_y — annual economy, or results which are reached as a result of concrete activity;

E_{nc} — standard effectiveness ratio; a constant which depends on a concrete field of activity (0.15);

C — expenses for concrete activity for which economic benefit is counted up.

Annual economic benefit represents an absolute indicator of efficiency. The system is considered effective, if 0.

In the given work we will consider economic benefit of the gauge of speed of deterioration. As an example we take car "Gazelle".

Data for calculation of efficiency of the gauge of deterioration are resulted in the appendix 9.

To calculate economic benefit, it is necessary to count economy from acquisition of the gauge of deterioration. For this purpose it is necessary to count a difference between mid-annual expenditures of labour on THAT (with cost of materials in a usual mode of operation of the car without the deterioration gauge) and mid-annual expenditures of labour on THAT (with cost of materials in a mode of operation of the car with the deterioration gauge). We will receive:

- 1) $2500 - 1700 = 800$ rbl.;
- 2) $2100 - 1400 = 700$ rbl.;
- 3) $550 - 370 = 180$ rbl.;
- 4) $450 - 300 = 150$ rbl.;
- 5) $(11000 + 3000 + 450) - 250 = 14\,200$ rbl.;
- 6) $800 + 700 + 180 + 150 + 14200 = 16\,030$ rbl.

Annual economy at acquisition of the gauge of speed of deterioration:

- Cost of expenses for engine oil has decreased on 800 rbl.;
- Cost of expenses on трансмиссионное oil has decreased on 700 rbl.;
- Expenses for replacement of filters have decreased on 180 rbl.;
- Expenses for replacement of a cooling liquid — on 150 rbl.;
- Diagnostics and repair of the engine, distributing box is not required, as the deterioration gauge reveals defects at an early stage. Economy 14 200 rbl.

Total: 16 030 rbl.

For an indicator of expenses for concrete activity for which economic benefit is counted up we take cost of two gauges of deterioration with the computing block — 16 000 rbl.

Let's calculate economic benefit:

$$E = 16\,030 \text{ rbl.} - 0.15 \cdot 16\,000 \text{ rbl.} = 13\,360 \text{ rbl.}$$

It is important to notice, that after installation of gauges oil and filters vary in 1.5 times less often, the indicator of an average resource of the engine increases in 1.5 times, the indicator of an average resource of a distributing box increases by 50 000 km.

Economic benefit calculation in this case is calculated approximately as it is impossible to foresee exact

expenditures of labour on THAT, all depends on the different situations, different ecological, economic and other factors. Despite it, the deterioration gauge has a considerable indicator of economic benefit.

Having calculated economic benefit of the gauge of speed of deterioration it is possible to draw a conclusion, that this very favourable acquisition. Often enough there are breakages of the car owing to various factors, but the gauge of speed of deterioration allows to prevent them, is simple in application, is patented, has passed operational tests, its price corresponds to expected result.

In the present diagnostic device is in a transitive stage between individual and small-scale manufacture. Manufacturing of computing blocks is put on a stream — in them standard elements are used. Gauges demand an individual approach in connection with distinctions in a design of units of technics of different manufacturers. However in process of accumulation of experience of manufacturing of gauges for the different technics it will be possible to reduce the nomenclature to several types of the gauges divided on the landing sizes. The software already possesses all base functions (the conclusion of results of measurements, construction of schedules), is conducted work on optimisation of the interface and addition of new functionality.

The market is presented by two basic segments are large consumers (the industrial enterprises, motor-vehicle pools, etc.) and private consumers (automobile owners and the small enterprises where the technics with oil-filled units is used). Both segments are stable enough, in long-term prospect the small tendency to growth is observed.

In the foreign market there are manufacturers of similar devices, for example Gill Sensors and Controls, however in the Russian market there is no offer of their production.

At the Russian enterprises and in motor-vehicles of system of monitoring behind a condition of knots of a friction now are not used. There is a potential competitor — Open Company «MMK» with workings out «VECTOR» and «АИДА», however these workings out are not introduced now in manufacture.

The above-stated problem has laid down in a basis of statement of a problem on search of innovative decisions for decrease in expenses for service of objects of thermal power station.

Comparison of technical and economic characteristics (including quantitative, qualitative and cost characteristics of production) the created product with foreign and domestic analogues (table 1).

Table 1. – Comparison of technical and economic characteristics with analogues

Technical and economic parameters of a product	Analogue 1 — the VECTOR	Analogue 2 — АИДА	Analogue 3 — Condition Monitoring Sensor	The created product — the gauge of speed of deterioration
1. Definition of weight of particles of iron in mg.	Yes	No	Yes	Yes
2. Definition of weight of nonferrous metals in mg.	Yes	No	No	The heuristic
3. The division price	0.1 mg.	No	1 mg.	0.1 mg.
4. A range	0–200 mg.	«Norm»/«Above norm»	0–500 mg.	0–100 mg.
5. Connection to other devices	Wire, USB	No	Wire, USB	Wireless, Bluetooth
6. Complexity of a design of the gauge	The high	There is no information	The high	The low
7. Cost	It is not made	It is not made	£350-£570 (35 000–57 000 rbl.)	12 500 rbl.

Table 2. – Data for calculation of efficiency of the gauge of deterioration.

The name	If-chestvo	Cost (rbl.)
Cost of the car the Gazelle 4×4	1	700 000
The engine the Gazelle	1	86 000
Distributing box	1	13 000
Engine oil	1	900
Transmission oil	1	1000
Cooling liquid	1	350
The filter oil	1	350
The filter air	1	1600
Crankshaft	1	70 000
Sliding bearings	1	1200
Tsilindro-piston group	1	5000
Differential of a distributing box	1	2000
Bearings Rolling	1	1200
Epiloons	1	600
Two gauges of deterioration with the computing block	1	16 000
Mid-annual expenditures of labour on THAT with cost of materials in a usual mode of operation of the car without the deterioration gauge (average data of the car the Gazelle for 5 years): – replacement motor (through 10 000 km) and transmission oils (through 40 000 km); – replacement of oil and air filters; – replacement of a cooling liquid; – diagnostics of the engine; – repair of the engine; – repair of a distributing box; the Average resource of the engine; the Average resource of a distributing box	200 000 km of 150 000 km	2500 2100 550 450 450 11000 3000
Mid-annual expenditures of labour on THAT with cost of materials in a mode of operation of the car with the deterioration gauge: – replacement motor (through 15 000 km) and transmission oils (through 60 000 km); – replacement of oil and air filters; – replacement of a cooling liquid; – diagnostics of the engine; – repair of the engine; – elimination of the found out defects at an early stage; the Average resource of the engine; the Average resource of a distributing box	300 000 km of 200 000 km	1700 1400 370 300 — - 250

In comparison 3 analogues were used:

1. Device «VECTOR», developed Open Company «ММК» (Russia)
2. Device «АИДА», developed Open Company «ММК» (Russia)
3. Condition Monitoring Sensor 4212, realised Gill Sensors and Controls (Great Britain). Cost is resulted for variants Standard and Industrial.

In previous years in a thermal power station segment high investment activity is noted. For example, in an oil refining segment, according to Ministry for the Power Generating Industry, according to 18 quadrilateral agreements signed between the oil companies, ФАС, Ростехнадзор and Росстандартом, is provided to reconstruct 34 and to construct 99 technological installations. In total on 133 installations by the oil companies it is planned 1.9 bln. rbl. in the prices of 2014 To the beginning of 2016 the given plan it is executed on 50 %, many enterprises successfully modernised existing and have placed in operation new manufactures, having equipped new modern, including the dynamic equipment.

Discussion of results

In the conditions of falling of oil quotations and exchange rate growth, in a segment of thermal power station of the Russian Federation reduction of profitability of the enterprises is marked and sharply there is a problem of optimisation of expenses for equipment service, that along with problems of the government of the Russian Federation on import substitution, defines high solvent demand for innovative, effective, domestic systems of diagnostics for maintenance of working capacity and safety operating fire and explosion hazard manufactures.

By the present moment there are 9 contracts on delivery of 70 measuring blocks with gauges and in addition 96 gauges for a total sum of 1 538 600 roubles, and also 2 letters on intention of acquisition of 27 measuring blocks with gauges for a total sum of 337 500 roubles.

In the domestic market and in the CIS countries the offered product will make a confident competition to import analogues for the account considerably smaller cost,

and also decrease in expenses for delivery and customs registration.

The batch production organisation will draw possible a conclusion of production to the world market. The factors positively influencing competitiveness in the foreign markets — low cost of the device (owing to smaller complexity a design of the gauge, smaller in comparison with the countries of Europe in cost of a labour) at preservation of technical characteristics.

Conclusions

Thus strategy of advancement of a product on the market includes 3 stages:

1) the Exit on the market of the industrial enterprises, with priority orientation to the thermal power station enterprises. Individual and small-scale manufacture has allowed to begin work with the separate organisations, with device completion according to wishes and requirements of customers. In process of expansion of the covered market and experience accumulation gradual transition to serial release of universal devices will be carried out. Advancement methods: participation of the company in actions of industrial subjects (forums, conferences), offers to heads of factories and responsible for a condition of technopark, the publication and advertising in trade magazines, participation in actions petrochemical territorial кластера Republics Bashkortostan.

2) the Exit on the market of motor transport and professional motor-vehicles. In process of adjustment of a batch production cost of the gauge of speed of deterioration will decrease, that will raise its appeal to more and more wide range of automobile owners. Advancement methods: advertising in newspapers and magazines of automobile subjects, advertising at forums of motorists and contextual advertising in a network the Internet, Internet shop creation, cooperation with car repair shops and shops of autospare parts.

3) the Exit on the foreign markets. At this stage well debugged manufacture, flexible enough to adapt production under foreign standards will matter. Advancement methods — similar to methods of first two stages, but already for the foreign markets.

References:

1. Fuel, lubricants, technical liquids. Assortment and application: Help izdanie/Budyshtova K. N., Bershtandt L. A., Bogdanov S. K., etc. Under Shkolnikova V. M's edition/Chemistry. – 1989. – P. 108–139.
2. The Analysis of results of tests of oils in the engine taking into account an estimation of their quality in laboratory conditions/And, B. Vipper, V. L. Lahshi//Двигателестроение. – 1979. – № 9. – P. 58–59.
3. The Condition, problems and development prospects tribological aspect energy saving in engine building/With. V. Putintsev//News of high schools. Mechanical engineering. – 1995. – № 10–12. – P. 71–79.

Section 5. Food industry

DOI: <http://dx.doi.org/10.20534/AJT-17-1.2-59-63>

Gafurov Karim Khakimovich,

Bukhara Engineering-Technology Institute

E-mail: kgafurov@yahoo.com

Ibragimov Ulugbek Muradilloevich

E-mail: culugbek@list.ru

Fayziev Shavkat Ismatovich

E-mail: shavkatfayz@gmail.com

Statistical-mathematical model of the process of extraction of pumpkin seeds by CO₂-extraction

Abstract: An experimental study of the process of obtaining of oil from pumpkin seeds by CO₂-extraction is carried out. Statistical analysis of experimental results is carried out; statistical and mathematical model of the process is obtained, rational parameters of influencing factors are defined.

Keywords: CO₂ extraction, liquid and supercritical gas, pumpkin seeds, pressure, temperature, extractant.

Development of methods of energy-saving technologies, allowing getting new high-quality products in the pharmaceutical, cosmetics and food industry is due to a pressing social need for high-quality medicines and food products as well as cleaner production.

One of the solutions of this problem is the use of liquid and supercritical carbon dioxide as the extractant. CO₂ extraction is just spread in the world. This is due primarily to the fact that this process is highly cost-effective, more technological, allows processing not only high-quality raw materials, but also the production of waste in order to extract from them the main components to give a better quality of lower grade product. Extraction is carried out with liquefied gases under pressure, where removing extractant evaporates and extractives remain in pure form. Extraction with carbon dioxide in liquid and supercritical form significantly expands the range allocated to the active compounds, and also allows to obtain the concentrations of biologically active substances in the final product, which cannot be obtained by any other known extraction techniques [1, 2–5; 2, 1–2].

Structural features of vegetable raw of the Uzbekistan — fruit seeds, grape seeds, pumpkin, melons, etc. are suggest technological development mode liquid extraction using supercritical carbon dioxide and the kinetics and dynamics of the extraction process, the determine

extraction process effects on the yield and quality of the product [3, 5–6].

In this case, there is a need to develop technics and technology of CO₂-extraction designed for local raw materials.

Research of the extraction process of ingredients from plant raw material with liquefied and supercritical carbon dioxide was carried out on laboratory installation (fig. 1), which consists of the following elements: a high-pressure extractor with the cassette to accommodate the sample plant material, extracting supply system, the product collection system, condensation system, heat pump systems, control equipment.

High pressure extractor with sample cassette VII for placing plant raw is a thick-walled vessel made of stainless steel. The cassette, which has a design shape close to the internal volume of the extractor (cylinder of thin sheet material with a perforated bottom sieve) is also made of stainless steel. The extractor has a pressure sensor which transmits signals for controlling the flow of the extractant in the extraction, controlling the operation of the control valve 4. For controlling the temperature of the extractant supplied into the extractor, temperature sensor is put on inlet of the extractor, a signal from which is supplied to the electric heater thermoregulatory system extractant VI.

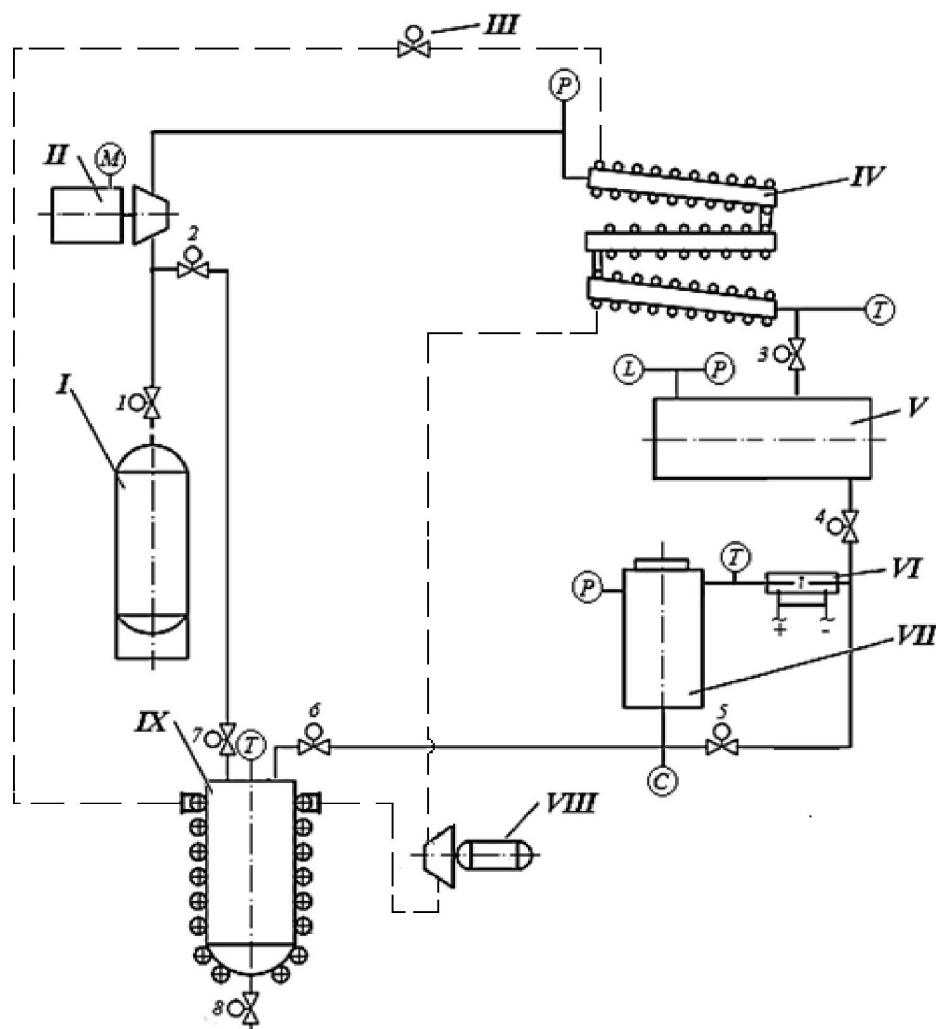


Fig.1. Schematic diagram of the laboratory equipment for the research of CO₂-extraction process from vegetable raw materials

Extractant feed system consists of a cylinder with CO₂ I, Compressor II, tanks for gas extracting V, an electric heater extractant VI, 1, 2, 5 stop valves and control valves 3, 4. The capacity for extract V has a pressure sensor and level sensor, which transmit signals to control valve performance 3.

Condensation extractant system consists of a condenser with a cooling jacket IV, in which the inlet pressure gauge, and at the outlet — the thermometer that perform control functions.

Product collection system consists of an evaporator-separator with a coil heater extract IX, the throttle valve 6 and valves 7 and 8.

The heat pump system consists of a compressor heat pump VIII, the throttle valve of the heat pump III. A working agent for the heat pump system is a Freon R-21, which serves as a refrigerant condenser for IV and thermal evaporation agent separator IX.

The laboratory setup is as follows (fig. 1). The crushed plant material pre-loaded into a mesh tape that

is installed in the extractor VII. After sealing the extractor, technology system with the product is purged with gaseous CO₂ in order to remove air.

Carbon dioxide from the tank I is transferred to the compressor II at an open valve 1 and closed 2 (during the first installation startup). CO₂ compressed by the compressor II passes through the condenser IV, wherein the agent is cooled by the working heat pump and becomes liquid ($P_1 = 8 \dots 10 \text{ MPa}$. and $t_1 = 25 \dots 30^\circ\text{C}$) and stored in tanks for extractat V at the open valve 3. In this case the pressure of the extractant at the entrance to the condenser and the temperature at the outlet of the condenser measured by pressure gauge and a thermometer, respectively. Pressure and level in the tank V measured pressure and level sensors, and the signals are transmitted to the control system for controlling the operation of the valve 3.

For carrying out the process of extraction the liquid extractant at the open valve 4 passes through the electric heater VI, which passes into a supercritical state

($P_2 = 8 \dots 10$ MPa. and $t_2 = 35 \dots 70$ °C) and fed to the top of the extractor *VII*, where a temperature sensor provides a signal to the controlled electrical heater system for controlling the temperature of the extractant. Consumption extractat regulated by valve 4. After passing through the layer of vegetable raw material extracting agent extracts the soluble components (eg, pumpkin seed oil) and excreted from the bottom of the extractor, ie, extraction is carried out by infusion for a time (the time depends on the type of infusion extractable feed) in the closed valve 5. If extraction technology requires extraction flow, then the process takes place at an open valve 5.

After reaching of process time the valve 5 opens and closes the throttle valve 6. When passing through the throttle pressure and temperature of the miscella is reduced below the critical parameters ($P_3 = 5.0 \dots 5.5$ MPa. and $t_3 = 25 \dots 30$ °C) and carbon dioxide passes to a gaseous state.

In the separator-evaporator *IX* is deposited dissolved in the extractant extract, which is necessary to maintain the temperature ($t_4 = 25 \dots 30$ °C). The temperature is maintained by means of the heat pump working agent serving to coil heater-evaporator heat separator agent. Thus precipitated extract removed from the bottom of the evaporator-separator with the valve 8 open, the gaseous carbon dioxide output from the top separator at the open-valve evaporator 7. A gaseous CO₂ passes through the valve 2 is compressed to the operating pressure of the compressor and the cycle is repeated.

The main operating parameters of the process are the pressure and temperature of the extractant in the extraction circuit, and a simple variation of these operating parameters can be used in the pre- and supercritical state extractant and thus to carry out directional change in the composition of the final extract.

The technological scheme is further coupled to a heat pump condenser *IV* in the cooling extractant and to maintain the desired temperature of the extract in the separator-evaporator *IX*. Operating agent — R-21-freon is compressed in the compressor of the heat pump *VIII*, passes through the evaporator coil separator-*IX*, gives up its heat and is cooled, exits the evaporator-separator coil and passes through the expansion valve *III*,

which loses pressure. Cooling agent is included in the jacket of the condenser *IV*, where taking heat from the extractant evaporates and comes in a gaseous state to the compressor and the cycle is repeated. Thus, as the heat pump condenser enters the coil-evaporator separator *IX*, here working agent, giving its heat, maintains the desired temperature for the separation of the extractant from the extract and condensed, and as the heat pump evaporator enters shirt capacitor *IV*, where the working agent, taking extratant heat from vaporized.

The purpose of the experiments was to determine the influence of the main influencing factors: pressure and temperature of extratant for CO₂ extraction on residual oil content meal (oil output).

As a fat-containing plant material are selected pumpkin seeds (*SEMINA CUCURBITAE*). The pumpkin seeds contain fatty oil (40%), which includes linolenic glycerides (45%), oleic (25%), palmitic and stearic (30%) acids; essential oil, phytosterols — kukurbitol, resinous substances, organic acids; vitamin C, B1 (0.2 mg/ %); carotene and carotenoids together — 20 mg/ %, amino acids [4].

Grinding of all raw materials used in the experiments carried out in the same mode type percussion grinder mill at 16000 rev/min for several seconds. The fineness of the material was determined by sieve analysis. At a sieve with a mesh size of 2 mm. was whole seeds (“leakage”), and their share was 9.2%. As a result, the calculation of the weighted average amount of ground seeds was 0.9 mm.

On the basis of the available information and analysis as influencing factors selected pressure and extracting temperature (supercritical CO₂). Processing time 60 min.

Varying levels of the two factors (x_1 — pressure and x_2 — temperature) are the following:

- The upper level (+): the pressure of 8 MPa, the temperature of 40°C.
- The lower level (–): the pressure of 7 MPa, the temperature of 30°C.

Coding of the factors is carried out (Table 1).

Since we have two influencing factors, and they change on two levels, get planning experiments to 2². Thus, it is necessary to carry out the experiment 4. Experimental design matrix is shown in Table 2.

Table 1. – Coding of the factors

Factors	Upper level x^+	Lower Level x^-	Center	Spacing variation, λ	encoded variable Dependency on natural
x_1	8	7	7.5	0.5	$(x_1 - 7.5)/0.5$
x_2	40	30	35	5	$(x_2 - 35)/5$

Table 2. – Experimental Design Matrix for 2²

№ of experiment	Factors		The effects of the interaction of factors	Results of the experiments			Average results
	x ₁	x ₂		x ₁ x ₂	y ₁	y ₂	
1	-	-	+	5.2	5	4.6	4.933
2	+	-	-	4.2	3.8	4	4.000
3	-	+1	-	3.5	3.7	3.3	3.500
4	+	+	+	2.8	3.2	3	3.000
						Σ y _j	15.433

The regression equation in this case is as follows:

$$y = b_0 + b_1x_1 + b_2x_2 + b_{12}x_1x_2.$$

The regression coefficients are calculated according to the formulas:

$$b_0 = \frac{\sum_{i=1}^N y_i}{N}$$

$$b_1 = \frac{\sum_{i=1}^N y_i x_{i1}}{N} \text{ etc.}$$

The calculation results are shown in Table 3.

Table 4. – The calculation of the dispersion of reproducibility

j	y ₁	y ₂	y ₃	y _j	(y _{j1} - y _j) ²	(y _{j2} - y _j) ²	(y _{j3} - y _j) ²	S ² _{repr.}
1	5.200	5.000	4.600	4.933	0.0711	0.0044	0.1111	0.0933
2	4.200	3.800	4.000	4.000	0.0400	0.0400	0.0000	0.0400
3	3.500	3.700	3.300	3.500	0.0000	0.0400	0.0400	0.0400
4	2.800	3.200	3.000	3.000	0.0400	0.0400	0.0000	0.0400
							Σ	0.2133

The standard deviation of the coefficients determined by the formula (2): S_{coef} = 0.0667.

From the distribution tables of Student [5, 283–284] according to the number of degrees of liberty: n(m - 1) = 4 · 2 = 8. With a level of significance of α = 0.05 we find t_{cr} = 1.86.

Estimated value of the t-test is determined by the formula (3):

$$|b_j| = t_{cr} \cdot S_{coef} = 1.86 \cdot 0.0667 = 0.124.$$

Comparing this value with 0.124 coefficients of the regression equation that all factors except b₁₂ are bigger in absolute value of |b_j|. Therefore all the coefficients except b₁₂ are significant. So this factor is excluded from the regression equation.

The regression equation is as follows:

$$y = 3.8583 - 0.3583x_1 - 0.6083x_2. \quad (4)$$

Adequacy of obtained regression equation is checked by using Fisher's exact test on formula [5, 74–75]

$$F = \frac{S_o^2}{S_v^2}. \quad (5)$$

Table 3. – The calculated values of the regression coefficients

Coefficients	b ₀	b ₁	b ₂	b ₁₂
Meaning	3.8583	-0.3583	-0.6083	0.1083

We determine the significance of these factors:

The dispersion reproducibility S_v made under the formula [5, 72–73]:

$$S_v^2 = \frac{\sum_{y=1}^{NN} (y_u^0 - \bar{y}^0)^2}{NN - 1}, \quad (1)$$

where: NN — number of replicates; y⁰ — average value of y, obtained in parallel experiments; y_u⁰ — values obtained when setting each of the additional experiments in the center of the plan.

The standard deviation of the coefficients:

$$S_{coef} = \frac{S_{repr.}}{\sqrt{15}}. \quad (2)$$

Estimated value of the t-test is given by [5, 73–74]:

$$t_{cr} = \frac{|b_j|}{S_{coef}}. \quad (3)$$

The calculation results are shown in Table 4.

where the residual dispersion is calculated using the formula:

$$S_o^2 = \frac{\sum_{i=1}^N (y_i - yr_i)^2}{N - L}, \quad (6)$$

where L — number of significant coefficients in the regression equation.

In our case S_o² = 0.14083. At the significance level α = 0.05 degrees of freedom and k₁ = n - r = 4 - 3 = 1 and k₂ = n(m - 1) = 8; F_{tabl} = 5.32 [5, 280–281]. Estimated value of Fisher's exact test on formula (5): F_{calc} = 2.64.

According to the results of calculations F_{calc} < F_{tabl}, so that the resulting model adequately describes the process.

Upon receipt of the equation (4) we construct a graph of the residual oil content of pumpkin seeds (meal) from influencing pressures and temperature on MathCAD program (fig. 2).

The graph shows that with increasing pressure and temperature oil content of meal decreases. According to fig. 4, rational values of the influencing factors are: pressure P = 7.75 MPa, t = 35 °C temperature. In this extraction mode the residual oil content of meal is 3.13%.

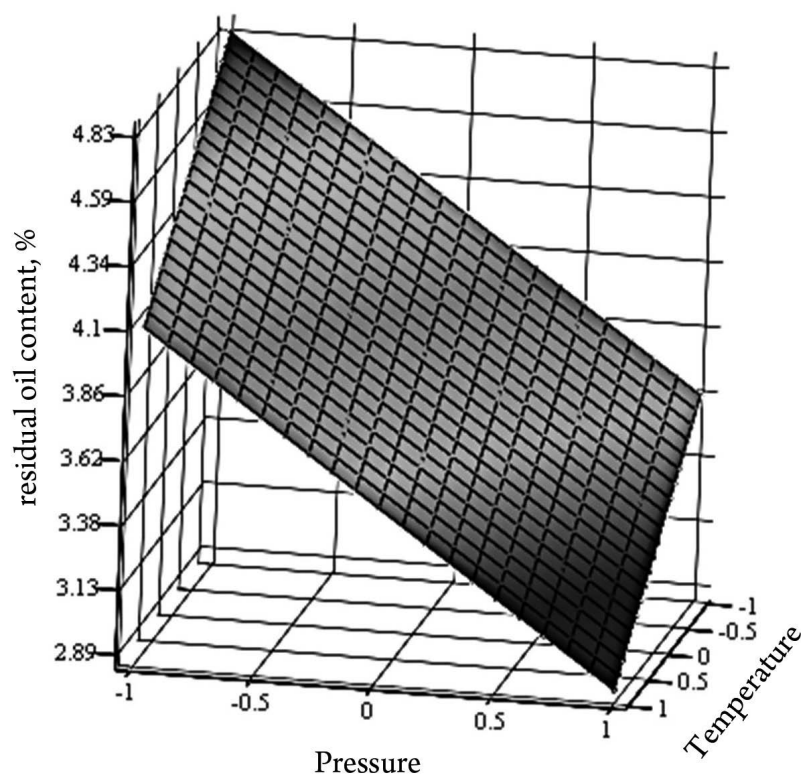


Fig. 2. Dependence of the residual oil content of pumpkin seeds (meal) from influencing pressures and temperatures

References:

1. Extraction with carbon dioxide in the food technology/E. P. Koshevoy, H. R. Blyagoz – Maikop: Maikop State technological institute, 2000. – 495 p.
2. The supercritical CO₂-extraction – opportunities and prospects//A. G. Lepeshkov, A. R. Vodyanik, K. M. Averin. SIC of environmental resources “GORO”. – Rostov-on-Don//[Electronic resource]. – Available from: <http://www.extract.ru/index.php?id=91>
3. Safarov A. F., Gafurov K. Kh. Modern technology in the extraction industry//Journal “Development of Science and Technology”. – 2015 – №1. – P. 5–9.
4. [Electronic resource]. – Available from: https://ru.wikipedia.org/wiki/Semena_tykvy
5. Grachev Y.P., Plaksin Y.M. Mathematical methods of experiment planning. – M.: DeLi print, 2005. – 296 p.

Section 6. Agricultural sciences

DOI: <http://dx.doi.org/10.20534/AJT-17-1.2-64-66>

*Ahmetov Adilbek Agabekovich,
d. t. s, main specialist in coordination of SRECW,
Ahmedov Sherzodbek Anvarhon o'g'li,
the design engineer, Special design bureau "Tractor" UE
Karimov Abror Kayumovich,
master TSTU, Tashkent, the Republic of Uzbekistan
E-mail: sheran1@mail.ru*

Priority directions of perfection construction cotton growing tractors

Abstract: In article is given the basic directions of perfection designs of cotton-growing four-wheel universal tractor-cultivators, providing with high their stability, passably and turning ability.

Keywords: a tractor, the front axle, a road clearance, passable, stability, inter-row processing wheels, a beam, a bar, a semiframe, a spindle and a wheel.

Cotton growing in the Central Asia has the specific features, specified in conditions of soil-environmental. The soil cover the irrigation earth where the cotton is cultivated, very various. But, despite these differences, after sowing almost all of them are condensed. Especially big consolidation occurs after watering. Long preservation of soil in the condensed condition detains development of root system of cotton, complicate them development of nutritious elements and air access, promotes development of weed plants, break a water-air mode of soil and in aggregate with a hot climate leads to intensive loss of a moisture. For removal the listed lack of these soils conduct interrow processing of crops of cotton. Multiplicity, which in dependences on a soil condition fluctuates from three until seven-eight and they are considered as the most labor-consuming operation at cotton cultivation [1; 2]. All given soil-climatic features of the Central Asia put specific requirements to the tractors applied at cultivation of cotton.

The specific demands are shown to universal-cultivator tractors of cotton cultivation, follow from necessity in process of their operation performance not only inter-row processes, but also other various kinds of technological operations on cultivation and cotton harvest, and also transport works.

The demands are shown to universal-cultivator tractors of cotton cultivation are rather various, which satisfaction presence at these tractors of some the operational

qualities characterizing in a complex efficiency of their work in those or other conditions if necessary.

Operational qualities cotton-growing universal-cultivator tractor can be divided into three basic groups: agro-technical, techno-economic and basic technical. Agro-technical qualities characterize fitness of a cotton-growing tractor to performance of the technology demands following from working conditions and, represent a number of the properties connected with agro-technical possibility and mobility, both the tractor, and created on its base machine-tractor units (MTU).

Techno economic qualities are defined basically by productivity and profitability MTU, made on the basis on cotton-growing tractor which at a concrete case depends on a mode building-block designing.

Basic technical qualities are connected basically with maintenance of convenience of work and service and safety conditions of work of the machinist-operator.

Inoperating program special design bureau "Tractor" on the basis of long-term study building-block design with a cotton-growing universal-cultivator tractor of car-tools, and also passably and turning ability a tractor, its stability to overturning with the account jumping and galloping are defined specific demands of a zone cotton growing [3], is shown to cotton-growing universal-cultivator tractors which consist of the following:

- At performance of transport works when the tractor moves on the raised speeds, for maintenance

of good stability it should have is minimum admissible low road clearance and the maximum length of base. As at smaller length of base of a tractor on the raised speeds of movement there can be “jumping” and galloping, and at a high road clearance, hence, huge distance of the centre of gravity from a basic surface on turns at the expense of centrifugal force the tractor loses stability that is undesirable;

– At performance of interrow works where speed of movement of a tractor small, on the contrary, for elimination damage high coalescent plants and knocking down flower and fetus elements the tractor should have the maximum agro-technical gleam, hence a high road clearance, and for reduction of the sizes of rotary strips it should have the minimum radius of turn, hence, the minimum length of base.

Widespread in cotton growing 3 and 4 wheel it is universal-cultivator tractors not to the full meet these requirements.

High agro-technical passably of 3 wheel universally-cultivator tractors until recently provided to the status of the basic power means for mechanization of field works in cotton growing. However tractors of this type have essential specific lacks, namely:

- The low cross-section stability doing their operation dangerous on biases and at turns on speeds above 12–13 km/h;
- Negative anthropogenic influence on soil in connection with the raised factor of a covering traces from wheels (three traces instead of two) and characteristic high condensing influence from the vertical loadings distributed on three wheels instead of four;
- An overload of tires, especially forward operated wheel, own vertical loadings of a tractor and from weights of agricultural cars and technological materials;
- Irrational distribution of weight MTU on tractor support;
- Inadmissibility of application on transport works because of their low stability;
- The low annual loading regulated only by a season of works on a cotton, i. e. not a demand in agricultural production during almost 4–5 (from November till March) months;
- Complexity of creation of an all-wheel drive design of a tractor with the wheel formula 3×2 that limits traction potential of a tractor only to pull chain qualities of tires of two leading back wheels;

- Application of 3 wheel tractors does not allow realizing completely advantage far-reaching MTU, because of deficiency of pull chain potential of a tractor and essential excess of admissible norms of ecological influence on soil.

The lacks set forth above of certain degree are absent at 4 wheel tractors. Reduction of negative anthropogenic influence by soil for the account of decrease in a total area of a covering traces of wheels (on 33.3%), reduction of the maximum pressure by soil in a zone of the basic area of the running device, more rational distribution of weights MTU on axes and decrease in slipping of wheels are the incomplete list of advantages of these tractors before 3 wheel. However they have the increased radius of turn and an insufficient agro-technical gleam under a beam of the forward bridge because of what they have not found application on interrow processes of crops of cotton. Whereas interrow processes is the most labor-consuming technological operation in cotton growing.

It is necessary to notice also that presence in zone-cotton growing two kinds: 3 and 4 wheel tractors leads to unreasonable increase in number of park of cars and accordingly expenses on their maintenance.

Proceeding from technology of cultivation of cotton, the basic demand to developed new generation of 4 wheel cotton-growing tractors is preservation of positive qualities of 3 wheel cotton-growing tractors, exactly:

- Negotiation designs in row-spacing with the developed bushes of a cotton in last inter-row processes, and also at defoliation and harvest;
- Increase maneuverability, providing the minimum radius of turn and loss of the productive areas in a zone swiveling strips at edges of irrigation sites with cotton crops.

Performance of specific requirements of zone cotton growing in aggregate with the basic constructive demands to 4 wheels is a universal-cultivator tractors considerably raises their consumer properties and expands area of their application.

At the positive decision of the problems set forth above concerning to 4 wheel tractors increase of productivity cotton MTU by increase lane agricultural cars to 6, 8 numbers on various schemes of crops for the account of the all-wheel drive scheme wheeled mover and increases of a traction class of a tractor is really provided. The problem of optimization of park of cars and all-the-year-round loading of cotton-growing tractors for the account usage not only on harvesting-transport, but also other kinds of works in cotton growing will dare, vegetable growing, feed producing, grain farming, on

cattle-breeding complexes, etc. Besides for the account of the qualities put in the scheme of the running device of 4 wheel tractors, controllability and stability of work transportations improves and at work in row-spacing of crops of a cotton and other cultures to demanded norms of safety.

For the decision of tasks in view in operating program special design bureaus "Tractors" are conducted research and developmental works in the most priority directions of working out of 4 wheel universally-cultivator tractors, including the decision of following problems:

- Increase of stability and agro-technical passably of universally-cultivator tractor without application of in addition mounted and dismantled devices and adaptations;
- Change maintenance, both a road clearance, and length of base of universally-cultivator tractor depending on a kind of carried out works;
- Increase of traction possibility of universally-cultivator tractor by transition on full driving a variant at the expense of application of the front axle;

- To minimize radius of turn of a four-wheel universally-cultivator tractor to level three-wheeled at the expense of perfection of a design of a steering drive and the front axle;
- Transition from traditional rear hinged systems building-block design cars-tools on the combined system (to hang cars-tools on universal-cultivator a tractor both behind, and in front, if necessary also on each side) for maintenance of uniform distribution of weight of building-block design cars-tools on forward and the rear axle of a tractor.

Decision mentioned above for the account creating four wheel universally-cultivator tractor with the raised stability, passably and turning, not conceding under the operational characteristics to a three-wheeled tractor, would allow to solve application questions in cotton growing widefar reaching manufacture tractor units essentially reducing power-both resources consumptions and raising labor productivity at cultivation of a cotton and cultures accompanying it.

References:

1. To Take care agricultural plants and producing products according to standard (model) technologic charts, for 2011–2015. – Tashkent: XILOLMEDIA, 2011. – I and II part. – 232 p.
2. System of cars and technologies for complex mechanization of agricultural production for 2011–2016 – Part 1, plant growing. – Tashkent: SPC at MAWRUz, 2012. – 199 p.
3. Ahmetov A. A. Frontaxles of universally-cultivator tractors of cotton appointment. – Tashkent, 2014. – 176 p.

Section 7. Technical sciences

DOI: <http://dx.doi.org/10.20534/AJT-17-1.2-67-69>

*Abdullaeva Sadokat Shonazarovna,
PhD student, Tashkent chemical-technological institute,
Department of «Processes and apparatuses of chemical technology»
E-mail: sadshon1975@yandex.ru*

*Nurmuhamedov Khabibulla Sagdullayevich,
Doctor of technical sciences, Professor,
Tashkent chemical-technological institute*

Issue of non-traditional cleaning root crops

Abstract: The paper presents the results of experimental studies on the treatment of root crops (sugar beet and red beet) by method instant pressure relief. Found that this method can achieve complete cleaning in the form of a thin skin and reduce the loss of raw materials in the 3–5 times. Experimental data are summarized and presented according to the calculation of the degree of purification.

Keywords: purification, roots, steam thermic treatment, method instant pressure relief, saturated steam, formula.

Industries for processing of these products are one of the fastest and most rapidly developing branches of agriculture today. One promising area is the rational and complete processing of root crops, such as red and sugar beets, potatoes, carrots, artichoke, etc.

It is rapidly developing production of food additives from roots and tubers [1, 54–56]. Analysis of different technologies for processing of root crops, in order to get new products show that cleaning of roots presents in all technologies. However, at present there is no effective cleaning process with low-loss materials. Cleaning to remove roots produce less valuable nutritionally skin raw. Intended for further processing raw materials purify by machines [2, 1–5].

The choice of the method and equipment for the cleaning of raw materials are received by the form of the processing of root. There are the following ways to clean roots from the skin: thermal (steam, steam water thermic), chemical (alkaline), mechanical (abrasive surface, blade system, compressed air), combined (alkaline steam, etc.) [3, 13–23].

Steam cleaning method tubers subjected to short-term treatment with steam under pressure $P = 0.3\text{--}0.5$ MPa. followed by removal of skin in washing and cleaning machine. Effect of pressure and temperature, pressure drop at the output of the machine, hydraulic (water jets) and

mechanical friction [4, 42–56]. Steamed potatoes peel in a drum washing machine. As a result of mechanical action plates located on the inner surface of the drum, water and friction between the tubers softened skin is removed and the water is removed through the hopper. In steam thermic Setting L9-KCHY designed to clean carrots uses saturated steam pressure of 0.5–0.8 MPa.

For the introduction of effective methods and technological modes of hydrothermal treatment plant products (potatoes, carrots and beets) to determine the nature of the changes in them, depending on the degree of exposure moisture and hot [5, 24–26].

Technology for production of natural syrup and dietary fiber is developed to get new types of food products from sugar beet and sugar in the North Caucasian Scientific Search Institute [6, 34–39]. Of course, getting natural syrup involves cleaning root of the bulk of heavy and toxic elements, pesticide residues, saponin by removing the surface layer of the skin, tail and head of the tuber, i. e. those parts of the beet, where these compounds tend to be concentrated.

Based on the theoretical analysis, we've selected and investigated experimentally way to clean roots, based on the short-term followed steam thermic treatment after instant pressure relief of saturated steam from an enclosed space [7, 28–30].

Fig. 1 shows that the function $S=f(P/P_0)$ is sharply increasing character regardless of the initial moisture content of the tuber. So, with a moisture content of sugar beet $U=68.9\%$, relative pressure steam $P/P_0=1.4$ purification $S=0.158$, with $P/P_0=2$, $S=0.32$, at $P/P_0=2.5$, $S=0.5$ and respectively at $P/P_0=3.4$ — achieved complete clearance, i. e. $S=1.0$. A similar relationship holds for other initial moisture content of the tuber. Increase in the relative pressure steam with $P/P_0=1.4$ to 3.4 increases the purity of 6 or more times, i. e., increased pressure steam positive effect on the efficiency of the cleaning process by instant pressure relief.

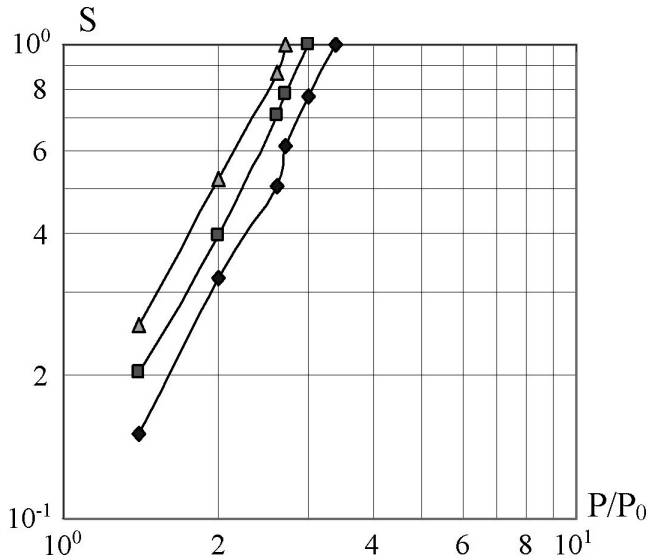


Fig. 1. Influence of pressure steam for purification of sugar beet:

◆ — $W=53.2\%$; ■ — $W=60.4\%$; △ — $W=68.9\%$

Experimental data on the method of cleaning instant pressure relief shows a significant influence on the degree of purification of the tubers. For example, with an increase in initial moisture content of sugar beet with $W=53.8$ to 60.4% degree of purification at $P/P_0=2.7$ increases with $S=0.615$ to $S=0.8$, and with increase of up to $W=68.9\%$ of the value of purity is increased to $S=1$. As can be seen, the intensification of the process of purification was 1.3–1.6 times. It is such a pattern of growth purity remains and other numerical values of P/P_0 . Similar results were obtained in the treatment of red beet.

The result of research on cleaning beet root is shown in fig. 2. As the graphs show, the initial moisture content $W=60.4\%$, relative pressure steam $P/P_0=2$ purification $S=0.395$, with $P/P_0=2.5$, $S=0.705$, with $P/P_0=2.75$, $S=0.8$, and, respectively, at $P/P_0=3$ — complete cleaning is achieved, i. e. $S=1.0$. Analysis of the results shows an increase in the intensification of purity 1.8–2.5 times.

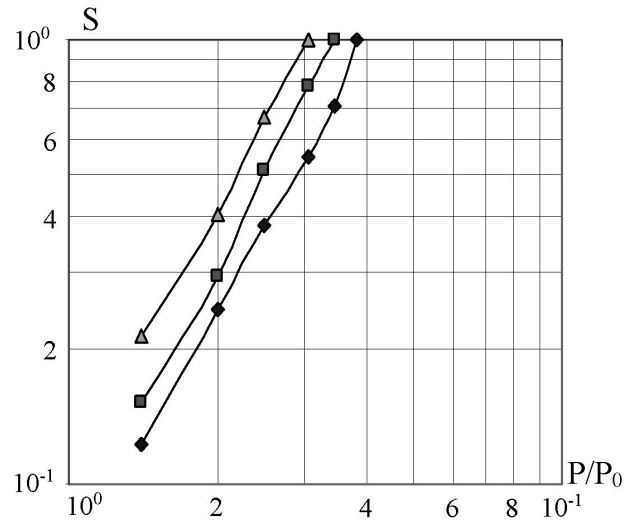


Fig. 2. Influence of pressure steam for purification of red beet:

◆ — $W=54.6\%$; ■ — $W=61.0\%$; △ — $W=68.1\%$

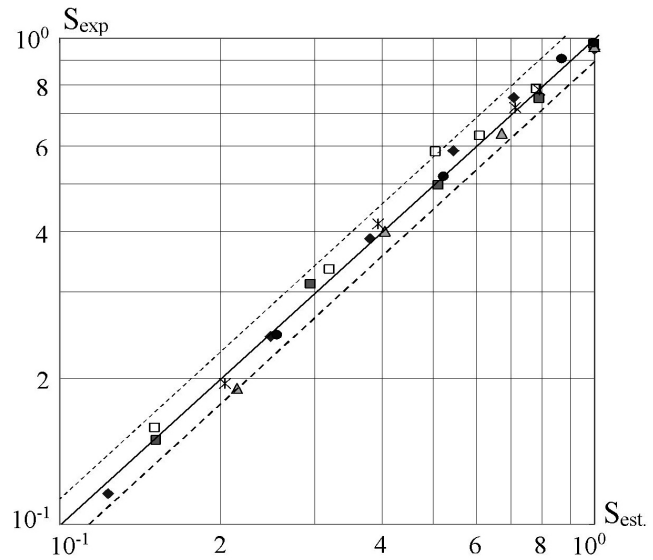


Fig. 3. Comparison of experimental data S_{exp} with estimated S_{est} . cleaning sugar beet by method instant pressure relief:

sugar beet:
□ — $W=53.2\%$; * — $W=60.4\%$; ● — $W=68.9\%$
beet root:
◆ — $W=54.6\%$; ■ — $W=61.0\%$; △ — $W=68.1\%$

The initial moisture content of roots also significantly affects the efficiency of the cleaning process. For example, with an increase in initial moisture content of red beets with $W=54.6$ to $W=68.1\%$ the degree of purification at $P/P_0=2$ increases with $S=0.35$ up to $S=0.405$ and at $P/P_0=2.5$ increases with $S=0.375$ to $S=0.67$. As can be seen, the intensification of the process is 1.15–1.8 times.

Generalization of experimental data purified by instant pressure relief possible to derive a formula to calculate the degree of purification of root crops in the form of:

$$S = A \cdot 10^{-3} \cdot \left(\frac{P}{P_0} \right)^m \cdot W_0^n \quad (1)$$

Coefficient for the red beet $A = 1.275$, the exponent $m = 2.08$ and $n = 2.245$, and for sugar beet respectively — $A = 4.52$, the exponent $m = 2.11$ and $n = 1.7$. Equation is valid in the following range of operating parameters: relative pressure steam $P/P_0 = 1.4-4.0$ and a relative of the original moisture content of $W_0 = 5.4-6.9$. The error in the above formula range of operating parameters shall not exceed $\pm 6.9\%$ (see fig.3).

Visual observations and experimental studies showed that the method provides instant pressure relief in the form of efficient treatment failure scraps thin skin over the entire surface of tuber, except for the top,

i. e. places sprouting leaves. Feature of the method of instantaneous pressure relief in the fact that it cleans pure eyes and even deeper place, filled with sand and soil. In addition, the presence of different types of litter and pollution raw material does not affect the efficiency of the process. Therefore, before clearing roots there is no need to process cleaning operations of raw materials from organic and metallic impurities, rocks and dirt.

Another distinctive feature of this method is that the purified tuber is not cooked, i. e. raw. Adhering after cleaning the pieces of skin can be easily removed in the process of hydraulic classification. This is a positive factor, as loss of raw materials decreased by 3–5 times. Preliminary studies on the treatment of other tuber roots also showed positive results.

References:

1. Магомедов Г. О., Петров С. М., Бывальцев А. И. и др. Новые способы получения продуктов из сахарной свеклы // Сахар. – 2003. – № 6. – С. 54–56.
2. Patent Germany № 3913172, МПК5 А23N 7/00, А47J 17/00. Verfahren zum mechanischen Schalen von Erd- oder Baumfruchten in Schalmaschinen // Dornow Karl-Dietrich. – P. 5.
3. Ковалев В. С., Воронков В. И. Промышленное производство продуктов питания из картофеля. – Киев: Урожай, 1987. – 80 с.
4. Переработка картофеля – стратегический путь развития картофелеводства России / Под общей ред. В. И. Старовойтовой. – М.: Техноэликс, 2006. – 156 с.
5. Остриков А. Н., Калашников Г. В., Калабухов В. М. Динамика качественных изменений в картофеле и овощах при влаготепловой обработке // Хранение и переработка сельхозсырья. – 2005. – № 7. – С. 24–26.
6. Колесников В. А., Лысый Н. А., Павлов П. П. Новые пищевые продукты из сахарной свеклы // Сахар. – 2008. – № 2. – С. 34–39.
7. Абдуллаева С. Ш., Нурмухамедов Х. С., Абдуллаев А. Ш. Очистка корнеплодов методом мгновенного сброса давления // Химическая технология. Контроль и управление. – 2008. – № 4. – С. 28–30.

DOI: <http://dx.doi.org/10.20534/AJT-17-1.2-69-71>

*Abdullaeva Sadokat Shonazarovna,
senior research associate – the researcher,
Tashkent chemical-technological institute,
Department of «Processes and apparatuses of chemical technology»
E-mail: sadshon1975@yandex.ru
Nurmuhamedov Khabibulla Sagdullayevich,
Doctor of technical sciences, Professor,
Tashkent chemical-technological institute*

The dehumidification during crushing of the peeled pulp root crops by method of instant dumping of pressure

Abstract: The results of experimental research on influence of relative pressure P/P_0 and further relative humidity φ of raw materials and time of dumping τ of pressure upon degree of crushing and final humidity of the product are given in the article. The analysis of influence of parameters on dehumidification in the

course of receipt of puree from root beets has also been carried out by the method of instant dumping of pressure (MIDP).

Keywords: dehumidification, heating rate, method of instant dumping of pressure, puree.

The processes to obtain of a ready-made product or a semifinished product by sharp change of pressure of the environment which placed the processed material in the food industry and other industries of production have been widely started to apply. Depending on appointment, the effect of dumping of pressure provides or drying [1, 79], crushing [2, 35–42] or hardening [3, 28–44] materials, by means of the maximum use of effect of intensive molar transfer of steam. The material is heated under the pressure which then decreased. The boiling of moisture and steam formation are resulted due to the accumulated heat in all weight of object. By regulating of boiling process, it is possible to achieve that the process is made destruction or modification of structure and properties of material [4, 135]. In general, by crushing solid materials, the method is implemented as following: heating the material with its moistening and swelling, dispersing and drying of obtained product.

Physical basis of this method is the effect of intensive molar transfer of steam which is observed after preliminary heating of damp material under pressure and it is later rapid decreasing [3, 135]. A change of aggregate state of moisture is occurred at the time of dumping of pressure in all volume of the material, therefore between the center and a surface of an object of processing is formed differential pressure, and contributing to form directed to particle surface of a stream in the form of steam and liquid.

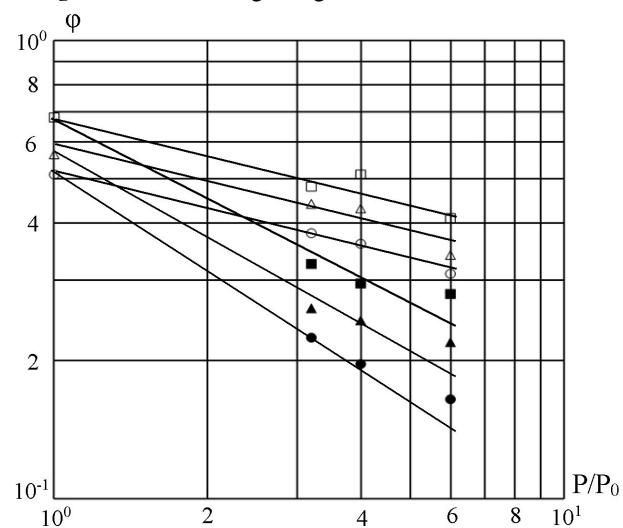
Conditions for realization of transfer of free moisture are created by physical and chemical changes of structure of damp material by its high-temperature heating under pressure. These changes of structure which takes place by heating of a sample proceed almost instantly with achievement of temperature necessary to start these transformations.

Increasing of initial moisture content material is led to increase of contents in an object of free moisture that leads to increase in pressure gradient which is formed by dumping. Gradients of temperature, humidity and pressure are proceeded in one direction, causing migration of moisture within material, leading it to be removed [5, 8–13].

The effect of dehydration with identical pressure is defined by a type of material as well as eventually its colloidal and capillary and porous structure [4, 141]. According to the researchs conducted by a number of

authors [3, 28–44; 6, 118–121], dumping of pressure allows to reduce the containing of moisture several times in comparison with initial depending on structure and properties of material. Intensity of dehydration of material significantly depends on the rate of dumping of pressure [4, 143].

In fig. 1 the results of pilot studies on influence of relative pressure P/P_0 , initial relative humidity φ of raw materials and time of dumping τ pressure upon extent of [7, 9–12; 8, 355–357] and final humidity of a ready-made product crushing are given.



$\tau = 0.070$ s: $\circ - \varphi_{\text{init.}} = 0.68$, $\Delta - \varphi_{\text{init.}} = 0.57$, $\square - \varphi_{\text{init.}} = 0.507$;
 $\tau = 0.005$ s: $\bullet - \varphi_{\text{init.}} = 0.68$, $\blacktriangle - \varphi_{\text{init.}} = 0.57$, $\blacksquare - \varphi_{\text{init.}} = 0.507$

Fig. 1. Dependence of relative humidity φ from pressure of saturated steam by crushing potatoes with the method of instant dumping of pressure

By processing potatoes in mashed potatoes with the method of instant dumping of pressure at initial relative humidity $\varphi = 0.678$ and time of dumping of pressure $\tau = 0.07$ it has the following results: at a relative pressure of saturated steam $P/P_0 = 3.4$ value of relative humidity $\varphi = 0.48$, at $P/P_0 = 4.0$ forms $\varphi = 0.51$, and, at last, at $P/P_0 = 6.0$ relative humidity it is equal $\varphi = 0.415$. Similar dependence is received also for initial relative humidity $\varphi = 0.51$.

So, with a relative pressure of saturated steam $P/P_0 = 3.4$ equal $\varphi = 0.37$ and at $P/P_0 = 6.0$ — $\varphi = 0.315$. It is clear that by growing of relative pressure of saturated steam with $P/P_0 = 3.4$ to 6.0 intensity of dehumidification forms 1.15–1.22 %.

By experimental studies on receiving puree of potatoes it is established that by reducing of time of dumping

τ pressure of saturated steam from the reserved system process of dehumidification is intensified.

Comparison of experimental data shows that at $P/P_0 = 4.0$ and initial humidity $\varphi = 0.678$, final humidity at time of dumping pressure $\tau = 0.07$ s is equal $\varphi = 0.51$, and at $\tau = 0.005$ s — $\varphi = 0.285$. It is clear, decrease in time of dumping of pressure leads to intensification of dehumidification process $\sim 1, 8$ times. The analysis of results for other values of relative pressure of saturated steam P/P_0 and humidity φ has shown that degree of intensity of dehumidification fluctuates within 1.5–2.2.

The analysis of experimental data shows that degree of dehydration of root crops pulp significantly depends on the rate of dumping pressure of saturated steam from the reserved system.

Similar experimental data on dehumidification by crushing with the MIDP are obtained for sugar, red beet and carrots. For these two products regularity of change of relative humidity also remains by crushing with the MIDP.

Explanation of high values of dehumidification in the following: with increase in excessive pressure of the heating steam rate of heating $dt/d\tau$ increases, is proceeded rapid penetration of the front of high temperatures deep into of pulp and intensive moistening of a thin skin. Naturally, at the same time for a high temperature of the heating steam and rather low temperature of pulp a root — or a tuber crop occurred the gradient of temperature which is directed in object of processing.

The object of processing surrounded with saturated water vapor with pressure $P/P_{atm} > 0$ has the temperature front, and inside of the object pressure is $P/P_{atm} = 0.1$. In other words the gradient of pressure of $grad P$ is directed into an object. The humidity vector has the same direction as well as working agent is saturated water vapor $U_{steam} > U_{mat}$.

After boiling of an object on a small depth is made dumping pressure of saturated steam from the reserved system to the environment. It should be noted that at the time of dumping of pressure in a pulp of root crop owing to the formed $grad P$ differential pressure $grad P = P_2 - P_{atm}$ aggregate state of superheated liquid in steam instantly changes. At the same time this phenomenon forms vapor-liquid a stream in the form of the smallest droplets of water and steam which directed from within outside. The amount of the formed water vapor at MIDP directly depends on temperature of the heating steam which much more temperature of boiling of water and temperature of pulp a root — or tuber crops.

At the time of dumping of pressure the above-named gradients of temperature of $grad t$, pressure of $grad P$ and humidity of $grad U$ are directed outside, i. e. from the center of an object of processing to its surface.

Thus, crushing of the deformed materials by method of instant dumping of pressure allows to obtain the crushed mass of necessary humidity and dispersion.

References:

1. Плановский А. Н., Муштаев В. И., Ульянов В. М. Сушка дисперсных материалов в химической промышленности. – М.: Химия, 1979. – 288 с.
2. Рабинович Д. И., Геллер З. И. Размол топлива методом сброса давления//Науч. запис. Одес. политех. ин-та. – 1960. – т. 22. – С. 35–42.
3. Шангареева Е. Ю. Разрушение влажных пористых материалов вследствие быстрого внутреннего испарения при тепловом ударе//ИФЖ. – 1994. – № 1. – С. 28–44.
4. Михайлов Ю. А. Сушка перегретым паром. – М.: Энергия, 1967. – 200 с.
5. Андрианов В. П., Сафин Р. Г. и др. Тепломассоперенос при сушке понижением давления//Современные аппараты для обработки гетерогенных сред. – Л.: ЛТИ им. Ленсовета, 1984. – С. 8–13.
6. Сажин Б. С. Основы техники сушки. – М.: Химия, 1984. – 320 с.
7. Абдуллаева С. Ш., Нурмухамедов Х. С., Абдуллаев А. Ш. и др. Влияние давления острого пара на подсушку корнеплодов при очистке методом мгновенного сброса давления//Хранение и переработка сельхозсырья. – Москва, 2016. – № 4. – С. 9–12.
8. Abdullaeva S. Sh., Nurmuhamedov H. S., Abdullaev A. Sh. Production of sugar beet puree by a method of instant pressure reset//5th World Conference on Intelligent Systems for Industrial Automation «WCIS-2008». – Т., 2008. – P. 355–357.

DOI: <http://dx.doi.org/10.20534/AJT-17-1.2-72-75>

*Bobokulova Oygul Soatovna,
Senior teacher of cathedral «Analytical, physical and colloid chemistry»,
Tashkent institute of chemical technology, Uzbekistan
E-mail: bobokulova79@mail.ru*

*Talipova Habiba Salimovna,
Associate professor, Tashkent institute of chemical technology
E-mail: bobokulova79@mail.ru*

*Mirzakulov Kholtura Chorievich,
Doctor of technical science, professor,
Tashkent institute of chemical technology
E-mail: khchmirzakulov@mail.ru*

Research of process of reception of the pure solutions of chlorides of sodium and magnesium from the dry mixed salts of lake Karaumbet

Abstract: Results of researches on reception of the solutions cleared of accompanying impurity from the dry mixed salts of lake Karaumbet are resulted. Conditions are established at which the maximum solubility of the dry mixed salts, chemical and salt contents of received solutions and solutions after cooling and branch of myrabilit, additional cleanings from sulphates with distiller liquid are established.

Keyword: dry mixed salts, dissolution, filtration, myrabilit, degree of sedimentation, desulphation.

Introduction

Compounds of magnesium and sodium sulphate are used in many industries. Chemical, metallurgical, glass, textile, power, pharmaceutical and other branches require magnesium compounds. Chloride magnesium or bischofite are initial raw materials in manufacture magnesium chloride defoliants [1]. In the absence of own manufactures of compounds of magnesium the requirement for them is completely provided at the expense of import.

Uzbekistan has enormous stocks of raw materials for reception of salts of magnesium and sodium. One of such kinds of raw materials are the dry mixed salts (DMS) of lake Karaumbet. Industrial stocks in a contour of a design open-cast mine of a deposit make 612.55 thousand t in recalculation on chloride magnesium. Dry mixed salts of lake Karaumbet on the average contains (weights, %): Na_2SO_4 — 43–61; MgCl_2 — 11–15; NaCl — 13–19; н. о. — 4–30. Except DMS huge stocks of salts of magnesium and sodium are concentrated and in leach of lakes Karaumbet and Barsakelmes [2].

Despite the big requirement for connections of magnesium and sodium sulphate, presence of a powerful raw-material base they in Republic are not made. It is connected, first of all, with absence of the developed technologies of processing of leach and the dry mixed salts. Therefore the researches directed on working out of

technology of processing of lake Karaumbet DMS with reception of compounds of magnesium are very actual.

For the purpose of involving of the dry mixed salts of lake Karaumbet in industrial production on an establishment of their solubility researches are carried out in water, clearing of solutions of accompanying salts and insoluble impurity in water, processing to hydroxide magnesium.

Objects and methods

For experiments used DMS of lake Karaumbet, contents, (weights, %): Na_2SO_4 — 60.69; NaCl — 18.81; MgCl_2 — 15.30; MgSO_4 — 0.42; CaCl_2 — 0.31; н. о. — 6.98; H_2O — others. The chemical analysis on the contents of the basic components in solutions, distiller liquids, mother solutions and a solid phase spent by known methods [3–5].

For an establishment of optimum technological parametres of preparation of solutions from DMS their solubility in water depending on ratio H : L is studied, at temperature 25 °C, constant speed of hashing and duration of process of 30 minutes. The received results are resulted in table 1.

From the resulted data it is visible, that maximum solubility of DMS in water is observed at H : L = 1 : 3 and makes 93.02 % from a total mass. Hence for reception of solutions with maximum solubility of DMS it is necessary to support H : L = 1 : 3.

Table 1. – Influence of H:L to solubility of DMS and speed of a filtration of suspension at temperature 25°C and durations of process of 30 minutes

Nº	H:L	Exit of a damp deposit, %	Exit of the dry rest, %	Degree of dissolution, %
1	1:20	22.63	13.02	73.96
2	1:2.5	6.72	4.46	91.08
3	1:30	4.69	3.49	93.02
4	1:40	4.70	3.49	93.02

From the table it is visible, that with increase H:L from 2:1 to 4:1 degree of dissolution of DMS increases and reaches 93.02%. Practically salt is dissolved at H:L = (2.5–3):1. This ratio corresponds to maximum

solubility of DMS in water at temperature 25 °C and durations of process of 30 minutes.

Researches of influence of duration of process at H:L = 3:1 have shown, that in 5 minutes dissolution degree reaches 89.25%, and in 15 minutes — 93.02% at temperature 25 °C and 92.5% in 5 minutes and 91.61% in 10 minutes at temperature 50 °C, that specifies that in water is enough 15 minutes (fig. 1) for dissolution of DMS.

For division of liquid and hard phases of solutions DMS researches on their filtration have been carried out. For this purpose used the condensed part after upholding. Upholding proceeds quickly and in 30 minutes clarification degree reaches 94.59% at temperature 20 °C and 95.51% at temperatures from 40 to 80 °C.

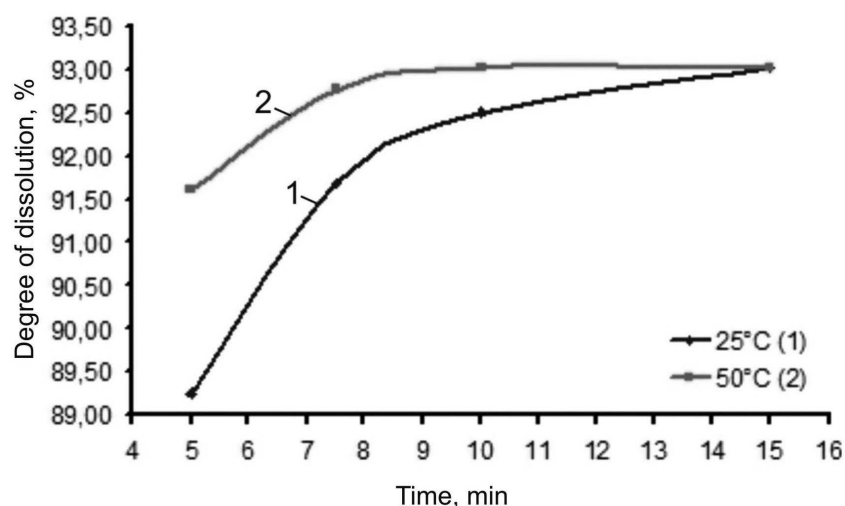


Fig. 1. Influence of duration of process on degree of dissolution of DMS at H:L = 1:3 and temperature: 1 — 25°C; 2 — 50°C

Results of researches of influence of temperature for speed of a filtration of the condensed part both on a pulp, and on a hard phase and a filtrate are presented in table 2.

Table 2. – Influences of temperature on speed of a filtration of the condensed deposit

Nº	Temperature, °C	Speed of a filtration, kg/m ² ·hour		
		on pulp	on a hard phase	on a filtrate
1	20	1028	132.64	895.88
2	40	1348	174.16	1176.84
3	60	1684	217.28	1468.84
4	80	2016	260.04	1756.28

The given tables show increase in speed of a filtration with rise in temperature. So at rise in temperature from 20 °C to 80 °C speed of a filtration on the condensed pulp raises about 1028 kg/m²·hour to 2016 kg/m²·hour, and on a filtrate about 895,88 kg/m²·hour to 1756,28 kg/m²·hour. It is thus formed from 132,64 kg to 260,04 kg solid phases.

In table 3 the average chemical compound of a deposit of the dry mixed salts after a filtration in recalculation

on dry weight is presented. The basic component of the insoluble rests in water are silicon oxide and its compounds. Except silicates there are carbonates of calcium, magnesium and calcium sulphate.

For acknowledgement of salt structure of the insoluble rests in water have been removed diffractogram and Ik-spectra.

Table 3. – Chemical coontents of the insoluble rests in water of DMS

Nº	The name	Chemical compound i. r., weights. %				
		CaO	MgO	SO ₃	CO ₂	SiO ₂
1	I.r. of DMS	16.01	1.25	19.90	6.59	51.33

On the roentgenogram there are the differential maxima concerning carbonates of calcium, magnesium, to double-water and waterless sulphate of calcium. Peaks 5.40; 4.56; 3.16; and 2.47 Å belong to calcium sulphate, 3.40; 1.875; 1.626 Å belong, and peaks 3.38; 2.75; 2.44; 1.818; 1.434 Å — to silicates.

On Ik-spectra there are strips of absorption of 1008.44 sm^{-1} concerning sulphatic groups. Strips of absorption 3557.42 ; 3430.55 sm^{-1} concern semihydrate and dihydrate calcium sulphate, and a strip of absorption 878.32 ; 467.21 sm^{-1} — to silicates. It also confirms the obtained data chemical and roentgen phase analyses.

After branch of the insoluble rests in water and rest of DMS are defined theological properties of formed solutions. The received results are resulted in table 4.

Table 4. – Influence of H:L and temperatures to density and viscosity of solutions from DMS lake Karaumbet

№	H:L	Density, g/sm ³			Viscosity, cPa		
		20 °C	40 °C	60 °C	20 °C	40 °C	60 °C
1	1:2	1.1874	1.1838	1.1800	220.50	168.30	139.10
2	1:3	1.1824	1.1788	1.1751	209.17	157.91	129.94
3	1:4	1.1778	1.1741	1.1705	197.30	148.30	120.70

Reception solutions at H:L = 1:(3–4) have density of 1.1778 – 1.1824 g/sm^3 at 20°C and decrease to 1.1705 – 1.1751 g/sm^3 at 60°C . Viscosity of solutions with rise in temperature from 20°C to 60°C decrease with 197.30 – 209.17 cPa . to 120.70 – 129.94 cPa . Solutions, irrespective of temperature, have good theological properties and are easily transported.

The dry mixed salts taken for experiment, contain more than 60% myrabilit. For allocation of sulphate of sodium the solutions received at H:L = 1:3, have subjected to cooling to temperature 0 , -5°C (tab. 5).

From the received data follows, that at cooling to temperature 0°C the contain of sodium sulphate in solution of DMS decreases from 15.31% to 2.51%. The contents

Table 5. – Influence of temperature to chemical and salt structures of solutions of the dry mixed salts and output of myrabilit

T, °C	Chemical content of a liquid phase, weights. %					Salt content of a liquid phase, weights. %				Output Na ₂ SO ₄ , %
	Na ⁺	Mg ²⁺	Ca ²⁺	Cl ⁻	SO ₄ ²⁻	Na ₂ SO ₄	MgCl ₂	NaCl	CaSO ₄	
25	7.92	1.01	0.024	5.83	10.41	15.31	3.97	4.74	0.08	–
0	3.44	1.43	0.032	8.22	1.75	2.51	5.52	6.68	0.11	83.61
-5	3.37	1.44	0.032	8.29	1.56	2.23	5.64	6.74	0.11	85.43

Table 6. – Norm influence of distiller liquids on chemical salt contents and degree of Desulphation solutions of DMS

Norm of dist. l., %	Chemical content of a liquid phase, weights. %					Salt content of a liquid phase, weights. %				Degree of desulphation, %
	Na ⁺	Mg ²⁺	Ca ²⁺	Cl ⁻	SO ₄ ²⁻	Na ₂ SO ₄	MgCl ₂	NaCl	CaSO ₄	
95	3.72	0.90	0.09	8.08	0.61	0.54	3.52	8.99	0.32	65.14
100	3.46	0.88	0.10	7.94	0.24	–	3.46	8.84	0.33	86.29
102	3.45	0.87	0.10	7.90	0.23	–	3.43	8.80	0.34	86.86
105	3.44	0.86	0.10	7.83	0.22	–	3.39	8.74	0.34	87.43

of other components of a solution raises. The content of magnesium chloride raises from 3.97% to 5.52%, sodium chloride from 4.74% to 6.68%. The content of calcium sulphate changes slightly and makes 0.11%. Received myrabilit further processed on sodium sulphate.

In view of the high residual content of sulphates in a solution (2.23–2.82%), after sedimentation of myrabilit, additional cleaning from sulphates carried out with distiller liquid — a waste of soda manufacture, structure (weights, %): Na⁺ — 2.18; Mg²⁺ — 0.007; Ca²⁺ — 3.03; Cl⁻ — 8.74; SO₄²⁻ — 0.03.

Desulphation spent at norm calcium of distiller liquids 95, 100, 102 and 105% on SO₄²⁻ a solution at temperature 25°C and durations of process desulphation at 30 minutes (tab. 6).

Thus content SO₄²⁻ decreases from 1.75% to 0.22–0.24%. Sodium sulphate co-operates with calcium chloride of distiller liquids with formation of sodium chloride and calcium sulphate. The content of sodium chloride raises to 8.74–8.84%, and magnesium chloride to 3.39–3.46%. At norm of distiller liquid of 100–102% in a solution does not have sodium sulphate and there is an insignificant quantity of calcium chloride.

The contents of calcium sulphate makes 0.33–0.34% that corresponds to its solubility in water solutions. Optimum norm of distiller liquids for desulphation are 100–102%.

The structures, the received solutions at norm of 100–102%, on the contents of impurity are close to structures of the cleared solutions received from leach of lakes Karaumbet and Barsakelmes which are processed with good technical and economic indicators to magnesium chloride and magnesium hydroxide [6; 7].

Conclusion

Thus, the carried out researches have shown basic possibility of processing DMS of lake Karaumbet with reception of the cleared of impurity solutions of chlorides of sodium and magnesium, suitable for the further processing to magnesium chloride, magnesium hydroxide and its other compounds. Thus in passing receive myrabilit, chemically besieged calcium

sulphate, sodium chloride at processing on bischofite, or its solutions at sedimentation of magnesium hydroxide. For this purpose it is necessary DMS to dissolve at $H:L=1:(3-4)$ within 15 minutes to separate the insoluble rests in water, to allocate at temperature $0, -5^{\circ}\text{C}$ myrabilit, mother solution additional clearing with distiller liquid at norm CaO of 100–102 % at the rate to SO_4^{2-} solution of DMS.

References:

1. Copyright certificate. № 1151507 SU, Cl. C01F5/30, A01N^o 59/06. Way of reception defoliants. M. N. Nabiev, S. To'xtaev, R. E. Shammasov, N. Yu. Musaev, R. A. Akramov and others. Publ. 23.04.1985. – Bubliten. № 15.
2. Bobokulova O. S., Usmanov I. I., Mirzakuloiv Kh. Ch. Salts of lakes Karaumbet and Barsakelmes – raw materials for reception of salts of magnesium // Chemistry and chemical technology. – 2014. – № 1. – P. 2–7.
3. Byurriel-Marti F., Ramires-Munos X. Photometry of flame. – Moscow: «Mir» Publ., 1972. – 520 p.
4. Methods of the analysis of phosphatic raw materials, phosphoric and complex fertilizers, fodder phosphates/Vinik M. M., Erbanova L. N., Zaytsev P. I. and others – M.: Chemistry, 1975. – 215 p.
5. GOST 7759–73. Magnesium chloride technical (Bischofite). Specifications. – M.: Publishing house of standards, 1986. – 10 p.
6. Bobokulova O. S., Tojiev R. R., Usmanov I. I., Mirzakuloiv Kh. Ch. Working out of technology hydroxide and oxide magnesium from leach of lakes Karaumbet and Barsakelmes // The Chemical industry. – 2015. – № 6. – P. 272–279.
7. Bobokulova O. S., Melikulova G. E., Sidikov A. S., Usmanov I. I., Mirzakuloiv Kh. Ch. Research of process of reception of magnesium chloride from leach of lakes Karaumbet and Barsakelmes // The Chemical industry. – 2016. – № 3. – P. 110–118.

DOI: <http://dx.doi.org/10.20534/AJT-17-1.2-75-79>

Kadirov Xasan,
associate professor,
Tashkent chemical-technological institute,
Tashkent, Uzbekistan
E-mail: Ulug8Sbek77@mail.ru

The use of complex composition in the preparation of water boiling and heating systems

Abstract: Proposed composition prepared on the basis of UFR and IOMS-1, as well as UFR + BRMEA + IOMS-1. It is found that these compositions under conditions of the tests are effective inhibitors of corrosion and scaling, with a concentration of 4–8 mg/l efficiency of not less than 90 %. Also, a composition for inhibiting scaling IOMS-1 ÷ BRMEA ÷ EPA ÷ AVK-extract ÷ H₂O. The use of this composition in water supply systems will prevent bio fouling, scaling and corrosion, ensuring a long and trouble-free operation of the closed water systems.

Keywords: complex composition, efficiency, preparation, boiling, heating, systems, salts.

Introduction

Dissolved in water, the substance causes certain problems in the energy equipment. This is mainly due to the formation in thermal units crustose deposits consisting of calcium and magnesium salts contained in the make-up water.

Reduce the tendency for scale formation on heat transfer surfaces are usually resorted to desalting using ion-exchange water or stabilization processing units via water scale inhibitors in which are introduced into the feed water chemicals that prevent the formation of scale [1].

The disadvantages of a water softener, sodium-cationization are continuous consumption of imported salt, fresh water consumption for auxiliaries chemical water treatment and water pollution by waste water containing a large amount of chloride, and neutralization and disposal of saline waste water boiler is one of the environmental problems. Currently, the cost of implementation of the various proposals for the treatment and recycling of waste water often exceed the cost of the water treatment. The current state of the domestic economy and the environment dictates the use of alternative softening environmentally friendly, low-cost technology solutions in the preparation of make-up water.

In techenie decades in thermal power plants to prevent deposits and reduce the rate of corrosion of equipment are widely used sequestering agents — chelators [2–4]. These compounds are used to correct water chemistry and for cleaning water heating equipment and pipelines from deposits. Significant interest alkildifosfonovye acid exhibiting high specificity of the interaction with the major cations [5].

An important representative of these acids are Nitrilotrimethylphosphonic acid (NTF) and hydroxyethylendiphosphonic acid (HEDP). Chelation have been very effective in preventing precipitation of sparingly soluble substances such as carbonates, sulfates and calcium phosphates. In particular, IOMS-1 (which is based on NTF) is effective for calcium carbonate is relatively ineffective in the case of calcium sulfate and is one of the most effective inhibitors of calcium phosphate deposition and has been successfully used in the boilers of Tashkent.

As a rule, the scope of the phosphonates is substantially limited scale-forming properties of water and thermal characteristics of equipment. In addition, the high cost of these inhibitors put limits to their use.

In order to obtain highly efficient, cheap inhibitors studied based composition NTF HEDP and adding phosphoric acid (EPA), urea-formaldehyde resins (UFR) and vacuum distillation bottoms monoethanolamine (BRMEA).

Objects and methods of research

The objects of research are — IOMS-1, HEDP and compositions prepared based on them, “IOMS-extra-1”, SUMONO-DU, EPA, BRMEA, UFR. Determine the efficacy of inhibition of scaling and shares of the main substances in the inhibitor.

Results and discussion

In order to prepare the compositions of mineral salt deposition inhibitors designed using a small quantity of the imported product, studied composition based on IOMS-1 with the addition of UFR and BRMEA. The prepared compositions were tested as inhibitors of mineral scales in real waters stiffness which varies in the aisles of 10–12 mg/g.

Of great interest from an economic point of view, the study of the inhibitory properties of the composition of the above products. Experiments show that the addition of a medium having 0.5 mg/l IOMS-1 in an amount of 1.5 mg/l UFR, increases the efficiency of 1.18 % inhibition relative IOMS-1 and 86 %; increase in UFR components relations and IOMS-1 (4.0:2.0) maximum efficiency — 94 %, which is the same as the requirements for standards. A further increase in the number of UFR and IOMS-1 does not lead to the desired result.

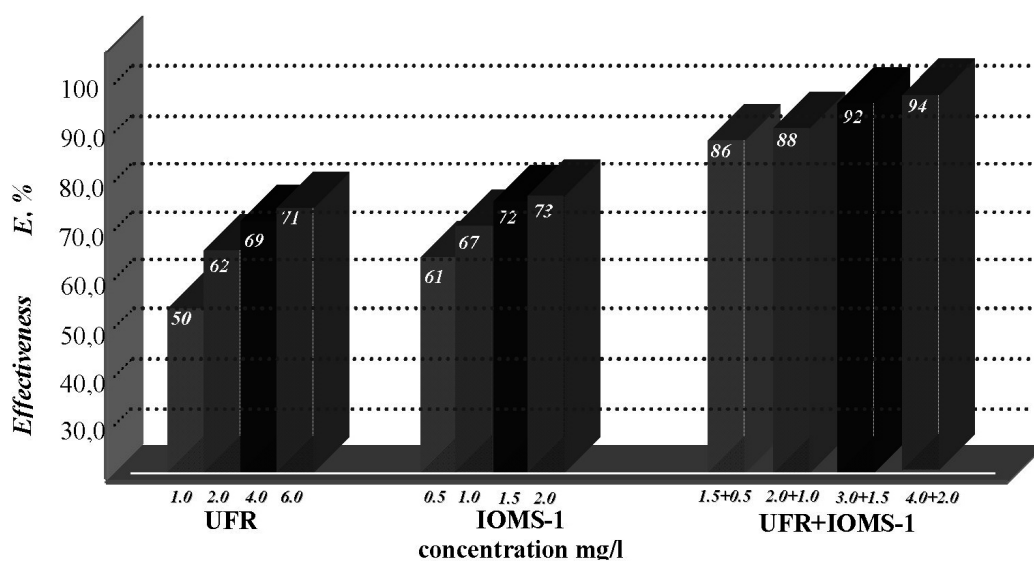


Fig. 1. The effectiveness of the inhibition of UFR, IOMS-1 and compositions thereof. The temperature of 90 °C

Table 1. — Investigation of the inhibitory activity of the obtained compositions

№	Inhibitor components, wt. %	Inhibitor concentration mg/l	Efficiency %		
			Hardness investigation water mg/l		
			4-6	7-9	10-12
1.	IOMS-1 ÷ BRMEA ÷ EPA (10+10+80)	2.0	88	86	84
		4.0	90	88	85
		5.0	91	90	88
		6.0	97	90	88
2.	IOMS-1 ÷ BRMEA ÷ EPA (15+10+75)	1.0	90	89	87
		2.0	92	91	88
		3.0	93	92	89
		4.0	93	92	90
3.	IOMS-1 ÷ BRMEA ÷ EPA (15+15+70)	1.0	90	88	86
		2.0	91	89	88
		3.0	91	90	89
		4.0	91	90	89
4.	IOMS-1 ÷ BRMEA ÷ EPA (10+15+75)	1.0	92	90	89
		2.0	93	91	90
		3.0	95	92	91
		4.0	96	92	91
5.	IOMS-1 ÷ BRMEA ÷ EPA (15+10+75)	1.0	90	89	87
		2.0	91	90	88
		3.0	92	90	89
		4.0	92	90	90
6.	IOMS-1 ÷ BRMEA ÷ EPA (10+20+70)	1.0	91	90	89
		2.0	92	91	90
		3.0	93	91	90
		4.0	93	91	90
7.	IOMS-1 ÷ BRMEA ÷ EPA (20+10+70)	1.0	91	90	89
		2.0	92	91	90
		3.0	92	91	91
		4.0	93	92	91

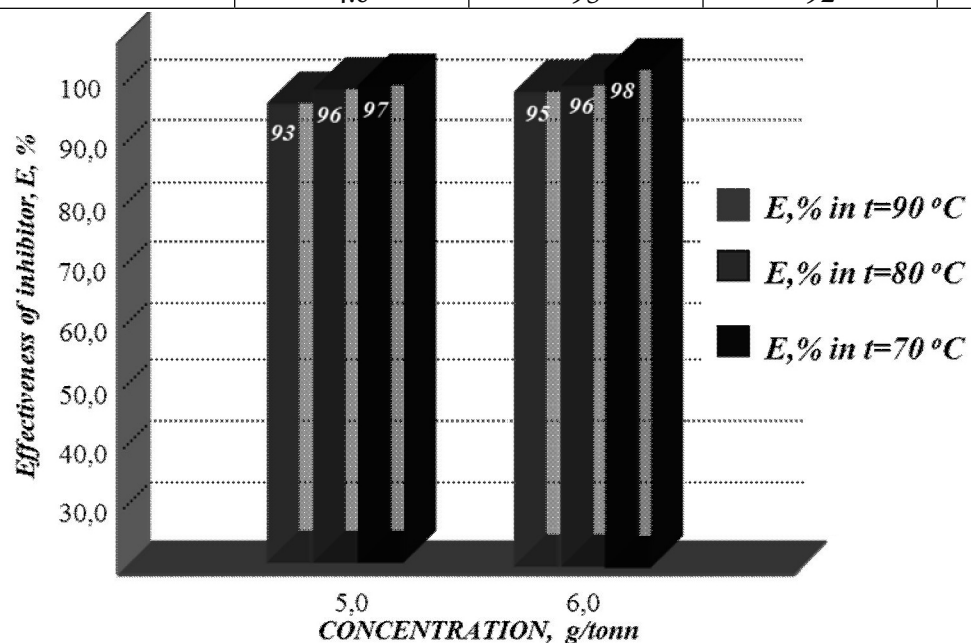


Fig. 3. The dependence of the efficiency of inhibiting deposition of mineral salts SUMONO-DU composition. Water hardness is 12 mg/l

As can be seen from table efficiency obtained composition is largely dependent on the amount IOMS-1: as further reducing the amount of the product leads to a dramatic deterioration in the effectiveness of the inhibitor minimum amount IOMS-1 is set to 10% by weight. The optimum ratio of these products can be considered IOMS-1 ÷ MEA ÷ EPA (10 + 15 + 75), in which the efficiency is 91–96% depending on the hardness of the water. But while the number of phosphate balance is slightly higher than the permissible norm, which does not allow the use of this product on a large scale.

In order to obtain high performance scale inhibitor provides a composition consisting of IOMS-1 ÷ BRMEA ÷ EPA ÷ AVK-extract ÷ H₂O (10 + 15 + 15 + 1 + 59). The composition conventionally named SUMONO-DU.

The graph shows the inventive composition is a highly effective inhibitor of scale (efficiency not less than 90%), while responding to physical, chemical and performance characteristics, requirements for such products of the chemical industry.

Experiments show that when using SUMONO-DU system in a closed water system allows you to get an unexpected result — the suppression of the microflora

while effectively inhibiting the corrosion and scaling. In our opinion, the presence of zinc complex mixture at a certain ratio with AVC-extract inhibits microbial activity. The use of this composition in water supply systems will prevent biofouling, scaling and corrosion, ensuring a long and trouble-free operation of the closed water systems, and with the required quality.

Summary

Thus, the compositions based on cooked and IOMS-1, UFR and UFR + IOMS-1 + BRMEA in terms of the tests are effective inhibitors of corrosion and scaling, with a concentration of 4–8 mg/l efficiency of not less than 90%. It was determined that the composition does not soften water and stabilizes it — does not allow to pass scaling processes. Water treatment with IOMS-1 in combination with UFR, BRMEA and allow to exclude water softening step, and in some water systems, and the step of de-aeration.

Also, a composition for inhibiting scaling IOMS-1 ÷ BRMEA ÷ EPA ÷ AVK-extract ÷ H₂O (10 + 15 + 15 + 1 + 59). The use of this composition in water supply systems will prevent biofouling, scaling and corrosion, ensuring a long and trouble-free operation of the closed water systems.

References:

1. Дрикер Б. Н., Михалев А. С., Пинигин В. К. и др. Ресурсосберегающие технологии в водоподготовке промышленных предприятий и теплоэнергетики // Энергосбережение и водоподготовка. – 2000. – № 3. – С. 45–47.
2. Кащавчев В. Е. и др. Предупреждение солеобразования при добыче нефти. – М.: Недра, 1985. – 215 с.
3. Chemistry of Organophosphonate Scale Growth Inhibitors: Physicochemical Aspects of 2-Phosphonobutane-1,2,4-Tricarboxylate (PBTC) and Its Effect on CaCO₃ Crystal Growth Konstantinos D. Dcmadis and Panos Lykoudis Department of Chemistry, University of Crete, 300 Leoforos Knossos, Heraklion, Crete, Greece GR-71409. Vol. 3, Nos. 3–4. – 2005. – P. 135–149.
4. Пат. (RU) № 1005667. Колотов В. Ю., Самошкин А. Л. N,N-бис(фосфатометилен)-N'-гидроксиметилен-N'-фосфонитометилен тиомочевина в качестве ингибитора и биоцида). Заявл. 05.01.2004. Опубл. 27.07.2006. Бюл. № 21.
5. МУ 1–322–03. Методические указания по стабилизационной обработке воды систем теплоснабжения, водогрейных котлов комплексонатами ОЭДФ-Zn, НТФ-Zn. – Ростов-на-Дону, 2003. – 18 с.

*Maksimova Sevinj Abusalat qizi,
PhD. Candidate, Department of Environmental economics,
Azerbaijan State University of Economics (UNEC)
E-mail: Sevinj_Mahsimova@unec.edu.az*

Research of new environmental methods for obtaining the organic–mineral fertilizers

Abstract: The essence of this research consists in that when municipal solid waste and sludge generated from waste water decompose with waste nitric acid produces organic-mineral fertilizers. As a result of the interaction the waste nitric acid with compounds contained in municipal solid waste and sludge, obtains high quality product: organic-mineral fertilizers with increased content of nitrogen, phosphorus and potassium. The technological process conducts in continuous mode. The result is solid and liquid phases of fertilizer. The released mixture of nitrous gases is absorbed and in the reaction with the limy milk obtained fertilizer. The heavy metals are also adsorbed during the process. Using the waste nitric acid significantly accelerates the decomposition process. Giving the title-product of fertilizer for agriculture increases the economic efficiency of the work done.

Keywords: solid waste management, decomposition, organic-mineral fertilizers.

Introduction

Development and growth capacities of different industries are based on waste-free technologies, and it calls for new approaches for the development of methods for recycling of household and industrial waste. And it is difficult to find the same point of views on the prospects of human society development on the issue of environmental protection and sustainable use of natural resources.

In parallel with the growth of world population the power of various industries is growing, despite the high requirements imposed on them. Due to this, environmental condition is getting worse and worse, and it has a negative impact on the food industry, agriculture, and as a consequence, the planet's health.

As it has been noted by many researchers, the main contradiction between economic and environmental development is that, on the one hand, the economy should be developed. On the other hand, the development increases harmful consequences for the environment (N. Rogojina, 1999).

For example, the analysis of the mining industries of some countries leads to the following conclusions. According to experts, opencast mining is damaging to natural ecosystems, despite the fact that it is a cheap way of production. In mining areas the enrichment and processing of raw materials are producing mountains of waste. This is a serious source of contamination of surface and underground waters, air and soil.

Efficient use of natural resources

Nowadays, all countries are taking measures to reduce the natural resource extraction. But it is not enough. It is necessary to undertake measures for nature restoration. For this approach, the scientists developed a system of measures for the environmental protection and restoration. These activities are carried out not only by the governments, but also by private organizations. Many scientists lead different methodologies of economic calculations of such activities. The economic results of the environmental protection measures, as E. D. Kazyanova argues (E. Kazyanova, 2003), are preventing the loss of natural resources and improving work efficiency in productive and non-productive areas of economy. Then, in her opinion, the economic justification for the protection of the environment should follow these steps:

1. More complete accounting of all positive and negative socio-economic impacts of different options of environmental protection measures, both in the short and in the long term perspective;
2. The most comprehensive accounting of cost, relevant to the implementation of various environmental action methods;
3. Accounting of the time factor in the assessment of costs and benefits;
4. Intersectoral approach to the selection of certain measures by taking into account saving costs for environmental improvement and ensuring more

effective usage of natural resources of the territory in question (M. Golubets, 1982).

In this case, as shown by M. A. Golubets in his research on the efficient use of mineral resources, you must base upon a few basic principles (M. Golubets, 1982). He offers three basic principles:

1. the use of a minimum of natural resources to produce target products;
2. decontaminate wastes;
3. taking into account the recycling of raw natural resources.

It is the fact, that, the world technologies are based on these principles.

Analyzing foregoing and other researches examining the impact of the growth of waste on the environment as a whole, it becomes obvious that one of the major challenges to address these issues is a creation of environmentally safe and non-waste technologies.

Many scientists have developed various methods of processing for solving these problems. Among the many existing recycling methods, the most important is a comprehensive solution of the problem with an economic effect. Considering the state of the issue to date, our research work was carried out in the direction of the most effective recycling and the least of environmental contamination.

Experimental part

This paper presents the results of investigation decomposition process of the waste nitric acid, a mixture of municipal solid waste and the sludge formed after wastewater treatment. Researches performed to recycling and obtain the desired product. Thus, besides the solid waste and sludge utilization, the importance of the test process is that: when the joint expansion of solid waste and the sludge waste nitric acid obtained organic-fertilizer improved quality (S. Sakmanli, 2015). In order to investigate the average composition of MSW tentative amount of waste from different areas of the city and in different seasons were taken.

The main indicators characterizing the physical properties of waste as raw material for producing fertilizers and fertilizer quality assessment include: an average density (volume weight), a morphological composition, fractional composition and humidity.

A. M. Kuzmenkova affirms that (A. Kuzmenkova, 1976), the volumetric weight of solid waste from the well-appointed apartment houses with a high level living conditions is 0.35 m/m, whereas the volume of waste by weight of poor areas reaches 0.65 t/m³ (based on date). According to our research, it is neces-

sary to take into account the volume of solid waste by weight, which is constantly changing and depends on many factors. For example, the humidity waste changes depend on the distance. The following shows the elemental and morphological composition of MSW, %, based of dry substance (table 1): (<http://portaleco.ru/ekologija-goroda/sostav-svoystva-i-obem-tverdyh-bytovyh-othodov.html>, 2016).

Table 1. – The elemental and morphological composition of MSW in %, based of dry substance:

Compo-nents	Content, % (humidity of MSW)	Elemental composition			
		Carbon	Hydrogen	Oxygen	Nitrogen
Food waste	15	41.7	5.8	27.6	2.8
Garden waste	10.1	49.3	6.4	36.3	3.0
Newsprint	11.6	48.8	6.1	42.7	0.1
Mixed paper	11.6	44.0	6.2	41.7	0.4
Corrugated cardboard	4.3	45.5	6.1	44.5	0.2
Plastic	11.5	59.8	8.3	19.0	1.0
Glass	5.0	0.5	0.1	0.4	0
Ferrous metals	3.9	0.8	0	0.2	0
Aluminum	1.2	0.8	0	0.2	0
Other inorganic waste	7.1	0.5	0.1	0.4	0
Other organic waste	8.8	48.8	6.1	28.3	1.8
Total	100.0	38.3	5.1	27.2	0.8

For Azerbaijan, the average chemical composition of solid waste is shown in table 2.

Table 2. – The average chemical composition of solid waste for Azerbaijan

Indicators	Climate zones, %	
	Middle	South
Organic substance	56–72	56–80
Ash content	28–44	20–44
Total Nitrogen	0.7–1.1	1.2–1.9
Calcium	2–3	4–5.7
Carbon	30–35	28–39
Phosphorus	0.5–0.8	0.5–0.8
Total Potassium	0.1–0.6	0.4–1.1
Humidity (% of the total weight)	40–50	35–70

For obtaining more exact results take we need to the average composition of solid waste in terms of the basic elements of which are presented in the tables 3 and 4 (S. Sakmanli, 2015).

Table 3. – The solid municipal waste, %

Nitrogen	Phosphorus*	Potassium**
0.8–1.5	0.5–0.8	0.3–0.6

Table 4. – Sludge from wastewater treatment, %

Nitrogen	Phosphorus*	Potassium**
1.7–5.5	0.9–6.5	1.8–1.9

Note: * — In terms of P_2O_5 , ** — In terms of K_2O

In the process is the waste nitric acid also used, which is a waste product electropolishing of steel and alloys of the following composition, %: HNO_3 — 27–35; F — 0.01; Cu — 1.1; Ni — 1.1; Cr — 1.2; CrO — 0.3; Mo — 0.3; Co — 0.1; Al_2O_3 — 0.03; organic impurities — 0.1–0.4; H_2O — the rest of it (M. Alosmanov, 1988).

Table 5. – The dependence of the degree of decomposition of municipal solid waste and sludge generated after waste water treatment waste nitric acid, the ratio of solid waste and sludge

№	Taken			Obtained					Decomposition degree, %
	municipal solid waste, kg.	sludge generated after waste water treatment, kg.	waste nitric acid, in terms of 100 %- HNO_3 , kg.	The solid phase, kg.	Liquid phase, kg.	including, %			
						P_2O_5	N_{total}	K_2O	
1.	80	15	5	64.0	36.0	5.0	6.6	1.6	88.6
2.	75	20	5	63.5	36.5	5.2	6.8	1.7	88.9
3.	70	25	5	62.0	38.3	5.25	6.9	1.8	88.7
4.	65	30	5	61.5	38.5	5.3	7.1	1.9	87.4
5.	60	35	5	59.5	40.5	5.36	7.6	1.95	86.3
6.	55	40	5	53.5	46.5	5.4	7.9	1.99	85.9
7.	45	50	5	47.5	52.5	5.5	8.1	2.1	85.8

Solid waste and sludge, generated from wastewater treatment, react with various acids by in different ways. As indicated above, the mineral acid used in our studies, is a waste of industrial production. Although, the low concentration of waste acid and impurities, a nitric acid is very strong by nature, so the waste decomposes sufficiently.

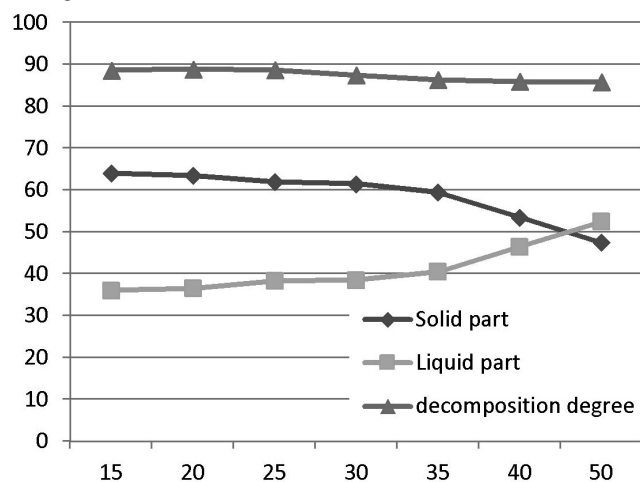


Fig. 1. Depending on the changes in the proportion of solid waste and sludge, and the degree of decomposition of waste

Conducted researches show that a continuous process, allows a large amount of solid waste and sludge generated from waste water. For research, we used a solid waste and sludge in the ratio of (80:45) : (15:50). Decomposition of resulting mixture with waste nitric acid takes place in a continuous mode (S. Sakmanli, 2015). Heavy metals contained in the solid waste and sludge is adsorbed from the liquid phase. At the same time, the process of capture and absorption of gases evolved. Table 5 shows the results of experiments, neutralization and utilization of solid waste and sludge. It was revealed that a change in the ratio of solid waste and sludge is inappropriate, since it is within the specified range to achieve the best results.

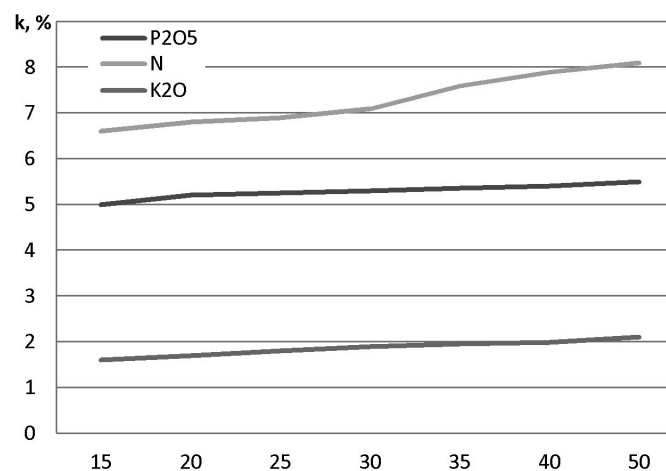


Fig. 2. The increased percentage of phosphorus, nitrogen and potassium in the obtained organic-mineral fertilizers

The study examines the degree of decomposition of solid waste and sludge with the waste nitric acid, combined in different proportions. The experimental results are shown in figures below. The experiments has been used the same amount of acid. Fig. 1 shows the change in the content of the solid and liquid phases, depending on

the changes in the proportion of solid waste and sludge, and the degree of decomposition of waste.

In fig. 2 we see the increased percentage of the basic chemical elements, phosphorus, nitrogen and potassium in the obtained organic-mineral fertilizers. This changes the percentage of solid waste and sludge at a constant amount of waste nitric acid. During the experiments, get steady indicators. As a result, it can be argued that the investigated process of obtaining organic-mineral fertilizer from solid waste and sludge is an efficient technological process (S. Sakmanli, M. Alosmanov, H. Bafadarova, 2010).

Conclusion

The organic fertilizer obtained in the process as the desired product and its usage shows the high importance in terms of economic efficiency of the work done. Additionally, all the prerequisites for creating a waste-free process are formed. Even the evolved gases in the

process are captured and absorbed, thus also get a valuable product.

As a result of this research, it has been achieved an acceleration of the process of decomposition of municipal solid waste and sludge generated from waste water, usage of waste nitric acid, obtaining organic — mineral fertilizer with a relatively high content of nitrogen, phosphorus and potassium, preventing of contamination of waste and sludge.

The Government of our country making major steps towards the rapid development of agriculture accepted many programs, laws, etc. in this area. Keeping the above principles the least use of natural resources and the maximum protection of the environment, the proposed technology allow to solve the problem of effective agricultural development and environmental protection. In order to improve this technological process researches continue.

References:

1. Kuzmenkova A. Using composts from municipal solid waste. – Moscow: Rosselhozizdat, 1976.
2. Kazyanova E. The damage caused by of environmental contamination. – Astrahan: Report, 2003.
3. [Electronic resource]. – Available from: <http://portaleco.ru/ekologija-goroda/sostav-svoystva-i-obem-tverdyh-bytovyh-othodov.html> (2016, 01).
4. Alosmanov M. Physical and chemical research and development of technology of phosphate fertilizers by using industrial wast and natural resources of the South Caucasus. – Baku: ANSA, 1988.
5. Golubets M. Actual matters of environment. – Kiev: Nauka, 1982.
6. Rogojina N. In search of answers to the environmental challenge. World economy and international relations. – 1999.
7. Sakmanli S. Patent No. i20150041. – Azerbaijan, 2015.
8. Sakmanli S., Alosmanov M., Bafadarova H. Physico-chemical research of processing of municipal solid wastes// Ecoenergetika. – 2010. – № 3.

DOI: <http://dx.doi.org/10.20534/AJT-17-1.2-83-88>

Salimova Nigar A.,

Professor and associate Professor

Mamedova Farida M.,

*Department of Oil-chemical Technologies
and Industrial Ecology, Azerbaijan State University*

of Oil and Industry, Baku, Azerbaijan

E-mail: farida.mamedova@yahoo.com

Removal of aromatic hydrocarbons from waste water of industrial oil processing

Abstract: Discharging waste water in marine environment without previous treatment has severe effects on the marine environment and produces aqua-toxicological effects, which is deleterious to aquatic life. The main contributors to acute toxicity of waste water have been found to be the aromatic and phenol fractions

of the dissolved hydrocarbons. Phenol is toxic to fish at a level of 0.05 mg/l, therefore the detoxification of phenols from waste water is of great importance. The aim of this research is studying the effect of treating aqueous solutions containing high concentrations of phenol, 8 mM phenol and low concentration of phenol, 1 m. mole phenol with the enzyme peroxidase extracted from horseradish. Hydrogen peroxide (H_2O_2) and poly ethylene glycol (PEG), It was found that the most effective addition of horseradish peroxidase and hydrogen peroxide was 1 U/ml and 10.0 m. mole respectively at neutral pH, for removing 70 % of the phenol from aqueous solutions containing 8 mM. phenol. It was also found that the most effective addition of horseradish peroxidase and hydrogen peroxide were 0.3 u/ml and 3.0 m. mole respectively at neutral pH, for removing 80 % of the phenol from aqueous solutions containing 1m. mole phenol. Precipitation of the phenolic oxidation products resulted from the enzymatic treatment. Through coagulation and precipitation by different coagulants, alumina and quick lime have been studied.

Keywords: Peroxidase, Enzymatic treatment, Phenolic polymers, Coagulation.

Introduction

Phenols in our environment come from various sources. For example, many are found in the waste waters of industries such as petroleum refineries, glue and resin manufacturers, coal processing, pulp and paper mills, and from the leaching of municipal landfills. Phenol is toxic to fish at a level of 0.05 mg/l, therefore the removing of phenols from waste water is of great importance. Most of the methods used for transformation of wastes and pollutants and treating wastewaters are physical, chemical or biological. Chemical transformations involve the application of reagents and reaction conditions to transform and treat target species.

Chemical methods involve the application of reagents and reaction conditions to transform and treat target species. Chemical processes often require the presence of excess quantities of reagents to accomplish the transformation to the desired extent. In addition harsh conditions (e. g., high temperature or extreme of pH) are sometimes required to facilitate the chemical transformation. Many chemical treatment processes are not highly selective in terms of the type of pollutants that are transformed during treatment. The high cost and disposal of contaminated media are the disadvantages of chemical treatment.

Biological processes make use of the natural metabolism of cells to accomplish the transformation or production of chemical species. The metabolic processes occur as a result of a sequence of reactions conducted inside the cell that are catalyzed by proteins called enzymes. Biological processes can often be conducted without the harsh conditions that are necessary during chemical transformations. Due to the large water hold-up volume and bacterial culture contact time, these systems are very large and heavy, and therefore only suitable offshore for low volume application. Also there are operational and

bacterial inhibition problems. The method is best suited to onshore installations where space and volume are not limitations [1].

The following potential advantages of an enzymatic treatment over conventional biological treatment were noted [2]; action on, or in the presence of, many substances which are toxic to bacteria; operation at both high and low concentrations: no shock loading effects: no delays associated with acclimatization of biomass; reduction in sludge volume (no biomass generation). The aims of this study were: extracting the enzyme peroxidase from horseradish roots by mixing with tap water, determining the optimum parameters of enzymatic treatment (Horseradish peroxidase dose, peroxide dose (H_2O_2)) for oxidation of phenol at aqueous solutions contains high and low phenol concentrations. To remove the phenolic oxidation products by coagulation and precipitation by different coagulants alum and quick lime (CaO).

Methods

H8P enzyme (EC 1.11.1.7) was extracted from horseradish in our lab. All the following chemicals were of analytical grade and were purchased from FECTON (Russian). Hydrogen peroxide (30 % w/v), solid phenol, 4-aminoantipyrine and potassium ferricyanide [$K_3Fe(CN)_6$] for analysis of phenol and activity of horseradish peroxidase. Quick lime (CaO) and alum (aluminum sulphate) were used as coagulants.

The horseradish peroxidase enzyme concentration and activity was determined by colorimetric assay [3]. The concentrations of total phenols were measured using a colorimetric method [4].

Batch experiments for enzymatic treatment were conducted at room temperature (approximately 25 °C). The batch reactors were glass vials of capacity 100 mL, which contained 50 ml. of synthetic waste water (phenol — distilled water) and predetermined doses of each

of horseradish peroxidase enzyme (HRP), hydrogen peroxide (H_2O_2) and poly ethylene glycol (PEG) has been added. A magnetic stirrer with a magnetic bar was used for mixing agitation of the synthetic waste water with the reactants for a specific time and at medium speed. After treatment the resulting solution was centrifuged for 30 minutes at 6 000 rpm. The supernatant was analyzed for phenol as described earlier.

For coagulation studies, jar tests were carried out. The objective of the jar test was to determine the optimum dose and the pH value at which a coagulant should be introduced to the waste water. Alum and quick lime were used as coagulants. After treatment of phenol with horseradish peroxidase HRP, H_2O_2 and PEG, the resulting solution contains colored products (phenolic polymers). Four samples of this solution were treated by a specific dose of alum in a jar test. Each sample of this solution has a 50 ml. volume, alum was added with a specific dose, and stirring occurred for 15 minutes and then stopped. The change in the color of the solution sample (clarification percentage) was measured at a specific time by measuring the relative absorbance of the solution sample at 400 nm. by a photoelectrocolorimeter.

Results and discussions

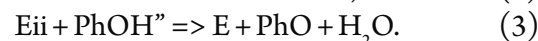
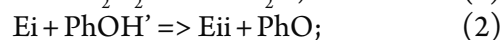
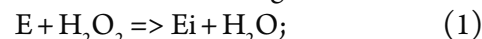
Extraction of horseradish peroxidase enzyme from minced horseradish roots using soft tap water occurred in a mixer at high speed for a specific time (1–4 hours). Two different ratios of horseradish to tap water were used 50 gram minced horseradish roots to 500 milliliter of tap water, and 100 gram minced horseradish roots to 500 milliliter of tap water. The resulting solution from mixing horseradish with water, for predetermined time, was filtered and the supernatant was centrifuged at 4 000 rev/min. The supernatant was stored at $-4^\circ C$. Every day the activity of HRP was analyzed before using the enzyme in the tests. The activity of the enzyme is defined in units, one unit of activity (U) is defined as the number of micromoles of hydrogen peroxide which are consumed in one minute at pH 7.4 and $25^\circ C$ [3].

Fig. 1 demonstrates the dependence of the activity of peroxidase on the extraction time. The parameters that were studied were horseradish roots weight to water ratio and time of extraction of enzyme. The activity of enzyme per milliliter extract was dependent on the ratio of horseradish roots weight to water, and the time of mixing the horseradish in tap water.

With increasing the time of mixing, the activity of the enzyme in the extract becomes higher, and reached 7 U/ml for ratio of horseradish roots (HR) to water equal 0.1 (50 gram HR per 500 ml. water), and 8 U/ml

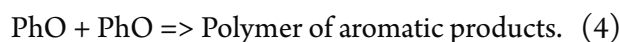
for ratio of HR to water equal 0.2 (100 gram HR per 500 ml. water). The total units of enzyme extracted were dependent on the volume of the water used for extraction. This means that the optimum ratio of HR to water was 0.1 (50 gram per 500 milliliter water) and also the optimum activity of HRP was 7 U/ml extract.

Horseradish peroxidase undergoes a cyclic reaction when reacting with phenolic substrates [5]. This sequence is summarized in the following reactions:



The enzyme starts in its native form (E) and is oxidized by hydrogen peroxide (H_2O_2) to form an active intermediate compound known as compound I (Ei). Compound I oxidizes one molecule of phenol (PhOH) to form a phenol free radical (PhO) and become compound II (Eii). Compound II oxidizes a second phenol molecule to produce another phenol free radical and complete the cycle by returning to its native form E. The free radicals polymerize and form insoluble compounds which precipitate from solution.

The polymerization reaction is illustrated in equation 4:



The pH of each sample was adjusted to be between pH 2 and pH 10 using concentrated HCl or NaOH. The pH of the solution was adjusted before stirring and after addition of the phenol, PEG, H_2O_2 , and HRP. Stirring of the aqueous solution in the presence of the chemical substances has been conducted in the sake of oxidation of phenol by using H_2O_2 in the presence of HRP enzyme. As a result of oxidation of phenol and formation of the oxidation products (phenolic polymers), which with less toxicity to the environment, the remaining phenol in the reaction solution was decreased and a measurement of the removal percentage of phenol has been achieved.

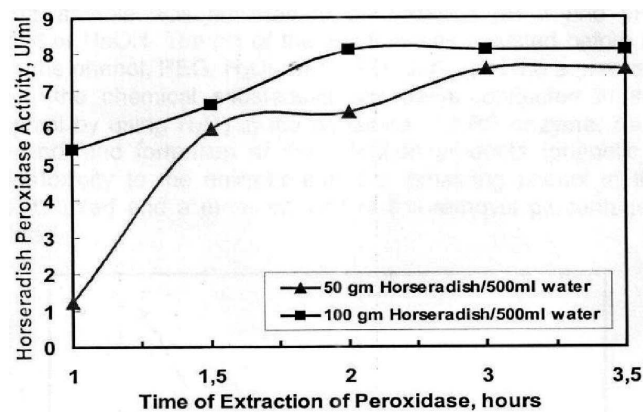


Fig. 1. The dependence of the activity of peroxidase on the mixing time of horseradish roots in water

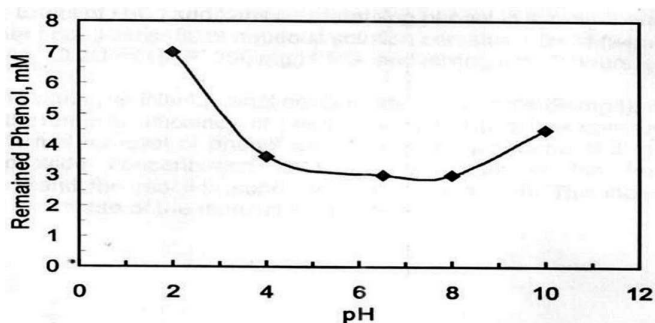


Fig. 2. Effect of pH on the removal of phenol using crude HDP. Experiment conditions: 50 ml. aqueous solution (distilled water) contains 8 mM. phenol, 8 mM. H_2O_2 , 0.8 U/ml HRP, 250 mg/l PEG, and mixing time 3 hours

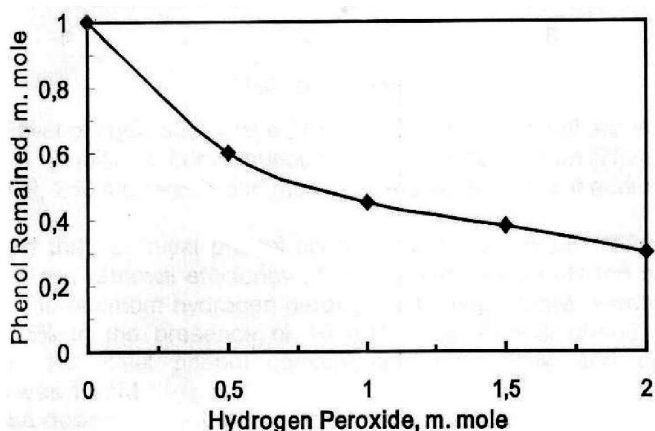


Fig. 3. Effect of H_2O_2 additions on remaining phenol in synthetic waste water. Experiment conditions: 50 ml. aqueous solution contains 1.0 mM. (94 mg/l) phenol, 0.2 U/ml HRP, 250 mg/l PEG, and mixing time 3 hours

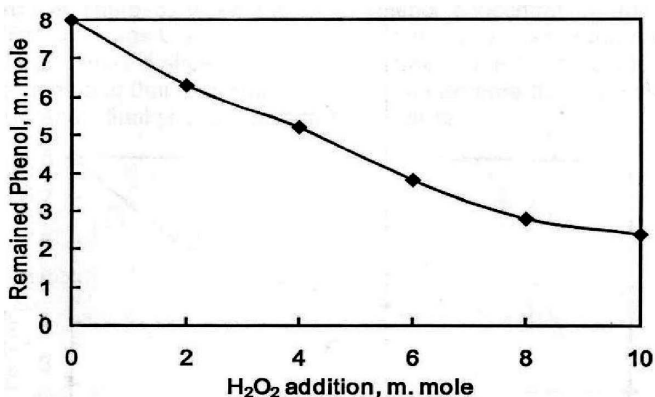


Fig. 4. Effect of H_2O_2 additions on remaining phenol in synthetic waste water. Experiment conditions: 50 ml. aqueous solution contains 8 mM. (752 mg/l) phenol, 1 U/ml HRP, 250 mg/l PEG, and mixing time 3 hours, without addition of PEG

Fig. 2 shows that the optimal removal of phenol from the aqueous solution occurred between pH 4 and 8, with optimum removal percentage 60% of phenol (Final phenol concentration 3.2 m. mole). The removal of phenol decreased at high acidic and alkaline conditions, this may

be due to the effect of OH and H ions on the oxidation reaction of phenol by using H_2O_2 and HRP. This study demonstrated that HRP is slightly less susceptible to pH changes and is probably suitable for the treatment of phenol at slightly acidic and alkaline conditions.

Two different phenol concentrations 1 mM. (94 mg/l) and 8 mM. were used in these tests. Hydrogen peroxide (H_2O_2) was added in predetermined amounts in order to determine the effect of hydrogen peroxide on extent the removal of phenol at initial phenol concentration 1 mM. or 8 mM.

Fig. 3 shows that, at initial phenol concentration 1 m. mole (94 mg/l), as H_2O_2 dose increases the removal efficiency of phenol increased until the optimum value was attained. Maximal removal of phenol was 70% in the presence of 3 mM. H_2O_2 . The optimum peroxide concentration H_2O_2 is a function of the treated phenol concentration and the reaction conditions (HRP dose, pH). The increase of H_2O_2 dose leads to increase of the removal of phenol.

Fig. 4 shows that, at initial phenol concentration 8.0 m. mole (752 mg/l), as H_2O_2 dose increases the removal efficiency of phenol increased until the optimum value was attained. The optimum hydrogen peroxide dose was 10 mM. Maximal removal of phenol was 65% in the presence of 10 mM. H_2O_2 . A final phenol concentration 2.4 mM, when the initial phenol concentration was 8 mM. and optimum H_2O_2 concentration was 10 mM.

Two different phenol concentrations 1 mM. and 8 mM. were used in these tests. Peroxidase was added in predetermined amounts in order to determine the effect of HRP dose on extent the removal of phenol at initial phenol concentration 1 mM. or 8 mM. The optimum HRP dose was determined at 1 mM. phenol and 3 mM. H_2O_2 concentration.

As appeared at fig. 5, when the initial phenol concentration was 1 mM, the effective HRP dose was 0.3 u/ml of the solution at H_2O_2 dose 3 mM, and the PEG dose 250 mg/L. Fig. 5 shows that with the increase in HRP dose, the removal of phenol increases and that maximal removal of phenol were 80%, at optimum HRP dose 0.3 U/ml and a final phenol concentration 0.2 mM.

As appeared at fig. 6, the optimum HRP dose was determined when the initial phenol concentration was 8 mM, the effective HRP dose was 0.8 u/ml of the solution at H_2O_2 dose was 8 mM. and PEG dose 250 mg/L. With the increase in HRP dose, the removal of phenol increases and that maximal removal of phenol was 70%, at optimum HRP dose 1.0 U/ml and a final phenol concentration 2.4 m. mole.

Poly ethylene glycol was prepared in a concentration of 5g/l, and stored in the refrigerator. A predetermined dose was added to each test to determine the effect of PEG on the enzymatic treatment efficiency.

Fig. 7 demonstrates the effect of poly ethylene glycol on the concentration of remained phenol in aqueous solution, when the initial phenol concentration was 8 mM. The effective PEG dose was 275 mg/L, when HRP dose was 1.0 U/ml of the solution and H₂O₂ dose was 10 mM. Fig. 7 shows that with the increase in PEG dose, the removal of phenol increases and that maximal removal of phenol were 75 %, at optimum HRP dose 1.0 U/ml and a final phenol concentration 2 m. mole.

Alum (aluminum sulphate) was used at two pH values, at slightly acidic conditions pH 5.6 and at slightly alkaline conditions, pH 8.0. Fig. 8 shows that at slightly alkaline conditions, pH 8.0, the coagulation of the colored products was little by alum. Maximum color removal of the colored products (clarification percentage) was only 40 %, at an alum dose 5.5 gm/l, after 18 hours (clarification time) from the moment of stopping the stirring in the jar test. Also figure 8 illustrates that when using alum at slightly acidic conditions, pH 5.6, the coagulation of the colored products were increased by increasing the alum dose and clarification time (time after the stopping the stirring). Maximum color removal of the colored products was only 5Q %, at an alum dose 3.0 gm/l, and after 3 hours, and increased to become 84 % at the same dose and after time 18 hours from the moment of stopping the stirring in the jar test.

Lime (CaO) is used for color removal (precipitation of color products by lime) from pulping and bleaching effluents [6]. Molecular weight of color products is one of the major factors influencing the precipitation of color products. Pulping and bleaching effluents was treated by horseradish peroxidase and H₂O₂ and found that the colored products from this treatment have high molecular weights greater than 5000. They found that lime can almost completely remove color products with molecular weights greater than 5000. This previous work was encouraging us to demonstrate the capability of lime to precipitate the color products resulting from oxidation of phenols by HRP and H₂O₂ in the presence of poly ethylene glycol.

Fig. 9 shows that as the addition of lime increases the pH of solution becomes above pH 10.5, and causes fast precipitation of the colored products. Maximum color removal (clarification) of the colored products was 60 %, at a lime dose 3 gm/l, after 30 minutes from the moment of stopping the stirring in the jar test (clarification time). The

percentage of color removal increases with the increase of the clarification time (after moment of stopping the stirring) in the jar test. Maximum clarification of the colored products was 85 %, at a lime dose 3 gm/l, after two hours. Fig. 9 shows fast and high efficiency of color removal using lime, as the lime doses increase and as the time after moment of stopping the stirring increases as well.

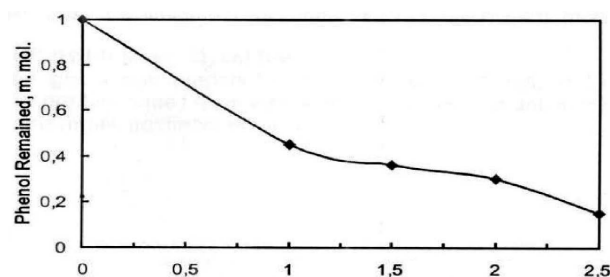


Fig. 5. Effect of additions of HPR on the phenol remaining in synthetic waste water, at initial phenol concentration, 1 m. mole. Experiment conditions: 50 ml. aqueous solution contains 1.0 mM. (94 mg/l) phenol, 3.0 mM. H₂O₂, 250 mg/l PEG, and mixing time 3 hours

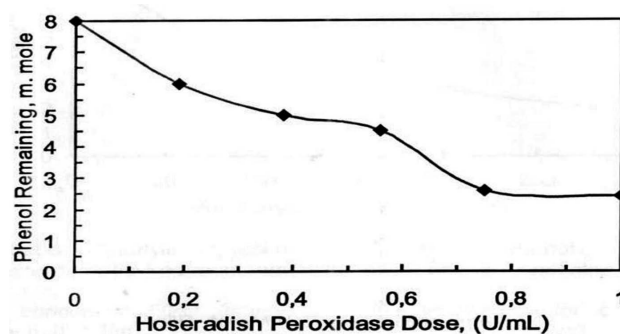


Fig. 6. Effect of additions of HPR on the phenol remaining in synthetic waste water, at initial phenol concentration, 8.0 m. mole. Experiment conditions: 50 ml. aqueous solution contains 8 mM. (752 mg/l) phenol, 8 mM. H₂O₂, 250 mg/l PEG, and mixing time 3 hours

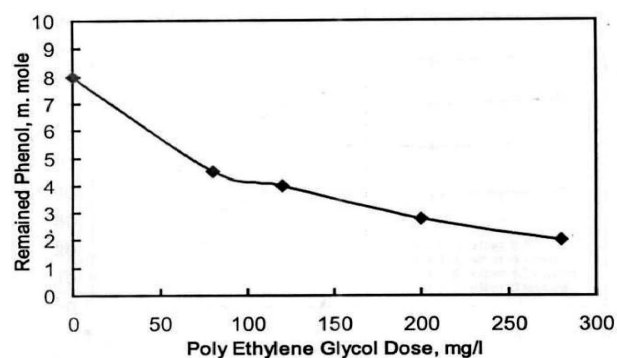


Fig. 7. Effect of polyethylene glycol dose on the remaining phenol conc. in aqueous solution after enzymatic treatment, when the initial phenol concentration was 8.0 m. mole. Experiment conditions: 50 ml. aqueous solution (distilled water contains 8 mM. (752 mg/l) phenol), 1 U/ml HRP, 10 mM. H₂O₂, and mixing time 3 hours

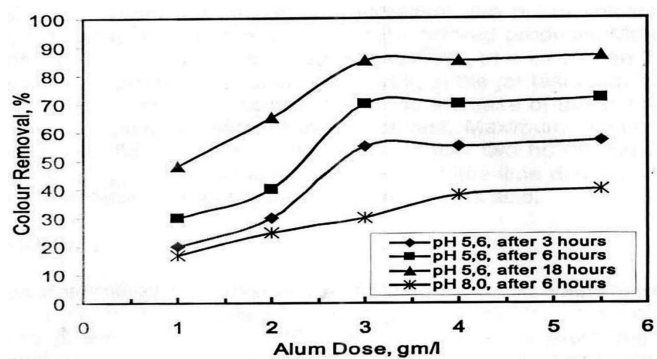


Fig. 8. Effect of alum addition on color removal (coagulation) of phenol polymers, at different pH values

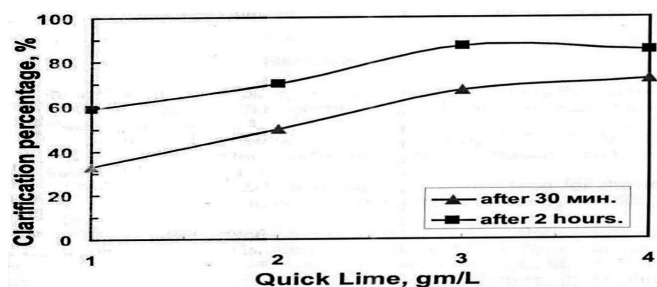


Fig. 9. Effect of coagulation with quick lime for phenolic polymers resulting from enzymatic treatment of phenol

Conclusions

This study has determined the possibility of treating synthetic waste water (distilled water contains both high amounts of phenol, 8 mM, and a low amount of phenol 1.0 mM) by the enzymatic system (HRP-Peroxide). The optimum parameters of enzymatic treatment of synthetic waste water containing 1 mM. initial phenol concentration were at pH 7.0, 0.3 U/ml HRPdose, 3.0 mM. H_2O_2 dose and PEG 275 mg/l achieved a final phenol concentration 0.2 mM. with a removal percentage of water contain 8 m. mole phenol were at pH 7.0, 1 U/ml HRP dose, 10.0 mM. H_2O_2 dose and PEG 275 mg/l achieved a final phenol concentration 2.0 mM. with a removal percentage of phenol 75 %. The optimum coagulant was quick lime used for precipitation of colored oxidation products of phenol and 85 % clarification could be attained after 2 hours.

Compliance with ethical standards

- Disclosure of potential conflicts of interest — there is not conflict of interest.
- Research involving Human Participants and/or Animals: For this type of study formal consent is not required.
- Informed consent: Informed consent was obtained from all individual participants included in the study.

References:

1. International association of oil and gas producers (I.A.O. G.P.) Aromatics in produced water: occurrence, fate and effects and treatments. – IAOGP, January 2002. – Report No. 1, 20/324.
2. Nicell J. A., Al-Kassim L., Bewtra J. K. and Taylor K. E. Treatment of waste waters by enzyme catalyzed polymerization and precipitation//Biodeterioration Abstracts. – 1993. – № 7(1). – P. 1–8.
3. Wright H. Characterization of soybean peroxidase for the treatment of phenilic waste water, Master of Engineering Thesis. – McGill University, Montreal, Canada, 1995.
4. Yiseon Han. Arthromyces ramosus peroxidase catalyzed phenol removal, Master of Engineering Thesis. – University of Alberta, Edmonton, Alberta, 1998.
5. Klibanov A. M., Alberti B. N., Mon-is E. D. and Felshin L. M. Enzymatic removal of toxic phenols and anilines from wastewaters//J. Applied Biochem. – 1980. – Vol. 2. – P. 414–421.
6. Schmidt R.L., Joyce T.W. An enzymatic pretreatment to enhance the lime precipitability of Pulp. Mill Effluents//Tappi. – 1980. – Vol. 63. – P. 63.

Nabiyev Akramjon Botijonovich,

Abdurahimov S.A.,

Namangan State University,

Tashkent Institute of Chemical Technology

E-mail: akramnabiyev@umail.uz

Preparation of surfactants reducing the viscosity of heavy oil from raw fatty acid of cotton soap stock

Abstract: This paper studied the effective viscosity of the local oil at a constant voltage shifts evaluate the effectiveness of synthetic surfactant to reduce the viscosity of the local oil. Studies for obtaining surfactants reducing the viscosity of the oil from the raw fatty acid of cotton soapstock (CS) show that a rational scheme was selected for gaining of surfactants from raw fatty acid of cotton soap stock in the form of higher fatty alcohols and their modification methods sorbitan or sulfation.

Keywords: oil, viscosity, sulfate, paraffin, gossypol, lecithin, cephalin.

Specific feature of oil from the Jarkurgan (Surkhandarya region) and Mingbulak (Namangan region) fields in Uzbekistan is the high content of paraffin, resins, asphaltenes of mineral salts and other related hydrocarbon components that significantly increase their viscosity and reduce their flow through the pipeline.

It is known that the high viscosity of the oil, not only complicates the process of its production from the wells, but also its industrial processing, which has a negative impact on their technical and economic indicators. To address these shortcomings in practice (especially in autumn and winter) the pipelines should be heated with steam where oil transport distance exceeds 10–15 km. The use of solvents for diluting high-viscosity oil is not desirable because it is related to fire safety oil explosion [1].

With in-plant transport of high-viscosity oil for less (less than 5 km.) distance it is effectively to use their electromagnetic processing (including microwaves), which, along with a decrease in viscosity of the oil increases its turnover and significantly reduces the deposition of waxes, resins and mineral salts in the pipes [2]. In this case, the problem of explosion, fire of oil pipelines requires their own individual solutions tailored to their construction.

It was offered the methods of application of ultrasonic cavitation and mechanical-chemical activation (MCA) on lowering the viscosity of oils of different composition [3].

Unfortunately, the influence of mechanical stress on the decrease in viscosity of the oil is not a long time and should therefore be used repeatedly, which significantly overstates their energy costs for transportation by pipeline.

Today, promising is the use of depressant i. e. surface-active agents (surfactants), and reduce the oil viscosity increase their fluidity in a pipeline.

It is known that the surfactants have the ability to lower surface tension in the interphase layer, as they dissolve selectively in one of the phases, the dispersion medium to be concentrated at the interface and there form an adsorption layer as a film. Reduced surface tension increases with the fineness of the disperse phase [4].

Mainly characterized by the oil viscosity, density, dispersion, electrical properties and stability of aggregate. Their viscosity usually varies within wide limits and depends on the intrinsic viscosity of the oil, the temperature and so on. They being dispersed systems have abnormal properties that under certain conditions are non-Newtonian fluids and characterized by an apparent (effective) viscosity [5].

We investigated on viscometer VPN-01 at a constant shear stress the effective viscosity of the local oil. This shear stress of test oil sample was calculated by the following formula [5]:

$$\tau = k_{\text{ass}} \cdot U, \quad (1)$$

where: k — the coefficient, which is equal to 0.63 Pa/V to 100 mm. gauge and 43 Pa/V to 20 mm. gauge;

U — stress in volts.

The shear rate was determined by the formula:

$$Y = A/T, \quad (2)$$

where: A — a constant measuring unit; T — Period of rotation, determined by the frequency indication.

Hence, the effective viscosity of the oil is determined by the formula [5]:

$$\eta = \tau_{\text{rear}} / \gamma. \quad (3)$$

Evaluation of the effectiveness of synthetic surfactant to reduce the viscosity of crude oils was produced using local viscometer VPN-01 and the above-mentioned formulas.

Analysis of the literature has shown that to reduce the viscosity of oils it is suggested many surfactants with ionic and nonionic nature. Moreover, the latter showed positive results in reducing the viscosity of crude oils of varying composition. For example, for the synthesis of ethoxylated fatty acids having more than 20 carbon atoms used bottoms fatty acid tar mixture. It found that the activity and physical properties of the surfactant depends on the number of oxyethylated groups with a carbon number of $C_{14}-C_{25}$ fatty acids per molecule. Thus a more active surfactant synthesized based on fatty acids with C_{25} ethylene oxide content of at least 70% [6].

Later surfactants synthesized from fatty acids, containing sulfonate group $-SO_2OH$ or a sulfite group OSO_2OH . For such purposes were different macromolecular sulfonated unsaturated fatty acids, hydroxy acids, their derivatives, alkylated amides or esters and glycerides of natural acids [7].

It is known that surfactant activity not only depends on its structure, but also on the location of the functional groups and on the value of hydrophilic-lipophilic balance (HLB) [8].

Currently, Uzbekistan has successfully operated more than 25 oil and fat enterprises, which produce about 500 thousand tons of refined cottonseed oil per year. Waste alkali refining cottonseed oil is soapstock, which contains up to 45% C_{16} , sodium salts of fatty acids $C_{16:0}$, $C_{18:0}$, $C_{18:2}$, $C_{18:1}$ and others up to 30% of neutral fat (oil) and 5% gossypol, chlorophyll and derivatives thereof, up to 3% phospholipids, and others. The current

technology this soapstock will be saponified the remaining with alkaline reagent (NaOH), decomposed with sulfuric acid (H_2SO_3) and gain raw fatty acids (RFA), which was distilled to improve the color and removing their low-boiling component [9].

RFA are a mixture of saturated and unsaturated fatty acids and therefore is considered the results of their tests averaged.

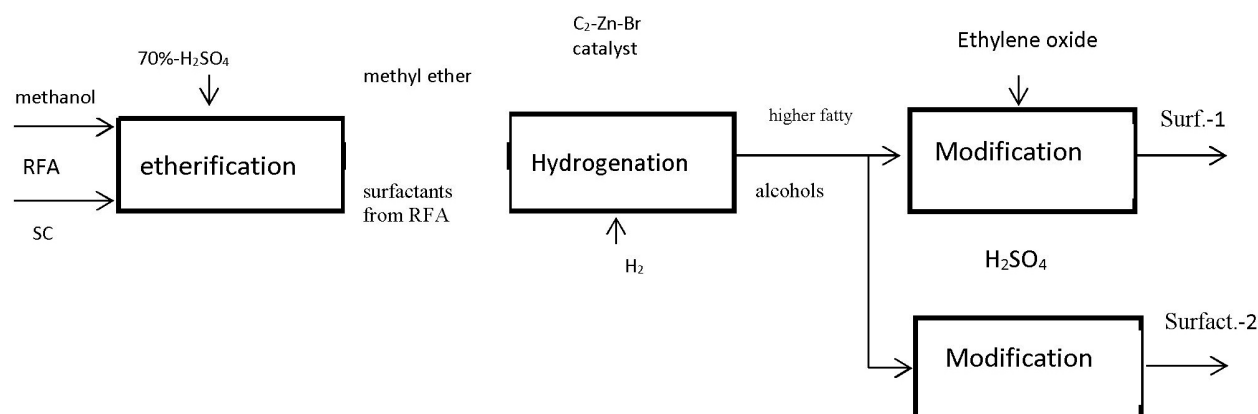
Table 1 presents the physical and chemical indicators of the RFA, which we have obtained from cottonseed soapstock. These tests are performed according to the approved standard [10].

From table 1 it is seen that raw fatty acids derived from cotton soapstock have substantial amounts of unsaturated fatty acids (110–112 g y. ch. = $J_2/100$ g), which gives them at room temperature liquid and low melting point. RFA relatively more reactive because it contains substantial amount of ethylene bonds which are necessary for the interaction with the other reagents in the preparation of surfactants.

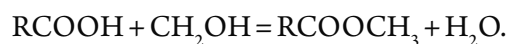
Table 1. – Physical and chemical parameters RFA cotton soapstock

RFA Indices	The values of the indicator
Appearance at 20 °C	The liquid mass of dark brown color
Acid number, mg KOH/g	201 ÷ 203
Iodine number, $gJ_2/100$ g	110 ÷ 112
Melting temperature, °C	19 ÷ 30
Mass fraction of unsaponifiables, %	2.1 ÷ 3.9
Water content, %	0.2 ÷ 0.6

Preparation of the surfactant in the form of higher fatty alcohols modified by various additives was carried out as follows:



We performed esterification process by reaction RFA cotton soapstock with methanol (CH_3OH) in the presence of 70% sulfuric acid (catalyst) at 115–120°C. The chemical reaction proceeds according to the formula:



In this case, the remaining sulfuric acid and fatty acid was removed by neutralization with a 5% caustic solution at 80°C.

The results of analysis of the main indicators of methyl RFA cholesterol are shown in Table 2.

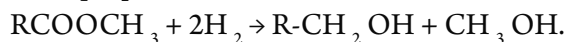
Table 2. – Physical and chemical indicators of cholesterol and free fatty acids methyl ester

The name of indicators	CS RFA	Methyl RFA cholesterol
Acid number, mg KOH/g	201.5	1.4
Essential numbers, mg KOH/g	0.7	187
Iodine number, % J _{2/100}	117.2	115.8

Table 2 shows that the two parameters in the process and the acid number of the esterification essential basically changed, which is 14 and 187 mg KOH/g, respectively. In the course of the ether synthesis, we sought to increase its output as during removal of the formed esterification water which was azeotropically escaping to condense in the reflux condenser, and gradually accumulates in the trap, the reaction equilibrium shifts toward increasing the yield of ester. In this way we were able to increase the yield of methyl RFA CS up to 93 %, against 56 %. The ester is a liquid and odor, readily soluble in many hydrocarbons.

Analysis showed that the resulting methyl ester RFA CS has a boiling point lower than the boiling temperature of the acids themselves.

Hydrogenation of the methyl ester RFA CS to obtain high-molecular (higher) fatty alcohols was carried out in the presence of a copper-chromium-barium catalyst at a temperature of about 300 °C and a pressure of 30 MPa, where the chemical reaction takes place according to the equation [11]:



The resulting alcohol is separated from the soap (reaction product of unreacted methyl ester RFA CS with sodium hydroxide) by distillation.

Physical and chemical parameters resulting higher fatty alcohol are presented in table 3.

Table 3 shows that the higher fatty alcohol obtained from the RFA CS has indicators, relevant non-ionic surfactant.

Table 3. – The organoleptic and physico-chemical characteristics of fatty alcohols derived from RFA CS

The name of indicators	The values of the indicator
Appearance and color	Liquid light yellow
Smell	With a slight characteristic odor
Temperature, °C	45.5
congeal	350
ignition -kipeniya	155
hydroxyl number, mg KOH	230
The content of hydrocarbons, %	0.85

Modification i. e. ethoxylation of higher fatty alcohols it will be modified the properties of the resulting surfactant. This process we conducted at 135–145 °C and pressures of ethylene oxide equal to 1.8–2.0 atm., Within 1.5–2.0 hours and in the presence of potassium (as a catalyst) in an amount of 1 % alcohol. Herewith the reaction proceeds as follows [12]:



where: n — is the number of ethylene oxide.

Study obtained by ethoxylation of higher alcohol from RFA CS showed that the surfactant containing 10–12 moles of ethylene oxide per mole of alcohol is a water soluble liquid which with increasing chain length of the ethoxylated surface tension of the latter increases. We conditionally to name a surfactant-1 and the resulting liquid were examined by lowering the viscosity of the local oil.

Next, we sulfited higher fatty alcohol, free fatty acids derived from cholesterol sulfuric acid solution at a temperature of 50 °C to a depth of 86 %. In the process of sulfonation of higher alcohols, a large amount of heat, so we surfactant cooled to room temperature. And, humidity higher alcohol should not exceed 0.2 %.

Table 4 presents the colloid-chemical parameters ethoxylated (surfactant 1) sulfited (surfactant –2) and the higher fatty alcohol derived from RFA CS.

Table 4. – Basic colloidal-chemical characteristics of surfactant 1, surfactant 2 and higher fatty alcohol obtained from the RFA CS

Naimeno-SURFACTANT tion	Viscosity, east	pH	surface tension of, dyne/cm	Blowing capacity at 25 °C, sec ³	Wetting-ability
Higher fatty alcohols of the RFA CS (control)	0.85	8.7	65	355	eleven'
SURFACTANT 1	0.53	9.8	35	230	19''
SURFACTANT 2	0.47	6.9	22	335	17''

From table 4 it is seen that obtained surfactant 1, surfactant 2 and higher fatty alcohol of RFA CS differ among themselves; despite the identity of the feedstock SURFACTANT-1 is more soluble in water than the SURFACTANT-2, which has a lower foaming capacity.

We have studied the reduction of the effective viscosity Mingbulak oil fields of administration depending on the surfactant1 and surfactant 2.

The results of analyzes are presented in table 5.

From table 5 it is seen that the addition of 0.05 % surfactant 2 in oil composition containing high paraffin from Mingbulak deposits compared with SURFACTANT-1 in

the same amount effective to reduce its viscosity to about 10–13 times, while the SURFACTANT-1 decreases 6–9 times (depending on the composition of researched oil).

Thus studies for obtaining surfactants reducing the viscosity of the oil from the RFA CS show that a rational scheme of the selected surfactants of RFA CS in the form of higher fatty alcohols and their modification methods sorbitan or sulfation.

It is found that the use of the resulting surfactant 2 in an amount of 0.05 % by weight of oil to reduce its effective viscosity 10–13 times (depending on the composition containing high paraffin from Mingbulak oil deposits).

Table 5. – Changes the rheological properties of oil deposits Mingbulak depending on the type of surfactant used

Configurable shear stress, Pa	Higher fatty alcohols RFA CS *)		SURFACTANT 1		SURFACTANT 2	
	The shear rate of oil, ⁻¹	Effective viscosity, Pa.s	The shear rate of oil, ⁻¹	Effective viscosity, Pa.s	The shear rate of oil, ⁻¹	Effective viscosity, Pa.s
6.30	1.902	3.341	11.614	0.547	25.425	0.251
9.45	2.921	3.283	17.388	0.552	37.531	0.255
12.60	3.935	3.209	22.815	0.561	51.292	0.259
15.75	4.974	3.172	29.104	0.569	62.814	0.267

References:

1. Lutoshkin G.S. Collection and preparation of oil, gas and water to transport. – M.: Nedra, 1972. – P. 324.
2. Lobkov A. M. Collection and transportation of oil on fields. – L., M.: Gostantehizdat, 1955. – P. 282.
3. Rehbinder P.A. Physico-chemical mechanics of disperse structures//AT Sat. Physical – chemical Mechanics disperse structures – M.: Science, 1966. – P. 12–16.
4. Voyutsky S. S. Course colloidal chemistry. – M.: Chemistry, 1975. – P. 512.
5. Sukhanov V.P. Oil recycling. Second addition, altered.4, extra. – M.: Higher School, 1979. – P. 335.
6. Jalilov S. S. Development of technology for producing nitrogen-containing surfactant-based RFA cotton soap-stock, Abstract of a thesis of the candidate of technical sciences. – T.: THTI, 2003. – P. 24.
7. Manual production of soap factories//Under. Ed. Tovbin I.M. – M.: Food Industry, 1974. – P. 518.
8. Adamson A. Physical chemistry of surfaces. – M.: Mir, 1979. – P. 320.
9. The surface active agent. Reference book//under Ed. A. A. Abramzon. – A.: Chemistry, 1979. – P. 376.
10. Nevolin F.V. Chemistry and technology of synthetic detergents. – M.: Food Industry, 1971. – P. 424.
11. Rehbinder P.A. Book Surfactants and their use in the chemical and petroleum industries. – Kiev: Science Dumka, 1971. – P. 3–4.
12. Paronyan V.H., Grin V.T. Technology of detergents. – M.: Chemistry, 1984. – P. 224.

DOI: <http://dx.doi.org/10.20534/AJT-17-1.2-93-97>

*Nabieva Iroda Abdusamatovna,
Doctor of science, the faculty of textile industry and technology,
Tashkent institute of textile and light industry, Republic of Uzbekistan*

*Khasanova Makhfuza Shukhratovna,
Assistant professor, the faculty of textile industry and technology*

*Artikboeva Ruza Maxsudjanovna,
Student, the faculty of textile industry and technology*

E-mail: niroda@bk.ru

Studying technological tools that prepare materials with a combination of polyether and cotton fiber for finishing-touch process

Abstract: Preparation thread and fabric containing polyether and cotton fiber in various ratios for polishing process are studied. The ways how to give strong capillarity by boiling process with flimsy alkaline condition are shown. Possibility of higher alkali fiber material than mixed fiber material is scientifically proved. Bleaching machine for fabrics containing synthetic fiber is introduced. Increase in hygroscopic and durability of fabrics during mercerization process is emphasized.

Keywords: polyether, cotton, yarn, fabric, mixed yarn, boiling, bleaching, mercerization process, capillarity, degree of whiteness.

Introduction

Solving science-technological problems associated with textile and light industry related to recycling local raw material profoundly, localizing the range of goods is essential. In this sphere expanding the usage of polyether fiber manufactured in the Republic, including the availability of manufacturing technologies that produce new types of products from the mixture of synthetic and natural fibers is considered as a crucial issue. Likewise, expanding the range of recycling of locally manufactured cotton fibers, developing assortment of readymade textile products is regarded as an important task.

The process of preparing materials that are made of synthetic fibers for dyeing and polishing includes cleaning from lubricate emulsion, the solution of antistatic substance and starch that is used to soak the thread before weaving material. To achieve this, the cloth is treated in the solution of surface active substances with the aid of soda and rinsed several times. It is obvious that the nature and structure of fibers contain variety of polymer, so the process of dyeing and polishing differs completely. To prepare fabrics produced from the mixture of those fibers special condition that is suitable for the features of both fibers which ensures qualified coloring is required. Certainly, the condition of process is also linked to the component of substances and features of fabric in textile process. In practice, the amount of starch that is used for fabrics with mixed fibers consists of 6–8%. To clean

the fabrics from that it should become water-soluble in alkaline condition, afterwards it excludes from the fabrics through the rinsing process. The feature of textile materials obtained from the mixture of those fibers varies according to the nature of fiber.

Types and ratio of fiber components in the mixture that makes up textile material defines the range of usage and is regarded as a basic factor in organizing recycling technologies. As chemical polishing technologies of materials containing different fiber are available, manufacturing problem of products which can meet the demands of consumers is tackled. But, the condition of production cannot be utilized on polishing of mixed fiber materials because not only the nature and structure of mixed fibers but also ratio of fibers should be taken into consideration by a machine. It is known that, the process of mercerizing cotton fiber is performed under the influence of highly concentrated corrode alkali. In this condition, to prevent polyether fiber from changing its traits technology through which the process of mercerizing with the aid of reducers is done has been studied. To bleach fabrics made of the mixture of cotton and polyether fibers, alkali concentration and process temperature are paid a special attention. Through the surveys chances of bleaching the cotton with the presence of hydrogen peroxide in neutral environment is learned. In published works the possibility of getting positive results from the method of polishing through the combination of hypochlorite

and peroxide and with the presence of complex creator with the mixture of cotton and polyether fiber fabrics is shown. When polishing process is performed according to this method silicate sediment is not produced, high quality whiteness is obtained, fabrics coloring improves. Simple and economical methods to bleach cotton based products have been suggested. This method can also be applied to compounds of cotton and polyether fibers, Classic method of bleaching solution of cotton made materials differ from composition of alkali processing solution which leads synthetic fibers to destruction. Developed technology of bleaching fabrics without deterioration of the mechanical properties achieved a sufficient degree of whiteness. In recent years, to carry out the structure of cotton and synthetic fiber textile materials in a soft condition continuously a special attention has been paid.

Object and research method

Material consisting polyether and cotton ratio in unequal degree is the object of investigation and is made up through cotton and polyether fibers (South Korea, formed in production of polyether chips) Cotton and polyether fibers made of a mixture of textile materials, the two-step method of polishing is needed. Indicators of quality prepared polishing materials are identified through capillarity, whiteness degree and physic-mechanic traits.

Achieving results and discussion

It is known that, preparation fabrics for dyeing and polishing includes the processes of cleaning and constant rate of bleaching. In the basis of these processes there is colloid-chemical process with presence of surface active substances, because hydrophobic greasy water insoluble featured substances are excluded through the help of surface active substances which have emulsion capabilities. Starch and natural coloring substances are dissolved with the aid of selected from the special structure oxidizers and through the rinsing process will be disposed of. But in this processes avoiding the destruction of basic polyether is required.

To work out the ratio condition of boiling process, achievement of high capillarity in mixed fiber thread and fabric is regarded as a boundary task. The boiling process of mixed fiber fabric is held by dimming in the solution containing hydroxide-25, natrium silicate ($d = 1/44$)-3, 38 % of NaHSO_3 -2, CAM-1 for 5 minutes at up to 70°C . Then the material will be squeezed up to 130 % and evaporated at 100°C for an hour, then be rinsed with cold as well as hot water. Acquired results are demonstrated in fig. 1.

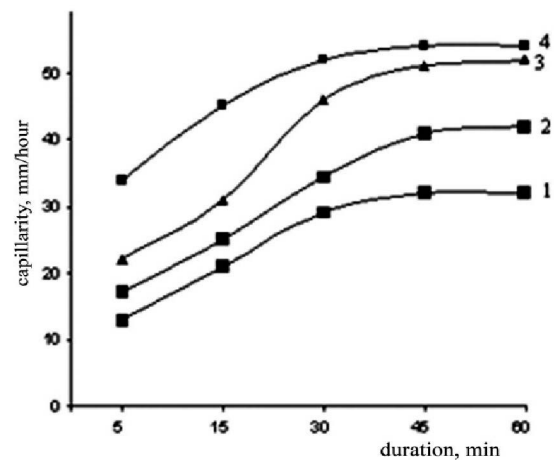


Fig. 1. The link between capillaries and the length of boiling process. Thread structure, cotton fiber: 1 — 80/40; 3 — 40/60; 4 — 20/80. It can be seen that capillarity of mixed fiber thread increases accordingly as amount of synthetic increases. Samples of cotton and polyether fibers used to obtain mixed fiber prepared separately in the same boiling condition and the capillarity has been checked

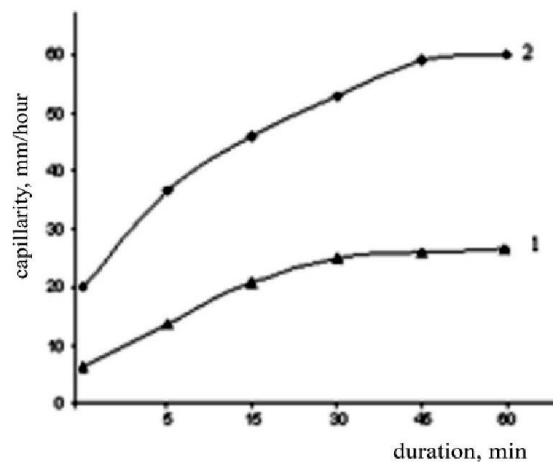


Fig. 2. The impact of boiling process upon cotton and polyether fibers: 1 — cotton, 2 — polyether

In the second figure it can be seen that the samples of boiled in separate conditions show the same results as above. It can be explained through the thread structure. Emptiness will be created as cotton fiber rotates freely around polyether fiber while weaving thread. Besides when mutual pushing occurs between synthetic and polyether fibers in the weaving machine this also leads to the space manifestation. Such spaces in thread weaved from cotton fiber are scarce. Rooting in the literature facts spaces among fibers can have more impact upon liquid absorbing process in preference to capillaries.

The nature of fiber also has something to do with liquid absorbing process. Hydrophilic — water goes up to the fiber through the reaction between physic-chemical and polymer instead of going up mechanically, in case

of polyether fiber it occurs conversely, that is liquid penetrates in spaces between fibers according to physic law without getting absorbed mechanically. That's why as the

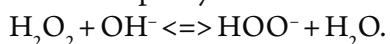
amount of synthetic fiber increases, the value of capillaries grows. Next surveys were conducted on learning how to boil mixed fiber fabrics.

Table 1. – Connection between capillarity of mixed fiber fabric and the length of boiling process

Duration Min	Capillarity mm/hour			
	Samples, cotton/polyether, %			
	100/0	75/25 warp – 55/45 weft – 0/100	57/43 warp and weft – 57/43	44/56 warp – 55/45 weft – 89/11
5	30	89	98	98
10	95	119	127	132
15	112	139	150	156
30	135	160	180	190
60	140	162	180	191

From the experiment in the fig. 1 it can be observed that, researches on boiling thread show repeatable results. That is, capillarity of fabric made of 100 % cotton is lower compared to the capillarity of mixed fiber fabric. But fabric capillarity which consists of rope thread with 100 % polyether fiber and basic thread with 55 % cotton and 45 % polyether fiber is lower than the one with mixture of basic and rope thread. So, it is possible to achieve the capillarity when the liquid runs through the spaces of thread and fiber capillaries. Obtained results can be utilized on planning the polishing process of mixed fiber fabrics. Namely, polishing process consists of 4 steps: the first is color diffusion toward fiber. The second step is color-molecule toward fiber sorption. By providing these two steps running in a short time opportunity to accelerate polishing process of textile fabrics will emerge.

In the boiling step of preparation natural color substances in fiber and colored pigment used while weaving process don't fade away, consequently they grant particular image to fabric. Increasing the rate of whiteness in fabrics that are meant to be used only in white appearance and the ones which should be bleached is required. Fabrics should be treated with oxidizer decays in order to achieve this. In industry peroxide, sodium hypochlorite and sodium chlorite are widely used as oxidizers. Each oxidizer has its own pros and cons. This matter has caused a lot of surveys as a result hydrogen peroxide is promoted in production. Taking these facts in to consideration we found this oxidizer the most suitable. Its mechanism of oxidizing performance can be explained as follows. Hydrogen peroxide is dissociated in PH 10.5–11.0 diffusive environment in order to create per hydronium ion.



This ion has the capability of destroying natural and synthetic pigment of fiber. Temporary hydro peroxide

bleaching on boiled materials is done at 85–90°C for 2 hours in the solution that includes components hydroperoxide 100 %, sodium hydroxide – 8, sodium silicate (d = 1.44) – 14, CAM-1. In this bath module is 50, after the process materials were washed with cold and hot water. Results are given in fig. 3, 4.

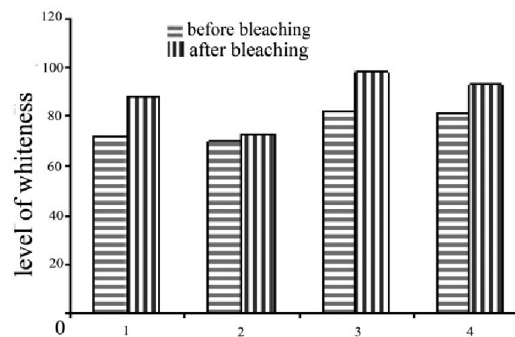


Fig. 3. Level of whiteness of fixed fiber fabrics. Cotton/Polyether: 1 – 100/0; 2 – 75/25; 3 – 57/43; 4 – 44/56

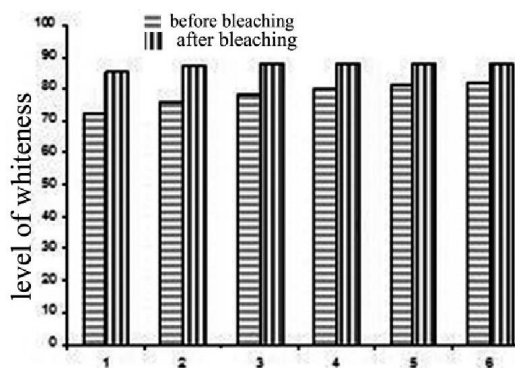


Fig. 4. Level of whiteness of mixed fiber thread's sample. Cotton/Polyether: 1 – 100/0; 2 – 80/20; 3 – 60/40; 4 – 40/60; 5 – 20/80; 6 – 0/100.

Result of experiments shown in diagram match with laws on bleaching textile materials. By treating row fabric or yarn with alkaline solution demand level of constant whiteness can be achieved. Comparison of

whiteness raw and processed materials made of polyether fiber it can be seen that whiteness of raw material is as in a good quality as it is in ready one, but as the level of cotton share decreases whiteness of material increases inversely proportionally. So when bleaching or coloring mixed fiber textile material with bright colors is needed, bleaching process isn't necessarily needs to be implemented separately. Mercerization process is performed in order to improve consumer property of fabric containing cotton and polyether fiber. When

mercerized cotton fiber based mixed fiber fabrics proper condition which prevents synthetic forming from being destructed have to be chosen. Polyether fiber which is one of the components of the mixture is not resistant to caustic alkalis effect under high temperature condition. But as mercerizing process generally occurs with the omission of heat the process is implemented at 15–20°C. According to the information above alkali concentration effect upon durability of mercerized fiber is learned.

Table 2. – Link between durability of mixed fiber fabric and alkali concentration

Alkali concentration	Samples, Cotton/Polyether, %			
	100/0	75/25 warp – 55/45 weft – 0/100	57/43 warp and weft – 57/43	44/56 warp – 55/45 weft – 89/11
	the strength of a delay			
200	531.23	579.81	576.78	576.53
220	551.23	580.23	572.58	570.35
260	568.78	579.91	568.27	565.27
280	570.54	577.25	565.27	560.09
300	570.96	576.68	537.80	523.70

As alkaline concentration increases in mercerization solution the strength of delay of samples containing polyether fiber will decrease. As cotton fiber increases fiber durability grows proportionally in value. It occurs because changes in morphology and molecular structure of cotton fiber influence it. During mercerization process fiber absorbs liquid to excess resulting in its walls get thick,

consequently diameter of fiber streams diminish. As a result cotton fiber alters its ribbon like shape to cylinder shape. It is obvious in mercerization process cotton hygroscopic rises. When studied the affect of alkaline concentration upon mixed fiber fabric hygroscopic it shows that indicator of concentration lower 220 is incompatible with purpose.

Table 3. – Link between mixed fiber fabric capillarity and alkaline concentration

Alkaline concentration	Samples, Cotton, Polyether, %			
	100/0	75/25 warp – 55/45 weft – 0/100	57/43 warp and weft – 57/43	44/56 warp – 55/45 weft – 89/11
	Capillarity, mm/hour			
200	150	170	179	188
220	160	196	210	218
260	165	200	227	230
280	166	220	230	235
300	168	225	232	238

Growth in mercerized fabric durability and hygroscopic terms can be explained as follows. As a result of processing upon cellulose with concentrated alkaline solution and rinsing it with water leads primarily changing gradually into alkaline cellulose, later into hydrocellulose. Such modification in cellulose without affecting to its chemical structure can have significant impact upon molecular structure. At first decrystallization occurs in cellulose, that is its amorphous part increases up to 10–20%, instead of cellulose 1 new crystal typed

cellulose 2 emerges. While conversion from cellulose 1 to cellulose 2, slight changes can be observed in multi-link configuration of macromolecular elements. Pyran rings in cellulose 1 placed fluently, some of the hydroxyl groups are interconnected through hydrogen ties. In cellulose 2 pyran rings are placed relatively at 90°C to each other. Consequently intermolecular hydrogen ties destroy and cellulose amorphous rises, this leads to grow in reaction and sorption capability of cotton fiber. Shown changes in mercerization process occur only on the sur-

face because of the low temperature and speed, that's why fiber durability doesn't weaken.

Resume. This article shows that mixed yarns and fabrics which were done by two ways for preparing to cloth finishing must have been achieved the fineness

and whiteness of the fabric. Conducting mercer process which mixture makes 220 g/l in these conditions, increasing the positive influence in order to receive the fine threads not allowing its negative influence for fabrics have been determined in the article.

References:

1. Каримова А., Сафина Л.А. Использование полимерных волокон для получения новых материалов для одежды. Международная молодежная конференция «Современные тенденции развития химии и технологии полимерных материалов». – Казань, 2012. – С. 178–181.
2. Хамраев Н.Х. Таркибида пахта нитрон толалари тенг, никобланган тўқималарни гул босишга тайёрлаш технологиясини ишлаб чиқиш: Дис... канд. техн. наук. – Т., 2005. – 125 с.
3. Zhang Liyan, Ke Meiling, Xu Guangbio, Wang Fumei. Research on the relationship between PTT content and property of cotton blended fabric//China Text. Sci. – 2010. – № 4. – P. 9–12.
4. Мерсеризация и пожелтение целлюлозы при высокой температуре. Li Mei-zhen, Jia Xiu-li, Zheng Ai-ping. Maofang keji = Wool Text. J. – 2010. – 38, № 6. – P. 21–23.
5. Saravanan D., Vasanthi H. S., Raja K. S., Das A., Ramachandran T. Bleaching of cotton fabrics using hydrogen peroxide produced by glucose oxidase//Indian J. Fibre and Text. Res. – 2010. – 35, № 3. – P. 281–283.
6. Tutak Mustafa. Optical whitening of cationised cotton: effect on whiteness and whiteness tint//Colorat technol. – 2011. – 127, № 5. – P. 340–345.
7. Abdel-Halim E. S. Simple end economic bleaching process for cotton fabric//Carbohydr. Polym. – 2012. – 88, № 4. – P. 1233–1238.
8. Energie- und Kosteneinsparungen in der Ausrüstung von Mächenware. Melliand Textilber. – 2011. – 92, № 3. – P. 199.
9. Abdukarimova M.Z., Nabiyeva I.A., Ismoilova G.X. To'qimachilik mahsulotlarini pardoqlash kimyoviy texnologiyasi fanidan laboratoriya va amaliy mashg'ulotlar uchun o'quv qo'llanma. – T.: TTYeSI bosmaxonasi, 2015. – 366 b.
10. Жерницын Ю.Л., Гуламов А.Э. Методическое указание по выполнению научно-исследовательских и лабораторных работ по испытанию продукции текстильного назначения. – 2007. – 96 с.
11. Браславский В.А. Капиллярные процессы в текстильных материалах. – М.: Легпромбытиздат, 1987. – 112 с.
12. Xu Changhai, Long Xiaoxia, Du Jinmei, Fu Shaohai. A critical reinvestigation of the TAED-activated peroxide system for low-temperature bleaching of cotton//Carbohydr. Polym. – 2013. – 92, № 1. – P. 249–253.
13. Кричевский Г.Е. Химическая технология текстильных материалов. Том 1. Волокна, подготовка. – М.: Легпромбытиздат, 2000. – 545 с.

*Ochilov Shuhratulla Atoyevich,
Senior Research Fellow – Competitor,
Faculty of Engineering Geology and Mining,
Tashkent State Technical University
E-mail: o.shuhrat84@yandex.ru*

*Nasirov Utkir Fatidinovich,
Head of the Department of Mining,
Faculty of Engineering Geology and Mining
E-mail: unasirov@yandex.ru*

*Toshniyozov Lazizjon Golib ugli,
Master of Mining machinery and equipment,
Faculty of Engineering Geology and Mining
E-mail: toshniyozovlaziz@gmail.com*

Theoretical study of the fracture mechanism of less fissured rocks

Abstract: The article deals with the fracture mechanism of rock in explosion of concentrated deep-hole charges. The factors, causing involvement of environment at explosion in progress were determined and the fracture mechanism of rock under the influence of kinetic energy of wave was found out. Calculations of distance change between deep-hole charges in less fissured rocks are illustrated. It has been determined that at explosion of ideal flat charges fracture of rocks occur under only compressive stress (in a near zone) and slabbing phenomenon (in a remote zone) appearing at reflexion of a compression wave from a free surface.

Keywords: crushing, cracking, downhole charges, explosives, destruction, rock, wave energy, strain, slabbing phenomenon.

After the detonation of the explosive charge voltage wave propagates in the environment. At distances of several radii of the charge pressure in a wave commensurate with the pressure of the detonation products and the tens of thousands of atmospheric pressure. At this pressure, there is a plastic flow of the medium, so that at the initial moment it is displaced expanding explosion products. As propagation happens, the surrounding is involved in the movement in the radial direction. If an explosion occurs near the free surface, after reflection of stress waves the displacement among the products of the explosion in the upper half.

The explosion energy in the less fissured environment is transmitted through wave and expanding explosion products in the form of elastic and kinetic components. Calculations and direct experimental measurements [1, 25–33] show that the elastic and kinetic components in the same order of magnitude. The experimental and theoretical studies imply that located at a given distance from the center of the charge volume of the rock starts to not break at the time when it spreads

the stress wave. Experiments in optically transparent media and monitoring under production conditions shown [2, 85–96; 3, 77–100], that failure in this volume begins shortly after its passage. This is proved by the fact that the speed of propagation of failure cracks in the rock volume is less than the speed of the stress wave. Depending on the physic-mechanical properties of the medium, the crack propagation rate ranges from 30 to 90 % of the acoustic speed.

Environment, located close to the explosion, due to higher pressures (of the order of tens of thousands of atmospherics) behaves like a liquid. Therefore, all three principal stresses δ_1 , δ_2 , and δ_3 are equal.

According to the energy theory of strength, generally good agreement with experiment, the reason for failure is the potential energy of forming, proportional to the value:

$$\left[(\delta_1 - \delta_2)^2 + (\delta_2 - \delta_3)^2 + (\delta_3 - \delta_1)^2 \right]. \quad (1)$$

In view of the equality $\delta_1 = \delta_2 = \delta_3$ have:
 $U_\phi = 0.$

It follows that in the near field by an elastic component of the wave environment and the pressure of the explosion products will not disintegrate.

In the far field given voltage δ_{mp} in wave according to the theory of energy equals strength $(1-2\mu) \delta (1-\mu)$, where: δ — pressure in the compression wave, μ — Poisson's ratio. Calculations show that δ_{mp} value in the far zone is less than the tensile strength of rocks (at least for the rocks with factor of a fortress $f > 5$). Consequently, in the far field rock under the action of the elastic component also will not deteriorate.

Going from the free surface of the expansion wave, interacting with the incident (forward) wave is slabbing phenomenon that for environments with a large acoustic stiffness are the main cause of the destruction. Studies have shown [4, 6–11; 5, 103–109; 6, 263–285; 7, 30–31; 8, 34–39; 9, 172–174; 10, 184–196] that the destruction of these environments are on the charge and the amount of destruction created by spall phenomena, is a small part of the total volume of the destroyed environment. With increasing line of least resistance (LLR), the average size of the largest piece of a fragmented masses increases. At the center of the explosion equal relative distances will be the same voltage δ_{pr} . For these conditions in a unit volume of rock will be the same elastic component.

When fragmentation covers the entire volume of the medium, the stress wave due to a sharp lag general destruction front leaves to a distance δ several times the size of the amount of fragmentation. If calculate the elastic component of the wave energy integrated across the blasted volume for that period, the energy of the wave is much less than the kinetic part of the same volume.

To elucidate the fracture mechanism under the influence of a wave kinetic energy we consider symmetric explosion, when a spherical or cylindrical charges are located, respectively, in the center of the spherical or cylindrical volumes of the medium axis.

After the explosion of the charge and the reflection of stress waves on the free surface and the expanding gas cavity is set symmetric quasi-stationary motion of the medium in the direction of the free surface. Elementary protection layer thickness d_r at a distance r from the charge will be in the complex stress state, characterized by radial compressive and tensile δ_r and δ_τ tangential stresses (fig. 1). At the same time it will move from the charge center in the radius direction with a speed \mathcal{G}_r and stretch in the perpendicular direction at a rate \mathcal{G}_τ (fig. 2).

As the strain rate increases towards the center of the charge, the considered elementary layer thickness will be subjected to breed uneven stretching: the lower layer of

rock fibers will be stretched upper. This fact leads to the fact that the elementary rock layer is simultaneously subjected to deformation of tensile shear and impact shift.

Impact shift (skew) is manifested in the fact that some mentally leased plane from the position $a-a$ by stretching velocity gradient rotates γ_p to position $b-b$ (fig. 3a).

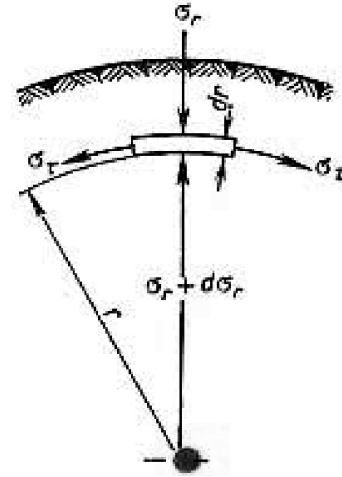


Fig. 1. Diagram of the complex state of stress of an elementary volume of the medium in the explosion of the explosive charge

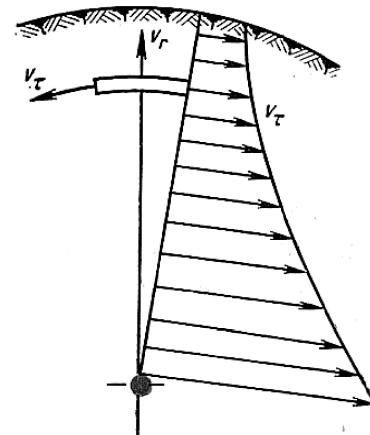


Fig. 2. The velocity field, which is formed in a medium with the explosion of the explosive charge

To impact tensile is exposed rock with layer thickness Δr and length l at a rate v_τ (fig. 3b). When the shock tension at an average speed v_τ if $\Delta v_\tau / \Delta r$ gradient disruption will happen in time Δt_p when in elementary layer elongation r reach destructive values ε_p .

As:

$$\varepsilon_p = \frac{\Delta l}{l} = \frac{v_\tau \Delta t_p}{2\pi r}, \quad (2)$$

where l — length of circumference of radius r , given kinematic dependence.

$$v_\tau = 2\pi r v_r, \quad (3)$$

we get:

$$\varepsilon_p = \frac{v_r \Delta t_p}{r}. \quad (4)$$

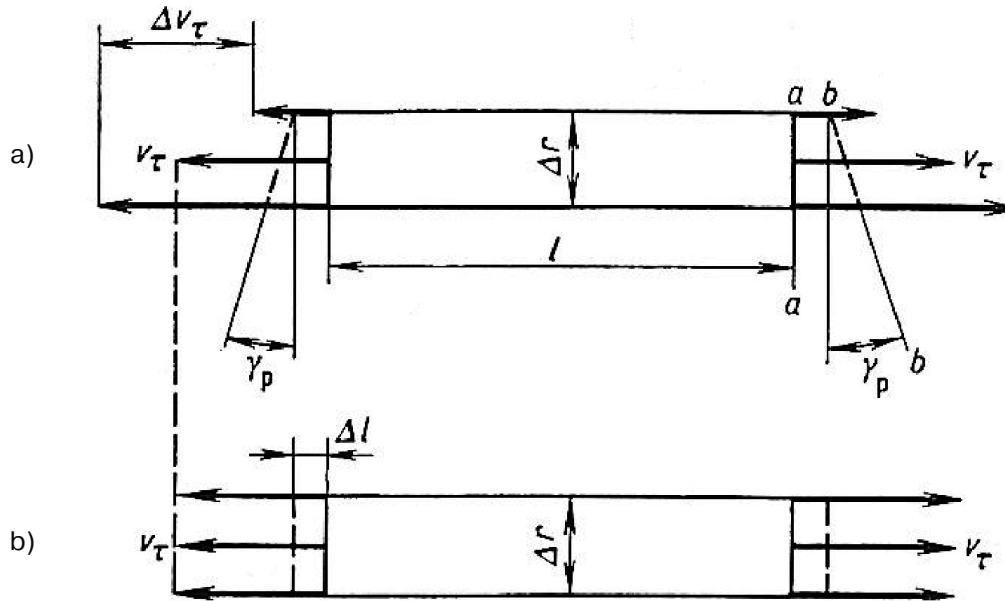


Fig. 3. Types of strain of elementary volume of the medium:
 a) — a shock shift under the influence of the velocity gradient; b) — uniaxial tension

It is known that:

$$\varepsilon_p = \frac{\delta_B}{E}, \quad (5)$$

where δ_B — tensile strength of rock under shock tensile;
 E — modulus of elasticity.

Therefore:

$$\Delta t_p = \frac{\delta_B}{E} \cdot \frac{r}{v_r}. \quad (6)$$

In the second case, breed destruction will happen when the relative shift of γ (the plane of rotation of the position a - a position b - b) reach destructive values γ_p . From fig. 3, a it follows that:

$$\gamma_p = \frac{\Delta v_\tau \Delta t_c}{\Delta r}, \quad (7)$$

where Δt_c — the time during which the elementary layer of rock will collapse under the influence of shear shock.

Since shear:

$$\gamma_p = \frac{t_p}{G_c}, \quad (8)$$

where: t_p — destroying the value of the shear stress;
 G_c — shear modulus, given the ratio.

$$G_c = \frac{E}{2(1+\mu)}; \quad (9)$$

$$\tau_p = \delta_B, \quad (10)$$

where μ — Poisson's ratio, we get:

$$\Delta t_c = \frac{2(1+\mu)\delta_B}{E} \frac{dv_\tau}{dr}. \quad (11)$$

Differentiating relationship (3), we find:

$$\frac{dv_\tau}{dr} = 2\pi \frac{dv_r}{dr}, \quad (12)$$

that substituting into (11) we find:

$$\Delta t_c = \frac{2(1+\mu)\delta_B}{\pi E} \frac{dv_r}{dr}. \quad (12)$$

Drinking $\Delta t_p : \Delta t_c$ obtained from the expression (6) and (12):

$$\frac{\Delta t_p}{\Delta t_c} = \frac{\pi}{1+\mu} \cdot \frac{r}{v_r} \cdot \frac{dv_r}{dr}. \quad (13)$$

The law changes the value v_r with the distance r can be approximated by:

$$v_r = v_0 \left(\frac{r_0}{r} \right)^n, \quad (14)$$

where: v_0 - the initial velocity of the breed on the border with the gas cavity; n — exponent, depending on the type of symmetry of the explosion and the physical and mechanical properties of the rock; r_0 — charge radius.

Differentiating, we obtain the absolute value:

$$\left| \frac{dv_r}{dr} \right| = n \frac{v_0 r_0}{r^{n+1}}. \quad (15)$$

Substituting formula (14) and (15) in relation (13) we finally find:

$$\frac{\Delta t_p}{\Delta t_c} = \frac{n\pi}{1+\mu}. \quad (16)$$

As a guideline for spherical and cylindrical symmetry, you can take the n values, respectively, equal to 2 and 1. For estimations μ value in comparison with unity can be neglected.

Then we find that the ratio $\Delta t_p : \Delta t_c$ for spherical and cylindrical explosions, respectively, equal to 2π and π . This shows that the rock is destroyed from the impact of

shear strain is several times faster than the tensile strain from the impact.

By simple calculations we can show that at the time of the destruction of shock rock due to the shear deformation ratio of the potential energy to stretch the same energy shift is $(1 + \mu) / 2(n\pi)^2$. For a cylindrical ($n = 1$) and spherical ($n = 2$), the symmetry ratio is respectively 1.16 and 1.64. Consequently, tensile energy calculations fragmentation can be neglected.

From this it follows that the failure mechanism at the basis of solid rock and concentrated blast hole charges lies shift shock, which is a consequence of the presence of the radial velocity gradient and is shown in misalignment erodible medium volume. For ideal flat charges at steady gradient of quasi-stationary motion is not speed. Consequently, there will be no impact and shear strain. Therefore, the ideal — flat charges as compared to the

focused provide a lesser degree of down hole rock breaking. This, in particular, can be seen in practice, explain the blasting quality deterioration array crushing rocks with decreasing distance between the wells (at a constant value of specific consumption of explosives). In this case, it becomes an ideal flat charge with decreasing distance to the ground a number of borehole charges. With the explosion of charges of ideal flat rock is destroyed by only one compressive, stress (near-field) and slabbing phenomenon (in the far field), arising from the compression wave reflected from the free surface.

Thus, the mechanism of crushing rocks is considered with the explosion of concentrated downhole explosive charges. It is found that the pressure wave is a factor causing the instantaneous movement involving environment. In the presence of the radial velocity the shift shock is generated, which is a major factor in the destruction of rocks.

References:

1. Hanukaev A. N. Stress wave energy in the destruction of rocks by explosion. – M.: Gosgortekhizdat, 1962. – 200 p.
2. Gaek E. V., Drukovanny M. F., Nishin V. V. The rate of propagation of cracks in the rocks and solids and methods of measurement. – In the book.: An explosive affair. – № 51/8. – M.: Gosgortekhizdat, 1963. – P. 85–96.
3. Mosinets V. N. Terms of brittle and ductile rock explosion. – Proc.: The destruction of rocks by explosion. – M.: Nedra, 1967. – S. 77–100.
4. Zverkov S. N., Okunev A. R. Experience in the use of parallel-contiguous wells in quarries GOK Zhdanov. – In the book: The use of parallel-contiguous wells and underground workings. – M.: IGD, 1967. – P. 6–11.
5. Maksimov E. P. Laboratory studies of the characteristics of lumpiness in crushing explosion. – In the book: An explosive affair. – № 47/4. – M.: Gosgortekhizdat, 1962. – P. 103–109.
6. Baum S. A. The process of destruction of rocks by explosion. – In the book.: An explosive affair. – № 52/9. – M.: Gosgortekhizdat, 1963. – P. 263–285.
7. Norov Yu. D., Bibik I. P., Norov J. A., Nasirov U. F., Normatova M. J. Production blasting in complex hydrogeological conditions//Mining journal. – 2013. – № 8–1. – P. 30–31.
8. Norov Yu. D., Bibik I. P., Zairov Sh. Sh. Effective management of the drilling and blasting parameters according to the criterion of the quality of blasted rock mass. News of the Higher Institutions//Mining Journal. – 2016. – № 1. – P. 34–39.
9. Filippov V. K. The direction of crack propagation appeared during the destruction of hard rock explosion. – In the book.: An explosive affair. – № 47/4. – M.: Gosgortekhizdat, 1961. – P. 172–174.
10. Drukovanny M. F. About the fracture mechanism of rocks with short-delay firing. – In the book.: An explosive affair. – № 47/4. – M.: Gosgortekhizdat, 1961. – P. 184–196.

*Khudoyberganov Abrorjon Akbarovich,
Bukhara refinery Deputy Chief Engineer
for the implementation of innovative projects
and technologies in production Bukhara refinery
E-mail: abrorjon_@mail.ru*

Studying of process steaming of kerosene fraction by hydrocarbonic steams

Abstract: In article resulted results of studying process of steaming kerosene fraction are by hydrocarbonic steams.

Keywords: hydrocarbonic, distillation, rectification, water steam, stripping — column, oil, gascondensate.

Introduction

As is known, by distillation of oil and a gas condensate receive hydrocarbonic fractions which are intermediate products for motor топлив. Process is carried out in installation of the primary distillation consisting in basic from rectification and the stripping-columns [1; 2; 3].

Under the existing «know-how» at steaming distillate fractions it is used heating water steam. As the steaming agent it is possible to carry to the basic lacks of application of water steam: increase in expenses of thermal energy at process; increase of loading of a column on steam, leading to increase in its diameter; condensate formation, its branch from fuel fractions and clearing of impurity demands additional expenses; strengthening of corrosion of working surfaces of the equipment under the influence of a water condensate, watery mineral oil and their necessity of the subsequent drying, etc. [2; 4].

For these reasons in the technological plan sharp reduction of the expense of water steam on process of distillation of oil is expedient, in particular, at steaming distillates, or carrying out of the given process without its participation. Thus one of technological decisions of a problem, use of steams of the oil fractions leaving from rectification of a column, as the alternative heat-carrier instead of water steam is [4]. Such technological decision promotes elimination of the above-stated negative phenomena which are taking place at distillation oilgascondensate of raw materials with participation of water steam.

The analysis of a condition of process of primary distillation of hydrocarbonic raw materials in oil refining factories shows, that because of not enough effective organisation of processes in rectification to a column the expense of thermal energy for process realisation raises, that is reflected in growth of the cost price of let out production. Therefore perfection of processes of distillation of hydrocarbonic raw materials, working out of

high efficiencies, energy — and resource saver up technological processes and rectification devices corresponds to the basic directions of dynamic development of oil refining branch.

Experiment

Proceeding from the above-stated, we collect the experimental stand for process studying steaming (decontaminations) of the kerosene fraction leaving from difficult rectification of a column of installation of primary distillation Bukhara oil treatment factory (fig. 1). The main objective of experimental researches was definition of quality indicators — fractional structure, density and temperature of flash of the kerosene fraction leaving installation of primary distillation and from the subsequent processing by its hydrocarbonic heat-carrier (the steaming agent).

Object of research is the kerosene fraction received from local oilgascondensate of raw materials (at a parity of 70 % of a gas condensate and 30 % of oil) on Bukhara OTF.

Experimental decontamination device consists of capacity 1 for easy fraction, thermometers 2, 7 and 9, electrotiles 3 and 10, a manometre 4, a sand bath 5, a gas torch 6, flask Angler 8, a refrigerator 11 and flasks for gathering of light fractions 12.

During experiments the capacity 1 is filled with easy fraction and it heats up by means of an electrotile 3. The capacity is supplied by the thermometers established in pockets 2 and manometres 4 for constant control of working temperature and pressure of investigated fraction. The working temperature of the hydrocarbonic heat-carrier in the given capacity is supported in limits from 350 T° to 400 T° by means of the sand bath 5 which are warmed up by a gas torch 6. The temperature of a sand bath is supervised under indications of the thermometer 7. During experiment in a flask 8 with volume three

litres fill in the kerosene selected from a sampler industrial rectification of installation, not subjected to steam processing — steaming. The investigated liquid in a flask 8 heats up by means of an electrotile 10 to temperature of 110 T° and the ferry easy fraction from capacity 1 is processed. Thus the liquid temperature in a flask 8 is supervised by the thermometer 9. Leaving steams of easy fraction from a flask 8 are condensed in water refrigerator

Libikha 11. The received condensate, i. e. the decontaminated easy fraction of kerosene, gathers in a flask 12.

At carrying out of experiences every 15 minutes defined temperatures and pressure of investigated fraction, according to regime parametres of the plant ($T_w = 30 \div 85$ °C and $P_w = 40 \div 150$ kPa). Results of experiences on decontamination of kerosene fraction of local hydrocarbonic raw materials are resulted in the table 1.

Table 1. – Results of experiences on decontamination of kerosene fraction of local hydrocarbonic raw materials

№	Indicators	Unit of measure	Kerosene fraction			Allocated easy fraction in the course of decontamination easy fraction		Easy fraction
			To stripping — columns	Decontaminated by water steam in a stripping-column	After decontamination easy fraction	on 52–280 T°	on 280–281 T°	
1	Density at 20 T°	kg/m ³	776.8	790.9	795.5	718.8	734	636
2	Fractional structure:							
	b. b.	T°	102	146	188	34	40	25
	10 %	T°	131	167	193	55	64	30
	20 %	T°	143	175	196	68	79	33
	30 %	T°	156	182	198	81	97	36
	40 %	T°	168	188	200	96	118	39
	50 %	T°	177	194	202	111	156	42
	60 %	T°	184	200	204	125	170	45
	70 %	T°	191	205	207	138	177	49
	80 %	T°	198	210	211	154	184	55
	90 %	T°	205	217	216	175	197	62
	e. b.	T°	216	228	225	198	211	67
3	Exit	%	98.0	98.0	98.0	97	98	95
4	The rest	%	1.0	1.0	1.0	1.2	0.8	0.5
5	Losses	%	1.0	1.0	1.0	1.8	1.2	4.5
6	Flash temperature	T°	–	38	46	–	–	–

From table data it is visible, that temperature of the beginning of boiling (b. b.) kerosene fraction to a stripping-column its temperature of the end of boiling (e. b. begins from 102 T°, and.) comes at 216 °C. Under production conditions, after decontamination of kerosene with water steam in a striping-column, it b. b. Makes 146 °C, and e. b. — 228 T°. After decontamination by the hydrocarbonic heat-carrier b. b. Kerosene fraction has made 188 °C, and e. b. — 225 T°. The allocated easy fractions in the course of decontamination of kerosene easy oil fraction at temperature of 52–280 T° had b. b. 34 °C and к. к. 198 T° accordingly. At realization of the given process at temperatures 280–281 T° easy fractions

of kerosene have н. к. 40 T° and e. b. 211 T°. Thus, the made experiments show, that after kerosene decontamination easy hydrocarbonic fractions from structure of kerosene fraction pass in structure easy oil fraction.

The basic results of experimental data by definition of fractional structure of kerosene and its easy fractions before decontamination process are represented on fig. 2. The analysis of curves shows, that with increase in temperature the exit of easy fractions from structure of steamed kerosene increases. At a temperature mode within 197–225 T° in all variants of experiences achievement of necessary clearness of division of kerosene fraction from the accompanying components,

corresponding to requirements of the standard of quality of production is observed.

As we see, process of decontamination of kerosene by steams easy fraction occurs at rather high temperature modes (a curve 1), than it steaming water steam in a stripping-column (a curve 2). Thus rate of allocation easilyflying components from structure of kerosene fraction more intensively (a curve 4), than at decontamination of kerosene with water steam (a curve 5).

On a course of experiments also are defined temperature of flash of kerosene fraction [2; 3] in accordance with GOST 6356 (the tab. see). The temperature of flash of kerosene fraction (at the expense $24 \text{ m}^3/\text{h}$), decontaminated by water steam (at the expense $1.5 \text{ m}^3/\text{h}$) in a stripping-column Bukhara OTF makes 38 T° , and the kerosene fraction decontaminated by hydrocarbonic steams in the conditions of experiment, had temperature of flash equal 46 T° . The difference in values of temperature of flash speaks distinction of the mechanism of intermolecular interactions of the steaming agent and the kerosene expressed in various degree flying of easy fractions at decontamination.

During experiences the density of kerosene fraction was defined areometric by a method [2; 3; 5],

according to GOST 1756. Apparently from the table, the density of kerosene fraction to a stripping-column makes $776.8 \text{ kg}/\text{m}^3$, and after its decontamination with easy oil fractions values of this indicator $795.5 \text{ kg}/\text{m}^3$ are equaled.

Conclusions

Generalising results of the spent experiments by definition of fractional structure of kerosene and its easy fractions in process steaming it is possible to draw a conclusion on possibility of an effective utilization of steams of hydrocarbonic fractions (for example, easy fraction, leaving of rectification columns) as the alternative steaming agent in exchange heated water steam. Application of the hydrocarbonic steaming agent promotes improvement of quality indicators of kerosene fraction, elimination of its possibility обводнения (especially aviakerosene and diesel fuel) and to clearness increase fraction distillates in rectification to a column. Because of distinction in physical and chemical and heatphysical properties of hydrocarbonic and water steams, efficiency spent warmly — and massechange processes at steaming kerosene fraction in a stripping-column raises; speed of corrosion of working surfaces of the equipment thus decreases and the expense inhibitors corrosion is reduced.

References:

1. Skoblo A. I., Molokanov J. K., Vladimirov A. I., etc. Processes and devices oilgastreatment and petrochemistry: the Textbook for high schools. 3 publ., the reslave. – M.: Bowels, 2000. – P. 103–104.
2. Technology of oil refining. In 2 parts. A part the first. Primary oil refining/Under the editorship of O. F. Glagolevoj and V. M. Kapustin. – M.: Chemistry, the Colossus, 2006. – P. 99–105, 143–146, 331–345, 390–392.
3. Manovyan A. K. Technolog of primary oil refining and natural gas. The manual for high schools. 2 publ. – M., 2001 – P. 104–107, 138–140, 357–389.
4. Salimov Z. S., Hudajberdiev A. A., Sharipov K. K., Hurmamatov A. M. The Effective utilization of hydrocarbonic steams in primary distillation oilgascondensate raw materials//the Uzbek magazine of oil and gas. – 2011. – № 2. – P. 34–35.
5. Tumanyan B. P. Practical of work on technology of oil. A small laboratory practical work. – M.: Technics, RSU oil and gas of I. M. Gubkin. Tuma groups, 2006. – P. 11–12.

DOI: <http://dx.doi.org/10.20534/AJT-17-1.2-105-107>

*Khudoyberganov Abrorjon Akbarovich,
Bukhara refinery Deputy Chief Engineer
for the implementation of innovative projects
and technologies in production*

E-mail: abrorjon_@mail.ru

*Saydakhmedov Shamshiddin Mukhtarovich,
Fergana oil refinery,
Chief of Fergana oil refinery*

Studying of process of decontamination of gasoil by hydrocarbonic couples

Abstract: In article results of pilot studies on use of kerosene fractions are given as the unpicking agent for decontamination of oil-gas condensate raw materials, change of density and kinematic viscosity, and also influence of the unpicking agent on quality ready production.

Keywords: pressure, temperature, kerosene, gasoil, water vapor, hydrocarbonic, gas condensate, distillation, water steam, light naphtha.

Development of the oil and gas processing and petrochemical industry at the present stage is characterized by considerable expansion of the range and products improvement of quality, increase in depth of oil refining, construction along with installations of big single power of modular low-tonnage installations of complex oil refining, gas and the gas condensate, allowing to receive wide scale of oil products taking into account needs for them oil and gas extraction areas [1; 2].

As a rule, oil and oil products divide by distillation into separate parts, each of which is less difficult mix. Hydrocarbonic fractions in difference from individual connections have no constant temperature of boiling. They boil away in certain intervals of temperatures. Temperatures I began and the end of boiling depend on a chemical composition of fraction. Thus, the fractional composition of oil and oil products shows the contents in them the various fractions which are boiling away in certain temperature limits. This indicator has great practical value. On fractional composition of oil judge what oil products and in what quantities can be emitted from it, and the fractional composition of gasolines and other motor fuels characterizes their evaporability, completeness of evaporation, etc. For the purpose of creation of a demanded steam irrigation in distant-pasture section of columns, and also evaporations of low-boiling fractions of oil in practice widely apply distillation with supply of water vapor [1]. At input of water vapor in distant-pasture section the partial pressure of vapors decreases and conditions under which liquid is as

though superheated that causes its evaporation (that is effect of water vapor similarly to vacuum) are created. The general consumption of water vapor entered into atmospheric columns of installations of distillation of oil makes 1.2–3.5, and in vacuum columns for fuel oil distillation — 5.8 % of masses. on overtaken raw materials. When using water vapor for distillation of oil there are following shortcomings: increase in expense of energy, increase of loading of columns on couples, deterioration of conditions of regeneration of heat in heat exchangers, increase in resistance and pressure increase in a column and other devices, flood of oil products and strengthening of corrosion of devices.

In this regard in recent years in world oil processing the tendency to existing restriction of application of water vapor and to transfer of installations on technology of dry distillation i. e. application of the hydrocarbonic steaming agent is shown.

Proceeding from the above, we collected model laboratory installation for carrying out experiments on decontamination of kerosene and gasoil fractions. Experiments are made in vitro Bukhara oil refinery to whom aviation fuel analyses Jet A-1 to an decontamination water vapor of stripping-columns and with an decontamination water vapor after stripping-columns are carried out. At creation of conditions of a temperature mode of stripping-columns experiments with application of light naphtha for an decontamination of kerosene fraction to stripping-columns [4] are in vitro made. The obtained experimental data are given in tab.1.

Table 1. – Results of analyses of Dzheta-1 kerosene before and after an decontamination water and hydrocarbonic ferry (light naphtha)

№	Name of indicators	Kerosene Jet A-1 to stripping- column	Kerosene Jet A-1 after a stripping- column (decontamination with water vapor)	Kerosene Jet A-1 after an decontamination from light naphtha
1.	Density at 20°C, kg/m ³	780	787	790
2.	The content of water, about %	0.0	0.0	0.0
3.	Contents fur of impurity, %	0.0018	0.002	0.0
4.	The contents about sulfurs, %	0.09	0.07	0.094
5.	Acidity, mg KOH/1000 cm ³	0.78	0.67	1.13
6.	Flash temperature, °C	13	40	47
7.	Copper plate	–	–	–
8.	Temperature turbidity, °C	3 a	3 a	1 a
9.	Temperature hardening, °C	20.4	19.2	22.5
10.	Kinematic viscosity at 20 °C, mm ² /sec.	26.8	27.48	25
11.	Fractional structure:			
	I began boilings, °C	109	151	154
	5 %, °C	121	158	164
	10 %, °C	138	162	167
	15 %, °C	144	165	169
	20 %, °C	149	169	171
	25 %, °C	155	172	173
	30 %, °C	160	175	174
	35 %, °C	163	178	175
	40 %, °C	169	180	176
	45 %, °C	172	182	177
	50 %, °C	181	185	178
	55 %, °C	183	187	180
	60 %, °C	185	190	181
	65 %, °C	187	192	182
	70 %, °C	192	195	183
	75 %, °C	195	198	186
	80 %, °C	199	202	188
	85 %, °C	203	206	190
	90 %, °C	209	211	194
	95 %, °C	217	218	199
	Boiling end, °C	227	225	209
	Exit, %	98.0	98.0	98.0
	Rest, %	1.2	1.1	1.2
	Losses, %	0.8	0.9	0.8

From table 1. is visible that kerosene density Jet A-1 before decontamination made 780 kg/m³, after its decontamination with water vapor density changed on 787 kg/m³, and decontaminations it with light naphtha this indicator made 790 kg/m³. The content of water after decontamination with water vapor of 0.01 %, and this indicator was absent when process is carried out with light naphtha. The indicator of temperature of flash made 40°C at decontamination with water vapor, and at

decontamination with kerosene fractions 44°C. Height not smoking a tribe (GNP) of kerosene before decontamination made 20.4 mm, at decontamination with water vapor made 19.2 mm, after decontamination of light naphtha of 22 mm. Acidity of kerosene to stripping-columns of 0.78 mg. the KOH/100 cm³, at decontamination with water vapor made 0.67 mg. KOH/100 cm³ after decontamination of light naphtha is absent. Kerosene decontaminations Jet fraction A-1 by means of water vapor as the

unpicking agent at initial temperatures of boiling 158°C was allocated 5 % of fraction, and at decontamination from light naphtha this indicator made 164°C. The boiling end with water vapor made 225°C, and about the ferry of light naphtha made 209°C. At the end of technological process the exit of hydrocarbonic fractions when using by water vapor made 98 %, the rest of 1.1 %, and with use of light naphtha as the unpicking agent the exit of fractions made 98.0 %, the rest of 1.2 %. From the conducted pilot researches it is visible that kerosene decontamination Jet

A-1 with hydrocarbonic couples proves to the advantages at their use as the unpicking agent.

Thus, uses of light naphtha as the unpicking agent for kerosene decontamination Jet A-1 to the advantages, after decontamination of their density, temperature of flash increases and acidity decreases this results from the fact that as a part of ready to production doesn't remain easy fractions and is absent an amount of water, besides temperature too decreases, this indicator it is possible will see their temperatures of flash.

References:

1. Skoblo A. I., Molokanov Yu. K., Vladimirov A. I., Shchelkunov V. A. Processes and devices of a neftegazoperabotka and petrochemistry. 3rd prod. reslave. and additional. – M: JSC Businessstentr-Nedra, 2000. – P. 5–7.
2. Technology of oil refining. In 2 parts. Part one. Primary oil refining/Under the editorship of O. F. Glagoleva and V. M. Kapustin. – M.: Chemistry, Colossus, 2006. – P. 331–345.
3. Manovyan A. K. Technology of primary oil refining and natural gas. Manual for higher education institutions. 2nd prod. – M.: Chemistry, 2001. – P. 138–140.
4. Salimov Z. S., Saydakhmedov Sh. M., Khudoyberganov A. A., Khurmamatov A. A., Hudayberdiyev A. A. Studying of process of an decontamination of kerosene fraction by hydrocarbonic couples//Oil processing Magazine and petrochemistry. – Moscow, 2012. – No. 9. – P. 10–13.

DOI: <http://dx.doi.org/10.20534/AJT-17-1.2-107-111>

*Shamshidinov Israiljon Turgunovich,
Candidate of technical science, associate professor,
Associate professor of cathedral «Professional education (Chemical technology)»,
Namangan engineering-pedagogical institute, Uzbekistan
E-mail: israiljon2010@mail.ru*

*Mirzakulov Kholtura Chorievich,
Doctor of technical science, professor,
Professor of cathedral «Chemical technology of inorganic substances»
E-mail: khchmirzakulov@mail.ru*

Research of process of washing of fluorine from phosphor gypsum

Abstract: Results of clearing of phosphor gypsum from fluorine compounds by washing by its solutions a chamois, a mix of sulfuric and phosphoric acids, 30 % a solution of ammonium nitrate and water are resulted. The maximum degree of washing phosphor gypsum from fluorine is observed at use of 60 % of sulfuric acid, a mix of sulfuric and phosphoric acid, 30 % by a solution of ammonium nitrate. Thus degree of washing makes 95.0–97.0 %, and the fluorine contents in phosphor gypsum decreases to 0.10–0.17 %.

Keywords: phosphorite, extraction phosphoric acid, phosphor gypsum, defluorination, filtration, degree of washing.

Introduction

At the average contents in extraction phosphoric acid (EPA) 1.2 % is fluorine, received of 716 thousand t washed burnt phosphor concentrate of Central Kyzylkum (CK), annually in soil is brought 8.59 thousand t of

fluorine. At achievement of full satisfaction of requirement of agriculture of Republic Uzbekistan in phosphoric fertilizers (the requirement for phosphoric fertilizers makes 518 thousand t. 100 % of P₂O₅) on fields will be brought 34.36 thousand t fluorine.

The average contents of fluorine in phosphor contents the fertilizers made in Republic, such as ammophos, superphos, makes superphosphate from 2.0 to 4.0 %. One of perspective methods of decrease the fluorine contents in fertilizers is its extraction from EPA by its manufacture as 70–80 % of fluorine at acid decomposition of phosphatic raw materials remain in EPA. It can achieve introduction in process sulfuric acid decomposition of phosphates of connections of alkaline metals with simultaneous reception fluorosilicate or by evaporation acid [1; 2]. These ways demand the additional equipment and are connected with the big expense of power resources.

Many researches are devoted to defluorination of EPA from phosphorites of Central Kyzylkum, which distinctive feature are low (0.13 %) the contents of acid-soluble compounds of silicon [3–5].

We develop a way of clearing of EPA from fluorine in a work cycle of manufacture of acid, by introduction of a carbonate of calcium before a filtration of extraction pulps [6]. Thus from 68.4 % to 82.5 % of fluorine it is besieged in the form of fluoride of calcium and remains in structure phosphor gypsum depending on norm of a carbonate of calcium (60–100 % on the fluorine content). At norm of 100–150 % of a calcium carbonate in phosphor gypsum passes 82.5–86.8 % of fluorine from available in phosphorite.

Fluorine is the necessary chemical element for manufacture of anticorrosive preparations, extraction

of precious metals, serves mineralizator at reception of cements. Therefore researches directed on extraction of fluorine from phosphor gypsum are very actual.

Objects and methods

On purpose allocation of fluorine from phosphor gypsum researches on washing of phosphor gypsum with sulfuric acid and phosphoric acid are carried out by solutions of various concentration, and also solutions of ammonium nitrate.

For this purpose received phosphor gypsum by introduction in sulfuric acid pulp of contents of EPA of a calcium carbonate in quantity providing norm of calcium on contents of fluorine of 100 %. After 30 minute hashing at temperature 80 °C, a pulp divided on funnel of Buxner, using lavesan fabric. The area of a filtering fabric of 131.8 sm².

Received phosphor gypsum contained 3.37 % of fluorine. Washing of phosphor gypsum was carried out by 5–60 % solutions of sulfuric acid, a mix of sulfuric acid with EPA, containing from 2.28 % to 6.97 % P₂O₅, the temperature was supported 60 °C.

The first washing phosphor gypsum spent washing solutions, and the second and third washing carried out hot water (60 °C).

Results of the residual contents of fluorine in phosphor gypsum and technological indicators reception EPA and washing of phosphor gypsum are resulted in table 1.

Table 1. – Technological indicators of washing phosphor gypsum from fluorine sulfuric- and sulfuric-phosphoric acid solutions

№ experiments	Washing solution		The contents of fluorine after washing phosphor gypsum	Technological indicators of reception of EPA			Degree of washing phosphor gypsum from fluorine, %
	Concentration H ₂ SO ₄ , % on SO ₃	Concentration EPA, % on P ₂ O ₅		K _p , %	K _{отм.} , %	K _{out} , %	
1.	60	–	0.42	99.80	99.30	99.20	87.54
2.	30	–	0.50	98.70	98.90	97.61	85.11
3.	20	–	0.55	98.48	98.60	97.11	83.68
4.	10	–	0.61	98.09	98.40	96.52	81.90
5.	5	–	0.77	97.87	98.21	96.12	77.15
6.	60	2.28	0.15	99.60	99.99	99.59	95.55
7.	30	4.29	0.30	98.60	99.99	98.58	91.10
8.	20	5.96	0.21	98.53	99.76	98.29	87.83
9.	10	6.97	0.10	98.38	99.70	98.08	97.03

With increase in concentration of sulfuric acid with 5 to 60 % the fluorine content in phosphor gypsum decreases from 3.37 % to 0.42–0.77 %. Degree of extraction of fluorine makes 77.15–87.54 %. The best results are received at use of sulfuric acid with concentration of 60 %. Thus the decomposition factor of phosphor raw material makes 99.8 %, factor washing 99.3 % and factor of an exit of 99.2 %.

At use of the sulfuric acid in addition containing EPA, technological indicators of process of washing improve, and the fluorine contents in phosphor gypsum decreases to 0.10–0.30 %, degree of extraction of fluorine makes 87.83–97.03 %. All factors — phosphorite decomposition, washing of phosphor gypsum and exit EPA raise also. Optimum techno-

logical parameters of washing fluorine from phosphor gypsum are: concentration of sulfuric acid of 60 % on SO_3 , 60 % SO_3 and with introduction of EPA in number of 2.28 % on P_2O_5 and 10 % on SO_3 with introduction of 6.97 % EPA on P_2O_5 .

In fig. 1 the given changes of the content of fluorine in washed phosphor gypsum 30 % by a solution of ammonium nitrate, 11 % a solution of sulfuric acid on SO_3 and hot water depending on temperature of washing solutions are cited.

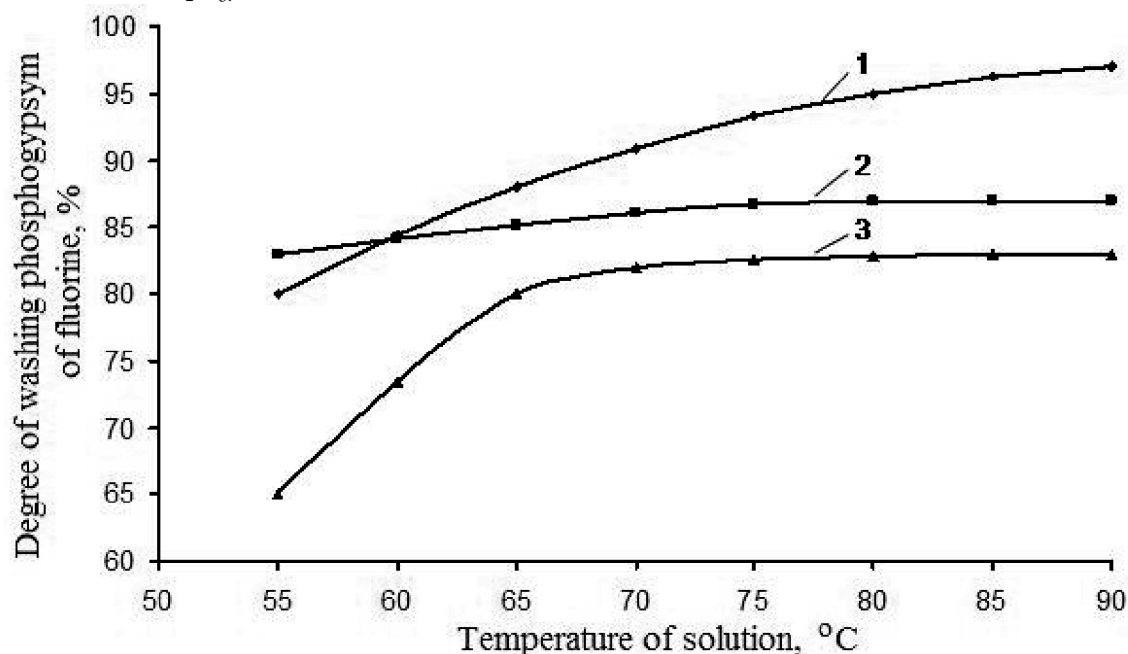


Fig. 1. Change of the contents of fluorine in phosphor gypsum at washing:
 1) 30 % solution of ammonium nitrate; 2) 11 % solution of sulfuric acid on SO_3 ;
 3) hot water depending on temperature of process of washing

Table 2. – Influence of temperature of washing on the fluorine content in production EPA and washing solutions (the fluorine content in not washed phosphor gypsum 3.37 %)

№ experiments	Washing temperature	The fluorine content, %				The fluorine content in phosphor gypsum, %	Degree of washing phosphor gypsum from fluorine, %
		I ϕ -T	II ϕ -T	III ϕ -T	IV ϕ -T		
Counterflow washing by hot water							
1	60	0.92	1.05	0.84	0.53	0.90	73.4
2	70	0.89	1.06	0.84	0.57	0.61	82.0
3	80	0.87	1.01	0.89	0.47	0.58	82.8
4	90	0.86	1.13	0.81	0.31	0.57	83.0
Washing of 30 % by solution NH_4NO_3							
5	60	0.84	0.66	0.60	0.74	0.53	84.4
6	70	0.92	0.76	1.17	0.39	0.31	90.9
7	80	0.77	0.64	1.82	0.78	0.17	95.0
8	90	0.81	0.87	1.94	0.75	0.10	97.0
Washing of 11 % by a solution on SO_3 sulfuric acid							
9	60	0.59	0.94	1.04	0.83	0.54	83.9
10	70	0.47	0.95	1.13	0.83	0.47	86.1
11	80	–	0.94	1.18	0.67	0.44	87.0
12	90	0.69	1.07	1.24	0.57	0.43	87.1

From the resulted of data it is visible, that the best indicators of washing are reached at use of 30 % of a solution of ammonium nitrate. Rise in temperature of a washing solution essentially influences washing degree phosphor gypsum at application of a solution of ammonium nitrate

and water. At use of 11 % on SO_3 a solution of sulfuric acid influence of temperature of a washing solution does not render appreciable influence. At temperature of a washing solution 80–90 °C washing degree of phosphor gypsum from fluorine a solution of ammonium nitrate

exceeds 97 %, 11 % sulfuric acid on SO_3 exceeds 87 %, water makes more than 83 %.

In table 2 data on change of the content of fluorine in washing solutions are cited at use for water washing, 30 % of a solution of ammonium nitrate and 11 % on SO_3 a solution of sulfuric acid.

From the table it is visible, that rise in temperature with 60°C to 90°C promotes decrease in the content of fluorine in phosphor gypsum at washing by water from 0.90 % to 0.57 %, at washing of 30 % by a solution of ammonium nitrate from 0.53 % to 0.10 % and 11 % on SO_3 a solution of sulfuric acid from 0.54 % to 0.43 %.

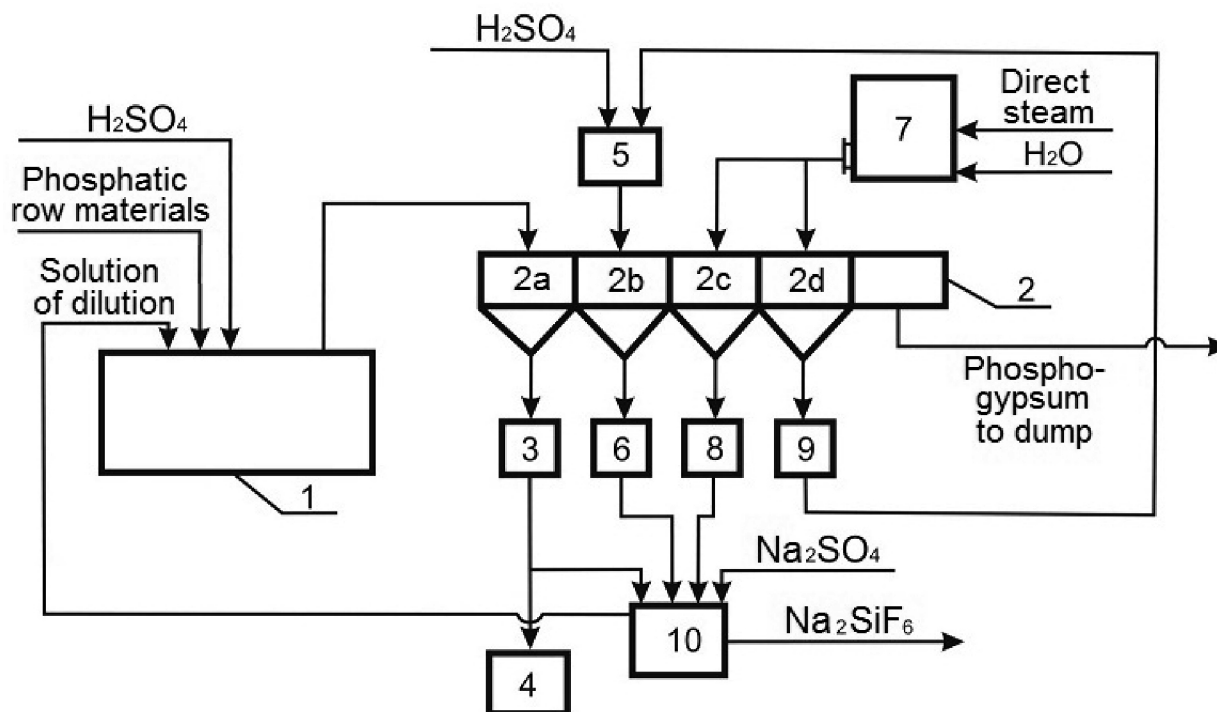


Fig. 2. The basic technological scheme of washing phosphor gypsum from fluorine: 1 – extractor; 2 – carousel vacuum-filter; 2a – first zone of a filtration; 2b – second zone of a filtration; 2c – third zone of a filtration; 2d – fourth zone of a filtration; 3 – collection of the first filtrate; 4 – warehouse of extraction phosphoric acid; 5 – amalgamator; 6 – collection of the second filtrate; 7 – pressure head tank; 8 – collection of the third filtrate; 9 – collection of the fourth filtrate; 10 – sediment bowl.

In fig. 2 the washing scheme phosphor gypsum with use for washing of sulfuric acid is resulted. The pulp sulphur-phosphoric acid decomposition of phosphatic raw materials from an ex-tractor moves on 1st zone of a filtration (poses. 2a) where occurs branch production EPA from phosphor gypsum. EPA arrives in the collection of 1st filtrate (poses. 3) and further in acid storehouse (poses. 4).

Phosphor gypsum at the first stage it is washed out by sulfuric acid (poses. 2b) also gathers in capacity (poses. 10). At the second and third stage it is washed out by hot water. A filtrate after the second stage (poses. 2c) also arrives in capacity (poses. 10), and after the third stage (poses. 2d) moves on the first stage of washing phosphor gypsum (poses. 2b),

In the second and third zones of washing (poses. 2c and 2d) occurs additional washing of fluorine from phosphor gypsum, passed under the influence of acid in the soluble form.

For sedimentation of soluble forms of fluorine in sediment bowl (poses. 10) it is entered sodium sulphate

for fluorine linkage in sodium fluorosilicate and its allocation for use to destination. Cleanliness sodium fluorosilicate makes not less than 96 %. Mother solution after branch sodium fluorosilicate comes back to a stage of decomposition of phosphorite.

Conclusion

Thus, the carried out researches have shown possibility of reception of EPA partially cleared of fluorine by introduction in extraction pulp of a calcium carbonate and washing phosphor gypsum from fluorine solutions a chamois, a chamois and EPA acids, ammonium nitrate.

The best results of washing phosphor gypsum from fluorine are reached at use of 60 % on SO_3 sulfuric acid, 60 and 10 % on SO_3 a chamois and EPA acids with the contents of 2.28 % and 6.97 % P_2O_5 , 30 % a solution of ammonium nitrate. Washing is desirable for carrying out at temperature $80\text{--}90^\circ\text{C}$. Thus degree of washing makes 95.0–97.0 %, and the fluorine content in phosphor gypsum does not exceed 0.10–0.17 %.

References:

1. Kochetkov S. P., Smirnov N. N., Il'in A. I. Concentrating and clearing of extraction phosphoric acid/GOUV-PO Ivan. gov. chem.-technolog. ins. – Ivanova, 2007. – 308 p.
2. Khujamkulov S. Z., Melikulova G. E., Mirmusaeva K. S., Mirsaidov M. H., Mirzakulov Kh. Ch. Research of processes of reception sodium fluorosilicate from extraction phosphoric acid on the basis of phosphorites of Central Kyzylkumov//Chemical technology. The control and management. – Tashkent: TGTU, 2016. – № 1 (67). – P. 34–40.
3. Khujamkulov S. Z., Asamov D. D., Bardin S. V., Mirzakulov Kh. Ch. Defluorination of extraction phosphoric acid with salts of sodium//Chemistry and chemical technology. – 2008. – № 2. – P. 16–19.
4. Khujamkulov S. Z., Asamov D. D., Bardin S. V., Mirzakulov Kh. Ch. Defluorination of extraction phosphoric acid of Central Kyzylkum in the presence of sodium silicate.//Chemistry and chemical technology. – 2008. – № 4. – P. 8–11.
5. Khujamkulov S. Z., Asamov D. D., Bardin S. V., Mirzakulov Kh. Ch. Technology working out defluorination of extraction phosphoric acid of Central Kyzylkum with recycling of sodium silicate//Chemical technology. The control and management. – Tashkent: TGTU, 2008. – № 4. – P. 41–45.
6. Arislanov A., Shamshidinov I., Gafurov K. Defluorination of EPA from phosphorites of KyzylKum in the process of decomposition//Scientific and technical journal FerPI. – Fergana: FerPI, 2006. – № 2. – P. 95–98.

DOI: <http://dx.doi.org/10.20534/AJT-17-1.2-111-113>

*Sharipov Khasan T.,
Tashkent State Technical University,
Professor, Doctor of Chemical Sciences,
Deputy Chairman of the SUE "Fan va tarakkiet"*

*Sharafutdinov Ulugbek Z.,
Navoi Mining and Metallurgical Combine,
Chief of the technical control service of the MA. of the NMMC
E-mail: u0505@mail.ru*

*Rajabboev Ibodillo M.,
Navoi state mining Institute, researcher*

*Khujaev Jasur E.,
Navoi state mining Institute, researcher*

Analysis of productive solutions and uranium sorption on anionits

Abstract: Currently of the uranium mined in Navoi Mining and Metallurgical Combine is obtained by means of underground leaching in the Kyzyl-Kum open pits. This method allows to reduce the cost of uranium mining and ensure the environmentally clean production.

Keywords: uranium, underground leaching, sorption, extraction, rhenium, environmental protection.

Currently, mineral raw resources compound economic roots of many developed countries therefore advances of industry and agriculture depends on rational and fruitful usage of them by means of creation of new technologies which provide complex processing. Especially it is about extraction of rare metals which composes interrelated and sophisticated cyclical process and obtaining final ready products in their pure forms. Nowadays in uranium industry the main part

of raw resources' basis consists of hydrogen mines which are based on processing by boreholes of underground leaching.

Uranium has had a severe impact on many aspects of intergovernmental relations which are far from science, particularly on international politics. Development of mining the uranium in *Kyzyl-Kum* region on the basis of physicochemical technology inseparably tied together with common tendency of the global

mining industry and takes place on the background of continuous changes of economic conditions and the demand for raw resources. A significant impact on our economy, along with the production of other rare metals has been made by mining, processing and further use of the uranium. Meanwhile, uranium production technology has many unresolved problems. One of such problems is the quality of incoming salts of sulfuric acid from In Situ Leaching (ISL) departments of Navoi Mining and Metallurgical Combine.

As already mentioned existing technology involves extracting uranium by the method of in situ leaching and further separation from productive solutions and accumulation on ion-exchange resins. Its use provides selective separation of uranium from solution and its concentration.

While leaching the uranium with sulfuric acid, many other admixture components of rocks are also partly dissoluble. Because of this many impurities enter productive solutions with uranium (table 1).

Table 1. – Efficiency of main components of ore in sulfuric acid dissolution

Reaction	Extraction in solution, %	Concentration of the component in solution, g/l
H_2SO_4		
SiO_2	1	0.1–0.5 (SiO_2)
$CaSiO_3 + H_2SO_4 \rightarrow CaSO_4 + H_2SiO_3$		
$Al_2O_3 + 3H_2SO_4 \rightarrow Al_2(SO_4)_3 + 3H_2O$	3–5	1–12 (Al_2O_3)
$Fe_2O_3 + \rightarrow Fe_2(SO_4)_3 + 3H_2O$	5–8	3–7 (Fe_2O_3)
$FeO + H_2SO_4 \rightarrow FeSO_4 + 3H_2O$	40–50	0.5–3.0 (FeO)
$FeCO_3 + H_2SO_4 \rightarrow FeSO_4 + H_2O + CO_2$	80–90	0.2–0.7 (FeO)
$CaCO_3 + H_2SO_4 \rightarrow CaSO_4 + H_2O + CO_2$	80–90	1.5–2.0 (CaO)
$MgCO_3 + H_2SO_4 \rightarrow MgSO_4 + H_2O + CO_2$	88–90	0.5–3.0 (MgO)
$MoO_3 + H_2O \rightarrow H_2MoO_4$	60–90	0.05–1.0 (Mo)
$K_2O * V_2O_5 * UO_3 * nH_2O + H_2SO_4 \rightarrow (VO_2)_3SO_4 + K_2SO_4 + (n+3)H_2O + UO_2SO_4$	92–95	0.5–5.0 (V_2O_5)
$CuO + H_2SO_4 \rightarrow CuSO_4 + H_2O$	30–70	0.1–1.0 (Cu)
$Ca_3(PO_4)_2 + 3H_2SO_4 \rightarrow 3CaSO_4 + 2H_3PO_4$	70–90	0.2–1.4 (P_2O_5)
$Ca_2F(PO_4)_3 + 5H_2SO_4 \rightarrow 5CaSO_4 + 3H_3PO_4 + HF$	–	–

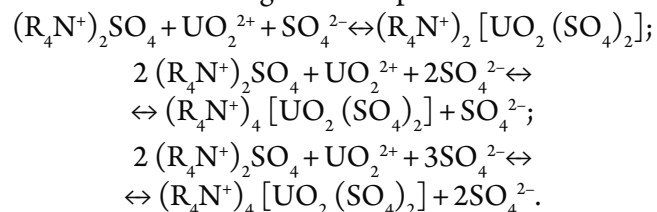
Thus the basic properties of solutions are not changed and are recycled. In the technology of leaching subsequent treatment of solutions are also taken into account. In sorptional extraction of uranium from solutions anionites are mainly used. Accompanying impurities in productive solutions behave inadequately. Cations of alkali and alkaline earth elements, ions of copper, iron, cobalt, manganese, practically are not sorbed. Sulfate, nitrate, chloride, fluoride and phosphate ions are well sorbed and are depressors at this point. In addition, there are anions that can be accumulated in resin and spoil its capacity. In this regard, in the productive solutions concentration of nitrate ions is allowed to appear no more than 0.1 mg/l, chloride and phosphate ions- no more than 0.2 and 0.4 mg/l subsequently. In sulfuric leaching sulfate-ions are accumulated up to 50–100 g/l, which strongly depress ion exchange sorption of uranium.

To prevent accumulation of salts in solutions more than permissible rates and normal performance of ion-exchange extraction of uranium from productive

solutions, partial withdrawal of them from main components to washing with subsequent use of them in technology of leaching. The easiest way of washing sulfuric solutions is lime treatment, in which occurs decreasing of sulfate-ion concentrations up to 5–8 g/l, ions of iron are almost completely precipitated. After the separation of sediment washed out solution is again used for preparation of working solutions.

During in situ leaching process close cooperation between minefield, receiving productive solutions and hydrometallurgical factory is set. If their distance is longer from each other in accordance with right technological and economical imagination, solutions are processed in minefields until having a concentrate or eluate, when the distance is short, saturated with uranium sorbent or productive solution is sent to the factory. The factory, by turn, accordingly is a provider of either containers or sorbent. The last may be profitable only in cases if the mining complex is situated in the same place with hydrometallurgical factory.

The process of uranium sorption from productive solutions by strong basis anionites is described by equalization of ion-exchange and complexation:



Low concentration of uranium in productive solutions ($6 \cdot 10^{-5} - 4.5 \cdot 10^{-4}$ M) specifies the features of the process of their sorptional processing using anion exchangers. Depending on the pH duration of the sorption of uranyl trisulfate ions with anionites of trimethylammonium takes from 100 (pH = 1.85) to 500 (pH = 3.6) minutes. In practice, the duration of ionites' contact with recyclable solutions lasts 6–8 hours.

Indicators of uranium sorption process — depth of extraction, capacity of the anion exchanger — depends upon its content in the processing solution, characteristics of anionites and number of ions in the solution-depressants of sorption such as sulfate, nitrate and chloride ions and ions

of iron and sulfuric acid. In the low area of uranium concentration ($1-2.5$ mg/dm³) coefficients of its duration is much higher than in high areas ($0.1-1.0$ g/dm³) (table 2).

Table 2. – Coefficient of uranium distribution during its sorption with anion exchangers from sulfuric productive solutions with pH = 1.8

Anion exchanger	Concentration of uranium in solutions, mg/m ³				
	1	10	25	100	1000
BD-706	$9.1 \cdot 10^2$	$6.6 \cdot 10^2$	$1.3 \cdot 10^3$	$5 \cdot 10^2$	$6.9 \cdot 10^1$

Acidity growth in productive solutions brings to the worsening of uranium sorption (table 3).

Anion exchangers have clearly expressed abrupt isotherm of sorption (K_{exch}), which provides deep extraction of uranium even from solutions with low concentration. As a rule, in the sorption process very low waste concentration of uranium is achieved and it does not exceed $1-2$ mg/dm³. Uranium dumping concentration in processed productive solutions (bittern) determined by residual capacity of ion exchange resins of uranium, produced in the desorption process.

Table 3. – Dependence of uranium distribution coefficient upon the acidity of solution during its sorption with anion exchangers from sulfuric productive solutions

Anion exchangers	Acidity of solution			
	pH = 1.8	5 g/dm ³ H ₂ SO ₄	10 g/dm ³ H ₂ SO ₄	20 g/dm ³ H ₂ SO ₄
BD-706	Concentration of uranium in the solution 50 mg/dm ³			
	$3.4 \cdot 10^2$	$3.1 \cdot 10^2$	$2.3 \cdot 10^2$	$1.6 \cdot 10^2$
BD-706	Concentration of uranium in the solution 5 mg/dm ³			
	$5.5 \cdot 10^2$	$5.1 \cdot 10^2$	$4.6 \cdot 10^2$	$2.6 \cdot 10^2$

Section 8. Physics

DOI: <http://dx.doi.org/10.20534/AJT-17-1.2-114-117>

Nadareishvili Malkhaz,
Tbilisi State University, Institute of Physics, senior researcher
E-mail: malkhaz.nadareishvili@tsu.ge

Kiziria Evgeni,
Institute of Physics, Leading researcher
E-mail: evgenikiziria@hotmail.com

Sokhadze Viktor,
Institute of Physics, senior researcher
E-mail: vsokhadze@yahoo.com

Tvauri Genadi,
Institute of Physics, Engineer
E-mail: gena_tvauri@yahoo.com

Tsakadze Severian,
Institute of Physics, senior researcher
E-mail: ztsakadze@gmail.com

Differential calorimeter of a new type

*The work was supported of Sh. Rustaveli Foundation
grant № FR/500/6–130/13*

Abstract: Discussed new type differential calorimeter, which uses impulse heating of cells during the scanning across the temperature, instead of continuous, which is commonly used in differential calorimetry. Pulse heating allows combine high speed of warming with measurements in equilibrium conditions, which strongly enhances the sensitivity and accuracy of the measurement of this installation.

Keywords: calorimeter, a differential calorimeter, continuous heating, pulse heating.

Introduction

Calorimetric studies play an important role for solution many problems existing in modern science and technology. These devices of different kinds are widely used in physics, chemistry, biology, materials science, medicine etc. [1–3], including for diagnosing cancer [4]. Modern calorimeters are divided into two basic groups: classical calorimeters, measuring the absolute heat capacity of bodies in the impulsive regime and differential scanning calorimeters (DSC) measuring the heat capacity difference between the research sample and the standard in the continuous heating regime.

The classical calorimeter consists of a single cell with a heater and a thermometer, where a sample is placed. A certain amount of heat ΔQ is supplied to the sample, and

the increase in temperature ΔT is measured. The heat capacity of the sample is calculated by the formula:

$$C = \Delta Q / \Delta T. \quad (1)$$

The differential calorimeter consists of two cells equipped with heaters and a thermometer and connected via thermocouples. In the cells, two samples, reference and analytical, are placed [3].

Equal power is applied to both samples, but they are heated differently because of different heat capacities of the samples. Leveling of heating rates happens with the help of the heat that transfers from one cell to another via the thermocouples and temperature difference δT between them. The difference between heat capacities is calculated by the formula:

$$\Delta C = 2 \Delta P / (\Delta T / \Delta t), \quad (2)$$

where ΔP is the power transferring from the one cell to another and $\Delta T/\Delta t$ is the heating rate of the samples. In the experiment, the heating rate $\Delta T/\Delta t$ is calculated by measuring the temperature and time with the help of a thermometer and a timer, respectively.

From the formula (2), it is evident that, the higher is the heating rate, the more power ΔP transfers from one cell into another. This means that, the smaller is the difference between heat capacities, the higher heating rate must be used to make the measurement of ΔP possible. At the same time, temperature gradients emerge in the sample, and the measurement becomes non-equilibrium, which causes mismatching of the measured and real values. Incompatibility of the high heating rate with the providing the measurement in equilibrium conditions, which does not allow studying many "fine" effects, is main important disadvantage of modern differential calorimeters [5].

It should be noted that DSC are characterized by higher sensitivity to the heat effects and by comparatively shorter time of measurements (that can be regulated by scanning rate) than the classical calorimeters, and they are used more widely [1]. That is why it is very important to eliminate all drawbacks of these calorimeters.

To eliminate the above-mentioned drawback of differential calorimetry, it was elaborated a new method the novelty of which consists in the use of pulse heating mode [6] instead of continuous heating, which is usually used in modern differential calorimeters. The high heating rate is achieved within a short, but powerful, pulse. At the same time the measurement proceeds under equilibrium conditions, because, at the beginning and at the end of the pulse, the samples are under equilibrium conditions.

Results and discussion

Based on the above-described pulse method, the differential calorimeter of a new type, a differential pulsed calorimeter (DPC), was designed. The main part of this calorimeter is differential container (fig.1). It consists of two identical cells (1), in which a sample and a standard (5) are placed. The cells are connected via thermocouples (3) that measure the temperature difference between the cells and, at the same time, provide the required thermal link between them.

Before applying a heat pulse of Δt duration and after a certain time of relaxation $\tau \gg \Delta t$, the sample under study and the standard are in thermal equilibrium and their temperatures are similar. During the entire process of measurement, the differential container is thermally isolated by radiation shields (6), and the process proceeds under adiabatic conditions.

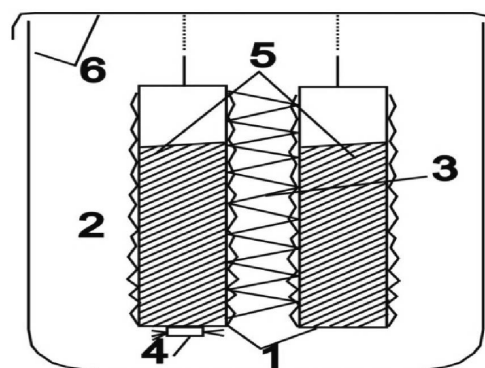


Fig. 1. Container of the differential calorimeter:
1 – Cells; 2 – Heaters; 3 – Thermocouples;
4 – Thermometer; 5 – Samples; 6 – Radiation shields

Measuring the difference between heat capacities, similar heat pulses $Q = IU \Delta t$ are applied to both cells by means of electric heater (2), where I is the current in heaters, U is the voltage at the heater ends, and Δt is the pulse duration, are applied to both cells by means of an electric heater (2). Due to the difference between the heat capacities of the samples, they are heated differently, the difference between the temperatures of cells emerges, and a certain amount of heat ΔQ transfers from one cell to another. Thus, after switching off of the heaters, after a certain time τ , which is called the relaxation time, the cells come into equilibrium again. During the whole process, the difference between the cell temperatures is registered by thermocouples located between the cells. A typical time dependence of emf of the thermocouples has the shape shown in fig. 2. As was shown in work [6], the difference between heat capacities of samples is calculated by the equation:

$$\Delta C = 2 \Delta Q / \Delta T, \quad (3)$$

where ΔT is the increase in the temperature, and ΔQ is the amount of heat transferred from one cell into another, being proportional to the area under the curve in fig. 2 and calculated by integration of this curve over time.

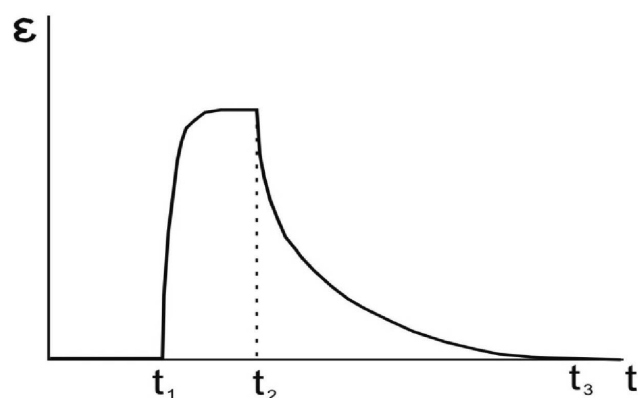


Fig. 2. The dependence of the emf of thermocouples versus time during a warm-impulse

The cryostat of the calorimeter allows measuring the Heat capacity from 1.5 K. For this purpose, it is equipped by a special chamber where liquid helium is pumped off. Liquid helium is supplied into the chamber through a special throttle. Parts of the container are made with high precise, the difference between the weights of the cells is less than a milligram.

The design of the cryostat, in combination with the electronics, provides high level of adiabatic conditions of differential container. This aspect is very important because the difference of heat flows to the cells should be less than the sensitivity of calorimeter (otherwise it will not be possible to use the maximum sensitivity). To solve this problem, some special technological and methodological measures were taken: to decrease the heat flows in the conducting wires, sapphire contacts will be used, which, at present, are considered as the best removals of heat flows from wires, to decrease the transfer of heat by conductors to the cells, the thinnest (0.03 mm. in diameter) golden wires with tungsten core was used, that are characterised by a good breaking strength at small diameters, by a rather poor heat conductivity and rather good electric conductivity. A special scheme of connection of wires with cells was used providing maximum similar values of heat flows, etc. To protect the cells against heat radiation, the gold-plating of cells and basic parts will be made. The design of cryostat provides the cooling of samples to the working temperature under the high-vacuum condition, this provides by using the special distribution of turn-off systems of thermal links. For the differential container the main problem is the providing of the maximum precision of temperature difference measurements between cells and very small thermal conductivity of the thermocouples defining the sensitivity and precision of the calorimeter. For this aim our original technology of production of thermocouples from a great number (~400 pcs) of thermoelectric couple for differential container was used. One should emphasize that the thermocouples are the most important element of the device and such a great number of thermoelectric couple in it provides a high sensitivity of the calorimeter. Most the work associated with the cryostat is performed under the microscope.

As for the electronics, first of all, the proportional-integral-differential amplifiers were created, which were assembled on the modern microcircuits and provide such

regulations of heat screen temperatures that heat flows in the cells are very small. In the measuring part of electronics the elements of high accuracy were used to provide a small error in measurements. The program of automatic control of calorimeter controls the experiments and the measuring units, creates the database and displays the obtained graphical results on the monitor.

The sensitivity of the pulsed differential calorimeter at low temperatures is 10⁻⁸ W/div. (1 div = 0.01 μV) and the precision $\delta C/C$ is 10⁻⁴, where δC is the error of measurement of ΔC , and C is the absolute heat capacity of sample.

The device is multifunctional and wide-range, it could be used for precision studies of solid state, liquids, and powders in the wide range of temperatures (1.5 k – 400 k).

The calorimeter is able to operate in two modes of heating: in the pulse and continuous, similar to the usual DSC. Such combination of modes makes it possible when it is necessary and it is not required a high precision or at carrying out the search experiments to carry out fast measurements in the continuous mode, to establish curves of heat capacity dependence on temperature, which frequently differs from real curves, according to our experience, but in difference with usual DSC, in our case they could be corrected using exact values of heat capacities obtained at several temperatures in pulsed mode.

Simultaneously with ΔC , the absolute heat capacities of studied and reference samples C_1 and C_2 , respectively, can be measured with the same accuracy as in the case of calorimeter measures absolute heat capacity of sample. The new calorimeter created by us is very effective also in case of measurement of heat capacity of a small sample (several milligrams of mass) in the equilibrium conditions. In this case, the investigated sample should be placed in one cell, and other cell remains empty. The difference of heat capacities between cells, measured in pulsed mode, would present the absolute heat capacity of sample.

Conclusion

Based on the pulse method developed by us for differential calorimetry, the differential calorimeter of a new type was designed. The calorimeter is highly sensitive and accurate over a wide temperature range, and shows high possibilities of pulse heating in differential calorimetry.

Acknowledgments

The authors express their gratitude to Prof. J. Monaselidze for very useful discussions.

References:

1. Kondepudi D. Introduction to Modern Thermodynamics. Wiley, Chichester, 2008. ISBN 978-0-470-01598-8.
2. Monaselidze J., Majagaladze G., Barbakadze Sh., Khachidze D., Gorgoshidze M., Kalandadze Y. Microcalorimetric investigation of DNA, poly (Da), poly (Dt) and poly [D (a-C)]poly [D (G-T)] melting in the presence

-
- of water soluble (Meso Tetra (4-N-Oxiethylpytidyl)pophirin) and its Zn complex//Journal of Biomolecular Structure and Dynamics. – 2008. – vol. 25. – P. 419–425.
3. Pooria Jill et al. Differential Scanning Calorimetry Techniques: Applications in Biology and Nanosciences// J. Biomol. Tech. – 2010. – vol. 21. – P. 4.
 4. Nemsadze G., Leshava T., Gorgoshidze M., Kiladze M., Gogelia N., Khachidze D., Lomidze E., Monaselidze J. Blood plasma main proteins stability of patients with ductal carcinoma in post surgery period//Int. J. Clin. Exp. Med. – 2016. – № 9 (2). – P. 1338–1345.
 5. Nadareishvili M., Kiziria E., Sokhadze V., Tvauri G. The problem of High Heating Rate in Differential Calorimetry. 13th European Conference on Innovations in Technical and Natural Sciences, Abstracts. – Vein, 2017.
 6. Nadareishvili M., Kiziria E., Sokhadze V., Tvauri G., Tsakadze S. New Method of Differential Calorimetry// European Science Review. – 2017. – №1–2.

Section 9. Chemistry

DOI: <http://dx.doi.org/10.20534/AJT-17-1.2-118-120>

*Abdurakhmanov Ergashboy,
Dr., assistant Professor Faculty of Chemistry,
Samarkand State University of Uzbekistan*

*Abdurakhmonov Gulomjon,
Assoc. Chemistry Department,
Samarkand State University of Uzbekistan
E-mail: abdugulom-81@mail.ru*

Technological scheme and regulation of production of fire retardant on the base of ammophos and ammonia

The work is supported by Fundamental Grant No. "F-7-06" from the Scientific Council of the Republic of Uzbekistan.

Abstract: The technological aspects of production of fire retardant structures on the base of central Kyzyl-Kum phosphorite are investigated. The optimal conditions to extract the fire retardant structures from the phosphorite ore are choosed.

Keywords: Fire retardant, phosphorite ore, technology, filtering, sedimentation, fire protection, physical-chemical properties.

The fire hazard of most distributed sewing materials calls for investigations those's ignition laws. And on the base of the laws creating a new generation of the fire protection instruments namely a fire retardants is today's topical scientific problem [1; 2].

To decrease the combustion hazard of the sewing materials an inorganic and organic bondings with various structures as a fire relievers that is the fire retardants are used. For the goal a few investigations were performed at Samarkand State University [3-5]. Here ammophos, ammonium nitrate, ammonium sulphate and other types of chemical materials produced in the cities of Uzbekistan as Samarkand, Almalik, Navoi, Chirchik were used.

Tests made on the structures of the fire protection materials obtained on the base of those chemical substances by handling with them the woody materials, the cotton during transportation and storing, the sewing materials which used by covering the cotton fibre clews gave efficient results. Therefore engineering of a technological scheme of the fire retardant production and its regulation on the base of the ammophos and the ammonia setted up as the topical task.

In present work the production technology of the fire retardant is proposed. It includes following steps:

- preparation of ammophos water solution;
- neutralization of the ammophos solution by ammonia;
- cleaning the solution from mechanical impurities by sedimentation.

Fig. 1 shows the principal technological production scheme of the liquid fire retardant. Here the ammophos mixed with water is delivered through admixer (1) to neutralizator reactor (2) and the ammonia is added to it by bubbler flask (3). Then the solution is mixed intensively by the admixer (4). Since the process finished the liquid bulk in the neutralizator (2) is filled into vertical type periodical sedimentator (5). At the end of the process the liquid phase is extracted and the product is stored in storage device (6). The leakless bulk in the bottom of the sedimentator (5) is carried then with water into horizontal type sectional sedimentator (7) and extraction process of the solid phase here takes place. After heating in (9) the sewage is delivered through water pump (8) to the top of the process (1) in order to mix it again with ammophos.

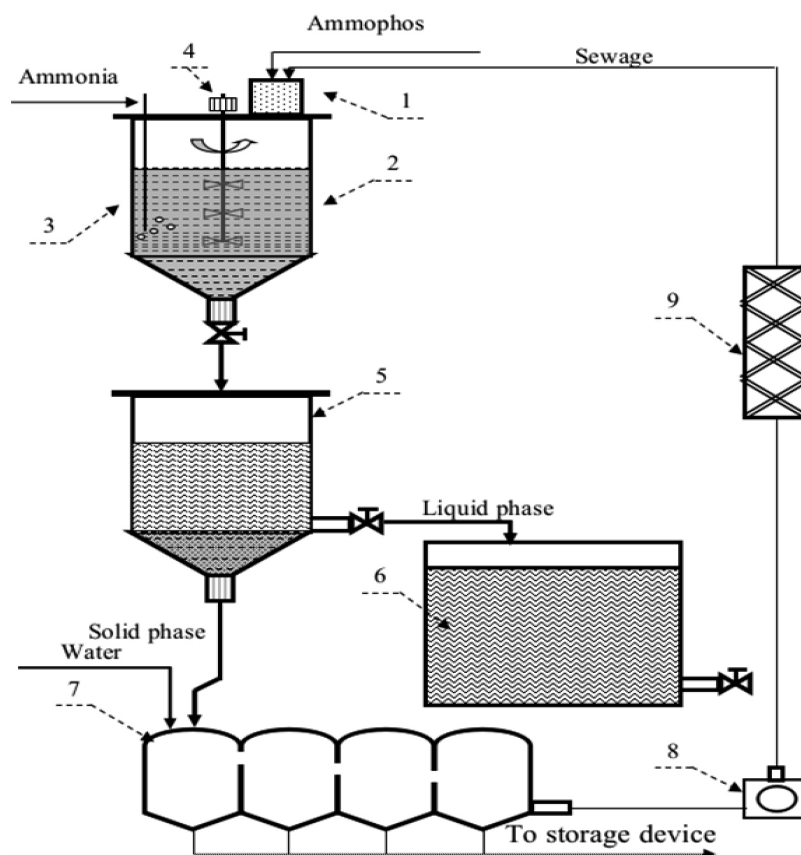


Fig. 1. The principle technological scheme of the ammophos based fire retardant production: 1 – mixer; 2 – neutralizer reactor; 3 – bubbler flask; 4 – admixer; 5 – sedimentator; 6 – storage device; 7 – horizontal type sectional sedimentator; 8 – water pump; 9 – heater

For production the fire retardant structure following technological regulation is recommended:

- the temperature region for the ammophos's melting in water should be $40 \div 60$ °C;
- the ammonation temperature should not be above than 60 °C;
- pH value should be in $7 \div 8$ region;
- holding time of the reaction bulk inside the reactor should be not less than 60 minutes;
- the mixing velocity should be 100 cycle/min;
- holding time in the sedimentator should be not less than 60 minutes.

Ready to use fire retardant should have following characteristics:

- the ammonia amount is not less than 4.5 %;
- the amount of P_2O_5 is in 12 ± 0.5 % region;
- pH value is $7 \div 8$ region;
- the density is 1.17 kg/litre.

In experiments the scheme of work material flow (fig. 2) and balance (tab. 1) for production of the fire retardant structure on the base of the ammophos and the ammonia are performed.

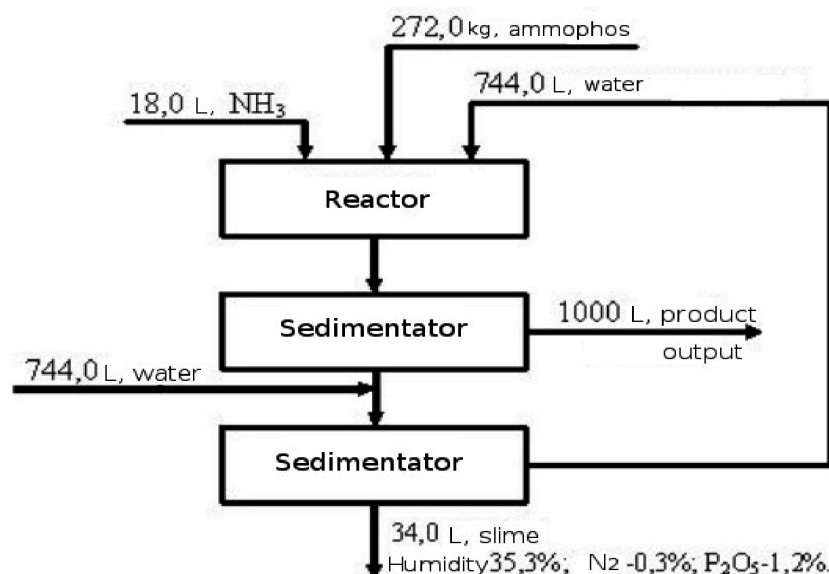
Thus on the base of various inorganic bonds (as ammophos, ammonium nitrate, ammonium sulphate,

ammonia, calcinated soda) it is proposed the method to product of the fire retardant structures. The optimal structures of the fire retardant preparation extracted from Central Kyzylkum phosphorites were chosen. It was improved their physical-chemical properties by using chemical and physical methods. The fire protection efficiency of the fire retardant structures obtained has been found.

It is proposed the method of neutralization by ammonia, the method of sand filtering cleaning and the improving method of the ammophos solution structure by sedimentation. The optimal parameters of cleaning of the liquid ammophos solution from the solid mechanical impurities are found.

Those parameters that allows to automatize the production of the fire retardant structures the physical-chemical and rheological properties such as the density, the viscosity, the pressure of saturated vapor as well as the conductivity that should be known by storing of the liquid products and their application are studied.

For production of the fire retardant preparation the principle technological schema and raw material balance are produced and proposed to production widely.



Fif. 2. The scheme of work material flow for production of the fire retardant structure

Table 1. – The balance of work material for production of the fire retardant structure on the base of ammophos and ammonia

Nº	Components (input)	Material amount	Nº	Product	Material amount, L.
1	Ammophos	272.0 kg.	1	Liquid fire retardant	1000.0
2	Water	744.0 L.	2	Slime	34.0
3	Ammonia	18.0 L.			
Summary		1034.0	Summary		1034.0

References:

1. Yerokhev K. ontemporary fire protection for building constructions and textile fabrics//Building materials. – 2002. – No. 6. – P. 14.
2. Modern city – the safe city//Journal “My Moscow”. – 2006. – No. 3. – P. 18–22.
3. Abdurakhmonov E., Tillaev S., Abdurakhmonov G., Sattarova M. Study of laws of fire spreading speed in textile materials//Scientific bulletin of Samarkand State University. – 2013. – No. 5. – P. 91–96.
4. Abdurakhmonov E., Tillaev S., Abdurakhmonov G. The burn process mechanism of cellulose materials treated by fire retardant//Journal “Bulletin of NUUz”. – Tashkent, 2015. – No. 3/1. – P. 261–265.
5. Abdurakhmonov E., Tillaev S., Ziyadullaev A., Abdurakhmonov G. Investigation of burn process mechanisms of textile materials treated by fire retardant by thermal analysis method//Journal of “Chemistry and chemical technologies”. – Tashkent, 2016. – No. 1. – P. 261–265.

DOI: <http://dx.doi.org/10.20534/AJT-17-1.2-121-123>

Aronbaev Dmitry,
Samarkand State University,
PhD, Associate Professor, Department of Chemistry
E-mail: diron51@mail.ru

Vasina Svetlana,
Samarkand State University,
PhD, Associate Professor, Department of Chemistry
E-mail: vasinas2003@mail.ru

Aronbaev Sergey,
Samarkand State University,
Doctor of Chemistry, Head of the Laboratory
«Ecological Systems and Devices»
E-mail: diron51@mail.ru

Interaction cells of brewing yeasts with ferro fluid

Abstract: Transmission electron microscopy studied the nature of the interaction of *Saccharomyces cerevisiae* yeast cells with magnetic fluids. It was shown that the modification of brewing yeast *Saccharomyces cerevisiae* based ferrofluid magnetite nanoparticles is an active process, which should be done with the cultured cells are in the exponential growth phase.

Keywords: *Saccharomyces cerevisiae*, yeast cells, the magnetic fluid, transmission electron microscopy, incubating, nanoparticles of magnetite, endocytosis.

Introduction

The use of magnet materials opens new possibilities of sorption technologies to extract toxicants from water [1–3]. Giving sorbents magnetic properties is carried out by treating the alleged sorption materials magnetic fluids (MF) on the basis of magnetite [4]. In recent years, in the world are increasingly began to be used for remediation of wastewater and surface water bio-sorptional technologies based on the use of living or dead organisms of different taxonomic groups, in particular yeast cells *Saccharomyces cerevisiae*, constitute an almost inexhaustible resource for learning based on these cheap sorbents.

In our previous papers were shown sorption analytical properties of yeast cell walls and the possibility of using biosorbents on their basis [5]. Joint immobilization RACs and magnetite in Ca-alginate gel led to the creation of a promising new smart material wider engineering and technology and environmental purpose [6; 7]. In this regard, the study of the interaction of the microorganism with ferromagnetic fluids is of particular relevance.

We note that the study of the interaction of living cells with nanomaterials in general is of great interest, since the evaluation of such interactions can be used to identify the toxic properties of nanomaterials and directional change

cell properties, visualization of cellular organelles, highly accurate identification of micro-organisms and the use of cells as three-dimensional templates [8].

The purpose of this paper is to examine the nature of the interaction of cells brewing yeast *Saccharomyces cerevisiae* with the components of magnetic fluids on the basis of the synthesized magnetite.

Materials and methods

We used yeast *Saccharomyces CEREVISIAE* strain W37, which are in the growth phase and after heat treatment in boiling water for 20 minutes. For this purpose, 2 g. of yeast sample was suspended in 10 ml. of 0.1 M. acetate buffer at pH 5.2. Then precipitate was separated from the liquid phase on Centrifuge at 3000 rev/min for 15 min.

The resulting yeast biomass was incubated for 2 hours with a magnetic fluid based on a synthetic magnetite stabilized by perchloric acid. Magnetite was obtained by [9; 10]. The concentration of magnetite nanoparticles in magnetic fluid sample was determined by a colorimetric method using photocolormeter KFK-3 [11].

Procedure for obtaining magnetically responsive yeast cells was as follows:

3 ml. of the yeast suspension was mixed with 1 ml. of ferrofluid and incubated at 30°C during 2 hours with

stirring. Thus, most of the yeast cells got properties as magnetically responsive. Magnetic and nonmagnetic yeast cells were separated by using permanent magnet. The residual magnetic fluid is also removed by using multiple washing of acetate buffer solution to obtain a clear supernatant.

In a similar manner it was carried out magnetic modification dead yeast cells obtained by heat treatment of yeast.

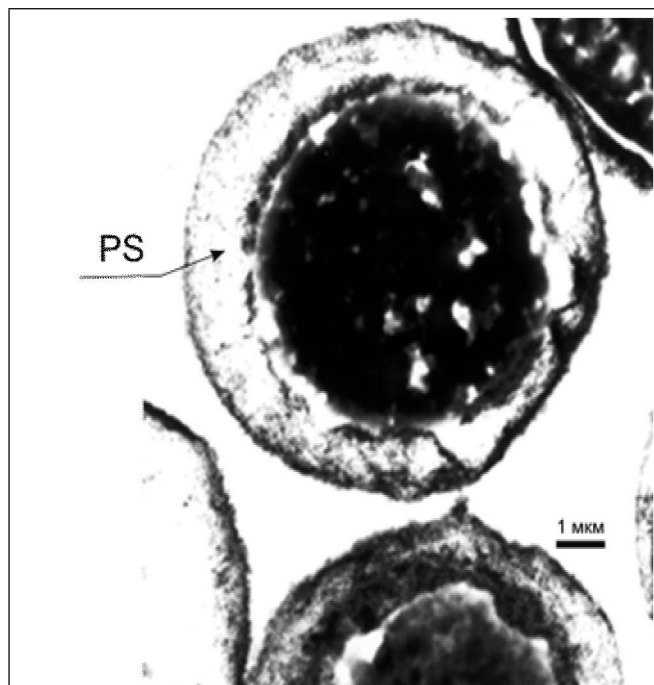


Fig. 1. TEM pictures of yeast-cells is incubated with magnetic nanoparticles of magnetite. Note the presence of magnetic nanoparticles inside of cell and in the periplasmic space PS (arrow)

On the fig. 1 shows the micrograph obtained by TEM. Images showed small amount of magnetic nanoparticles on the surface of the yeast cell wall and much larger number of cells in the inner space. Here also shows that the nanosized particles of magnetite is located between the cell wall and the plasma membrane, i. e. in periplasmic space PS (Periplasmic Space).

On the fig. 2 shows microphotographs of a magnetic modification dead yeast cells yeast cells subjected to heat treatment. Here there is a greater accumulation of nanoparticles on the surface of the CWY (Cell Wall of Yeast), and not in the periplasmic space and inside the cells.

It should be noted that the magnetic nanoparticles were able to cross the cell wall, but not the cell membrane. But we know that it is the cell membrane, instead of yeast cell wall may be responsible for the selective sorption of toxicants.

This means that the procedure of physical effects on cells, for example, heating, and the procedure of

The resulting samples of the modified yeast cells were washed, fixed and prepared for transmission electron microscopy (TEM) [12]. Images were captured on a microscope Jeol 1200 EX (Japan) at an accelerating voltage of 80 kV.

Results and discussion

Transmission electron microscopy is one of the main tools used to study the interaction between nanoparticles and living cells.

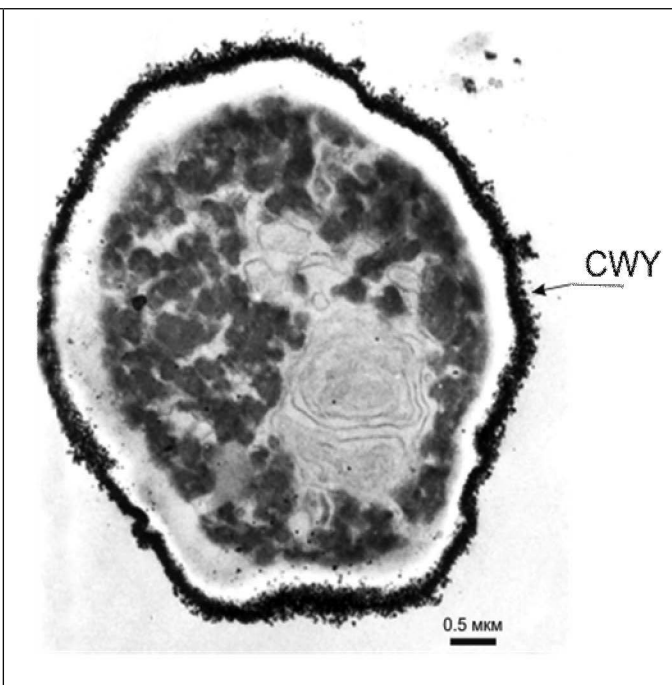


Fig. 2. TEM pictures of a magnetic modification dead yeast cells subjected to heat treatment. Note that magnetic nanoparticles are outside the cells instead of in the periplasmic space (PS)

magnetic updating has more importance in terms of adsorption capacity of cells.

We have also studied the effect of phase yeast cell growth on its ability to be magnetically responsive.

For this experiment was performed incubation the normal yeast biomass with a magnetic fluid and incubation with magnetic fluid cultured yeast in the growth phase.

Transmission electron microscopy shown that in the latter case, i. e. when incubated with ferrofluid cultured yeast cells in the growth phase, magnetite nanoparticles incomparably greater than that for normal yeast cells.

This is due to the fact that for cultured cells of yeasts in exponential growth phase, an acceleration of cellular functions, and hence the ability endocytosis — capture magnetite nanoparticles by incubating such cells with ferrofluid [13]. This, in turn, shows that the process of internalization of nanoparticles is active and not passive phenomenon. The same conclusion were made by researchers [8].

Conclusions

As a result of the research, we came to the following conclusions:

1. Modifying of yeast *Saccharomyces cerevisiae* with ferrofluid based on magnetite nanoparticles is an

active process, which should be carried out with the cultured cells are in the exponential growth phase.

2. We offer magneto-modified yeasts, as a promising bio-sorptional smart material for engineering and environmental applications.

References:

1. Ebner A. D., Ritter J. A., Ploehn H. J., Kochen R. L., Navratil J. D. New magnetic field-enhanced process for the treatment of aqueous wastes//*Separ. Sci. Technol.* – 1999. – Vol. 34. – P. 1277–1300.
2. Kurinobu S., Uesugi J., Utumi Y., Kasahara H. Performance of HGMS filter and recycling of magnetic seeding material on magnetic seeding method//*IEEE Trans. Magn.* – 1999. – Vol. 35. – P. 4067–4069.
3. Safarik I., Safarikova M. Use of magnetic techniques for the isolation of cells//*J. Chromatogr.* – 1999. B. – Vol. 722. – P. 33–53.
4. Robinson T., McMullan G., Marchant R., Nigam P. Remediation of dyes in textile effluent: A critical review on current treatment technologies with a proposed alternative//*Bioresource Technology* – 2001. – Vol. 77. – P. 247–255.
5. Aronbaev S. D. Biosorbciya ekotoksikantov saharomicetami. Primenenie v analize (Monografiya)/LAP. Lambert Academic Publishing/Deutchland. – 2016. – 224 p.
6. Aronbaev S. D., Nasimov A. M., Aronbaev D. M. Magnitoupravlyaemye smart-biosorbenty na osnove kletochnyh stenok pivovarenyh drozhzhey i nanostrukturirovannogo magnetita//*Vestnik NUU.* – 2016. – № 3/2. – S. 242–244.
7. Aronbaev S. D., Nasimov A. M., Aronbaev D. M. Potential of biosorptional technologies//*WORLD SCIENCE “New Opportunities in the World Science”* – 2015. – № 1 (August 22–23, 2015, Abu-Dhabi, UAE). – P. 22–26.
8. Azevedo R. B., Silva L. P., Lemos A. P. C., Báo S. N., Lacava Z. G. M., Safarik I., Safarikova M., Morais P. C. Morphological study of *Saccharomyces cerevisiae* cells treated with magnetic fluid//*IEEE Trans. on Magn.* – 2003. – Vol. 39, № 5. – P. 2660–2662.
9. Aronbaev D. M., Aronbaev S. D., Nasimov A. M., Vasina S. M., Ergashev I. M., Nasimov H. M., Ali-Ahunov A. Sintez i issledovanie superparamagnitnyh svoystv nanochastic magnetita i magnitnyh zhidkostey na ih osnove//*Nauchnyy Vestnik SamGU.* – 2013. – № 5. – S. 97–101.
10. Massart R. Preparation of aqueous magnetic liquids in alkaline and acidic media//*IEEE Trans. Magn.* – 1981. – Vol. MAG-17. – P. 1247–1248.
11. Kiwada H., Sato J., Yamada S. Feasibility of magnetic liposomes as a targeting device for drugs//*Chem. Pharm. Bull.* – 1986. – Vol. 34. – P. 4253–4258.
12. Zamaleeva A. I., Alimova F. K., Ishmuhametova D. G., Fahrulina R. F. Mikroskopicheskie metody dlya harakteristiki nano-modificirovannyh kletok mikromicetov//*Uchenye zapiski Kazanskogo gosudarstvennogo universiteta. Estestvennyye nauki.* – 2010. – t. 152. – S. 110–120.
13. Aronbaev D. M., Ismailov Z. F., Nasimov A. M., Aronbaev S. D., Kabulov B. D. Eta tonkaya gran mezhdu «nano» i «bio»//*Nauchnyy Vestnik SamGU.* – 2014. – № 5. – S. 110–123.

Makhmudova Feruza Akhmadjanova,
The senior scientific researcher,
Tashkent chemical-technological institute
E-mail: feruza_ahmadjonovna@mail.ru

Maksumova Oytura Sitdikovna,
The Doctor of Chemistry sciences, professor
E-mail: omaksumovas@mail.ru

Synthesis on a basis olefines

Abstract: possibility of obtaining unsaturated monatomic alcohols by the condensation reaction of olefines with formaldehyde in the presence of catalysts is shown. Kinetic regularity of reaction interacting of olefines with formaldehyde from the relationship of initial reagents, the nature of catalyst and temperature are studied.

Keywords: olefins, unsaturated alcohols, the catalyst, condensation, solvent, formaldehyde.

Liquid olefines are important inter-mediats in organic synthesis. As chemical raw materials, they draw attention of researchers in the respect that at the synthesis on their basis, reactions can undergo at atmospheric pressure in milder conditions. Liquid olefines enter into various reactions which compounds of other classes, including unsaturated alcohols are formed. Unsaturated alcohols can be used in various spheres of national economy. In chemical, food and other industries for allocation of firm suspended matters, for the separation of synthetic organic ion exchangers, for clearing of industrial flow and intermediate products in organic synthesis etc [1, 10].

Unsaturated alcohols can be synthesized in the various ways [2, 3]. Among them Prins reaction, which is understood as interaction of olefines with aldehydes in the presence of catalysts, is a convenient method. However, in Prins reactions depending on the nature of olefine and aldehyde, from reaction conditions, and also on the character of the catalyst and dissolvent it is possible

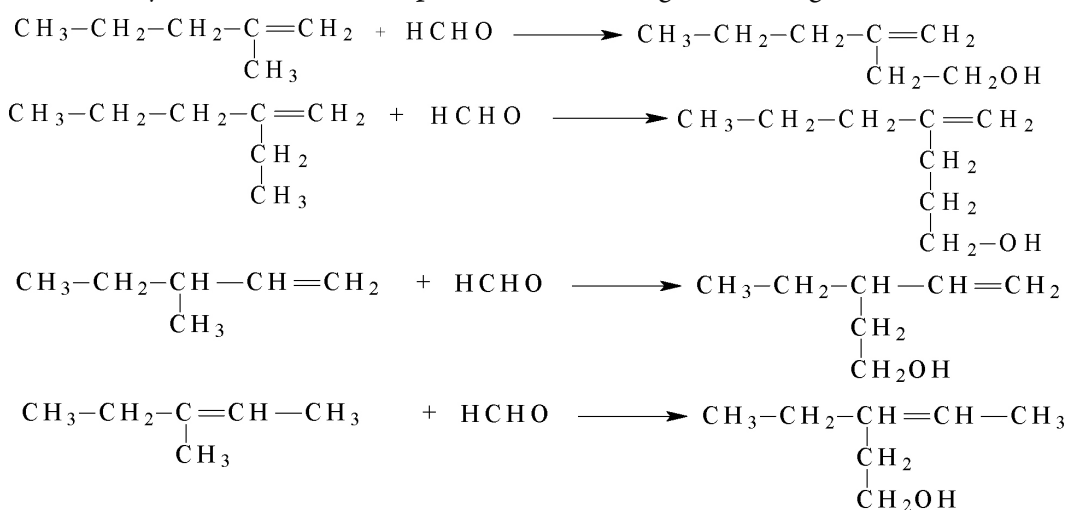
to obtain organic compounds of different classes, including unsaturated alcohols. The analysis of this data shows the possibility of two regimes of process with anhydrous formaldehyde:

1) at 20–100 °C in the presence of catalysts and dis-solvents;

2) thermal condensation at 150–240 °C, 5–10 atm. pressure. For our researches the first regime as in the laboratory environment it is technologically more preferable chosen.

The purpose of the present work is the synthesis of unsaturated alcohols by the condensation reaction tertiary isomers of hexene with formaldehyde.

During the undergone reactions by interacting of tertiary olefines: 2-methyl-1-pentene, 2-ethyl-1-pentene, 3-methyl-1-pentene, 3-methyl-2-pentene with formaldehyde at rather low temperatures in the presence of the catalysts have been detected unsaturated alcohols under following circuit designs:



For the purpose of detection of optimum conditions of process, the influence of the nature of dissolvent, the catalyst, olefine, and temperatures on the reaction product yield is investigated. In the capacity of dissolvent are chosen dioxane-1,4 and diethyl ether, the catalyst of halogenide metals: $ZnCl_2$, $CuCl_2$.

A series of experiments have been carried out and solvent has been chosen for the condensation reaction of olefines with formaldehyde (tab. 1).

Table 1. – Influence of the nature of solvents on the yield of obtained alcohol; $T = 80^\circ C$

Compound	Names of solvents	The yield of alcohol, %
2-methyl-1-pentene	Dioxane	63.0
	Diethyl ether	82.6
2-ethyl-1-pentene	Dioxane	52.0
	Diethyl ether	72.5
3-methyl-1-pentene	Dioxane	48.7
	Diethyl ether	65.3
3-methyl-2-pentene	Dioxane	36.0
	Diethyl ether	54.8

It is found out that is smooth also good exits condensation chosen olefines with formaldehyde proceeds at presence of diethyl ether. Comparison of relative activity of the specified catalysts is carried out in condensation reactions on an example of 2-methyl-1-pentene at $60\text{--}80^\circ C$ in diethyl ether.

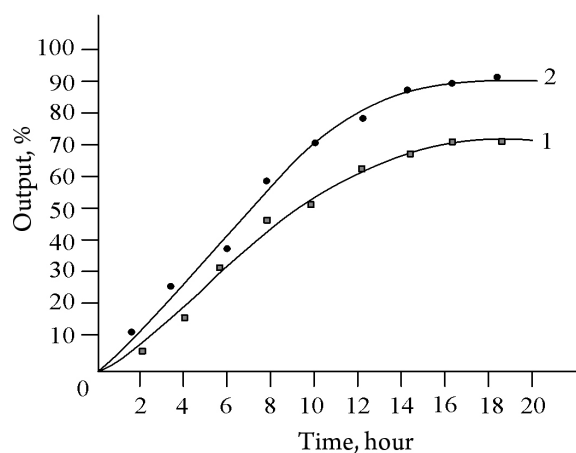
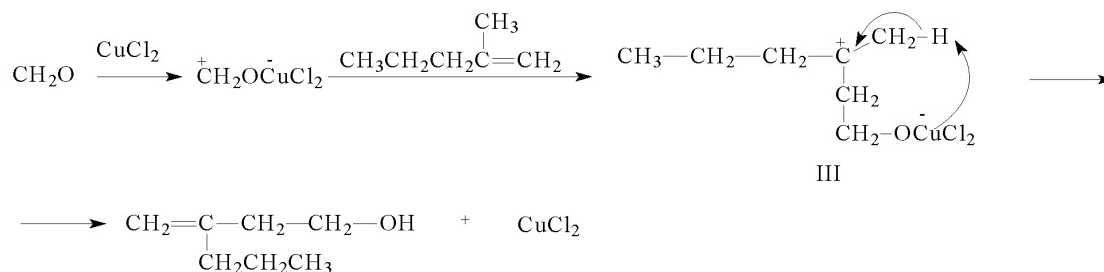


Fig. 1. Relative activity of catalysts at the condensation of 2-methyl-1-pentene. $T = 80^\circ C$, $[K] = 0.25$ mole/l: 1 – $ZnCl_2$; 2 – $CuCl_2$



The gained results show that $CuCl_2$ manifests the best catalytic activity (fig. 1). These results allow to have catalysts for the given reaction in the following row of relative activity: $CuCl_2 > ZnCl_2$.

The influence of a molar relationship of olefine, formaldehyde and catalyst is studied. At equimole relationship of olefine, formaldehyde and catalyst is equal to 1 : 1 : 0.25 within 14–18 hours the yield of appropriate unsaturated alcohols made only 20–30%. Intensive formation of coproducts has been observed. With increase in the molar relation of olefine to formaldehyde the maintenance of alcohols in reaction particles increased. At quintuple excess of olefine the quantity of coproducts decreased and an yield of unsaturated alcohols formed within 70–85%.

Study of the influence of temperature on the obtaining process of unsaturated alcohols shows that alongside with increase in reaction temperature of condensation the alcohol yield increases. At the temperature of $80^\circ C$ the yield of alcohol attains to 82%, the further increase in temperature does not promote increase in the yield of alcohol.

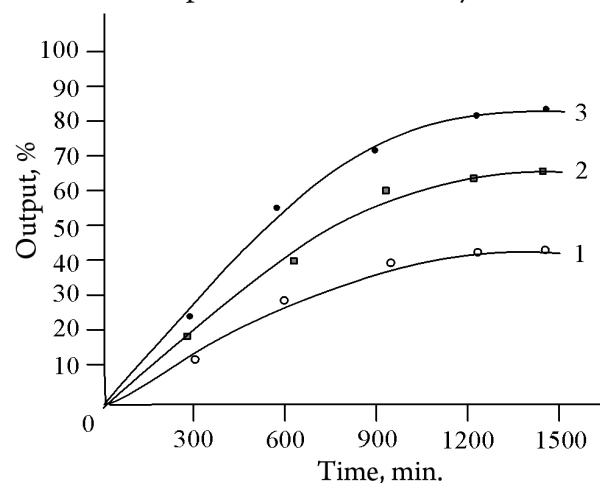


Fig. 2. Dependence of an yield of alcohol on the base of 2-methyl pentene-1 on the reaction temperature, $^\circ C$: 1 – 60; 2 – 70; 3 – 80

On the basis of the gained results and the literary data the codensation reaction mechanism of 2-methyl pentene-1 with formaldehyde in the presence of $CuCl_2$ it is possible to present as follows: in the presence of Lewis acids the intermediate compound III, stabilized as a result of detachment of Lewis acid and proton transfer, is formed:

Structure of the synthesized alcohol identified IR-spectral analysis. In IR-spectrum of the obtained unsaturated alcohol on the base of 2-methyl-1-pentene with formaldehyde new absorption bands of valence oscillation of C-O bond in the field of 1031–1170 cm^{-1} ; valence oscillation of olefinic bond C=C are manifested in the field of 1605 cm^{-1} ; absorption bands CH_3 , CH_2 groups at 2661–2731 cm^{-1} and a wide absorption band ν_{OH} carbonyl groups in the field of 2900–2958 cm^{-1} .

Thus, condensation process of 2-methyl-1-pentene, 2-ethyl-1-pentene, 3-methyl-1-pentene, 3-methyl-2-pentene, heptene-1 with formaldehyde is studied. Optimum conditions of obtaining monatomic unsaturated alcohols are determined. Influence of the nature and concentration of the catalyst, temperature and dissolvent on the product yield is investigated.

In the capacity of subjects of investigation there have been chosen tertiary olefines 2-methyl-1-pentene, 2-ethyl-1-pentene, 3-methyl-1-pentene, 3-methyl-2-pentene that have been separated by the method of fractionation from hexine fractions of the Shurtan gas-chemical complex, formaldehyde, sulphuric acid.

In the capacity of dissolvent there have been chosen dioxane and diethyl ether, the catalyst of halogenide metals: ZnCl_2 , CuCl_2 .

IR-spectrums of the synthesized alcohols and their initial reagents have been removed on IK- Fourier spectrophotometer SISTEM-200.

Purity of the synthesized compounds has been controlled thin-layer chromatography on plates Silufol: eluent -benzol-acetone.

References:

1. Касимова К. А., Шарф В. З., Литвин Е. Ф. Алкилбензол-сульфокислоты – эффективные катализаторы кислотно-катализируемого взаимодействия олефинов с формальдегидом (реакция Принса)//Тез. докл. УП Всесоюзной конференции: «ПАВ и сырьё для их производства. Химия и технология ПАВ», 1988. – С. 10.
2. Шеманаева М. Н., Мельник Л. В., Крюков С. И., Москвичев Ю. А., Среднев С. С., Суровцев А. А., Карпов О. П. Способ получения кислородсодержащих органических соединений – смеси кетонов и непредельных спиртов и возможно альдегидов. Патент РФ № 2174113. Дата публикации 27.09.2001.
3. Астахова А. С., Хидекель М. Ф. Способ получения непредельных спиртов. Авторское свидетельство № 232966, 1969.

DOI: <http://dx.doi.org/10.20534/AJT-17-1.2-126-129>

Mirkhamitova Dilorom,
candidate of chemical science, dotsent
E-mail: dmirkhamitova@mail.ru

Nurmanov Suvonkul,
doctor of technical sciences, chair of department

Halimova Oygul, magister
National University of Uzbekistan, Tashkent

Investigation of catalytical reaction of acetylene with morpholine

Abstract: Method of N-vinylmorpholine synthesis by vinylation of morpholine was elaborated in homogeneous and heterogeneous conditions and also in the presence of nanostructural catalysts on the base of activated coal and potassium hydroxide.

Keywords: morpholin, heterogeneous catalyse, nanostructural catalysers, vinylation, kinetics of this process, energy of activation.

In last years a great progress has been achieved in obtain and investigation of properties of modified nanostructural heterogeneous catalysts for vinylation of organical compounds having in their composition an active atoms of hydrogen [1].

It is known that vinyl compounds are used in different braches of industry and agriculture and ther are synthesized by different methods, among which by importance and actuality is vinylation of corresponding organical compounds by action on them by acetylene [2–4].

From above-mentioned reaction of vinylation of morpholine in the presence of KOH with using super base systems such as KOH-DMSO and KOH-DMF

(DMSO-dimethylsulfoxide; DMF-dimethylformamide) has been investigated and it was determined that reaction is carried out according to following scheme:



At this influence of solvent nature on carrying out of this reaction was investigated. Experimental results have shown that in absence of dipolar aprotonical solvents vinylmorpholine also has been obtained but in small quantities (before 2.0 %). In solution of DMF at 70 °C and duration 4 h. aproduct was obtained with yield 8–10 %. At substitution of DMF and DMSO the yield of forming N-vinylmorpholine has increased in high degree (at the same conditions as at using DMF the maximal yield of product was equaled 22 %). In all cases yield of N-vinylmorpholine has been increased with increasing of reaction duration (1–4 h.).

Influence of quantity of catalyst on vinylation was investigated by chanding it's quantity in reaction system from 10 to 20 % from mass of morpholine in the presence of solvent — DMSO. Obtained results have shown that quantity of catalyst has influenced on the yield of forming N-vinylmorpholine with increasing of it's contant in interval 10–15 % yield of product also was increased. The following increasing of catalyst quantity negatively influenced on formation of N-vinylmorpholine what canbe explained by following fact — at content of KOH in system more 15 % quantity of oligomers or polymers has increasing of resinous compounds during reaction of vinylation. Correspondenly it is possible to conclude, that optimal contance of catalyst (KOH) for vinylation of morpholine by acetylene is 15 mass. %.

Also it was investigated influence of nature of using catalysts hydroxides LiOH, NaOH and KOH (in solid state) on the vinylation of morpholine. It was determined that in all cases N-vinylmorpholine was formed but KOH was the most active catalyst — in it's presence yield of N-vinylmorpholine was equaled 23.0 % (in the presence of LiOH or NaOH yield of product was equaled 16.6 and 19.4 % correspondenly).

Kinetics of vinylation of morpholine with acetylene at atmospheric presence in the presence of system KOH-DMSO and different temperatures and durations of reaction carrying out has been investigated. On the base of obtained kinetical data the graph in coordinates lgW-1/T has been constructed (fig. 1) and also value of the activation energy (E) of vinylation of morpholine has been calculated which was equaled 55.6 kDj/mole.

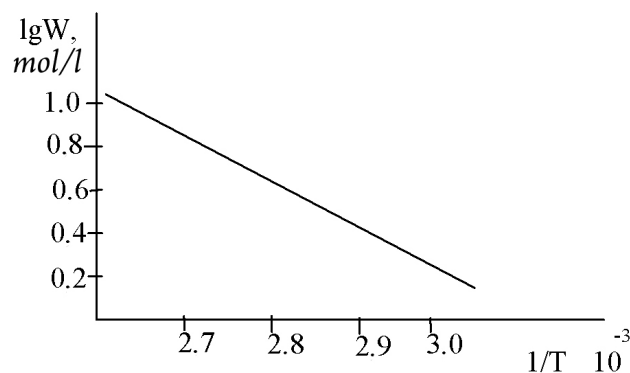


Fig. 1. Dependence of lgW from 1/T for reaction of morpholine vinylation

Also heterogeneous — catalytical vinylation of morpholine in running reactor in the presence of heterogeneous catalyst (KOH) beared on granulated activated coal (30 % from mass of bearer) has been carried out. It was determined that in these conditions also N-vinylmorpholine was formed.

For optimization of conditions of morpholine vinylation influence of temperature on it's carrying out in heterogeneous system that is on yield of the forming at this N-vinylmorpholine has been investigated. Obtained results are presented in table 1.

Table 1. – Effect of temperature on vinylation of morpholine

№	Temperature, °C	Yield of N-vinylmorpholine, %	№	Temperature, °C	Yield of N-vinylmorpholine, %
1	65–70	–	6	210–215	23.2
2	100–105	10.6	7	225–230	25.0
3	120–125	18.4	8	250–255	31.7
4	140–160	19.8	9	280–285	19.0
5	180–190	21.5	10	290–300	12.0

Obtained results have shown that with increasing of temperature in interval 100–255 °C yield of forming N-vinylmorpholine was increased from 10.0 to 31.7 % correspondenly. Than increasing temperature above 225 °C has carried out to shar decreasing of yield of synthesised compound and for example at temperatures 280–285 °C and 290–300 °C it was equaled 19 and 12 % correspondenly.

Structure of synthesised N-vinylmorpholine was proved by method of IR-spectroscopy.

In IR-spectrum of N-vinylmorpholine there are following bands: 1520–1610 cm^{-1} – valent vibrations C=C bond of vinyl group; 1050–1250 cm^{-1} valent vibrations C-O-C fragment of morpholine molecule; 2950–2960 cm^{-1} symmetrical and unsymmetrical vibrations of methylenic group ($-\text{CH}_2-$).

Determined experimental data have shown that catalyst KOH/activate coal has an enough activity at synthesis of N-vinylmorpholine by heterogeneous-catalytical vinylation of morpholine by acetylene.

For development of catalytical systems for reaction of acetylene with morpholine some nanostructural matrices of activated coal were obtained which were used as bearer of catalysts. It was determined influence of initial dimensions of obtained activated coal on carrying out synthesis of N-vinylmorpholine. The optimal dimensions of using of activated coal were equalled 1–3 μm .

Dispersion analysis was carried out by method of microscopy. With in of decreasing of dimensions of particles of activated coal sample before for fractionation were undergone to ultrasonic treatment, for which water suspension of activated coal has been prepared (150 ml. H_2O : 5g. of activated coal) and than it was undergone to ultrasonic treatment in regime 0.6 A; 38 kGc. during 60 min. Through every 3 min. the treatment was stopped and glass with mixture was cooled in during 30 sec. in water. Through 10, 20, 30 and 60 min. probes were separated and dimensions of particles of activated coal were determined by method of microscopy.

Analysis of obtained results has shown that dimensions of dispersed particles of activated coal were equalled 700–900 nm.

Sedimentation fractionation of particles of activated coal during 20, 30, 40 and 60 min. has shown that in investigated intervals of time their distribution by dimension has changed markedly.

Dimensions of particles of obtained fraction after 20 min. dispersion were equalled 500–750 nm, and after intervals 30, 40 and 60 min. of dispersion they were equalled 300–350; 200–320 and 200–250 nm. correspondently. Obtained results are presented in table 2.

Such the results of dispersion analysis by method of microscopy have shown that in installation of ultrasonic disperser UZDH2T by dispersion of suspension of activated carbon by water it is possible to active of dimensions of particles of activated coal to 200–250 nm. during 60 minutes. Increasing of dispersion time didn't influenced on dimensions of obtained particles.

Table 2. – Influence of dispersion time on dimensions of particles of activated coal

Time of dispersion, min.	Dimensions of particles of activated coal, nm.
–	1–3 μm .
10	700–900
20	500–750
30	300–350
40	200–320
60	100–250

Heterogeneous — catalytical reaction of acetylene with morpholine in the presence of catalyst on the base of nanostructural activated coal with dimensions of particles 200–250 nm. has been investigated. Conditions of carrying reaction were the same as in the presence of catalyst activated coal/KOH. Quantity of KOH in the presence of catalyst was equalled 30 mass. %. Influence of temperature on reaction of acetylene with morpholine in heterogeneous conditions in the presence of catalyst on the base of activated coal with dimension of particles 200–250 nm. has been determined.

It was determined that in this case also N-vinylmorpholine was synthesised. Obtained results are presented in table 3.

Table 3. – Influence of temperature on yield of N-vinylmorpholine in the presence of catalyst activated coal/KOH with particles dimensions of activated coal 200–250 nm

No	Temperature of reaction, °C	Yield of N-vinylmorpholine, %
1	160	24.3
2	180	27.0
3	200	29.5
4	220	34.4
5	240	38.2
6	260	25.6
7	280	20.4

Obtained results have shown that in this case temperature in interval 160–180 °C in graded degree has influenced on the yield of forming N-vinylmorpholine. In investigated interval of temperatures yield of N-vinylmorpholine was carried out through maximum (38.2 %) observed at 240 °C. With increasing of temperature in interval 160–240 °C yield of product has increased from 24.3 to 38.2 %. The following increasing of temperature has negative influence of yield of N-vinylmorpholine for example its yield at 260 °C and 280 °C was equalled 25.6 and 20.4 % correspondently.

Analysis of obtained data has shown that for reaction of acetylene N-vinylmorpholine in the presence of

catalyst on the base of nanostructural activated coal with dimensions of particles 20–250 nm. the optimal temperature was 240 °C and at this yield of N-vinylmorpholine was equaled 38.2 %.

Such heterogeneous — catalytical reaction of acetylene with morpholine in the presence of catalysts:

activated coal AV-L/KOH and nanostructural activated coal/KOH has been investigated. It was shown that in both cases N-vinylmorpholine was obtained. Activity of catalyst on the base of nanostructural activated coal was higher in comparison with catalyst on the base activated coal AV-L.

References:

1. Mackenzie J. D., Bescher E. Chemical Routes in the Synthesis of Nanomaterials Using the Sol-Gel Process // *Acc. Chem. Res.* – 2007. – № 40. – P. 810.
2. Темкин О. Н. Химия ацетилена, «Ацетиленовое дерево» в органической химии XXI века // *Соросовский образовательный журнал.* – Соросов, 2001. – Т. 7, № 6. – С. 35–38.
3. Трофимов Б. А. Некоторые аспекты химии ацетилена // *ЖОХ.* – Л., 1995. – № 9. – С. 1368–1370.
4. Трофимов Б. А., Нестеренко Р. Н., Михалева А. И. Новые примеры винилирования NH-гетероциклов ацетиленом в системе KOH-DMCO // *ХГС.* – Рига, 1986. – № 4. – С. 481–485.

DOI: <http://dx.doi.org/10.20534/AJT-17-1.2-129-132>

Parmanov Askar Basimovich,

Senior researcher fellow,

National University of Uzbekistan, Tashkent

E-mail: asqar.permanov@mail.ru

Nurmanov Suvonkul Erxonovich,

doctor of technical sciences, chair of department,

National University of Uzbekistan, Tashkent

Phayzullaeva Mariya Phayzullaevna,

teacher of the Karaganda State University

named after Korkyt Ata

Abdullaev Jakhongir Urozolievich,

magister National University of Uzbekistan

Soliev Mukhammadjon Ismatullaevich,

teacher Namangan Engineering Pedagogical Institute

Synthesis of vinyl esters of some carbonic acids

Abstract: Heterogeneous-catalytical vinylation of some carbonic acids (enanthic, pelargonic and cyclohexancarboxylic) was investigated. In each case the influence of the catalyst nature, temperature and mole ratio of reagents on the yield of the obtained vinyl esters of the corresponding acids was investigated.

Keywords: Heterogeneous-catalytical, acetylene, acids: enanthic, pelargonic and cyclohexancarboxylic, energy activation.

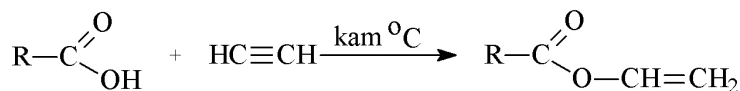
Vinyl esters are used in different branches as solvents, bactericidal preparates in perfumery [1; 2]. Polymers obtained on their base have a specific properties and are used as glue for different materials [3; 4].

From carbonic acids acetic acid as reagent for obtain vinyl esters has been investigated in large degree. Fat carbonic acids in this plane aren't investigated [5].

It is necessary to note that in Republic of Uzbekistan during last years the output of oil has been increased. Extraction from oil composition heteroatom-containing compounds such as fat carbonic acids and their processing has a great importance and future [6; 7].

In this work hetero-catalytical vinylation of acids such as enanthic, pelargonic and cyclohexanic extracted from oil

composition of our Republic was investigated. Acetylene was used as vinylation agent. All reactions were carried out in flowing reactor in presence of following catalysts: Al_2O_3 ; $\text{Zn}(\text{CH}_3\text{COO})_2$ and $\text{Cd}(\text{CH}_3\text{COO})_2$ bearing on



Where: $\text{R} = -\text{C}_6\text{H}_{11}$; $-\text{C}_6\text{H}_{13}$ and $-\text{C}_8\text{H}_{17}$.

Their yields have been depended on nature of catalysts, temperature of process and mole ratio of carbonic acids and acetylene.

It was investigated a mole ratio of initial reagents on yield of vinyl ester enantic acid in presence of catalysts $\text{Zn}(\text{CH}_3\text{COO})_2/\text{Al}_2\text{O}_3$ and $\text{Zn}(\text{C}_6\text{H}_{13}\text{COO})_2/\text{Al}_2\text{O}_3$. Obtained data are presented in table 1.

Table 1. – Influence of mole ratio enantic acid and acetylen on yield of it's vinyl ester (temperature 300°C)

Molar ratio of enantic acid : acetylene	Yield of vinyl ester of enantic acid
<i>catalyst $\text{Zn}(\text{CH}_3\text{COO})_2/\text{Al}_2\text{O}_3$</i>	
3 : 1	6.3
2 : 1	10.4
1 : 1	35.8
1 : 2	45.0
1 : 3	56.2
1 : 4	61.3
1 : 5	61.8
<i>catalyst $\text{Zn}(\text{C}_6\text{H}_{13}\text{COO})_2/\text{Al}_2\text{O}_3$</i>	
3 : 1	11.2
1 : 1	38.6
1 : 2	51.0
1 : 2.5	54.3
1 : 4	62.7
1 : 5	63.4

Obtained results have shown that molar ratio of initial reagent has influenced on yield of vinyl ester of enantic acid. In presence of used catalysts when molar ratio of acid is higher then acetylen the vinyl ester was formed with low yields but in case when content of acetylen was more then acid yields of product were higher. At using of catalyst $\text{Zn}(\text{CH}_3\text{COO})_2/\text{Al}_2\text{O}_3$ and molar ratio of regents 3 : 1 – 6.3%. With increasing of molar ratio enantic acid: acetylen 1 : 4 the yield of forming vinyl ester of enantic acid was increased to 61.3%. Following increasing of acetylen practically didn't influenced on yield of product. The same dependence was observed at using catalytical system $\text{Zn}(\text{C}_6\text{H}_{13}\text{COO})_2/\text{Al}_2\text{O}_3$. For example in it's presence at molar ratios enantic acid: acetone 3 : 1 and 4 : 1 yields of formed vinyl ester were

Al_2O_3 ; $\text{Zn}(\text{C}_6\text{H}_{13}\text{COO})_2/\text{Al}_2\text{O}_3$ pelargonic and cyclohexanic acids bearing on Al_2O_3 . It was determined that in all cases vinyl esters of corresponding acids were obtained with different yields according to following scheme:

11.2 and 62.7% correspondenly. Thus for synthesis of vinyl ester of enantic acid the most active catalyst was $\text{Zn}(\text{C}_6\text{H}_{13}\text{COO})_2/\text{Al}_2\text{O}_3$ and at this optimal ratio of enantic acid : acetylen was 1 : 4–5.

For carrying out of reactions especially heterogeneous-catalytical at high temperatures investigation of their kinetical constants in practical ratio is very important. By this reason kinetics of vinylation of enantic acid by acetylen in the presence of catalyst $\text{Zn}(\text{CH}_3\text{COO})_2/\text{Al}_2\text{O}_3$ was investigated at temperatures 150, 200, 250 and 300°C and at duration of 0.5; 1.0; 1.5 and 2.0 hours. Obtained kinetical data are presented on fig. 1.

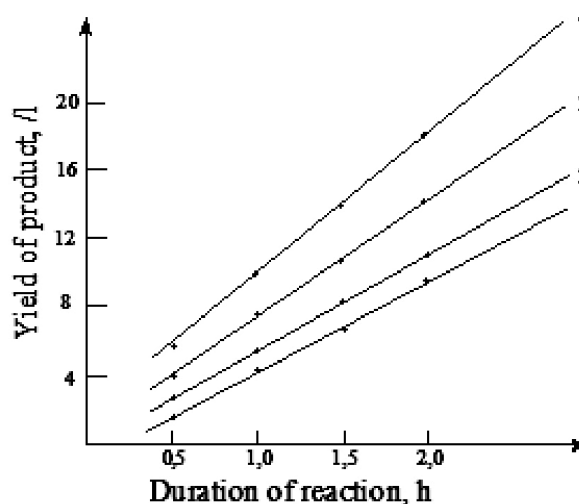


Fig. 1. Dependence of yield of vinyl ester of enantic acid from duration of reaction at temperatures ($^\circ\text{C}$): 1 – 150; 2 – 200; 3 – 250; 4 – 300; (catalyst – $\text{Zn}(\text{C}_6\text{H}_{13}\text{COO})_2/\text{Al}_2\text{O}_3$)

On the base of these data the rate of reaction of vinylation of enantic acid was calculated and also graph of dependence on of $\lg W/1/T$ was constructed (fig. 2), from which by equation of Arrhenius the activation energy of this reaction was determined which was equaled 4090 J/mole .

For determination of influence of nature of carbonic acids on vinylation and yields of forming vinyl esters vinylation of pelargonic acid by acetylen in presence of following catalysts; Al_2O_3 ; $\text{Zn}(\text{CH}_3\text{COO})_2$ /activated coal; $\text{Zn}(\text{CH}_3\text{COO})_2/\text{Al}_2\text{O}_3$; $\text{Cd}(\text{CH}_3\text{COO})_2/\text{Al}_2\text{O}_3$ and $\text{Zn}(\text{C}_6\text{H}_{13}\text{COO})_2/\text{Al}_2\text{O}_3$ also was investigated. Obtained maximal yields of vinyl ester of pelargonic acid in presence of these catalysts are presented in table 2.

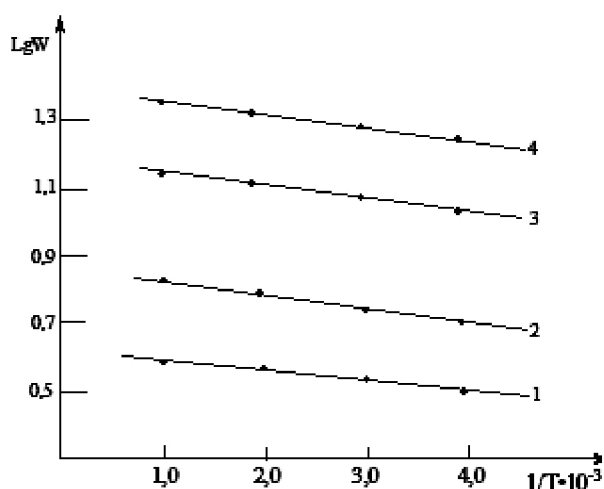


Fig. 2. Dependence of logarithm of rate from reverse temperature ($1/T$) for vinylation of enantiic acid at duration of rection (h.): 1–0.5; 2–1.0; 3–1.5; 4–2.0

Table 2. – Yields of vinyl ester of pelargonic acid in presence of different catalysts (mole ratio of acid: $C_2H_2 = 1 : 4-5$, $300^\circ C$, volume rate of initial reagents 43–46 l/l.kat. h.

Catalyst	Yield of vinyl ester of pelargonic acid, %
Al_2O_3	–
$Zn(CH_3COO)_2$ /activated coal	33.2
$Zn(CH_3COO)_2/Al_2O_3$	51.3
$Cd(CH_3COO)_2/Al_2O_3$	37.4
$Zn(C_8H_{17}COO)_2/Al_2O_3$	55.4

Obtained results have shown that between investigated catalysts for vinylation of pelargonic acid catalyst $Zn(C_6H_{13}COO)_2/Al_2O_3$ was the most active; in it's presence yield of vinyl ester of pelargonic acid was equaled 55.4%. Also influence of temperature on yield of this ester in the presence of the most active catalyst has been investigated (table 3).

Table 3. – Influence of temperature on yield of vinyl ester of pelargonic acid (catalyst $Zn(C_6H_{13}COO)_2/Al_2O_3$)

Nº	Temperature, $^\circ C$	Yield of vinyl ester of pelargonic acid, %
1.	230	15.4
2.	260	43.5
3.	280	49.8
4.	300	55.4
5.	320	57.2
6.	350	48.3

For determination of influence of presence of carbocyclical ring in molecule of carbonic acid on it's vinylation also it was investigated reaction of cyclohexancarboic acid

by acetylene in the presence of some above-mentioned catalysts and also influence of temperature on yields of obtained vinyl ester of this acid have been investigated in the presence of catalyst $Zn(C_6H_{13}COO)_2/Al_2O_3$. Obtained data are presented in table 4.

Table 4. – Vinylation of cyclohexancarboic acid at different temperatures (catalyst $Zn(C_6H_{13}COO)_2/Al_2O_3$)

Temperature, $^\circ C$	Yield of vinyl ester of cyclohexancarboic acid, %
220	22.5
240	33.2
260	38.7
280	45.3
300	53.0
320	51.4
340	43.6

Results have shown that in investigated temperature interval ($220-340^\circ C$) yield of obtained vinyl ester was carried out through maximum (53.0%) at $300^\circ C$. On fig. 3 comparasional data by influence of temperature on yields of vinyl esters of investigated carbonic acids in the presence of the most active catalyst are presented.

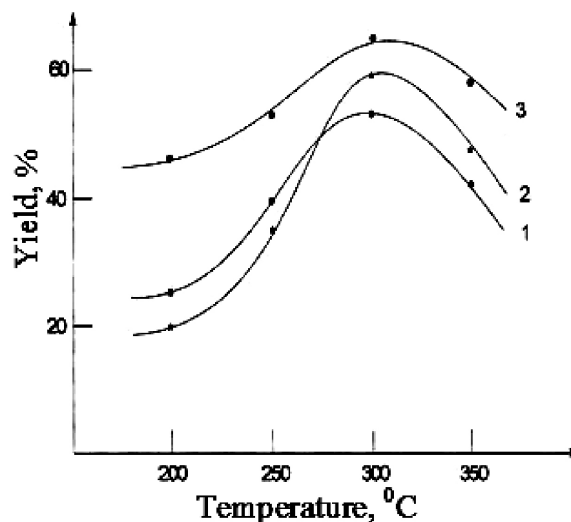


Fig. 3. Comparasional data by dependence on yield of vinyl esters from temperature (catalyst $Zn(C_6H_{13}COO)_2/Al_2O_3$): 1 — Vinyl ester of cyclohexancarboic acid; 2 — Vinyl ester of enantiic acid; 3 — Vinyl ester of pelargonic acid

Also yields of vinyl esters of investigated acids in presence of some elaborated catalytical systems also were determined (table 5). From these data it is possible to conclude that aliphatical carbonic acid are more active than cyclic acid at heterogeneous-catalytical vinylation of them by acetylene. Also it is shown that with increasing of molecular mass of aliphatical carbonic acids the vinylation is carried out at higher temperatures and yields of their obtained vinyl esters at this have been decreased.

Table 5. – Yields of vinyl esters of investigated carbonic acids in the presence of elaborated catalysts (mole ratio of carbonic acid : acetylene — 1 : 4–5, temperature 300°C)

Catalysts	Yields of products, %		
	I	II	III
Al ₂ O ₃	trace	–	–
Zn (CH ₃ COO) ₂ /activated coal	43.4	33.2	31.4
Zn (CH ₃ COO) ₂ /Al ₂ O ₃	61.8	51.3	48.5
Cd (CH ₃ COO) ₂ /Al ₂ O ₃	52.7	37.4	35.2
Zn (C ₆ H ₁₃ COO) ₂ /Al ₂ O ₃	63.4	–	–
Zn (C ₈ H ₁₇ COO) ₂ /Al ₂ O ₃	–	55.4	–
Zn (C ₆ H ₁₁ COO) ₂ /Al ₂ O ₃	–	–	53.0

In table 5 — I, II and III vinyl esters of enantic, pel-argonic and cyclohexancarboxylic acids.

This is caused by fact that with increasing of molecular mass of carbonic acids their acidity has decreased what is carried out to decreasing of yields of their vinyl esters. Results have shown that investigated acids by of their ratio to vinylation by acetylene can be presented by following row:



Maximal yields of their vinyl esters were 53.0 and 63.4%. At investigation of nature of catalysts at vinylation above mentioned acids by acetylene it was determined that zink salt of every acid is active catalyst for vinylation namely of this acid.

References:

1. Лебедев Н. Н. Химия и технология основного органического и нефтехимического синтеза. – М., 1988. – 245 с.
2. Раднаева Л. Д. Полимеры на основе ненасыщенных карбоновых кислот и их производных. – Улан-Удэ, 2005. – 354 с. // [Electronic resource]. – Available from: <http://bankrabot.com>
3. Плате Н. А., Сливинский Е. В. Основы химии и технологии мономеров. – М.: Наука, 2002. – 415 с.
4. Нарметова Г. Р., Хамидов Б. Н., Рябова Н. Д., Арипов Э. А. Очистка, идентификация и применение нефтяных кислот. – Ташкент, 1983. – 144 с.
5. Муратова С. Х., Нурманов С., Нарметова Г. Р., Сирибаев Т. С. Винилирование карбоновых (нефтяных) кислот // Узб. хим. журн. – Ташкент, 2003. – № 6. – С. 13–17.
6. Бродская Е. С. Нефтяные и синтетические нефтяные кислоты, их свойств и применение // Журн. орг. хим. – 1999. – Т. 35, Вып. 2. – С. 221–226.
7. Наметкин Н. С., Егорова Г. М., Хамаева В. Х. Нефтяные кислоты и продукты их химической переработки // Химия. – 1982. – С. 182–186.

DOI: <http://dx.doi.org/10.20534/AJT-17-1.2-132-134>

Smanova Zulaykho,
National University of Uzbekistan
E-mail: smanova.chem@mail.ru

Yangibayev Azim,

Yakhshieva Khurniso
E-mail: yaxshiyeva67@mail.ru

Raximov Samariddin,
National University of Uzbekistan
named after Mirzo Ulugbek

Chemism of complex formation of pyridine and anabasine dyes

Abstract: Between problems standing before investigators working in field of synthesis of organic reagents one of the important is finding of general principles of selection analytical reagents with help of which it is possible to determine content of different ions of metals with high sensibility. Decision of this problem is connected with investigation of particularities of spacial and electronical structure of reagents, ions of different metals, their complexes and also changing carrying out at their interaction.

Knowing all particularities has allowed to outline the base directions of synthesis and physico-chemical investigations for obtain newq important analytical reagents.

Keywords: immobilization, nitrozonafolov derivatives, heavy and toxic metals.

It was determined that new synthesized pyridine and anabasine dyes namely: N-methylanabazine α -azo-chromotropical acid; N-methylanabazine α -azo-1,8 aminonaphtol-4,6 disulfoacid; 6-methylpyridil -2-azo-n-aminophenol; 1-(5-methylpyridilazo)-5-diaminophenol; 1-(2-pyridilazo)-2-oxynaphtaline-6-sulfoacid-sodium have formed strong and coloured complexes with ions of different metals [1; 2; 5].

Formation of their complexes has carried out basically in acid and moderate acid mediums. Owingr multidentatntion and multybasicity of compounds on the base of anabasine and pyridine at examination of chemical structure of their complexes it is necessary to take into account state of azodyes in conditions of carrying out of reaction. On the base of spectral data [3; 4] it is possible to make conclusion that in different by nature mediums different protinozation has carried out at: pH 2 atom of nitrogen of pyridine and piperidine nucleuses is protenized in molecules of all dyes: pH 4.5 only atom of nitrogen of tertiary amino-group of piperidine nucleus is protonized but ionization of OH-group didn't carried out; pH = 10 tertiary atom of nitrogen is unde-gone to protenization but also it is possible ionization of OH-group; pH higher 12 tertiary atom of nitrogen of piperidine nucleuse is deprotinozed and also full dissociation of OH-group has carried out. Ability to formation to complexes can be examine in general aspect from the point of view their donoral ability to formation of coordinational bonds by oxygen atom owing to displacement of hydrogen atom. Degree of strong of complexes is depended on position of OH-group in aromatical nucleus.

Ability of phenoxylical anions to coordination is depended on strong of acceptation by ion of metal of π -electrons of anion of oxygen. From literature data [6] and obtain our data it is show that metals have displaced hudrogen atom from compounds also in acid medium; increasing of strong of bond Me-O in composition with H-O can be explain by transition of π -electrons of oxygen atom on free orbitals cenral o ion of metal. Strong of complexes is depended on degree of filling of d-orbitales (Ti^{3+} , Fe^{3+} , Co^{3+}).

The second coordinating group in molecules of azodyes is azo-group which has accepted hydrid-ions. Therefore if in metal ioness there are fulfilled d- orbitales then they are able to form coordinated bond which azo-group. In article [7] properties of PAA complexes have

been compared with complexes with α -o-hydroxophenylaminoethylpyridine; saliciliden-2-aminopyridine and some others ligands in which azo- group is substituted on pyridilazomethinal or phenoxy-methinal groups such comparison has carried out to conclusion that complexes with ligands having azo-group are stronger and their spectral characteristics have allowed to conclude that in chelated complexes of such type azo-group has entered in reaction of complex-formation. It is important that this ability is determined by energy of free π -orbitales of azo-group and by presence of fulfilled d-orbitales at complexoformator (that is at ioness of metals).

Owing to fact that oxygen atom of OH group has performed as π - donor and azo-group as π -acceptor than combination of theres two groups in orto-position of phenolical and naphtilical radicals has promoted to increasing of strong of obtained complex compounds.

To interaction of nitrogen atom of pyridine is devoted a great number of early investigated complexes of this reagent with great number of ions of different metals. But complex formation with pyridine it is impossible to explain by only using of undivided pair of electrons of nitrogen atom. More essential is interaction between free or fulfilled d- or f- orbitales of the central ion. Owing to these complexes with pyridine can exist in weak-acid mediums but at the same time it is impossible correlation between constants of basicity of different nitrogen-containing aliphatic and aromatical bases with constant of unsta-bility of complexes of these ligands. Position of pyridil radical in meolecules, of azodye such that in mort cases it is possible it's interaction by tertiary coordinate of ion of given metal at presence of bond with -OH⁻ or azo-groups.

Essential peculiarity of azodyes synthesised and investigated in our laboratory is presence in their olecules N-methylpiperidine unclous. As far as ternary N-methyl group is a strong basical and nitrogen atom of aliphatical amines didn't able to formation of π -bond with ions of met-als and correspondenly it is impossible to wait of forma-tion of strong coordinational bond by this nitrogen atom of azo-dye, Owing to coplasity of molecules of dyes im-portant role is devoted to spherical factors at formation of complexes. In this plane N-methylpiperidine system can manifiast double role: to create difficulties to interaction of pyridine nucleus by third coordinate of six and more coordinating ion creating conditions for introduction of second or third molecule of dye in coordinational sphere

or contrary this grouping can to prevent introduction of second molecular of azodye in coordinational sphere. Obviously this effect must to became apparent for ions forming 3, 4 and 5 coordinating bonds.

Presence of this group in molecule of organical reagent has allowed as is shown from experimental date to carried out reactions in more acid mediums. increazing of acidity of medium is connected with possibility of protonization N-methylpyperidine, owing to this fact using of azodyes as analytical reagents is more comfortable. At this also it is necessary to take into account fact, that many ions of investigated metals in weak-base and neutral mediums able to formation of forms uncomfortable for interaction with

ligands (owing to such reactions as hydrolysis, polymerization and so on) and by this reason increasing of acidity has carried out to increasing of precision and sensibility of determination. Also it is important increasing of molecular mass of reagents leconrse at this sensibility of analytical methods of determination of metal ions and their affinity to used organical reagents.have been increazd.

Owing to purpose ful changing of structure of azodyes not only by effect of additional coordinating groups by also of their immobilization it is possible essential changing of properties of complexes and also theoretical and practical preconditions to selection of specifical analytical reagents are created.

References:

1. Smanova Z. A., Manzurhojaev V. M. Extraction – photometrical determination of Ni by azoreagent 2- (5-methylpyridilazo) – 2-hydroxy – 5-methoxybenzole//Vestnik of NUUz. – Tashkent, 2005. – № 4. – P. 124–126.
2. Smanova Z. A. Reagent 1- (4-antipyrilazo)-2-naphtol-6 – sulphoacidal sodium for determination of some heavy and toxical metals//Usb. chem. journal. – Tashkent, 2008. – № 2. – P. 52–55.
3. Ivanov V. M. Geterocyclical nitrogen – containing azocompounds. – M.: Zeience, 1982. – P. 129–136.
4. Smanova Z. A. Immobilized organical reagents and their analytical application at determination of heavy toxical metals. Avtoreferat of doctor dis. On the competition of d. ch. s. – Tashkent, 2015. – 88 p.
5. Smanova Z. A. Elaboration of sorptionno – spektroskopical methods of analysis with using of immobilized organical reagents (review)//Vestnic NUUz. – Tashkent, 2010. – № 4. – P. 67–71.

DOI: <http://dx.doi.org/10.20534/AJT-17-1.2-134-138>

*Shomurotov Shavkat Abduganievich,
PhD, Senior Researcher, Department of Chemistry of Polysaccharides,
Institute of Bioorganic chemistry UzAS
E-mail: shsha@mail.ru*

*Akhmedov Oliy Ravshanovich,
Institute of Bioorganic chemistry UzAS, Researcher
E-mail: oliy86@bk.ru*

*Mamatmusaeva Nilufar Erkinovna,
PhD, Researcher Department of Chemistry of Polysaccharides
E-mail: erkinova81@mail.ru*

*Sagdullaev Bakhodir Takhiroviich,
DSc, Senior Researcher, Department of Chemistry of Polysaccharides
E-mail: bsagdullaev29@gmail.com*

*Turaev Abbaskhan Sabirkhanovich,
DSc, professor, Institute of Bioorganic chemistry UzAS
E-mail: abbaskhan@mail.ru*

Modified derivatives of polysaccharides having anti tuberculosis activity

Abstract: The research on the synthesis of polymeric complexes of polygalacturonic acid with anti-TB preparations having antituberculosis activity was conducted. The structures were ascertained and studied

the physicochemical properties of polymeric systems. Pharmaco-toxicological studies have shown that polymeric complexes are less toxic than their low molecular analogues and *Mycobacterium of tuberculosis* show high sensitivity to the prepared preparations.

Keywords: polymeric complexes, tuberculosis, prolongation, polyglacturonic acid, isoniazide, ethambutol.

In connection with the specific treatment of tuberculosis — complex therapy (at the same time with several anti-TB preparations), duration of treatment, the need for the prescribing of multiple high doses of drugs and the emergence of this toxic and allergic complications — it is very important to find the method to reduce the dosage of anti-TB preparations. One way to improve the conditions of drug therapy is the creation and application of polymeric anti-TB preparations of prolonged action. Such long-acting anti-TB preparations are available including in polymer — carriers of known anti-TB preparations, which allows purposefully change their physico-chemical and medico-biological properties.

In this regard, were carried out the studies on obtaining the macromolecular drug delivery system by the addition of anti-TB preparations of hydrazide of isonicotinic acid (HINA) and ethambutol dihydrochloride (EBHC) to the macromolecule of polymer carrier. As the polymer carrier was used modified polygalacturonic acid (PGA) obtained by demethoxylation of citrus pectin.

Materials and methods

UV spectra were recorded on a UV spectrophotometer "UV 1280" manufactured by "Shimadzu", Japan, in quartz cuvettes with 1 cm thick, in the range of 200–500 nm. in aqueous solutions.

IR spectra were recorded on devices "Bruker Vektor-33", in the wavelength range of 500–4000 cm^{-1} in tablets with KBr.

Synthesis of dialdehyde polygalacturonic acid (DAPGA). Periodate oxidation of PGA was performed

at pH of 4.7 in 3 % aqueous solution of PGA, at oxidant concentration of 0.5M and temperature of 25 °C within 2.5 hours. Degree of oxidation of reaction in product was determined by iodometric method [1] and UV — spectrophotometric method [2] on flow rate JO_4^- of ions on intensity change of absorption band at $\lambda = 222 \text{ nm}$.

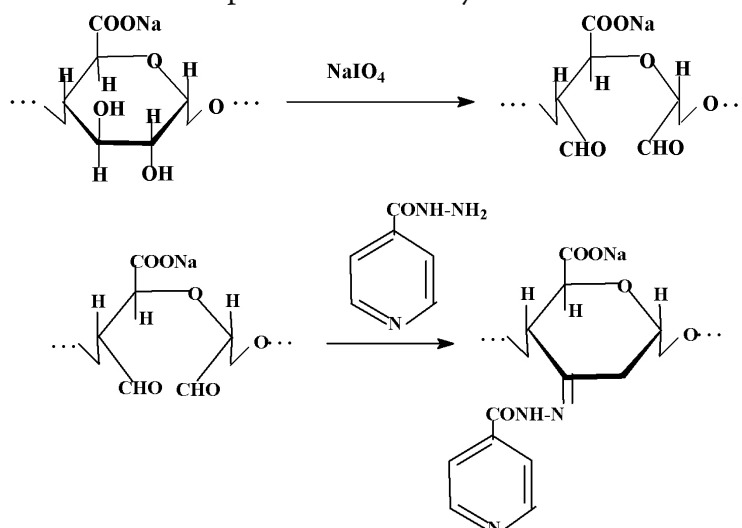
Synthesis of PGA with HINA. The reaction was performed in a three-necked thermostated flask equipped with thermometer and stirrer. Into the flask was placed 0.02 mole of DAPGA and 40 ml. of an aqueous solution containing 0.06 mole of HINA and stirred vigorously within 60 min. at 25 °C. Then the reaction product was filtered, washed repeatedly with mixture of alcohol: water (1:1) and dried over P_2O_5 in a desiccator. The content of bound HINA was determined by the content of nitrogen.

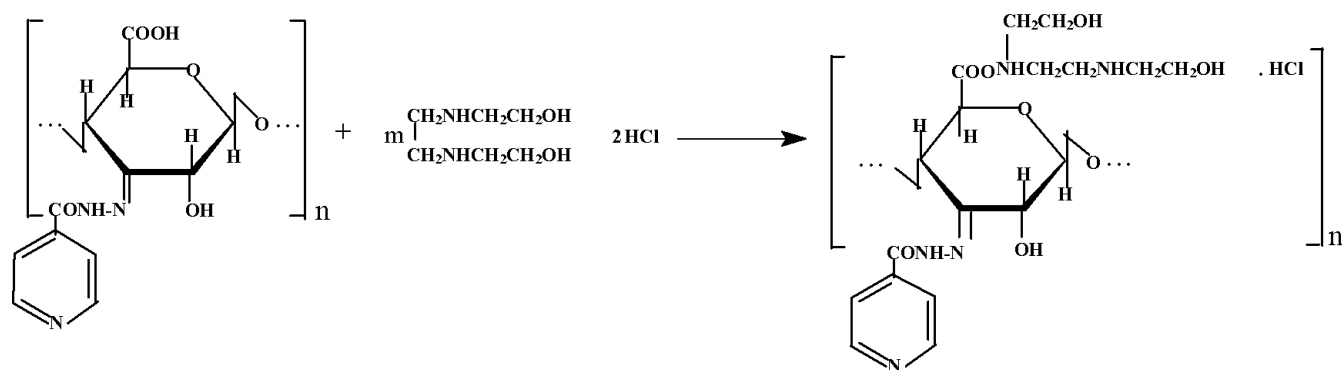
Synthesis of PGA complex with HINA and EB. The reaction was carried out at pH 5.5 in 3 % aqueous solution of the complex PGA with HINA at EBHC concentration of 0.5 M. and temperature of 20 °C for 60 min. The reaction mass was then dialyzed for 24 hours. The product was isolated by rotary drying. The content of HINA and EB was determined on nitrogen content and spectrophotometric method.

Results and discussion

We have studied the synthesis of polymeric complexes HINA and EB with modified macromolecule PGA, which was obtained by demethoxylation of citrus pectin (the content of OCH_3 groups, 7.6 %) [3].

Synthesis was carried out as follows.





DAPGA was obtained by periodate oxidation of PGA. The reaction was carried out homogeneously in aqueous solution of NaJO_4 . The reaction products were precipitated with acetone. The control of the oxidation process was carried out on the spending of periodate ion (spectrophotometric method) and on changing the content of aldehyde groups (iodometric method).

The dependence of the oxidation degree of the modified PGA on the reaction time, the molecular weight (MW) of PGA and ratio of reagents was studied.

As can be seen from table 1, with increasing of the reaction time increases the degree of oxidation, in all

samples it is nearly identical, suggesting that the MM almost doesn't influence on the degree of oxidation of PGA. Increasing the reaction time over 2.5 hours leads to some reduction in oxidation state (the content of aldehyde groups). Such a course of reaction, due to the fact that in addition to the main reaction proceeds adverse reaction — the oxidation of the resulting aldehyde groups to carboxyl [4].

Nucleophilic substitution reaction of DAPGA with HINA was conducted. The dependence of the interaction between HINA and DAPGA on the reaction conditions was studied.

Table 1. – The dependence of the oxidation degree of PGA on the reaction time and MW at periodate oxidation (Reaction conditions: PGA: $\text{JO}_4^- = 1 : 1.5$; $t = 20^\circ\text{C}$; $\text{pH} = 4.0$)

Time, hour	Molecular mass of PGA									
	48 500		44 000		40 000		30 000		15 000	
	I*	S*	I*	S*	I*	S*	I*	S*	I*	S*
0.25	8.6	8.7	8.8	9.0	8.4	8.7	8.4	8.5	9.3	9.5
0.5	15.0	15.4	15.3	15.6	14.4	15.2	15.7	16.3	15.6	15.9
1.0	23.2	23.8	24.1	24.2	24.3	24.6	24.7	25.2	25.2	25.5
1.5	32.7	33.0	32.9	33.2	36.5	37.2	36.6	37.3	35.2	37.5
2.0	43.8	46.4	43.3	47.3	45.8	49.5	44.4	46.6	46.7	47.6
2.5	52.4	55.6	51.6	52.8	51.3	56.1	54.4	56.8	52.9	54.5
3.0	51.5	57.2	49.6	55.8	48.3	48.9	46.9	59.5	50.5	56.7
5.0	49.3	60.8	47.4	58.6	47.2	59.4	46.3	61.7	49.2	58.2

Note: oxidation degree was determined: I* — iodometric method; S* — spectrophotometric method.

Table 2. – Dependence of nucleophilic substitution of DAPGA with HINA on MW and the ratio of DAPGA: HINA (Reaction time 30 min., $t = 20^\circ\text{C}$, $\text{pH} = 5$, content of oxidized parts 21 to 100 elementary parts)

Ratio of DAPGA: HINA, moles	Molecular weight of DAPGA, dalton				
	75 670	58 530	34 440	26 570	11 520
	Content of bound HINA, moles %				
1:0.25	7.8	7.2	6.9	7.0	7.2
1:0.50	13.2	15.6	14.4	16.6	15.8
1:1.00	16.6	17.4	16.2	16.4	17.6
1:1.50	18.4	18.8	18.8	19.5	19.3
1:2.50	20.2	19.8	20.7	20.7	20.9
1:5.00	20.8	20.2	21.4	21.6	21.0

Effect of reagents ratio DAPGA: HINA on content of bound HINA (table 2) shows that the increase of HINA in the reaction medium up to 2.5 mole leads to the increase in the content of bound HINA in polymer. However, further increase in its amount does not affect its content in the product, indicating the exhaustion of the aldehyde groups of the polymer matrix at certain ratios of components.

Nucleophilic substitution reaction of DAPGA with HINA passes homogeneously in aqueous solutions. Therefore MW of polymer hardly affects the nucleophilic substitution process. With increasing concentration of HINA increases the content of bound HINA, the limit value of bound HINA almost corresponds to the content of disclosed, pyranose parts, i. e. 50 % of the total number of aldehyde groups.

This indicates that in condensation reaction is involved only one aldehyde group in DAPGA. The second aldehyde group reacts the reduction reaction of pyranose cycle. Similar data was previously obtained by reaction with dialdehydecellulose with

phenylhydrazine [5]. To clarify this, the authors carried out a condensation reaction of dialdehyde triphenylmethylcellulose, in which is eliminated the formation of hemiacetal connection with tolilhydrazine (since all hydroxyl groups in C₆ are substituted). The authors demonstrated that during the condensation reaction of triphenylmethylcellulose with tolilhydrazine is proceeding the reduction of C₂-C₃ bond of glucopyranose cycle forming a compound containing arylnitro-group in the third carbon atom.

The reaction of interaction of complex PGA-HINA with EBHC was studied. The reaction was carried out in aqueous solution at pH 5.5. At this pH the largest part of the carboxyl groups is in salt form. Thus, there is a reaction of ion binding of EB with macromolecule of PGA, as evidenced by IR spectroscopy method and elemental analysis. The resulting product is readily soluble in water.

In order to study the effect of the ratio of reagents on the content of bound EB in the macromolecule PGA-HINA reactions were carried out at different ratios of PGA-HINA: EB. Results are shown in Table 3.

Table 3. – Dependence of content of bound EB on ratio of PGA-HINA: EBHC

Mole ratio of PGA-HINA*: EBHC	Nitrogen content, %	EB, moles %
1 : 0.1	4.25	5.64
1 : 0.5	5.88	22.7
1 : 1	5.99	24.5
1 : 2	6.58	30.4
1 : 5	7.80	42.6
1 : 8	7.77	42.5

Note: PGA-HINA* — MW 12 000 and containing 20.2 mole % of HINA with hydrozonic bond.

The table shows that with increase in the ratio of PGA-HINA: EBHC increases the content of bound EB in the reaction product. It is interesting to note that even with a molar ratio of PGA-HINA: EBHC = 1 : 1 and large ratios the reaction does not proceed to full substitution of ions Na⁺ to EB. The latter is due to steric difficulties of ion exchange along the chain of the macromolecule, and, of course, lower basicity of EB.

It is found that in the interaction reaction of PGA-HINA with EBHC molecular parameters of polymer-carrier hardly change. This is evidenced by results of a study of the characteristic viscosity and molecular weight determination of the original PGA-HINA and PGA-HINA associated with the EB. The characteristic viscosity, measured in 0.1 M. NaCl solution, almost doesn't change and is in the range of 0.34 ± 0.5.

Pharmaco-toxicological properties of the obtained polymeric complexes were studied, in particular, the

acute toxicity and anti-TB activity. The following polymeric complexes were studied:

- PGA-HINA-EB, containing 20.2 mole % of HINA and 25.6 mole % of EB;
- PGA-HINA, containing 20.2 mole % of HINA;
- PGA-EB, containing 24.5 mole % of EB.

As a control was taken HINA with activity of 99 % and EBHC with a content of active principle of 100 % of the German company «Sigma chemical». Determination of acute toxicity of preparations was carried out in 100 white mongrel mice weighing 18–20 g. of both sexes by intraperitoneal injection.

Experimental results were treated by variational statistics. LD₅₀ calculations were performed according to the method of Litchfield and Wilcoxon.

On the basis of experiments were determined LD_{50'}, which are summarized in table 4.

Table 4. – Composition of studied preparations and their LD₅₀

Composition	HINA content		Ethambutol content		LD ₅₀ mg/ml
	%	Mole %	%	Mole %	
HINA	100	100	–	–	224 (160÷300)
EB	–	–	100	100	1290 (1100÷1500)
CMC + HINA + EB	13.07	20.2	18.67	25.6	More than 5000
CMC + HINA	13.07	20.2	–	–	3600 (3200÷4300)
CMC + EB	–	–	17.85	24.5	More than 5000

Table 5. – The sensitivity of Mycobacterium tuberculosis to the studied polymeric complexes

Preparations	№ Cultures							
	646	824	831	956	806	743	552	765
CMC + HINA + EB	+	+	+	+	+	+	+	+
CMC + HINA	+	–	–	+	+	+	+	–
CMC + EB	+	–	–	+	+	+	+	+

Note: «+» — Sensitive to preparation; «-» — stable to preparation.

Based on the obtained results, we can conclude that the tested preparations by single intraperitoneal administration can be assigned to different classes of toxicity: «HINA» — to the class of low toxic substances; «Ethambutol» — to practically non-toxic class of substances; «PT», «PTE» and «PEB» — to the class of non-toxic substances.

We conducted the study of sensitivity of Mycobacterium tuberculosis to the synthesized polymeric complexes. The study was conducted under conditions in vitro in virulent strains of Mycobacterium tuberculosis H37Rv, Bovinus-8. Tests were conducted by the method of absolute concentrations with content of preparations in the medium of Lewenstein – Jensen 1 mkg/ml and 10 mkg/ml.

The results showed that to the complex CMC + HINA + EB all tested strains remained sensitive. To the CMC + EB complex of eight strains remained

sensitive six cultures, to the CMC + HINA complex five strains of Mycobacterium cultures were sensitive and in all cases, the efficacy depends on active substance concentration in the preparation. The higher the concentration, the more effective its action on mycobacteria. Combinations of two preparations increase the inhibitory effect on mycobacteria.

Conclusions

Thus, in the course of the research were obtained macromolecular medicinal systems having anti-TB action. The reaction conditions were determined and ascertained the structures of the obtained macromolecular systems.

Pharmaco-toxicological studies have shown that strains H37Rv, Bovinus-8 show high sensitivity to the synthesized polymeric complexes, and also was observed the decrease in toxicity compared to the initial medicinal preparations.

References:

1. Sjutkin V.N., Nikolaev A. G., Sazhin S. A., Popov V.M., Zamoryansky A. A. Nitrogen-containing derivatives of dialdehyde cellulose//Chemistry of plant raw materials. – 1999. – No. 2. – P. 91–102.
2. Akhmedov O. P., Shomurotov Sh. A., Turaev A. S. Features of synthesis of the dialdehyde derivatives of polysaccharides//Uzbek chemical journal. – Tashkent, 2013. – No. 1. – P. 30–33.
3. Shomurotov Sh. A., Muydinov N. T., Akhmedov O. R., Boymirzaev A. S., Turaev A. S. Study of molecular-mass characteristics of carboxymethyl cellulose and polygalacturonic acid by hydrolytic cleavages//Uzbek chemical journal. – Tashkent, 2015. – No. 4. – P. 15–18.
4. Amanova D. M., Shomurotov Sh. A., Turaev A. S., Ergashev M. R. Study of features of periodate oxidation of galactomannan. Conf. “Actual Problems of Chemistry of Natural Compounds”. – Tashkent, 2012. – P. 128.
5. Nadzhimutdinov Sh., Sarymsakov A., Usmanov Kh. U. Study of some of the laws of synthesis for dialdehydes of cellulose and its ethers//Cellulose Chem. Technol. – 1981. – No. 16. – P. 613–628.

DOI: <http://dx.doi.org/10.20534/AJT-17-1.2-139-140>

*Yakhshieva Zukhra,
Ph.D. Assoc. Chemistry Department,
National University of Uzbekistan n. a. M. Ulugbek
E-mail: yaxshiyeva67@mail.ru*

*Smanova Zulayxo,
Dr., assistant Professor Faculty of Chemistry
E-mail: smanova.chem@mail.ru*

*Khaydarov Islomjon,
Undergraduate chemistry*

*Mirzakhmedov Rustam,
Student of IV course of the faculty of chemistry
National University of Uzbekistan n. a. M. Ulugbek*

Amperometrical determination of palladium ions by organical azoreagents

Abstract: Possibility of using of 4-(2-N-methylanabazinazo)-m-phenyldiamine as reagent for determination ions of palladium was shown and conditions of their amperometrical titration on different by acid — base properties phone electrolytes and buffer imixtures have been optimized. Elaborated methods were used to analysis of binarical, triple and more complexe model mixtures imitating industrial materials and natural objects. In all cases the obtained results were treatment by methods and procedures known in literature and were valued from value of metrology.

Keywords: selectivity, amperometry, electroconductivity, titration, expression.

Small content of noble metals in geological and production materials has caused necessity their preliminary concentration with following determination by hybrid and combinational methods. This problem is very actual for Uzbekistan owing to finding of noble metals and determination of production of their deposits.

To presence time optical, phisical and some others methods of determination of ions Pt (II) have been elaborated but they don't charaeterised by high metrological parameters and analytical characteristics they are low selective, complicated, didn't pressision and so on.

By this reason it was necessary to elaborate new, more modern method of determination of ions of noble metals corresponding to all peresence demands. Selectivity of determination of ions palladium in solution can be increased by precission sorptional concentrat-ing for following their electrochemical determination, it is very important that complexes of palladium have given sensible analytical signal.

Aim of this work was investigation of possibility of amperometrical determination of palladium in solutions of complex composition after it's concentrating.

Selective and sensible microquantitave ampero-metrical method of determination of palladium's ions based on their electrochemical reaction with azoreagent 4-(2-N-methylanabazinazo)-m-phenyldiamine has been elaboratel.

One of advantage of voltamperometry is it's accesibility and determination of small quantities of the determined ions of metal. Modern method of determination of palladium ions have included the stage of decomposition of probe what is caused by partienlitres of apparntnes used for determination and also by necesarity of garantie vesohreunoun probe [1]. At determination of microquantities of palladium ions including in solutions of complex composition obtained after ores decomposition it is necessary previons concentrating. For this extractional [2] and sorptional methods [3–5] in combination with electrochemical method are wide used. The method of dinamical sorptional concentrat-ing don't requed phases division and elowed to acheave high coefficients of concentrating during very small time what very perspecitival [6].

4-(2-N-methylanabazinazo)-m-phenyldiamine is azoreagent which was proposed as selective and sensible

reagent for photometrical determination of ions of palladium was used in our work as electrochemical reagent for their determination [7].

The task of this investigation was concluded in finding of optimal conditions for amperometrical determination of ions of palladium by reagent 4-(2-N-methylanabazino)-m-phenyldiamine at their electrochemical titration.

Optimal conditions of carrying out of amperometrical titration of palladium ions at optimal concentration of reagent in investigated solution were following: $\text{pH} < 4.2$; concentration of buffer 0.1–0.3 M and concentration of reagent $1 \cdot 10^{-4}$ M.

Determined molar ratio (2 : 1) in complex of palladium with 4-(2-N-methylanabazino)-m-phenyldiamine by photometrical method has proved also by amperometrical titration. Obtained curves of titration have witnessed about rightness and reproduction of the elaborated method.

In result of amperometrical titration of palladium ions by new azocompound 4-(2-N-methylanabazino)-m-phenyldiamine at right optimal conditions it was shown that this new nitrogencontaining reagent is selective and sensible reagent for amperometrical determination of palladium ions.

References:

1. Bemish Ph. Analytical chemistry of noble metals. – M.: Mir, 1969. – № 1. – P. 267–272.
2. Shmidt V. S. Extraction by amines. – M.: Atomizdat, 1980. – P. 311–314.
3. Kavalv I. A., Phormanovskiy A. A. and others // Journal of neorg. Chemistry. – 1995. – T. 40, № 5. – P. 828–832.
4. Gurjeva R. F., Savin S. B. // Journal of analyt. chemistry. – 2000. – T. 52, № 3. – P. 247–250.
5. Curjeva R. F., Savun S. B. // Journal of analyt. Chemistry. – 2000. – T. 55, № 3. – P. 280–283.
6. Kovalev I. A., Tsysin G. I., Zolotov Yu. A. // Mendeleev Commun. – 1995. – № 3. – P. 111–116.
7. Smanova Z., Yahshiyeva Z., Juraev I., Mirzahmedov R. Using azoreagents in determining the platinum ions / European research: Innovation in science, education and technology XIX international scientific and practical conference. – London, 2016. – № 8 (19). – P. 26.

Contents

Section 1. Biology	3
<i>Nenko Natalya Ivanovna, Ilyina Irina Anatolyevna, Kiselyova Galina Konstantinovna, Sundryeva Mariya Andreyevna</i> Physiological and biochemical characteristics of resistance of grape varieties of different ecological and geographical origin to the stress factors of summer season	3
<i>Sukhov Evgeny Evgenyevich</i> Kungurian foraminifera of Starostinskaya suite of Spitsbergen Island	12
<i>Sukhov Evgeny Evgenyevich</i> Permian foraminifera of parastratotype of the river Usolka	17
<i>Khuzhanazarov Uktam Eshtemirovich, Islamov Imongali, Sadinov Jasur Samandarovich, Ishmuminov Bobur</i> A description of some pasture plant communities in adyr (steppe) territory of Chirakchi district in Kashkadarya basin	20
Section 2. Mathematics	23
<i>Druzhinin Victor Vladimirovich, Holuskin Vladimir Semenovich</i> Necessary conditions of the existence the sums of fermat	23
Section 3. Materials Science	26
<i>Bukleshev Dmitry Olegovich, Sharaukhova Anastasia Grigoryevna, Buzuev Igor Ivanovich</i> Industrial danger reduction of the pipelines operation by assesment of the weld-affected zones in a stress-strain state	26
<i>Maksudova Nasima Atkhamovna, Iskandarov Asilbek Akrom ugli</i> Research project of metal oxide nanofluids reaching an increase of heat transfer rate capacity in solar absorption refrigerator	30
<i>Turaev Erkin, Mikitaev Abdulah, Djalilov Abdulakhat</i> The properties of polyethylene nanocomposites based on organo-modified montmorillonite	35
Section 4. Mechanical engineering	38
<i>Vasenin Valery Ivanovich, Bogomyagkov Aleksey Vasilevitch</i> Investigation of the work of the P-shaped gating system	38
<i>Maslov Ivan Vasilevich</i> Numerical simulation of underwater curtain welding with various configurations of water nozzle	51
<i>Salahov Timur Zufarovitch, Migranov Mars Sharifullovitch, Nigmatullin Rashit Gajazovich, Hamidullin Ruslan Galeevitch</i> Economic calculation of efficiency of introduction of the gauge of deterioration and temperature in the car engine	55
Section 5. Food industry	59
<i>Gafurov Karim Khakimovich, Ibragimov Ulugbek Muradilloevich, Fayziev Shavkat Ismatovich</i> Statistical-mathematical model of the process of extraction of pumpkin seeds by CO ₂ -extraction	59
Section 6. Agricultural sciences	64
<i>Ahmetov Adilbek Agabekovich, Ahmedov Sherzodbek Anvarhon o'g'li, Karimov Abror Kayumovich</i> Priority directions of perfection construction cotton growing tractors	64
Section 7. Technical sciences	67
<i>Abdullaeva Sadokat Shonazarovna, Nurmuhamedov Khabibulla Sagdullayevich</i> Issue of non-traditional clearing root crops	67

<i>Abdullaeva Sadokat Shonazarovna, Nurmuhamedov Khabibulla Sagdullayevich</i>	
The dehumidification during crushing of the peeled pulp root crops by method of instant dumping of pressure .	69
<i>Bobokulova Oygul Soatovna, Talipova Habiba Salimovna, Mirzakulov Kholtura Chorievich</i>	
Research of process of reception of the pure solutions of chlorides of sodium and magnesium from the dry mixed salts of lake Karaumbet	72
<i>Kadirov Xasan</i>	
The use of complex composition in the preparation of water boiling and heating systems	75
<i>Maksimova Sevinj Abusalat qizi</i>	
Research of new environmental methods for obtaining the organic–mineral fertilizers.	80
<i>Salimova Nigar A., Mamedova Farida M.</i>	
Removal of aromatic hydrocarbons from waste water of industrial oil processing.	83
<i>Nabiyev Akramjon Botijonovich, Abdurahimov S. A.</i>	
Preparation of surfactants reducing the viscosity of heavy oil from raw fatty acid of cotton soap stock.	89
<i>Nabieva Iroda Abdusamatovna, Khasanova Makhfuza Shukhratovna, Artikboeva Ruza Maxsudjanovna</i>	
Studying technological tools that prepare materials with a combination of polyether and cotton fiber for finishing-touch process	93
<i>Ochilov Shuhratulla Atoyevich, Nasirov Utkir Fatidinovich, Toshniyozov Lazizjon Golib ugli</i>	
The oretical study of the fracture mechanism of less fissured rocks	98
<i>Khudoyberganov Abrorjon Akbarovich</i>	
Studying of process steaming of kerosene fraction by hydrocarbonic steams	102
<i>Khudoyberganov Abrorjon Akbarovich, Saydakhmedov Shamshiddin Mukhtarovich</i>	
Studying of process of decontamination of gasoil by hydrocarbonic couples	105
<i>Shamshidinov Israiljon Turgunovich, Mirzakulov Kholtura Chorievich</i>	
Research of process of washing of fluorine from phosphor gypsum.	107
<i>Sharipov Khasan T., Sharafutdinov Ulugbek Z., Rajabboev Ibodillo M., Khujaev Jasur E.</i>	
Analysis of productive solutions and uranium sorption on anionits	111
Section 8. Physics	114
<i>Nadareishvili Malkhaz, Kiziria Evgeni, Sokhadze Viktor, Tvauro Genadi, Tsakadze Severian</i>	
Differential calorimeter of a new type.	114
Section 9. Chemistry	118
<i>Abdurakhmanov Ergashboy, Abdurakhmonov Gulomjon</i>	
Technological scheme and regulation of production of fire retardant on the base of ammophos and ammonia.	118
<i>Aronbaev Dmitry, Vasina Svetlana, Aronbaev Sergej</i>	
Interaction cells of brewing yeasts with ferro fluid	121
<i>Makhmudova Feruza Akhmadjanova, Maksumova Oytura Sitdikovna</i>	
Synthesis on a basis olefines.	124
<i>Mirkhamitova Dilorom, Nurmanov Suvonkul</i>	
Investigation of catalytical reaction of acetylene with morpholine.	126
<i>Parmanov Askar Basimovich, Nurmanov Suvonkul Erxonovich, Phayzullaeva Mariya Phayzullaevna, Abdullaev Jakhongir Urozolievich, Soliev Mukhammadjon Ismatullaevich</i>	
Synthesis of vinyl esters of some carbonic acids.	129
<i>Smanova Zulaykho, Yangibayev Azim, Yakhshieva Khurniso, Raximov Samariddin</i>	
Chemism of complex formation of pyridine and anabasine dyes	132
<i>Shomurotov Shavkat Abduganievich, Akhmedov Oliy Ravshanovich, Mamatmusaeva Nilufar Erkinovna, Sagdullaev Bakhodir Takhirovich, Turaev Abbaskhan Sabirkhanovich</i>	
Modified derivatives of polysaccharides having anti tuberculosis activity	134
<i>Yakhshieva Zukhra, Smanova Zulayxo, Khaydarov Islomjon, Mirzakhmedov Rustam</i>	
Amperometrical determination of palladium ions by organical azoreagents	139